MRR 2007–1

New Nouveau
Brunswick

Natural Resources
Minerals, Policy and Planning

Mineral Resource Report

GEOLOGICAL INVESTIGATIONS IN NEW BRUNSWICK FOR 2006

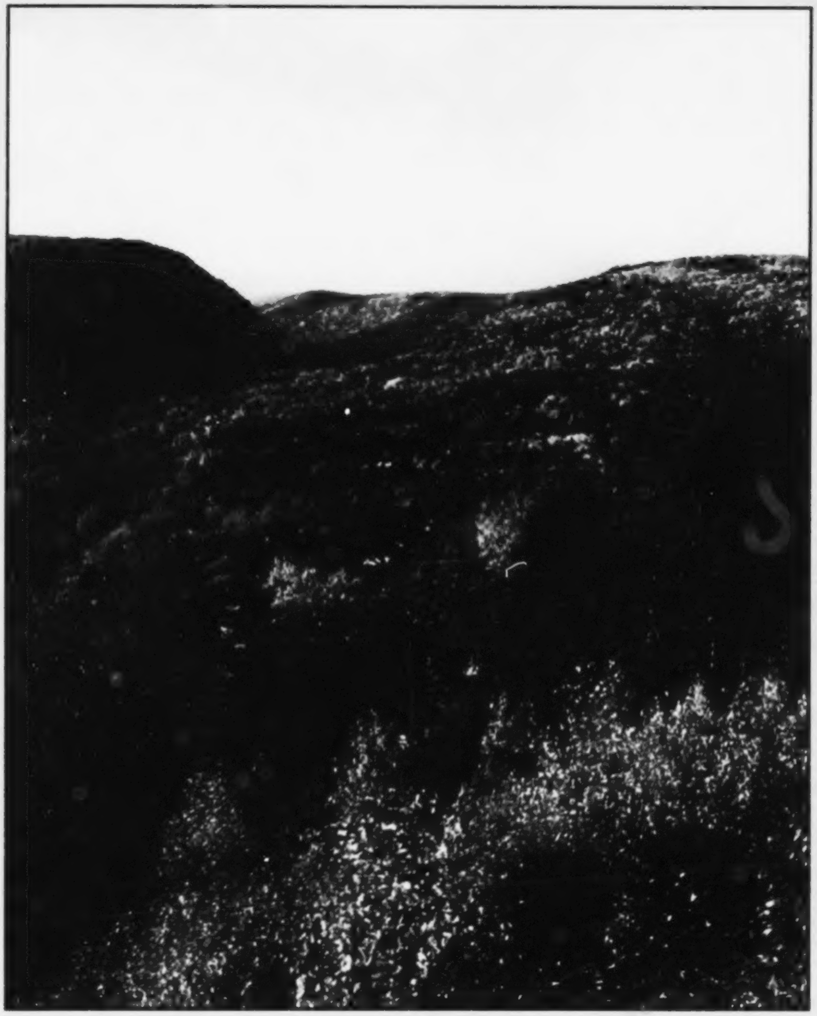

Gwen L. Martin, editor

2007

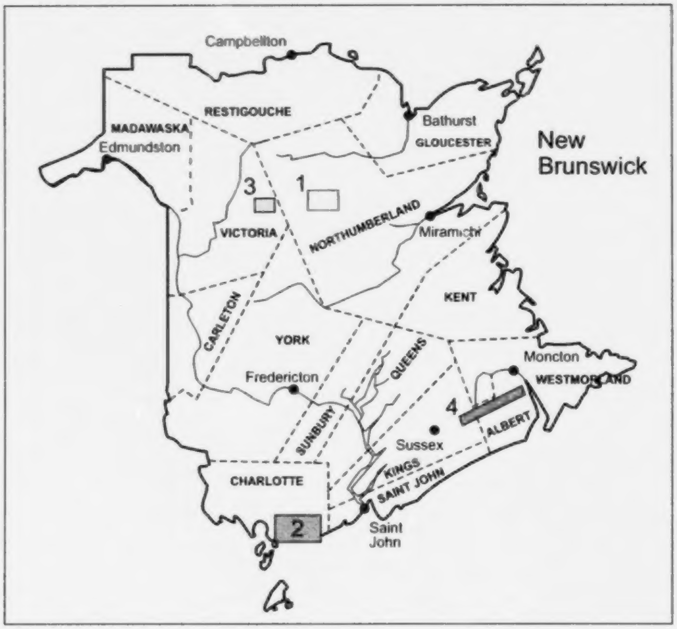
Campbellton
RESTIGOUCHE
MADAWASKA
Edmundston
Bathurst
GLOUCESTER
New
Brunswick
3
1
VICTORIA
NORTHUMBERLAND
Miramichi
KENT
CARLETON
YORK
QUEENS
Moncton
WESTMORLAND
Fredericton
4
SUNBURY
ALBERT
Sussex
KINGS
SAINT JOHN
CHARLOTTE
2
Saint
John

Mineral Resource Report 2007-1

GEOLOGICAL INVESTIGATIONS IN NEW BRUNSWICK FOR 2006

Print Edition
ISBN 978-1-55396-401-8
ISSN 0548-4014

Online Edition
ISBN 978-1-55396-402-5
ISSN 1717-1237

CD Edition
ISBN 978-1-55471-000-3
ISSN 1911-7582

Numbers on location map refer to papers in this volume, as listed in *Table of Contents* (facing page).

Cover illustration *Caledonia Highlands in southeastern New Brunswick, looking northwest up Crooked Creek from about 7 km south-southeast of Caledonia Mountain (see Park and St. Peter, this volume). The rugged landscape is typical of Precambrian crystalline rocks of the Caledonia Uplift.*

Photograph courtesy of Martin Marshall, New Brunswick Department of Natural Resources

Figure preparation Terry Leonard

Editing, design, layout Gwen L. Martin

Translation Le Bureau de traduction, Ministère de l'Approvisionnement et des Services du Nouveau-Brunswick (Translation Bureau, New Brunswick Department of Supply and Services)

Recommended citation

Martin, G.L. (editor). 2007. Geological investigations in New Brunswick for 2006. New Brunswick Department of Natural Resources; Minerals, Policy and Planning Division, Mineral Resource Report 2007-1, 126 p.

This report has been prepared by:

Minerals, Policy and Planning Division
New Brunswick Department of Natural Resources

Hon. Donald Arseneault
Minister of Natural Resources

October 2007

TABLE OF CONTENTS

PAGES

1 **Revised Age of the Clearwater Stream Formation, and New Structural Observations Near the Chester Deposit, Bathurst Mining Camp, Northeastern New Brunswick** 1–20

REGINALD A. WILSON [1] AND SANDRA KAMO [2]

[1] Geological Surveys Branch, New Brunswick Department of Natural Resources
[2] Department of Geology, University of Toronto

2 **Surficial Geology of the St. George Map Area (NTS 21 H G/02), Southwestern New Brunswick** 21–48

SERGE ALLARD

Geological Surveys Branch, New Brunswick Department of Natural Resources

3 **Cheaver Lakes East Occurrence: Setting of Porphyry-Dyke-Related Cu–Zn–Sn–W–Mo Mineralization, North-Central New Brunswick** 49–86

JAMES A. WALKER

Geological Surveys Branch, New Brunswick Department of Natural Resources

4 **Structural Styles in Late Devonian–Early Carboniferous Rocks Along the Southern Margin of the Moncton Subbasin: Caledonia Mountain to Elgin, Southeastern New Brunswick** 87–125

ADRIAN F. PARK [1], CLINTON J. ST. PETER [2], AND DAVID G. KEIGHLEY [1]

[1] Department of Geology, University of New Brunswick
[2] Geological Surveys Branch, New Brunswick Department of Natural Resources

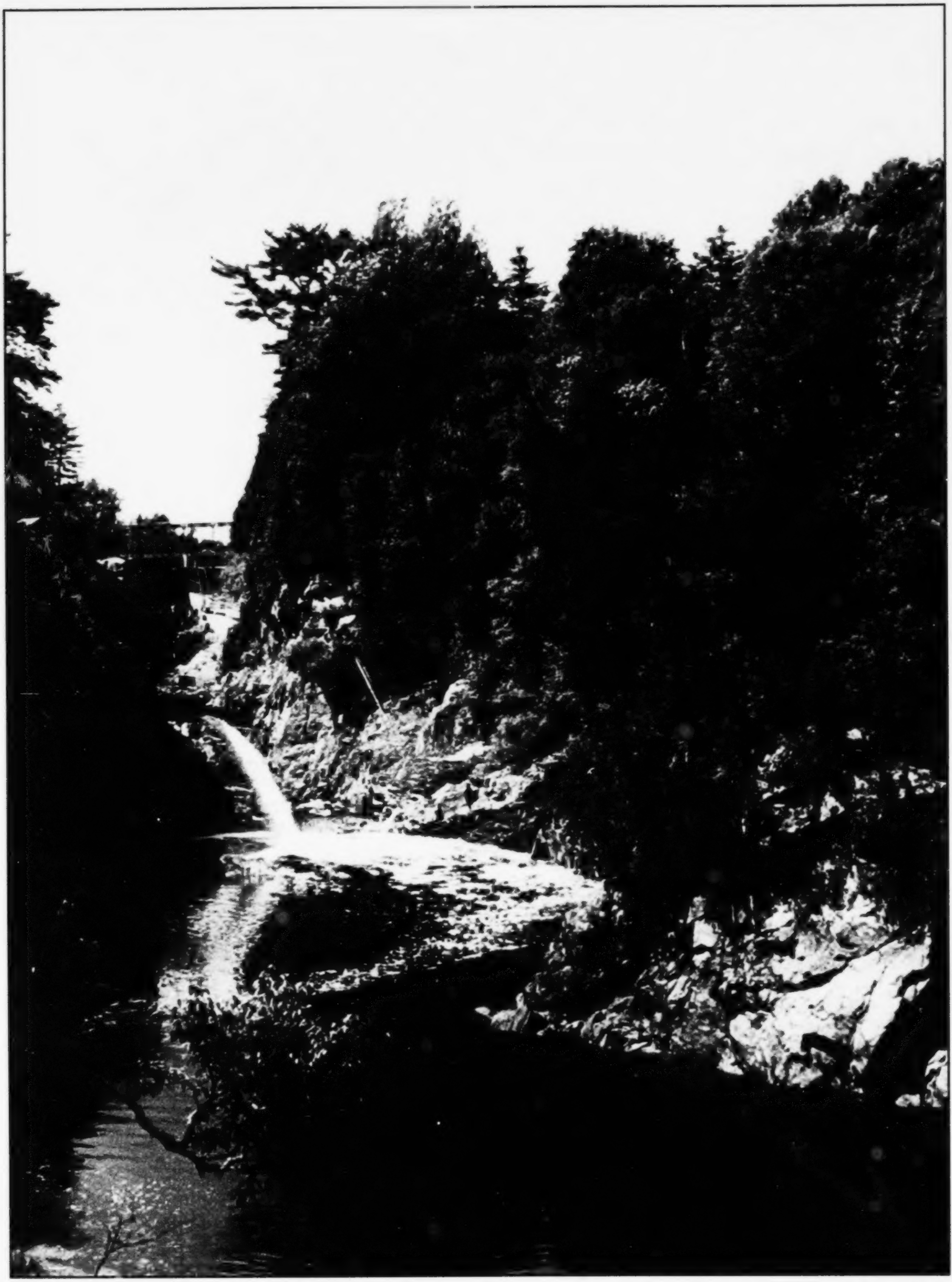

Frontispiece. Mouth of Magaguadavic River in the St. George map area, southwestern New Brunswick (see Allard, this volume). Foreground shows sedimentary rocks of the Silurian Mascarene Group. *Photograph courtesy of Kay Thorne, New Brunswick Department of Natural Resources.*

REVISED AGE OF THE CLEARWATER STREAM FORMATION, AND NEW STRUCTURAL OBSERVATIONS NEAR THE CHESTER DEPOSIT, BATHURST MINING CAMP, NORTHEASTERN NEW BRUNSWICK

REGINALD A. WILSON [1] **AND SANDRA KAMO** [2]
[1] Geological Surveys Branch, New Brunswick Department of Natural Resources,
P.O. Box 50, Bathurst, New Brunswick, CANADA E2A 3Z1 (*reg.wilson@gnb.ca*)
[2] Jack Satterly Geochronology Laboratory, Department of Geology, University of Toronto,
22 Russell Street, Toronto, Ontario, CANADA M5S 3B1

Wilson, R.A., and Kamo, S. 2007. Revised age of the Clearwater Stream Formation, and new structural observations near the Chester deposit, Bathurst Mining Camp, northeastern New Brunswick. *In* Geological Investigations in New Brunswick for 2006. *Edited by* G.L. Martin. New Brunswick Department of Natural Resources; Minerals, Policy and Planning Division, Mineral Resource Report 2007–1, p. 1–20.

The Clearwater Stream Formation in the southern part of the Bathurst Mining Camp, northeastern New Brunswick, is the oldest unit of the Sheephouse Brook Group and hosts the Cu-rich Chester deposit. A new U–Pb (zircon) age of 469.0 ± 0.9 Ma for the Clearwater Stream Formation demonstrates that the unit is significantly younger than previously thought. The new age is essentially identical to the age of other first-cycle felsic volcanic rocks in the Bathurst Camp (that is, the Nepisiguit Falls and Spruce Lake formations). The new age is also in accord with the 466 ± 2 Ma age of conformably overlying rhyolites of the Sevogle River Formation. This stands in contrast with a previously determined Clearwater Stream age that gave a large gap in radioisotopic ages between the Clearwater Stream and Sevogle River formations, thereby implying the existence of an unconformity between the two units for which no field evidence could be found.

New lithogeochemical analyses of volcanic rocks intersected in drillholes west of the main belt of Clearwater Stream rocks reveal signatures typical of that unit. This indicates that the unit extends in the subsurface far west of its present surface distribution and lies structurally below the stratigraphically underlying Patrick Brook Formation (uppermost Miramichi Group). The large-scale structure on the west side of Clearwater Stream is therefore interpreted to define a synform overturned to the east, with a shallowly west-dipping axial surface. The main foliation in the Chester area is an intense, differentiated schistosity — now recognized as S_3 — that dips shallowly to the west, southwest, or south. Newly exposed outcrops in the district reveal the existence of two foliations that developed before this schistosity. Existence of the shallowly dipping S_3 supports structural observations made throughout the Bathurst Camp; however, in the Chester area, earlier foliations are commonly transposed, except in the rarely exposed hinges of F_3 folds.

La Formation de Clearwater Stream dans le sud du Camp minier de Bathurst, dans le Nord-Est du Nouveau-Brunswick, constitue l'unité la plus ancienne du groupe du ruisseau Sheephouse; elle abrite le gîte cuprifère de Chester. Une nouvelle datation U–Pb (zircon) de 469,0 ± 0,9 Ma de la Formation de Clearwater démontre que l'unité est substantiellement plus récente qu'on le pensait auparavant. Le nouvel âge attribué est essentiellement identique à celui des autres roches volcanofelsiques de premier cycle à l'intérieur du Camp minier de Bathurst, c'est-à-dire celles des formations de Nepisiguit Falls et de Spruce Lake. Le nouvel âge correspond également à la datation de 466 ± 2 Ma des rhyolites sus-jacentes concordantes de la Formation de Sevogle River. Ce fait marque un contraste avec la détermination antérieure de l'âge de Clearwater Stream, qui établissait entre les datations radioisotopiques des formations de Clearwater Stream et de Sevogle River un vaste écart laissant supposer l'existence entre les deux unités d'une discordance dont on ne pouvait pas trouver de preuve sur le terrain.

De nouvelles analyses lithogéochimiques de roches volcaniques croisées dans des puits de forage à l'ouest de la ceinture principale des roches de Clearwater Stream révèlent les signatures typiques de cette unité. La présence de ces signatures signifie que l'unité s'étend dans le sous-sol loin à l'ouest de sa distribution en surface actuelle et qu'elle se trouve structuralement au-dessous de la formation stratigraphiquement sous-jacente de Patrick Brook (partie supérieure du groupe de Miramichi). On interprète en conséquence la structure à grande échelle du côté ouest de Clearwater Stream comme un synforme déversé vers l'est présentant une surface axiale peu profondément inclinée vers l'ouest. La principale foliation dans le secteur de Chester est une schistosité varvée intense — désormais désignée à titre de S_3 — qui s'incline peu profondément vers l'ouest, le sud-ouest ou le sud. Des affleurements récemment découverts dans le district révèlent l'existence de deux foliations qui se sont développées avant cette schistosité. L'existence de la foliation peu profondément inclinée S_3 appuie les observations structurales réalisées à l'intérieur du Camp de Bathurst; les foliations antérieures sont toutefois communément transposées dans le secteur de Chester, sauf dans les charnières rarement visibles des plis F_3.

INTRODUCTION

Knowledge of the tectonostratigraphy and geological evolution of the polydeformed volcanic and sedimentary rocks of the Bathurst Mining Camp was significantly improved during the multidisciplinary EXTECH-II project conducted in the late 1990s (van Staal et al. 2003). Interpretation of Bathurst Camp geology was based largely on detailed structural and stratigraphic analysis, and on lithogeochemical characterization of volcanic units, but it also relied extensively on radioisotopic dating of felsic volcanic rocks.

In recent years, First Narrows Resources Corp. has been conducting an exploration program, including diamond drilling, near the Chester base-metal deposit (Fig. 1, 2). To help guide their exploration efforts west of the deposit by confirming that the Clearwater Stream Formation, which hosts the Chester deposit, was in fact being intersected, the company submitted two core-section samples in 2006 to a commercial laboratory for radioisotopic dating. The analytical results gave a significantly younger date than the previously reported age of the Clearwater Stream Formation (Wilson et al. 1999) in the southern Bathurst Mining Camp. To resolve the discrepancy, rocks of the Clearwater Stream Formation were re-collected from an identical lithotype near the originally dated surface outcrop. At the same time, new bedrock exposures were examined on recently constructed logging roads, mainly west of the Chester deposit, to obtain additional clues concerning structure in that part of the Bathurst Camp.

REGIONAL GEOLOGY

The northern Appalachians have been divided into several tectonostratigraphic zones (Williams 1979) which record the evolution and destruction of an ancient ocean (Iapetus) that lay between two major cratons: Laurentia to the west and Gondwana to the east (Dewey 1969; Bird and Dewey 1970). Northern New Brunswick is underlain by volcanic and associated sedimentary rocks from two of these zones (van Staal and Fyffe 1991), those being the Gander Zone (siliciclastic rocks of the peri-Gondwanan passive margin) and the Dunnage Zone (volcanic and sedimentary rocks of the largely allochthonous oceanic domain).

The Bathurst Mining Camp is part of the Dunnage Zone and comprises a polydeformed, Ordovician volcano-sedimentary complex known as the Bathurst Supergroup (van Staal et al. 2003). Rocks of the supergroup were deposited within the complex, ensialic Tetagouche–Exploits back-arc basin (van Staal et al. 1991; van Staal 1994) that developed behind the Popelogan–Victoria arc during eastward-directed subduction on the Gondwanan side of Iapetus (van Staal 1994; van Staal et al. 1998). The Bathurst Supergroup rests unconformably to conformably on crust of the Gander Zone, represented in northern New Brunswick by the Cambrian–Early Ordovician Miramichi Group (van Staal and Fyffe 1991).

The Tetagouche–Exploits back-arc basin comprises several distinct subbasins or volcanic centres that were juxtaposed along D_1 thrust faults. The thrusts formed as back-arc crust was being incorporated into a subduction complex in the Late Ordovician to at least Early Silurian (van Staal et al. 2003). The major subbasins are thus represented by distinct nappes that correspond to the four main groups composing the Bathurst Supergroup: from south to north, they are the Sheephouse Brook, Tetagouche, California Lake, and Fournier groups (Fig. 1). The Fournier Group consists dominantly of basalt and sedimentary rocks; the remaining three units comprise voluminous felsic volcanic rocks overlain by interbedded basalts and sedimentary rocks. Each nappe/subbasin comprises a sequence of coeval but chemically and lithologically distinct volcanic and sedimentary rocks (Rogers et al. 2003; Rogers and van Staal 2003). The Sheephouse Brook Group is situated on the south side of the Moose Lake–

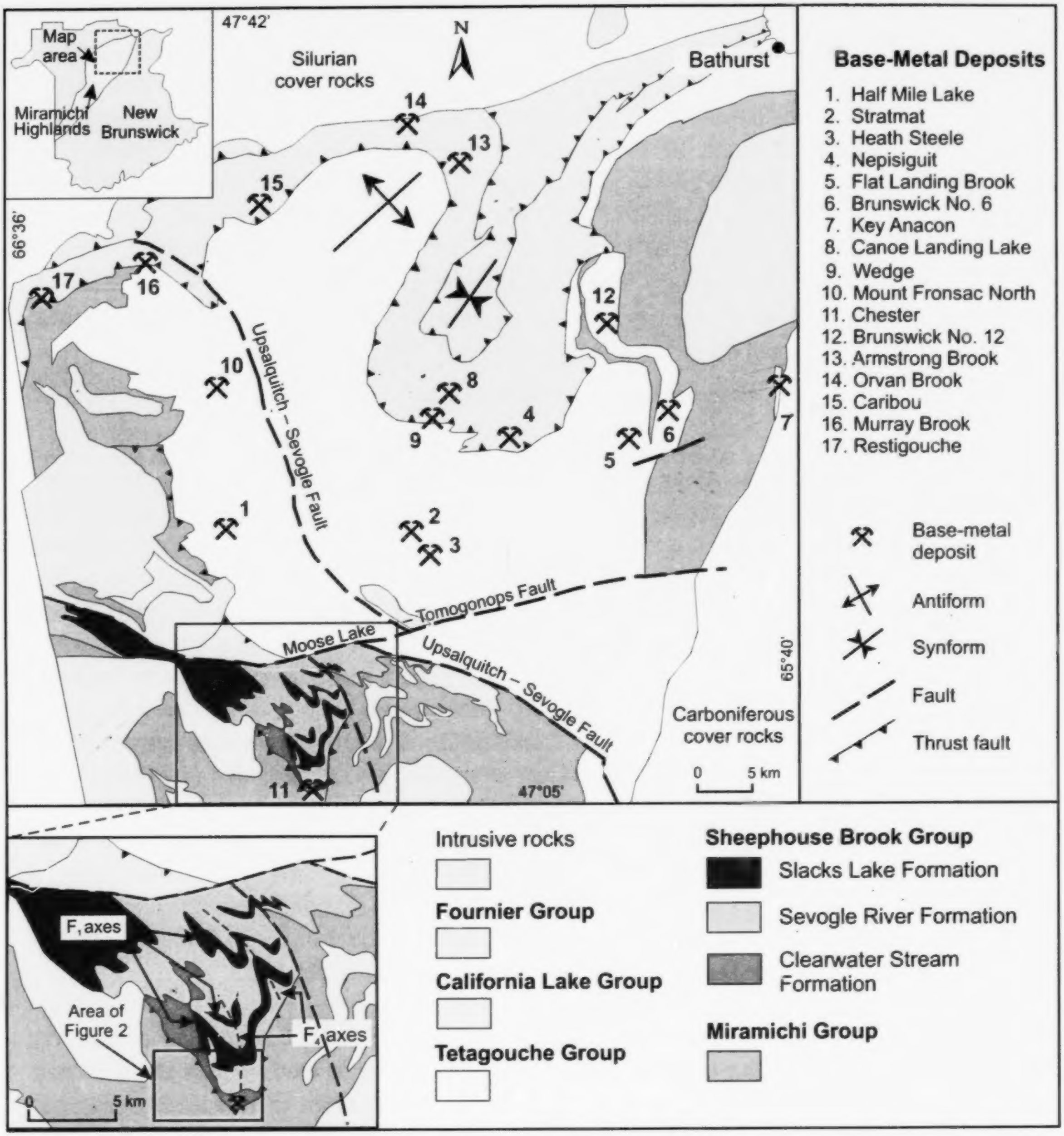
Map area
Miramichi Highlands
New Brunswick
47°42'
Silurian cover rocks
N
Bathurst
66°36'
Upsalquitch – Sevogle Fault
Tomogonops Fault
Moose Lake
Carboniferous cover rocks
65°40'
47°05'
0 5 km
Base-Metal Deposits
1. Half Mile Lake
2. Stratmat
3. Heath Steele
4. Nepisiguit
5. Flat Landing Brook
6. Brunswick No. 6
7. Key Anacon
8. Canoe Landing Lake
9. Wedge
10. Mount Fronsac North
11. Chester
12. Brunswick No. 12
13. Armstrong Brook
14. Orvan Brook
15. Caribou
16. Murray Brook
17. Restigouche
Base-metal deposit
Antiform
Synform
Fault
Thrust fault
F₁ axes
F₄ axes
Area of Figure 2
0 5 km
Intrusive rocks
Fournier Group
California Lake Group
Tetagouche Group
Sheephouse Brook Group
Slacks Lake Formation
Sevogle River Formation
Clearwater Stream Formation
Miramichi Group

Figure 1. General geology of the Bathurst Mining Camp and the report area, highlighting constituent formations of the Sheephouse Brook Group and major base-metal deposits. Cutout map delineates traces of F_1 and F_4 fold axes in the Chester deposit area.

Tomogonops Fault and is the least areally extensive of the four major lithostratigraphic units (Fig. 1). From oldest to youngest, the group consists of the Clearwater Stream, Sevogle River, and Slacks Lake formations (Wilson et al. 1999).

During the EXTECH-II program, radioisotopic dating of basal felsic units in the Tetagouche and California Lake groups (Nepisiguit Falls and Spruce Lake formations, respectively)

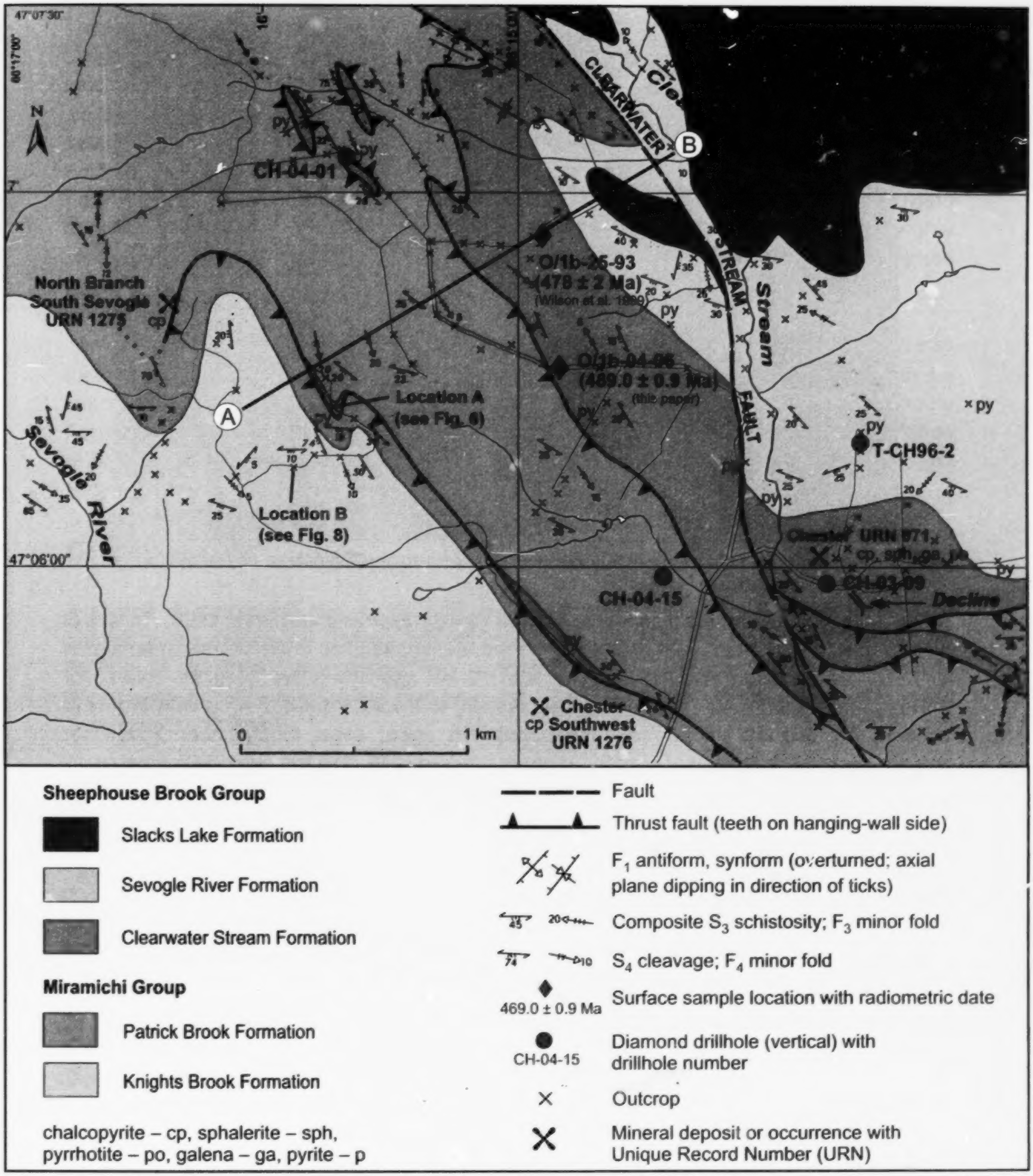
47°07'30"
66°17'00"
N
CLEARWATER STREAM FAULT
Clearwater Stream
B
A
CH-04-01
py
O/1b-25-93
(478 ± 2 Ma)
(Wilson et al. 1999)
O/1b-04-06
(469.0 ± 0.9 Ma)
(this paper)
North Branch
South Sevogle
URN 1275
cp
Location A
(see Fig. 6)
Location B
(see Fig. 8)
Sevogle River
T-CH96-2
Chester URN 971
cp, sph, ga, po
CH-03-09
Decline
CH-04-15
47°06'00"
Chester
cp Southwest
URN 1276
0
1 km
Sheephouse Brook Group
Slacks Lake Formation
Sevogle River Formation
Clearwater Stream Formation
Miramichi Group
Patrick Brook Formation
Knights Brook Formation
chalcopyrite – cp, sphalerite – sph,
pyrrhotite – po, galena – ga, pyrite – p
Fault
Thrust fault (teeth on hanging-wall side)
F1 antiform, synform (overturned; axial plane dipping in direction of ticks)
45
20
Composite S3 schistosity; F3 minor fold
74
10
S4 cleavage; F4 minor fold
469.0 ± 0.9 Ma
Surface sample location with radiometric date
CH-04-15
Diamond drillhole (vertical) with drillhole number
Outcrop
Mineral deposit or occurrence with Unique Record Number (URN)

Figure 2. Geology of the Chester deposit and vicinity (modified after Fyffe 1993). This interpretation assumes that the Clearwater Stream–Patrick Brook boundary is a thrust contact and that the shallowly dipping S_1 foliation of Fyffe (1993) is a composite S_3 fabric. Cross-section A–B is shown in Figure 7. Map location is outlined in Figure 1.

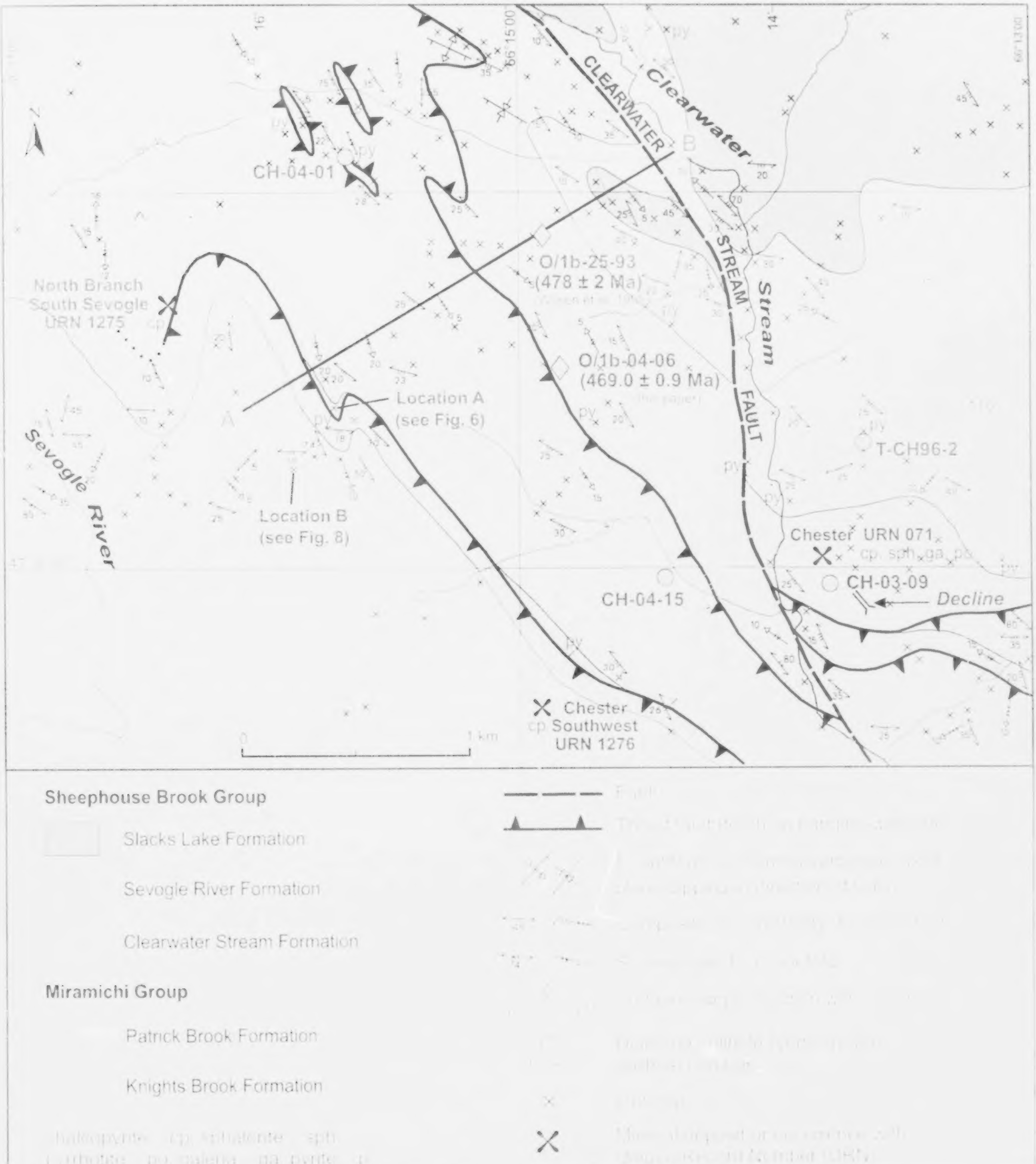
66°15'00"
66°13'00"
16'
14'
N
CH-04-01
North Branch
South Sevogle
URN 1275
cp
O/1b-25-93
(478 ± 2 Ma)
O/1b-04-06
(469.0 ± 0.9 Ma)
(this paper)
A
B
Location A
(see Fig. 6)
Location B
(see Fig. 8)
Sevogle River
CLEARWATER STREAM FAULT
Clearwater Stream
T-CH96-2
Chester URN 071
cp, sph, ga, po
CH-03-09
CH-04-15
Decline
Chester
Southwest
URN 1276
py
0
1 km
Sheephouse Brook Group
Slacks Lake Formation
Sevogle River Formation
Clearwater Stream Formation
Miramichi Group
Patrick Brook Formation
Knights Brook Formation
chalcopyrite = cp, sphalerite = sph
pyrrhotite = po, galena = ga, pyrite = py
Fault
Thrust fault (teeth on hanging wall side)
Outcrop
Mineral deposit or occurrence with
Unique Record Number (URN)

Figure 2. Geology of the Chester deposit and vicinity (modified after Fyffe 1995). This interpretation [illegible] Clearwater Stream–Patrick Brook boundary is a thrust contact and that the shallowly dipping S [illegible] (1995) is a composite S fabric. Cross section A–B is shown in Figure 3. Map projection is [illegible]

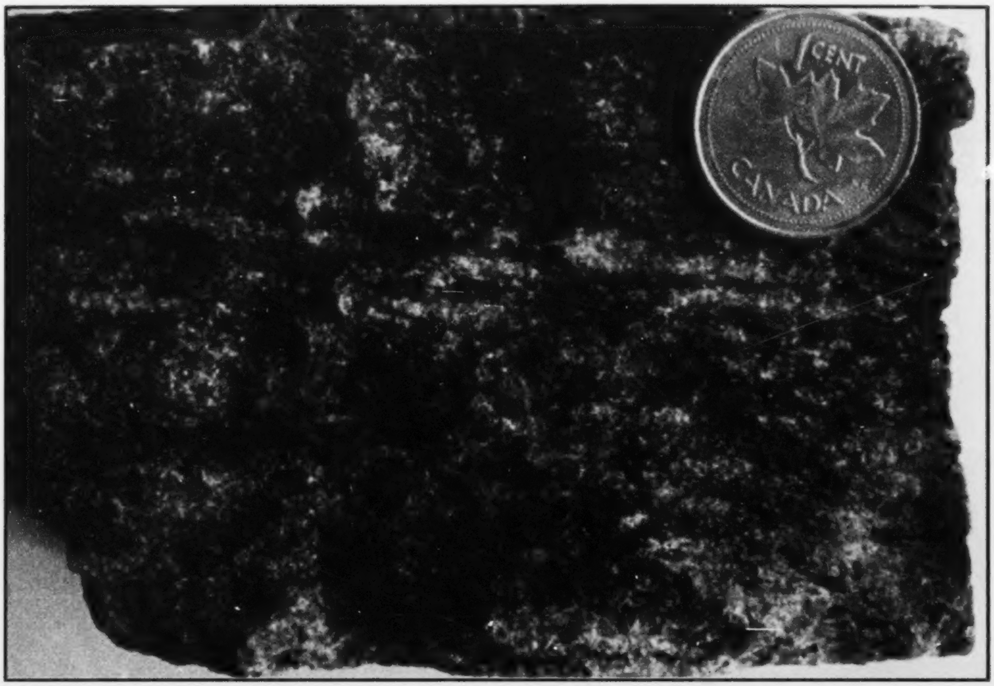

Figure 3. Typical chlorite + biotite-rich metavolcanic rock (plagioclase-phyric dacite) of the Clearwater Stream Formation.

revealed they are essentially coeval at ca. 470 Ma (Sullivan and van Staal 1996; Rogers et al. 1997). However, the Clearwater Stream Formation yielded an anomalously older age of 478 +3/-1 Ma (Wilson et al. 1999). The 466 ± 2 Ma age of the overlying Sevogle River Formation (Wilson et al. 1999) made it necessary to invoke a fault or an unconformity to account for this 12-million-year discrepancy in ages, even though the Clearwater Stream–Sevogle formational contact appears conformable, and the two units share many chemical characteristics.

LOCAL GEOLOGY OF THE CHESTER DEPOSIT

The Chester base-metal deposit is hosted by the Clearwater Stream Formation. The deposit features two small Pb–Zn-enriched massive-sulphide zones that subcrop north of the old exploration decline (Fig. 2), and a Cu-enriched stringer zone that has been traced westward at progressively greater depths in exploration drillholes (Irrinki 1986; Fyffe 1995).

Geology of the deposit and vicinity has been described by Petruk (1959), Van de Poll (1963), Irrinki (1986), Fyffe (1995), and Wilson and Fyffe (1996), and is only summarized here. Geological interpretations have been hampered by complex deformation, metamorphism, and poor exposure. Furthermore, none of the drill core from extensive exploration programs in the 1950s and 1960s was retained, with the result that subsequent workers have been unable to benefit from re-examining or relogging the older core. Several resource estimates of the deposit have been made (Wilson and Fyffe 1996), the most recent being 1.02 Mt of 3.95% Zn, 1.58% Pb, and 0.67% Cu; and 6.4 Mt of 1.22% Cu (McCutcheon et al. 2003).

The Clearwater Stream Formation consists of medium to dark green, strongly foliated plagioclase-phyric volcanic rocks (Fig. 3) that are dominantly dacitic and contain abundant muscovite and about 25% biotite + chlorite (Fyffe 1995; Wilson and Fyffe 1996; Wilson et al. 1999). Deformation and metamorphism generally obscure primary features, but local subtle bedforms suggest pyroclastic emplacement (Wilson et al. 1999). The Clearwater Stream Formation is conformably overlain by alkali-feldspar-phyric rhyolite of the Sevogle River Formation, which in turn is overlain by alkali basalt of the Slacks Lake Formation. Underlying the Clearwater Stream Formation are rocks of the Miramichi Group (Fig. 2), namely dark grey shale, siltstone, and feldspathic wacke of the Patrick Brook Formation; and grayish-green quartzite and shale of the Knights Brook Formation (Fyffe 1995; Wilson and Fyffe 1996).

The nature of the Clearwater Stream–Patrick Brook formational contact is unclear. Intense foliation is consistent with a tectonic (thrust) contact, but its displacement, if any, may be minor (see *Structural Geology*, below). Near the Chester deposit, the Clearwater Stream Formation is altered to a quartz–chlorite schist that has experienced significant mass addition of Si, Fe, Mg, base metals, Cr, and Co, and almost total depletion of Ca, Na, K, Ba, Rb, and Sr (Wilson and Fyffe 1996).

GEOCHRONOLOGY

A sample of dacitic tuff (No. O/1b-25-93 in Fig. 2) was collected in 1993 from a surface outcrop of the Clearwater Stream Formation and subsequently was dated at 478 +3/-1 Ma (Wilson et al. 1999). Age dating was conducted in the Geological Survey of Canada geochronology laboratory using high-precision, isotope dilution thermal ionization mass spectrometry (ID-TIMS).

About a decade later, First Narrows Resources Corp. sunk drillholes CH-04-01 and CH-04-15 northwest and southeast, respectively, of the original site as part of its exploration program in the area (Fig. 2). Two core-section samples, one from each drillhole, were dated at Activation Laboratories Ltd. (Actlabs) and the results reported in 2006 (First Narrows Resources 2006). Those published radioisotopic ages of 469.3 ± 0.3 Ma and 469.4 ± 0.4 Ma were considerably younger than the 478 +3/-1 Ma reported by Wilson et al. (1999) from the surface sample of the Clearwater Stream Formation.

Because it appeared likely that the First Narrows drillholes had indeed intersected rocks of the Clearwater Stream Formation, it was considered necessary to redetermine the crystallization age of the Clearwater Stream Formation to confirm or refute the 478 Ma age. Consequently, another dacite tuff sample (No. O/1b-04-06 in Fig. 2) was collected in 2006 from an outcrop situated about 600 m south of, but in the same lithologic unit as, the outcrop that yielded No. O/1b-25-93. This new Clearwater Stream sample was dated by ID-TIMS at the Jack Satterly Geochronology Laboratory at the University of Toronto; methods and results of its analysis are described below.

Analytical Methods

Zircon from Sample No. O/1b-04-06 was separated using standard heavy liquid and magnetic separation techniques (Fig. 4a). All zircon fractions underwent an air abrasion treatment (Krogh 1982). Mineral dissolution in the presence of a mixed ^{205}Pb–^{235}U tracer followed the procedure of Krogh (1973). Anion exchange column chemistry was used to purify Pb and U. No chemical separation procedure was performed on the zircons. The dissolved sample solutions were dehydrated and redissolved in 3.1 Normal HCl, and the bulk dissolved sample was analyzed in the mass spectrometer.

Pb and U were loaded together with silica gel (Gerstenberger and Haase 1997) onto outgassed rhenium filaments. The isotopic compositions of Pb and U were measured using a single collector with a Daly pulse-counting detector in a solid-source MM354 mass spectrometer. Data were corrected for a mass discrimination of 0.033%/atomic mass unit (AMU) and a dead-time correction of 19.5 nsec. The thermal-source mass discrimination correction was 0.1%/AMU for both Pb and U. The total amount of common Pb in each analysis in this study ranged from 0.23 pg to 0.44 pg. This is the lowest value attainable at any laboratory; it signifies that laboratory blanks are at this level or slightly lower, and that correction for initial common Pb from geological sources is unnecessary.

Error estimates were calculated by propagating known sources of analytical uncertainty for each analysis, including 1) ratio variability (within run), 2) uncertainty in the fractionation correction (0.038% and 0.015% (1 σ) for Pb and U, respectively, based on long-term replicate measurements of the standards SRM982 and CBNM072-6), and 3) uncertainties in the isotopic composition and amount of laboratory blank. Decay constants are those of Jaffey et al. (1971). All age errors described below in the text, shown in Table 1, and depicted as error ellipses on the concordia diagram (Fig. 4b), are given at the 95% confidence interval.

Results

The processing of approximately 13 kg of a strongly deformed, plagioclase-phyric dacitic tuff yielded a moderate quantity of clear, euhedral, pale yellow, generally equant zircons with minor melt inclusions (Fig. 4a). The clearest unaltered zircons were given an air abrasion treatment to remove surface-related Pb loss, and four single zircons with the highest quality were selected and analyzed for Pb and U. Results of the analysis are shown in Table 1.

Three of the single-grain data points (Points 1, 2, and 4 in Fig. 4b and Table 1) give consistent ^{206}Pb/^{238}U ages of 469.1 ± 1.4 Ma, 469.1 ± 1.2 Ma, and 468.4 ± 3.0 Ma. The weighted mean age derived from these data is 469.04 ± 0.88 Ma (Mean Square of Weighted Deviates (MSWD) = 0.091; probability = 0.91). The fourth data point has a ^{206}Pb/^{238}U age of 466.4 ± 3.1 Ma, which is slightly younger than, but within analytical uncertainty of, the first three data points. The analyzed zircon appears to have lost very little Pb. Including this slightly

Table 1. U–Pb isotopic data from four high-quality zircons, Sample No. O/1b-04-06, Clearwater Stream Formation, Bathurst Mining Camp (latitude N47°06'31.6", longitude W66°14'51.3").

Zircon No.	Weight (milligrams)	U (ppm)	Th/U	Pb^{tot} (picograms)	Pb^{com} (picograms)	$^{206}Pb/^{204}Pb$ measured	$^{207}Pb/^{204}Pb$ measured
1	0.0019	98	0.37	14.2	0.38	2380.7	149.0
2	0.0001	179	0.64	14.6	0.44	1980.2	125.2
3	0.0006	83	0.57	4.0	0.34	731.3	55.9
4	0.0004	122	0.48	3.8	0.23	1045.3	72.8

Zircon No.	$^{206}Pb/^{238}U$	2 σ	$^{207}Pb/^{235}U$	2 σ	$^{207}Pb/^{206}Pb$	2 σ	$^{206}Pb/^{238}U$ Age (Ma)	2 σ
1	0.07548	0.00024	0.5875	0.0036	0.05645	0.00029	469.10	1.44
2	0.07548	0.00021	0.5813	0.0044	0.05585	0.00037	469.10	1.24
3	0.07503	0.00051	0.5841	0.0109	0.05647	0.00097	466.36	3.06
4	0.07537	0.00049	0.5785	0.0083	0.05566	0.00074	468.44	2.95

Zircon No.	$^{206}Pb/^{238}U$ Age (Ma)	2 σ	$^{207}Pb/^{235}U$ Age (Ma)	2 σ	$^{207}Pb/^{206}Pb$ Age (Ma)	2 σ	% Disc	Rho
1	469.10	1.44	469.29	2.29	470.2	11.3	0.2	0.549
2	469.10	1.24	465.29	2.80	446.6	14.7	-5.2	0.489
3	466.36	3.06	467.10	6.99	470.8	38.3	1.0	0.385
4	468.44	2.95	463.47	5.31	438.9	29.5	-7.0	0.383

Notes:

1. All single zircon analyses.
2. Pb^{com}= common Pb assuming the isotopic composition of laboratory blank: 206/204 = 18.221; 207/204 = 15.612; 208/204 = 39.360 (errors of 2%).
3. Th/U calculated from radiogenic $^{208}Pb/^{206}Pb$ and $^{207}Pb/^{206}Pb$ age assuming concordance.
4. Disc = per cent discordance for the given $^{207}Pb/^{206}Pb$ age.
5. Rho = correlation coefficient ($^{206}Pb/^{238}U$ and $^{207}Pb/^{235}U$).
6. Uranium decay constants are from Jaffey et al. (1971).

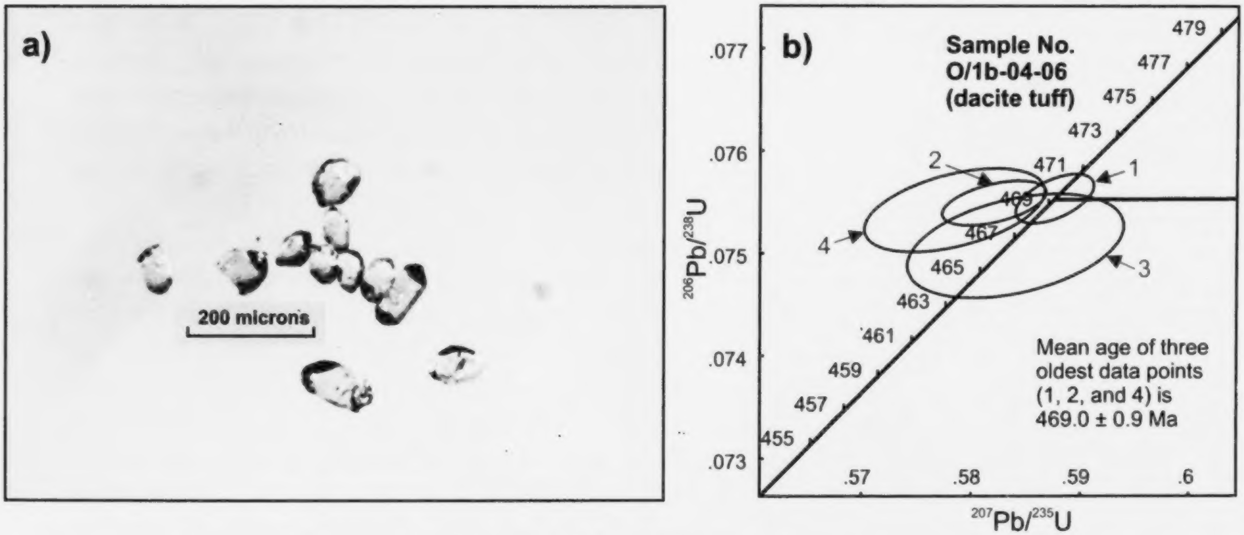

Figure 4. a) Zircons recovered from Sample No. O/1b-04-06, Clearwater Stream Formation. b) U–Pb concordia diagram for Sample No. O/1b-04-06 from the Clearwater Stream Formation. Red arrows indicate data points for the four analyzed zircons.

anomalous datum in the weighted mean $^{206}Pb/^{238}U$ age adjusts the overall age downwards only slightly to *468.83 ± 0.84 (MSWD = 1.00; probability = 0.39), well within error of the* 469.04 Ma age. However, the most robust and accurate age interpretation is the mean of the three oldest data points, that being 469.0 ± 0.9 Ma.

GEOCHEMISTRY

The geochemistry of volcanic rocks from the Sheephouse Brook Group, including the Clearwater Stream Formation, has been previously described (Wilson et al. 1999) and will not be repeated in detail here. Instead, the present section aims to establish the stratigraphic affiliation of volcanic rocks intersected in holes drilled by First Narrows Resources Corp., particularly the radioisotopically dated rocks in drillholes CH-04-01 and CH-04-15 (Fig. 2). This involves comparing the lithogeochemical data from CH-04-01 and CH-04-15 with 1) regional lithogeochemical data of Wilson et al. (1999), and 2) lithogeochemical data from First Narrows Resources drillhole CH-03-09. The data sets shown in Figure 5 and Table 2 thus comprise:

- 15 analyses of surface samples from the Clearwater Stream Formation (Wilson et al. 1999);
- 14 analyses of core-section samples from the Clearwater Stream Formation, collected from First Narrows drillhole CH-03-09 by J. Walker of the New Brunswick Department of Natural Resources (J. Walker, unpublished data);
- 124 analyses (trace elements only) of core-section samples from First Narrows drillhole CH-04-01;
- 34 analyses (trace elements only) of core-section samples from First Narrows drillhole CH-04-15; and
- 31 analyses of surface samples from the Sevogle River Formation (Wilson et al. 1999).

The Walker samples are, by definition, from the Clearwater Stream Formation, as drillhole CH-03-09 was collared in the unit hosting the Chester deposit (J. Walker, pers. comm.). These rocks are variably altered and mineralized, but significantly mineralized samples were excluded from the data set. Geochemical data for the overlying Sevogle River Formation are included to illustrate similarities and contrasts between these rocks and those of the Clearwater Stream Formation (Fig. 5a–f).

On the Y + Nb vs Rb tectonic discrimination diagram (Fig. 5a), both Clearwater Stream and Sevogle River volcanic rocks typically plot in the within-plate granite field. However, the First Narrows data from holes CH-04-01 and CH-04-15 fall in the volcanic-arc granite field. First Narrows samples from these holes were analyzed by less sensitive methods, and only partial extraction was achieved for most elements. This is reflected in comparatively low abundances of rare-earth and high-field-strength elements, especially Y, which is so low that a spurious peralkaline affinity is implied by anomalously high Nb/Y (Table 2). On a primitive-mantle-normalized spidergram (Fig. 5b), average values for each data set show parallel profiles, with the Sevogle River Formation slightly enriched in most elements when compared with the Clearwater Stream Formation. The First Narrows samples are significantly more depleted, particularly in heavy rare-earth elements, but again, this is because of incomplete extraction.

Table 2. Averaged chemical composition of felsic volcanic rocks in the Chester deposit area, Bathurst Mining Camp.

	Clearwater Stream Fm. (from Wilson et al. 1999)	**Clearwater Stream Fm. – Drillhole CH-03-09 (from J. Walker, unpub. data)**	**First Narrows Resources – Drillhole CH-04-01**	**First Narrows Resources – Drillhole CH-04-15**	**Sevogle River Fm. (from Wilson et al. 1999)**
	Surface Samples	**Core Sections**	**Core Sections**	**Core Sections**	**Surface Samples**
n	15	14	124	34	31
SiO_2	64.75	68.53	–	–	69.02
TiO_2	0.70	0.35	–	–	0.40
Al_2O_3	15.18	11.65	–	–	14.57
Fe_2O_3	5.45	7.23	–	–	3.24
MnO	0.07	0.19	–	–	0.06
MgO	3.11	3.49	–	–	1.91
CaO	1.53	0.19	–	–	0.58
Na_2O	2.10	0.71	–	–	1.87
K_2O	3.26	4.05	–	–	5.47
P_2O_5	0.28	0.08	–	–	0.11
Cr	25	5	76	40	15
Ni	8	5	48	10	4
Co	9.2	9.3	19.9	8.2	4.0
Sc	17.0	16.9	14.4	16.9	10.9
V	71	15	101	24	26
Cu	–	138	43	111	–
Pb	20	68	33	34	27
Zn	81	161	103	171	94
Ga	20.2	20.9	23.1	21.4	20.9
Rb	106	156	81	120	153
Ba	681	557	318	392	743
Sr	100	23	58	41	77
Ta	1.45	1.28	1.10	1.31	1.85
Nb	19.2	17.0	14.6	20.8	26.5
Hf	9.04	7.12	4.23	7.52	9.23
Zr	316	245	142	244	319
Y	54.9	45.1	7.5	10.7	60.0
Th	20.0	15.8	9.8	11.8	22.6
U	4.2	4.4	4.2	4.3	5.5
Nb/Y	0.35	0.38	1.95	1.94	0.44
La	55.11	45.24	18.25	34.72	55.86
Ce	113.45	93.88	36.75	64.61	108.70
Pr	–	10.99	–	–	–
Nd	51.96	42.69	23.89	40.44	51.09
Sm	10.56	9.32	5.11	8.96	10.28
Eu	1.62	1.15	0.88	1.10	1.23
Gd	–	8.55	–	–	–
Tb	1.77	1.49	0.58	0.75	1.80
Dy	–	8.14	–	–	–
Ho	–	1.61	–	–	–
Er	–	4.88	–	–	–
Tm	–	0.73	–	–	–
Yb	5.44	4.56	1.26	2.15	5.92
Lu	0.76	0.69	0.18	0.35	0.89

Notes: 1. Oxides are in wt % (hydrous). Trace elements are in ppm. Dash (–) indicates "not analyzed."
2. All core-section data show the average of unmineralized samples.

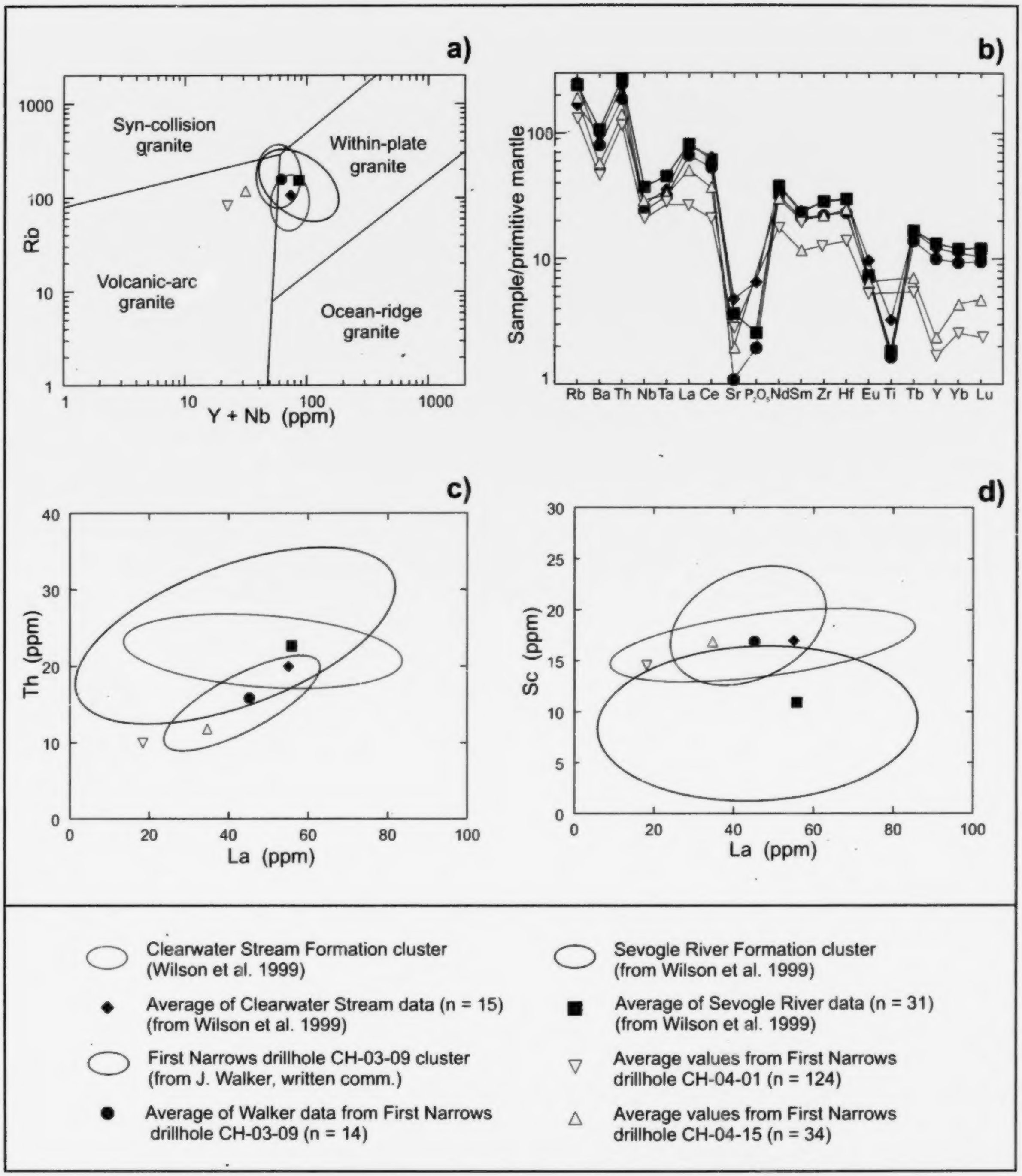

Figure 5. Geochemistry of felsic volcanic rocks from the Clearwater Stream Formation and Sevogle River Formation. a) Rb vs Y + Nb granitoid discrimination diagram (Pearce et al. 1984) for felsic volcanic rocks from the Clearwater Stream and Sevogle River formations. b) Primitive-mantle-normalized spidergram for felsic volcanic rocks from the Clearwater Stream and Sevogle River formations; normalizing values from Sun and McDonough (1989). c) Th vs La, and d) Sc vs La bivariate plots for felsic volcanic rocks from the Clearwater Stream and Sevogle River formations.

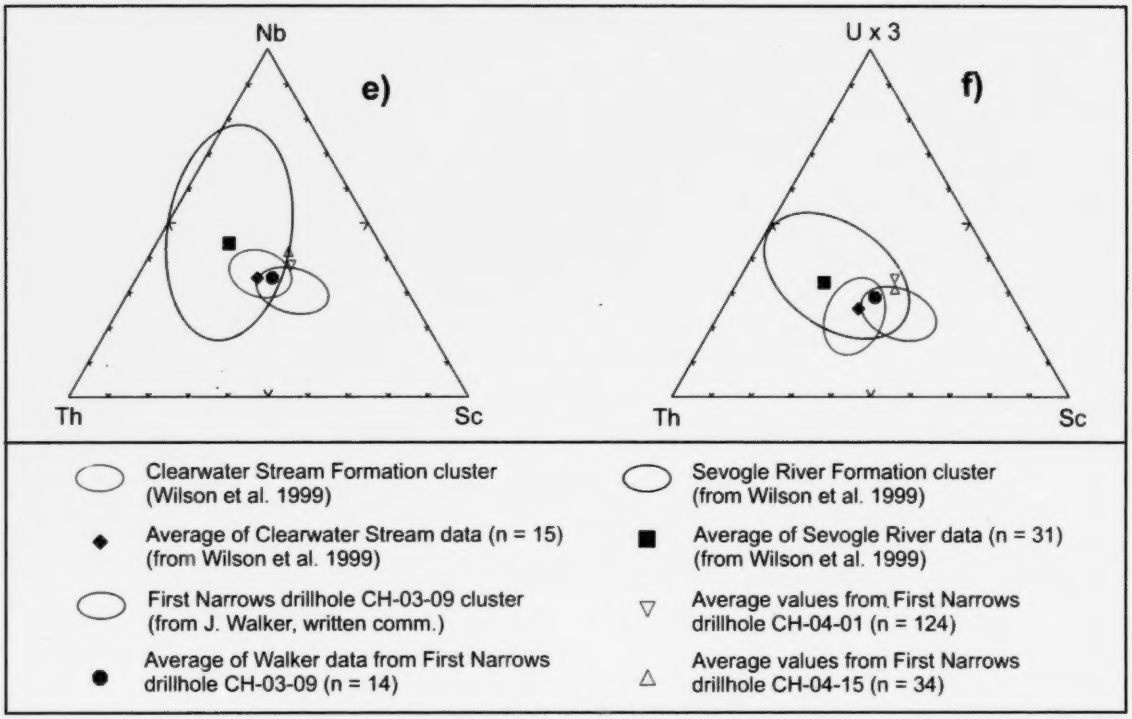

Figure 5. *(cont'd).* e) Th–Nb–Sc, and f) Th–U–Sc ternary diagrams for felsic volcanic rocks from the Clearwater Stream and Sevogle River formations.

Th vs La and Sc vs La bivariate plots (Fig. 5c, 5d) present two of the elements that best discriminate between Sevogle River and Clearwater Stream rocks, namely Th and Sc. The First Narrows data again show comparatively low Th and La values when compared with those from average Clearwater Stream rocks, although Sc is unaffected (Fig. 5d). The Th–Nb–Sc and Th–U–Sc ternary diagrams are particularly effective in distinguishing Sevogle River from Clearwater Stream samples (Fig. 5e, 5f). It thus can be concluded that the First Narrows samples clearly resemble those from the Clearwater Stream Formation, despite displaying somewhat lower average Th.

STRUCTURAL GEOLOGY

West of the Clearwater Stream Fault (CSF), the Clearwater Stream Formation occupies a northwest-trending belt parallel to the dominant foliation (Fig. 2). Volcanic rocks of the formation are also present in scattered outcrops west of this belt, where the dominant exposures are sedimentary rocks of the Patrick Brook Formation (Fig. 6a, 6b). The volcanic rocks have been intersected elsewhere in the shallow subsurface by diamond drilling such as in drillhole CH-04-15 (Fig. 2). Another drillhole, CH-04-01, intersects 263 m of Clearwater Stream volcanic rock, although the hole was collared only 50 m from an outcrop of Patrick Brook Formation.

The gross structure west of the CSF is therefore interpreted as a tight, overturned synform with a shallowly west-dipping axial plane (Fig. 7). Irrinki (1986) and Wilson and Fyffe (1996)

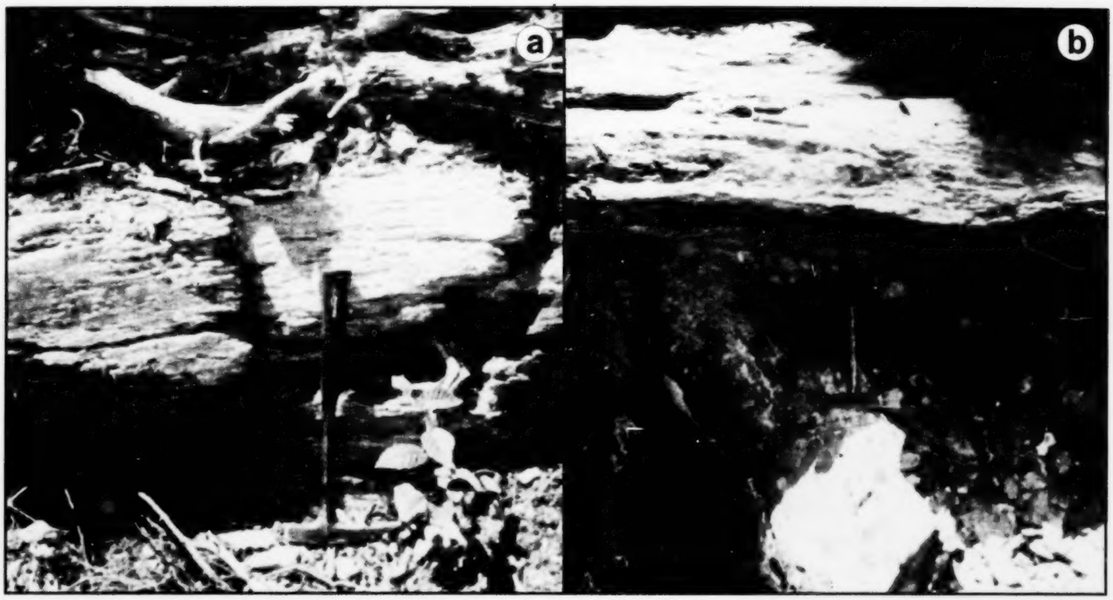

Figure 6. Outcrop of silicified, pyritiferous volcanic rocks of the Clearwater Stream Formation exposed at Location A in Figure 2. This exposure is interpreted to lie in the immediate footwall of a thrust fault. Rusty aspect in Figure 6b is a result of pyrite oxidation. Hammer is 41 cm long.

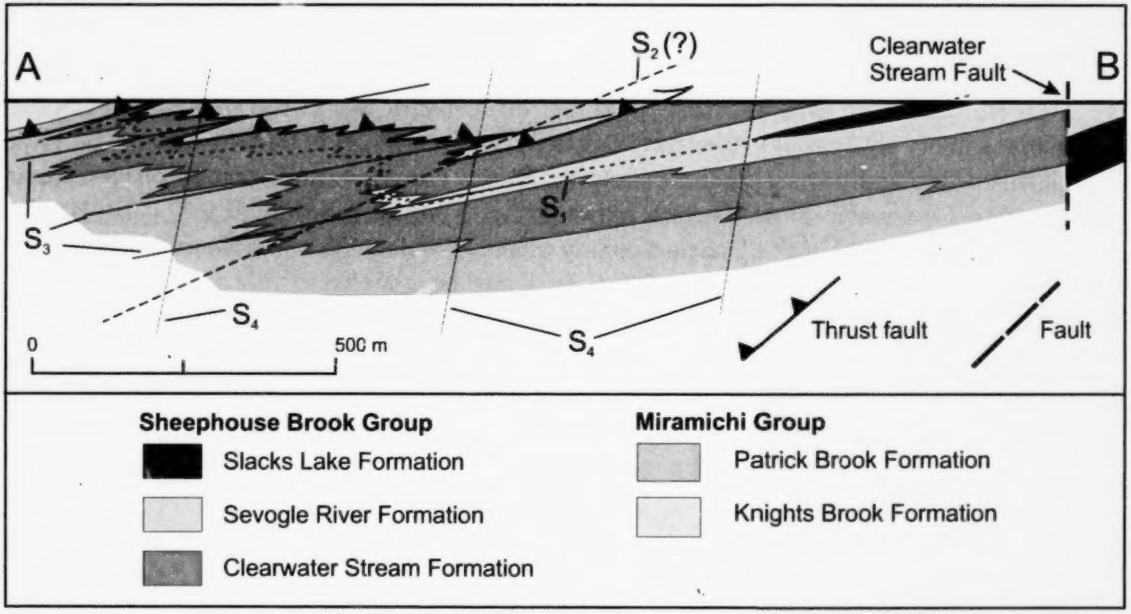
A
B
S_2(?)
Clearwater Stream Fault
S_1
S_3
S_4
S_4
0
500 m
Thrust fault
Fault
Sheephouse Brook Group
Slacks Lake Formation
Sevogle River Formation
Clearwater Stream Formation
Miramichi Group
Patrick Brook Formation
Knights Brook Formation

Figure 7. Structural interpretation of cross-section A–B (located in Fig. 2), looking northwest. Overturned F_1 folds and associated thrust faults have been modified by 1) upright F_2 folds reflecting continued convergence, 2) recumbent F_3 folds related to gravitational collapse, resulting in intense vertical shortening and transposition of S_1 and S_2 into shallow S_3 foliation, and 3) upright, doubly plunging F_4 folds related to late orogenic dextral transpression (van Staal 1994; de Roo and van Staal 1995). F_4 folds (not shown) are probably responsible for locally bringing Clearwater Stream rocks to surface as small "whalebacks" within the Patrick Brook Formation on the left (west) side of this figure.

both interpret this structure as an F_2 fold, although it is more likely an F_1 macrofold overprinted by D_2 through D_4 (see below). Northwest of the Chester deposit, this structure is cored by basaltic rocks of the Slacks Lake Formation (Fig. 2) and appears to plunge southeast (Fyffe 1993).

Elsewhere in the Bathurst Mining Camp, overturned F_1 sheath folds are associated with development of D_1 thrust faults (van Staal 1994), and at Chester, thrusting can similarly be invoked to explain geometry of the local structure. For example, a thrust fault may well account for the anomalously thin interval of Patrick Brook Formation between some outcrops of Clearwater Stream Formation and the Patrick Brook–Knights Brook contact between the Chester Southwest and North Branch South Sevogle mineral occurrences (Fig. 2). Moreover, the abrupt termination of the Clearwater Stream Formation just east of the Chester deposit (Fig. 1, 2) is probably a result of tectonic cutoff, as originally suggested by Fyffe (1995). "Overthickening" of the Clearwater Stream Formation at Chester may be related to some thrust imbrication in this area (Fig. 2). West of Clearwater Stream, the Patrick Brook–Clearwater Stream contact occurs within a broad zone of high strain that may also represent a tectonic contact (Fig. 2).

The Chester deposit is situated within that part of the Bathurst Camp referred to as the "flat belt" (de Roo and van Staal 1994; Fig. 1). In the flat belt, vertical shortening related to extensional collapse has produced recumbent F_3 folds of S_2, or of composite S_1/S_2, and a shallowly dipping S_3 transposition foliation. At Chester and vicinity, overprinting relationships are rare, and most outcrops display a single intense schistosity that dips south or southwest at shallow to moderate angles. Fyffe (1993) recognized S_3 in some outcrops, but where overprinting relationships were lacking, the main foliation was generally mapped as S_1. However, a key new exposure (Location B in Fig. 2) in sedimentary rocks of the Knights Brook Formation (Miramichi Group) contains three foliations, all characterized by a differentiated layering, that shed new light on the structural history of the area. Overprinting relationships at this outcrop (Fig. 8) indicate that the dominant, shallowly dipping foliation is a composite S_3 transposition foliation. Composite S_3 is commonly thrown into open to close, doubly plunging F_4 folds with steeply west-dipping axial planes (Fig. 9). Outliers of Clearwater Stream Formation near drillhole CH-04-01 are best explained as "whalebacks" along the hinges of these F_4 folds. The attitude of the S_0 and S_1 enveloping surfaces at the macroscale is still somewhat speculative, but a possible model has been developed that incorporates current knowledge (Fig. 7).

West of the Clearwater Stream Fault, S_3 dips mostly west-southwest on the western limb of a major F_4 fold. East of the CFS, this same composite foliation is folded around the nose of an F_4 fold and typically dips at shallow to moderate angles to the south, southwest, or southeast (Fig. 1). In the latter area, interpretation of subsurface geometry is again hampered by lack of information on the attitude of S_0 and S_1 enveloping surfaces. If the macroscale D_1 structure can be extrapolated eastward across the CSF, as is likely, then the Clearwater Stream

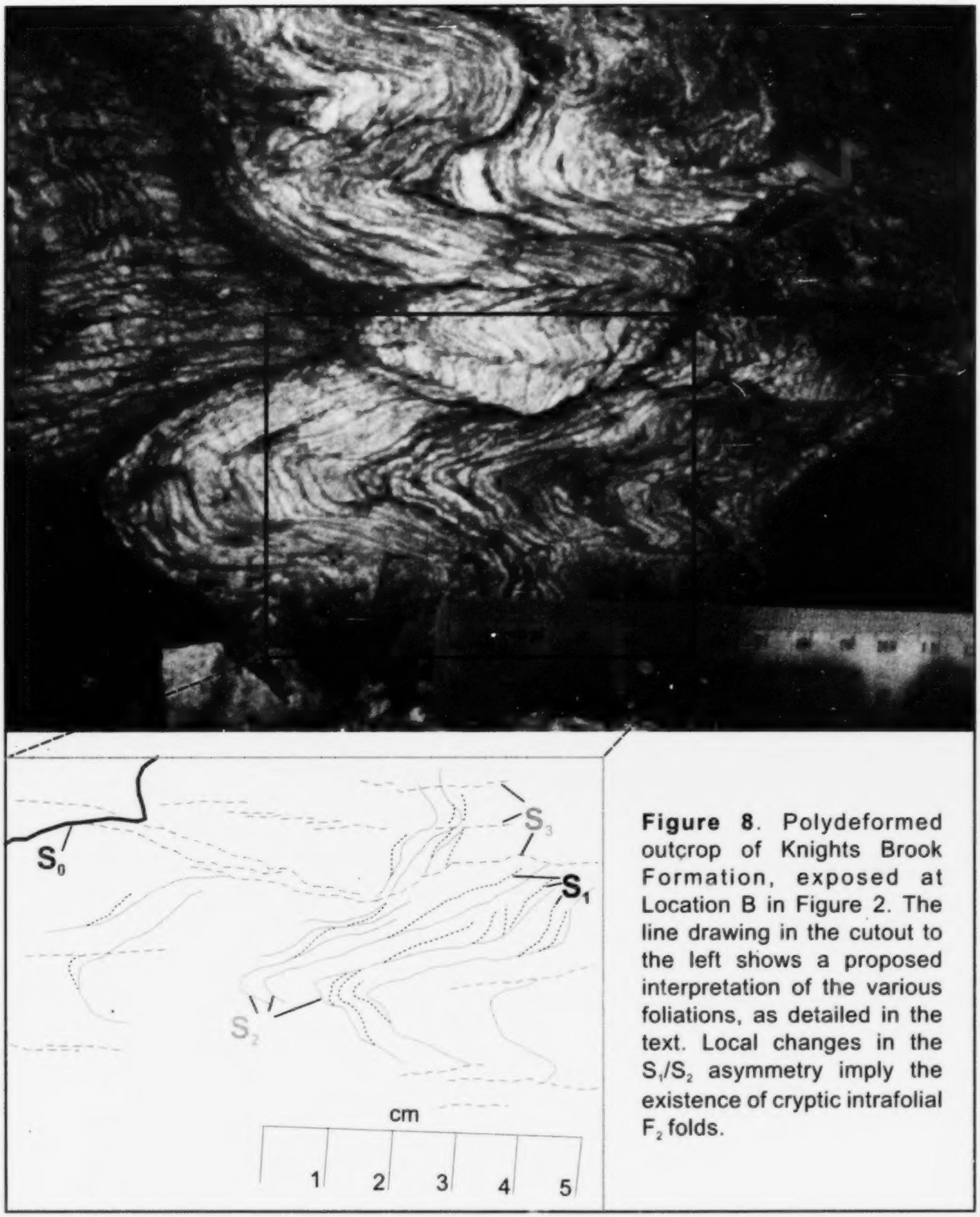

Figure 8. Polydeformed outcrop of Knights Brook Formation, exposed at Location B in Figure 2. The line drawing in the cutout to the left shows a proposed interpretation of the various foliations, as detailed in the text. Local changes in the S_1/S_2 asymmetry imply the existence of cryptic intrafolial F_2 folds.

Formation can be interpreted to dip south below the Patrick Brook Formation. However, no holes have been drilled through the Patrick Brook Formation in this area to confirm the interpretation. A deep hole drilled by Teck Exploration (drillhole T-CH96-2 in Fig. 2) in 1996 (Clark 1997) just north of the Clearwater Stream–Sevogle River formational contact intersected only Sevogle River volcanic rocks, thereby establishing that the contact does not dip north. North of the Chester deposit, keels of Slacks Lake Formation outline the surface trace of F_1 fold axes (Fig. 1).

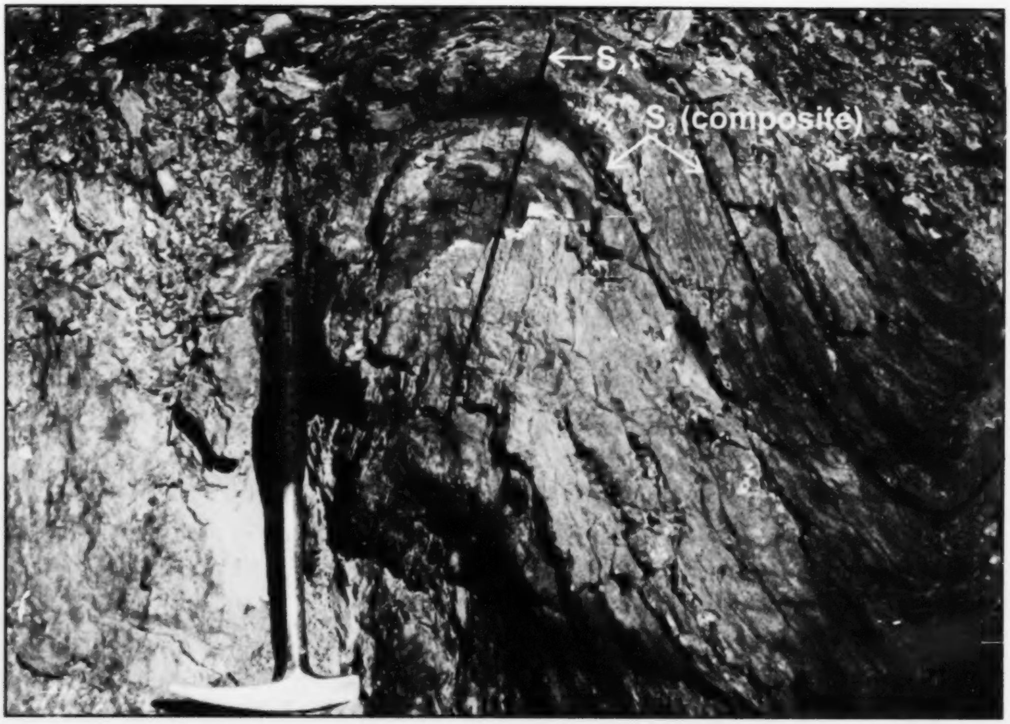

Figure 9. Outcrop of the Patrick Brook Formation, showing development of an F_4 fold of composite S_3, with axial planar S_4 cleavage. Hammer is 41 cm long.

SUMMARY

The newly determined 469.0 ± 0.9 Ma age of the Clearwater Stream Formation conforms with the age of other first-cycle felsic volcanic rocks in the Bathurst Mining Camp and is congruous with the radioisotopic age obtained from conformably overlying rhyolites of the Sevogle River Formation. Previously, the large gap in radioisotopic ages between the two units implied the existence of an unconformity/disconformity, which is not consistent with the lithologically and chemically gradational character of the Clearwater Stream–Sevogle River contact. Trace element signatures of volcanic rocks intersected at depth in First Narrows Resources Corp. drillholes CH-04-01 and CH-04-15 (and dated at ca. 469 Ma) resemble those of the Clearwater Stream Formation, confirming that the latter formation occurs at depth and lies below older Patrick Brook sedimentary rocks that crop out at surface.

Structural observations at newly exposed outcrops along logging roads west of Clearwater Stream indicate the existence of two foliations that developed prior to the dominant, shallowly dipping schistosity, now recognized as S_3. The shallowly dipping attitude of S_3 is consistent with observations made throughout the Bathurst Camp. The difference between the "flat belt" and "steep belt", located west and east of the Upsalquitch–Sevogle Fault, respectively (Fig. 1) is in the far greater intensity of S_3 in the flat belt, where S_1 and S_2 are commonly transposed. In the steep belt, subhorizontal S_3 is locally noted, especially in vertical exposures, but does not transpose earlier foliations or affect the gross distribution of rock units. The proposed structural model for the Chester deposit and vicinity presented herein (Fig. 2, Fig. 7) explains some of the observations at surface. The model remains to be tested, however, and much additional work, probably involving trenching to expose more bedrock, is required to complete the structural picture.

ACKNOWLEDGEMENTS

The authors thank Earnest Brooks and Peter Gummer of First Narrows Resources Corp. for providing geochemical data, access to drill core, and discussions on the geology of the Chester area. John Langton provided expert opinion on structural minutiae. The manuscript was improved by critical reviews by Steve McCutcheon and John Langton.

REFERENCES

Bird, J.M., and Dewey, J.F. 1970. Lithosphere plate — continental margin tectonics and the evolution of the Appalachian Orogen. Geological Society of America Bulletin, **81**, p. 1031–1060.

Clark, D. 1997. Report of work, Chester Property, Teck Explorations Ltd. New Brunswick Department of Natural Resources; Mineral Resources Division, Assessment Report # 474864.

de Roo, J.A., and van Staal, C.R. 1994. Transpression and extensional collapse: steep belts and flat belts in the Appalachian Central Mobile Belt, northern New Brunswick, Canada. Geological Society of America Bulletin, **106**, p. 541–552.

Dewey, J.F. 1969. Evolution of the Appalachian–Caledonian Orogen. Nature, **222**, p. 124–129.

First Narrows Resources. 2006. First Narrows completes age dating study at Chester: Chester footwall volcanics are same age as host rocks of Falconbridge's No. 12 VMS deposit. < http:// www.uno.ca/NewsRelease/2006/02/NewsRelease643/ >

Fyffe, L.R. 1993. Geology of the Clearwater Stream area (NTS 21 O/1b), Northumberland County, New Brunswick. New Brunswick Department of Natural Resources and Energy; Minerals and Energy Division, Plate 93-325 (revised 1999).

Fyffe, L.R. 1995. Regional geology and lithogeochemistry in the vicinity of the Chester VMS deposit, Big Bald Mountain area, New Brunswick, Canada. Exploration and Mining Geology, **4**, p. 153–173.

Gerstenberger, H., and Haase, G. 1997. A highly effective emitter substance for mass spectrometric Pb isotope ratio determinations. Chemical Geology, **136**, p. 309–312.

Irrinki, R.R. 1986. Geology of the Big Bald Mountain map area. New Brunswick Department of Natural Resources and Energy; Minerals and Energy Division, Map Report 86-2, 55 p.

Jaffey, A.H., Flynn, K.F., Glendenin, L.E., Bentley, W.C., and Essling, A.M. 1971. Precision measurement of half–lives and specific activities of 235U and 238U. Physical Review, **4**, p. 1889–1906.

Krogh, T.E. 1973. A low contamination method for hydrothermal decomposition of zircon and extraction of U and Pb for isotopic age determinations. Geochimica et Cosmochimica Acta, **37,** p. 485–494.

Krogh, T.E. 1982. Improved accuracy of U–Pb ages by the creation of more concordant systems using an air abrasion technique. Geochimica et Cosmochimica Acta, **46,** p. 637–649.

McCutcheon, S.R., Luff, W.M., and Boyle, R.W. 2003. The Bathurst Mining Camp, New Brunswick, Canada: history of discovery and evolution of geologic models. *In* Massive Sulfide Deposits of the Bathurst Mining Camp, New Brunswick, and Northern Maine. *Edited by* W.D. Goodfellow, S.R. McCutcheon, and J.M. Peter. Economic Geology Monograph 11, p. 17–35.

Pearce, J.A., Harris, N.B.W., and Tindle, A.G. 1984. Trace element discrimination diagrams for the tectonic interpretation of granitic rocks. Journal of Petrology, **25**, p. 956–983.

Petruk, W. 1959. The Clearwater copper–zinc deposit and its setting, with a special study of mineral zoning around such deposits. Unpublished Ph.D. thesis, McGill University, Montreal, Quebec, 122 p.

Rogers, N., and van Staal, C.R. 2003. Volcanology and tectonic setting of the northern Bathurst Mining Camp – Part II: mafic volcanic constraints on back-arc opening. *In* Massive Sulfide Deposits of the Bathurst Mining Camp, New Brunswick, and Northern Maine. *Edited by* W.D. Goodfellow, S.R. McCutcheon, and J.M. Peter. Economic Geology Monograph 11, p. 181–201.

Rogers, N., Wodicka, N., McNicoll, V., and van Staal, C.R. 1997. U–Pb zircon ages of Tetagouche Group felsic volcanic rocks, northern New Brunswick. *In* Radiogenic Age and Isotopic Studies: Report 10. Geological Survey of Canada, Current Research 1997-F, p. 113–119.

Rogers, N., van Staal, C.R., McNicoll, V., and Thériault, R. 2003. Volcanology and tectonic setting of the northern Bathurst Mining Camp – Part I: extension and rifting of the Popelogan Arc. *In* Massive Sulfide Deposits of the Bathurst Mining Camp, New Brunswick, and Northern Maine. *Edited by* W.D. Goodfellow, S.R. McCutcheon, and J.M. Peter. Economic Geology Monograph 11, p. 157–178.

Sullivan, R.W., and van Staal, C.R. 1996. Preliminary chronostratigraphy of the Tetagouche and Fournier groups in northern New Brunswick. *In* Radiogenic Age and Isotopic Studies: Report 9. Geological Survey of Canada, Current Research 1995-F, p. 43–56.

Sun, S.-S., and McDonough, W.F. 1989. Chemical and isotopic systematics of oceanic basalts: implications for mantle composition and processes. Geological Society Special Publication No. 42, p. 313–345.

Van de Poll, H.W. 1963. Geology of the Chester copper occurrence, Northumberland County, N.B. (Chesterville Mines Ltd. Option). Report for Newmont Mining Corporation. New Brunswick Department of Natural Resources; Minerals, Policy and Planning Division, Assessment File # 470729.

van Staal, C.R. 1994. Brunswick subduction complex in the Canadian Appalachians: record of the Late Ordovician to Late Silurian collision between Laurentia and the Gander margin of Avalon. Tectonics, **13**, p. 946–962.

van Staal, C.R., and Fyffe L.R. 1991. Dunnage and Gander Zones, New Brunswick: Canadian

Appalachian region. New Brunswick Department of Natural Resources and Energy; Mineral Resources, Geoscience Report 91-2, 39 p.

van Staal, C.R, Winchester, J.A., and Bédard, J.H. 1991. Geochemical variations in Middle Ordovician volcanic rocks of the northern Miramichi Highlands and their tectonic significance. Canadian Journal of Earth Sciences, **28**, p. 1031–1049.

van Staal, C.R., Dewey, J.F., Mac Niocaill, C., and McKerrow, W.S. 1998. The Cambrian–Silurian tectonic evolution of the northern Appalachians and British Caledonides: history of a complex, west and southwest Pacific-type segment of Iapetus. *In* Lyell: The Past is the Key to the Present. *Edited by* D.J. Blundell and A.C. Scott. London: The Geological Society, Special Publication 143, p. 199–242.

van Staal, C.R., Wilson, R.A., Rogers, N., Fyffe, L.R., Langton, J.P., McCutcheon, S.R., McNicoll, V., and Ravenhurst, C.E. 2003. Geology and tectonic history of the Bathurst Supergroup, Bathurst Mining Camp, and its relationships to coeval rocks in southwestern New Brunswick and adjacent Maine — a synthesis. *In* Massive Sulfide Deposits of the Bathurst Mining Camp, New Brunswick, and Northern Maine. *Edited by* W.D. Goodfellow, S.R. McCutcheon, and J.M. Peter. Economic Geology Monograph 11, p. 37–60.

Williams, H. 1979. Appalachian Orogen in Canada. Canadian Journal of Earth Sciences, **16**, p. 792–807.

Wilson, R.A., and Fyffe, L.R. 1996. Geologic setting of mineralization in the Big Bald Mountain area (NTS 21 O/1), Bathurst Camp, New Brunswick. *In* Current Research 1995. *Edited by* B.M.W. Carroll. New Brunswick Department of Natural Resources and Energy; Minerals and Energy Division, Mineral Resource Report 96-1, p. 179–217.

Wilson, R.A., Fyffe, L.R., McNicoll, V., and Wodicka, N. 1999. Lithogeochemistry, petrography and geochronology of Ordovician rocks in the Big Bald Mountain area (NTS 21 O/1), Bathurst Mining Camp, New Brunswick. *In* Current Research 1998. *Edited by* B.M.W. Carroll. New Brunswick Department of Natural Resources and Energy; Minerals and Energy Division, Mineral Resource Report 99-4, p. 89–142.

SURFICIAL GEOLOGY OF THE ST. GEORGE MAP AREA (NTS 21 G/02), SOUTHWESTERN NEW BRUNSWICK

SERGE ALLARD
Geological Surveys Branch, New Brunswick Department of Natural Resources,
P.O. Box 6000, Fredericton, New Brunswick, CANADA E3B 5H1 (*serge.allard@gnb.ca*)

Allard, S. 2007. Surficial geology of the St. George map area (NTS 21 G/02), southwestern New Brunswick. New Brunswick Department of Natural Resources; Minerals, Policy and Planning Division, Mineral Resource Report 2007-1, p. 21–48.

Unconsolidated surficial sediments in the St. George map area (NTS 21 G/02), southwestern New Brunswick, reveal a complex sequence of glacial erosion, deposition, and deglaciation. Major fluctuations in glacial activity, water levels, and land levels occurred during the Wisconsinan and had a profound effect in shaping the regional landscape. Recent investigations involved mapping and characterizing the extensive, well preserved Pleistocene–Holocene deposits and erosional features in the report area. No evidence of pre-Wisconsinan glaciation was documented. Early–Middle Wisconsinan glaciation (ca. 100–20 ka B.P.) gave rise to large-scale erosional features and basal till deposits. Most surficial deposits in the report area derive from the Late Wisconsinan (ca. 20–10 ka B.P.), during which period the basal till deposits were reworked or eroded, and depositional processes related to glacial downwasting (that is, glaciofluvial and ablation till deposition) were dominant.

By the end of the Late Wisconsinan, the Bay of Fundy was ice-free, and fluctuations in the relative sea level led to deposition or erosion caused by glaciomarine activity in coastal regions. The most spectacular glaciomarine landforms in the report area are the Pennfield–Utopia Delta Complex and the Pocologan Delta. These glaciomarine deposits typically occur as shallow-water, Gilbert-type deltas with well defined topset, foreset, and bottomset configurations. Both deposits form extensive sand and gravel plains that stand as high as 89 m above the current Bay of Fundy sea level and can reach 35 m thick.

Given that the Pennfield–Utopia Delta Complex and Pocologan Delta cover areas of about 39 km^2 and 40 km^2, respectively, the two deposits represent a tremendous source of unconsolidated granular aggregate materials. Geotechnical test results demonstrate that sand and gravel from the deposits could be used in high-specification products such as Portland cement concrete.

Des sédiments de surface meubles dans le secteur cartographique de St. George (SNRC 21 G/02), dans le Sud-Ouest du Nouveau-Brunswick, révèlent une séquence

complexe de phénomènes d'érosion glaciaire, de dépôt et de déglaciation. Des fluctuations marquées de l'activité glaciaire, des niveaux d'eau et des niveaux terrestres sont survenues au cours du Wisconsinien et ont eu un profond effet sur le profilage du paysage régional. Des études récentes ont comporté une cartographie et une caractérisation des dépôts vastes et bien préservés du Pléistocène-Holocène et des signes d'érosion dans le secteur visé. Aucun indice de glaciation antérieur au Wisconsinien n'a été documenté. Une glaciation du Wisconsinien précoce à moyen (environ 100 à 20 millions d'années avant nos jours) a engendré une érosion visible à grande échelle et des dépôts de till de fond. La majorité des dépôts de surface dans le secteur remontent au Wisconsinien tardif (environ 20 à 10 millions d'années avant nos jours), période au cours de laquelle les dépôts de till de fond ont été remaniés ou se sont érodés et où les processus sédimentaires apparentés à l'amaigrissement du glacier (c'est-à-dire le dépôt de till fluvioglaciaire et de till d'ablation) ont prédominé.

À la fin du Wisconsinien tardif, la baie de Fundy était libérée des glaces, et les fluctuations dans le niveau relatif de la mer ont abouti au dépôt et à l'érosion de vastes dépôts glaciomarins dans les régions côtières. Les formes de relief glaciomarines les plus spectaculaires dans le secteur visé sont le complexe deltaïque d'Utopia-Pennfield et le delta de Pocologan. Ces dépôts glaciomarins se manifestent généralement sous forme de deltas de type Gilbert en eau peu profonde comportant des configurations bien définies des couches sommitale, frontale et basale. Les deux dépôts forment des plaines sableuses et graveleuses étendues qui s'élèvent jusqu'à 89 mètres au-dessus du niveau de la mer actuel de la baie de Fundy et qui peuvent atteindre 35 mètres d'épaisseur.

Comme le complexe deltaïque d'Utopia-Pennfield couvre une superficie de 39 kilomètres carrés et que le delta de Pocologan s'étend sur 40 kilomètres carrés, les deux dépôts représentent d'énormes sources d'agrégats granulaires meubles. Les résultats d'essais géotechniques ont démontré que le sable et le gravier de ces dépôts pourraient servir à la fabrication de produits répondant à des normes élevées, comme le ciment Portland.

INTRODUCTION

An understanding of surficial geology is invaluable for assessing granular aggregate potential in a given region; it also has applications to conducting activities such as mineral exploration, forestry, agriculture, land-use planning, and climate change studies. A program of surficial mapping and granular aggregate sampling was recently carried out in the St. George area (NTS 21 G/02) of southwestern New Brunswick (Fig. 1) and is detailed in Allard (2007a). A primary objective of the work was to evaluate the extensive, Crown-managed aggregate resources near the Bay of Fundy coast between the communities of Utopia and New River (Fig. 1). Of particular interest were the thick (up to 35 m) glaciomarine delta deposits, which consist largely of sand and gravel, and which blanket about 79 km^2 of the district.

Subsidiary objectives of the recent investigations were to 1) classify surficial deposits in the area and produce a surficial geology map (Allard 2007b), and 2) delineate the regional glacial history. The current paper discusses both topics further and is intended to complement information presented in Allard (2007a, 2007b).

PREVIOUS WORK

An early, detailed surficial geology map of the St. George map area was produced by Gadd (1968), who also (1973) described the composition and extent of surficial materials in southwestern New Brunswick and presented an interpretation of their glacial history. Much of his preliminary work is summarized in Rampton et al. (1984).

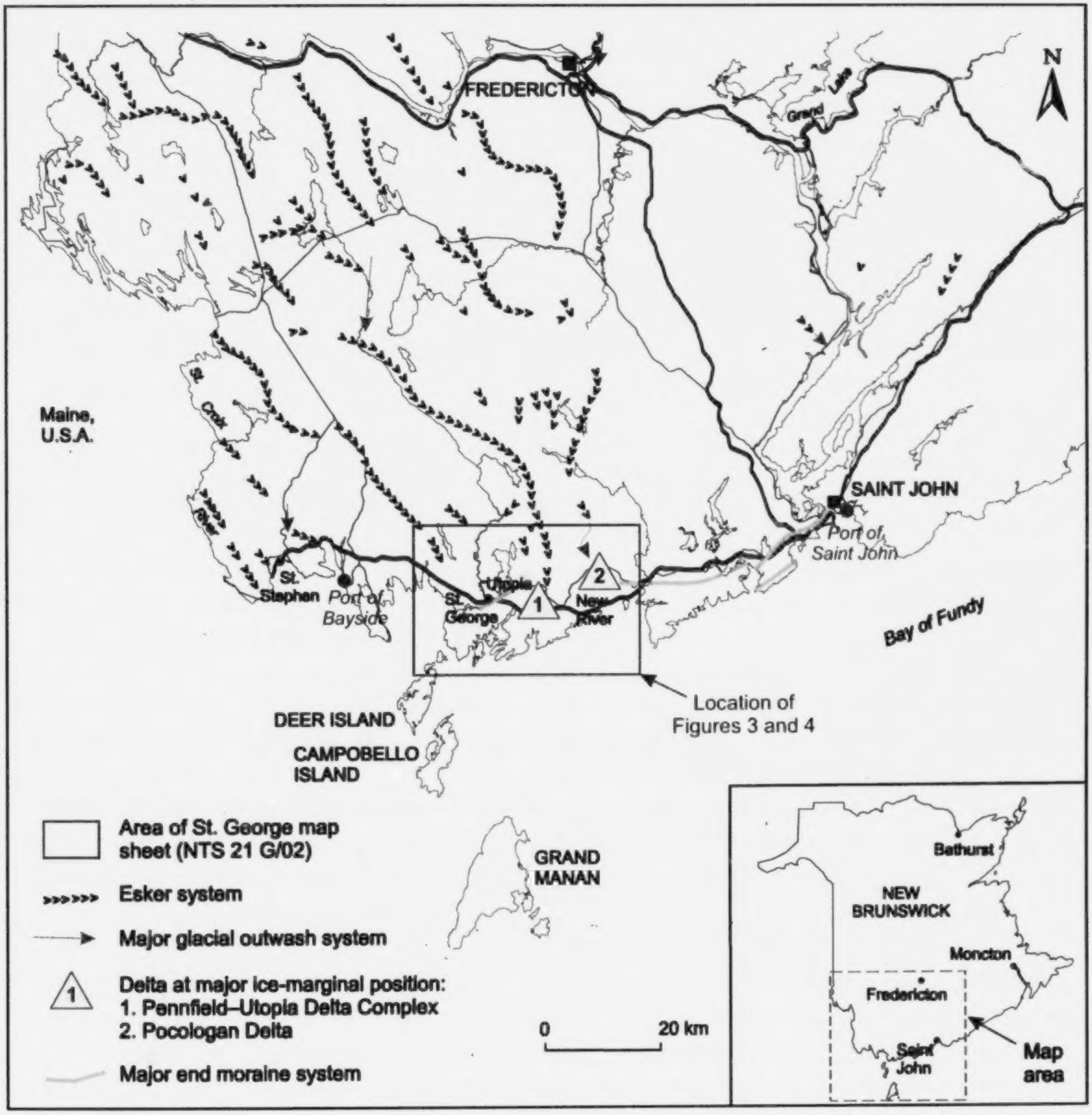
FREDERICTON
Grand Lake
N
Maine, U.S.A.
St. Croix River
SAINT JOHN
Port of Saint John
St. Stephen
Port of Bayside
St. George
Utopia
1
2
New River
Bay of Fundy
Location of Figures 3 and 4
DEER ISLAND
CAMPOBELLO ISLAND
GRAND MANAN
Area of St. George map sheet (NTS 21 G/02)
Esker system
Major glacial outwash system
Delta at major ice-marginal position:
1. Pennfield–Utopia Delta Complex
2. Pocologan Delta
Major end moraine system
0
20 km
Bathurst
NEW BRUNSWICK
Moncton
Fredericton
Saint John
Map area

Figure 1. Location of the St. George map area (NTS 21 G/02) in southwestern New Brunswick.

Finamore (1977) conducted reconnaissance mapping and sampling of surficial deposits in the report area to assess the development potential of its aggregate resources as part of a province-wide granular aggregate inventory program (New Brunswick Department of Natural Resources and Energy 1987). The granular aggregate inventory of the entire St. George map area was completed at a later date (Finamore and Seaman 1988). Interpretive cross-sections derived from seismic surveys of the area (Chandra 1976) gave a preliminary indication of surficial stratigraphy and unit thicknesses in the Pennfield–Utopia and Pocologan district.

Seaman (1989a, 1989b) and Seaman et al. (1993) documented the complex glacial geology of southwestern New Brunswick, including the report area. A till geochemistry survey of the St. George map area (Pronk et al. 2004) yielded geochemical data as well as detailed textural and lithological data for basal till and, to a lesser extent, ablation till.

Finamore (1977) and Finamore and Seaman (1988) presented an excellent account of the aggregate resource quantity on both Crown and freehold land. However, they did not provide enough geotechnical data on which to base a reasonable qualitative assessment of the resource. Allard (2007a) addressed this issue by providing detailed qualitative data for aggregate resources in the eastern half of the St. George map area, focusing on data relevant to current industry specifications. Allard (2007a) also outlined the impact of land commitments and other constraints on the regional availability of aggregate material on property owned and managed by the Crown.

PHYSIOGRAPHIC SETTING

The report area lies entirely within the St. Croix Highlands physiographic division of the New Brunswick Highlands (Bostock 1970; Rampton et al. 1984). The St. Croix Highlands consist of several subdivisions, three of which occur in the map area: the Musquash Lowlands, Clarendon Hills, and Bocabec Hills (Fig. 2). The following descriptions are derived from Rampton et al. (1984).

The Musquash Lowlands occupy almost 75% of the report area. They form an undulating plain, locally interrupted by clusters of hills adjacent to the Bay of Fundy. Maximum elevations seldom exceed 90 m, and coastal cliffs range in height from 10 m to 30 m. Drainage patterns in this district are deranged, the result of intense glacial activity and post-glacial submergence and emergence. The Musquash Lowlands are moderately well drained in most locales. However, poor drainage prevails where broad depressions are scoured directly into bedrock.

The Clarendon Hills occupy the north-central to northeastern part of the report area and comprise intrusive rocks of the Saint George Plutonic Suite. These well defined hills rise in sharp contrast to the adjacent Musquash Lowlands (Fig. 2), from which they are separated by a 60 m to 90 m high, fault-controlled escarpment. Maximum elevation in the Clarendon Hills ranges from 300 m to 350 m. Local relief generally varies between 50 m and 100 m but

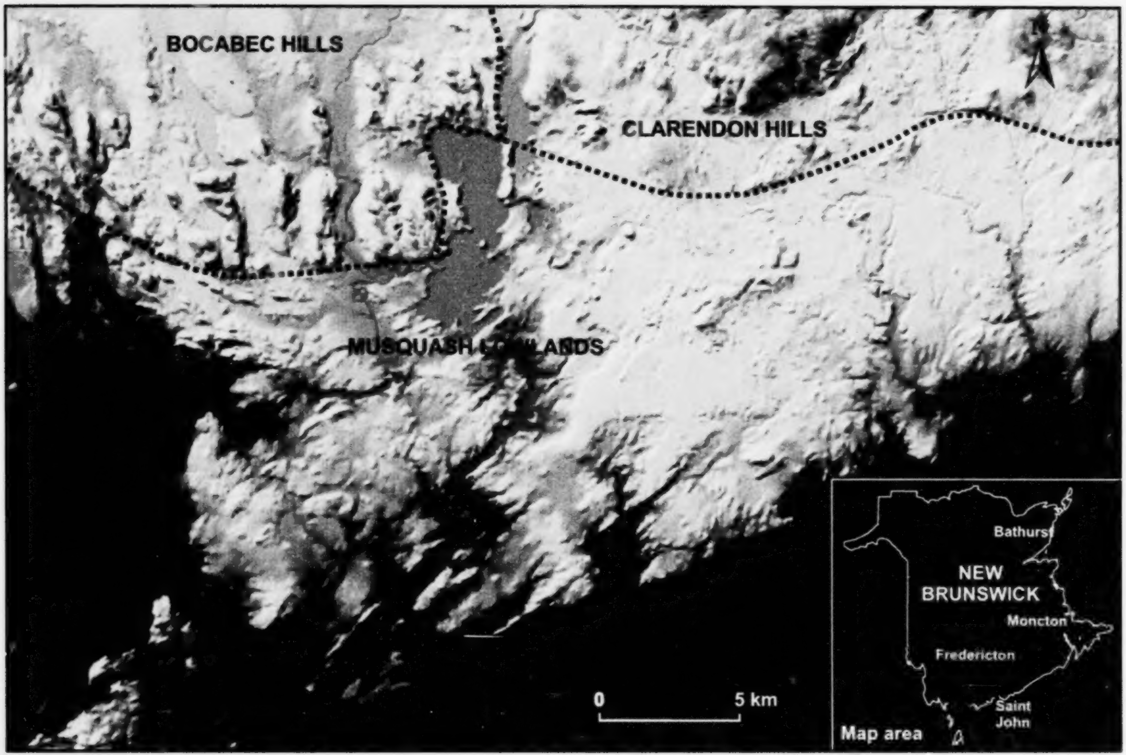

Figure 2. Physiography of the St. George map area, southwestern New Brunswick.

reaches as much as 180 m. Lakes formed by glacial sediment damming their outlets are common in incising valleys of this physiographic subdivision. Most of the subdivision drains into the Bay of Fundy via the Pocologan, New, and Lepreau rivers.

The northwestern part of the report area is occupied by the rugged ridge-and-valley terrain of the Bocabec Hills that separate the undulating upland surface to the north from the low-lying Musquash Lowlands to the south. In the report area, the ridges are generally streamlined into megaflutes with a north-northwest alignment, which has created a parallel drainage system (Fig. 2). The area is predominantly well drained, although drainage obstacles consisting of glacial debris are common.

BEDROCK GEOLOGY

Figure 3 shows a simplified bedrock geology map of the report area. A more detailed, 1:50 000 scale bedrock geology map is available (McLeod et al. 2005), as are 1:20 000 scale maps for parts of the report area (Fyffe 1998; Barr and White 2001a, 2001b). Comprehensive unit descriptions are available in *Lexicon of the Bedrock Nomenclature of New Brunswick* (New Brunswick Department of Natural Resources 2007).

The ages of bedrock units in the report area range from Neoproterozoic to Jurassic. The northern portion of the map is dominated by the Late Silurian–Late Devonian Saint George Plutonic Suite (Fig. 3), which comprises a large composite batholith of high-level intrusive

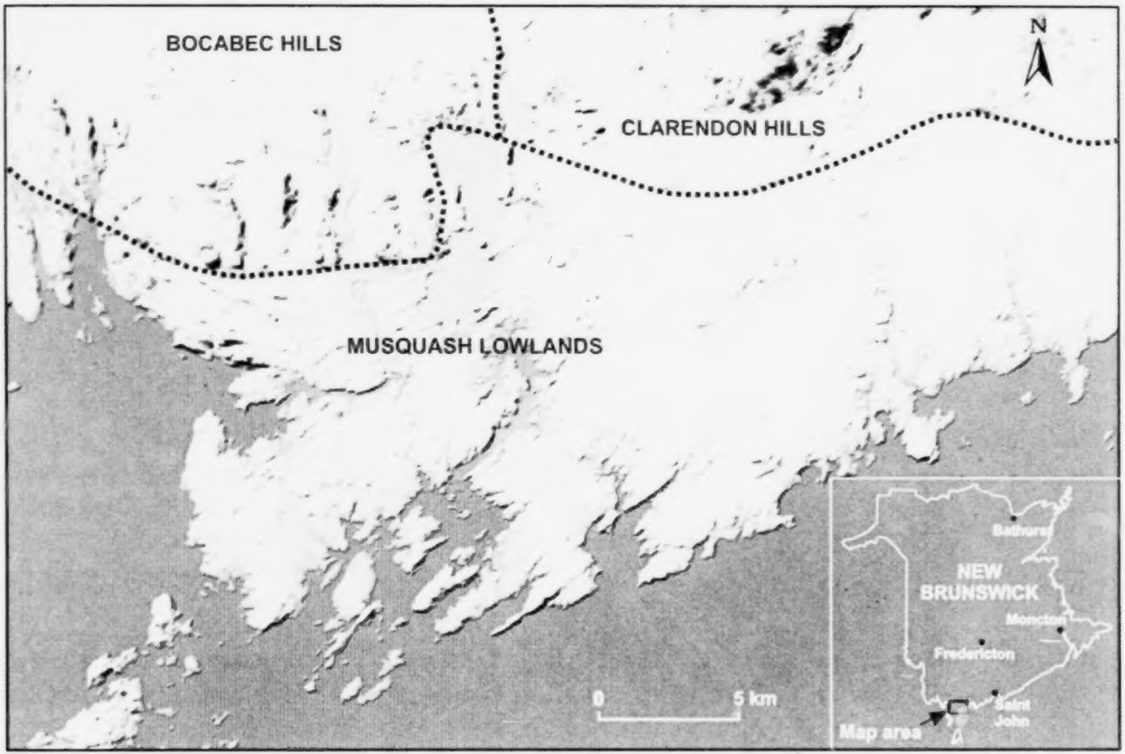

Figure 2. Physiography of the St. George map area, southwestern New Brunswick.

reaches as much as 180 m. Lakes formed by glacial sediment damming their outlets are common in incising valleys of this physiographic subdivision. Most of the subdivision drains into the Bay of Fundy via the Pocologan, New, and Lepreau rivers.

The northwestern part of the report area is occupied by the rugged ridge-and-valley terrain of the Bocabec Hills that separate the undulating upland surface to the north from the low-lying Musquash Lowlands to the south. In the report area, the ridges are generally streamlined into megaflutes with a north-northwest alignment, which has created a parallel drainage system (Fig. 2). The area is predominantly well drained, although drainage obstacles consisting of glacial debris are common.

BEDROCK GEOLOGY

Figure 3 shows a simplified bedrock geology map of the report area. A more detailed, 1:50 000 scale bedrock geology map is available (McLeod et al. 2005), as are 1:20 000 scale maps for parts of the report area (Fyffe 1998; Barr and White 2001a, 2001b). Comprehensive unit descriptions are available in *Lexicon of the Bedrock Nomenclature of New Brunswick* (New Brunswick Department of Natural Resources 2007).

The ages of bedrock units in the report area range from Neoproterozoic to Jurassic. The northern portion of the map is dominated by the Late Silurian–Late Devonian Saint George Plutonic Suite (Fig. 3), which comprises a large composite batholith of high-level intrusive

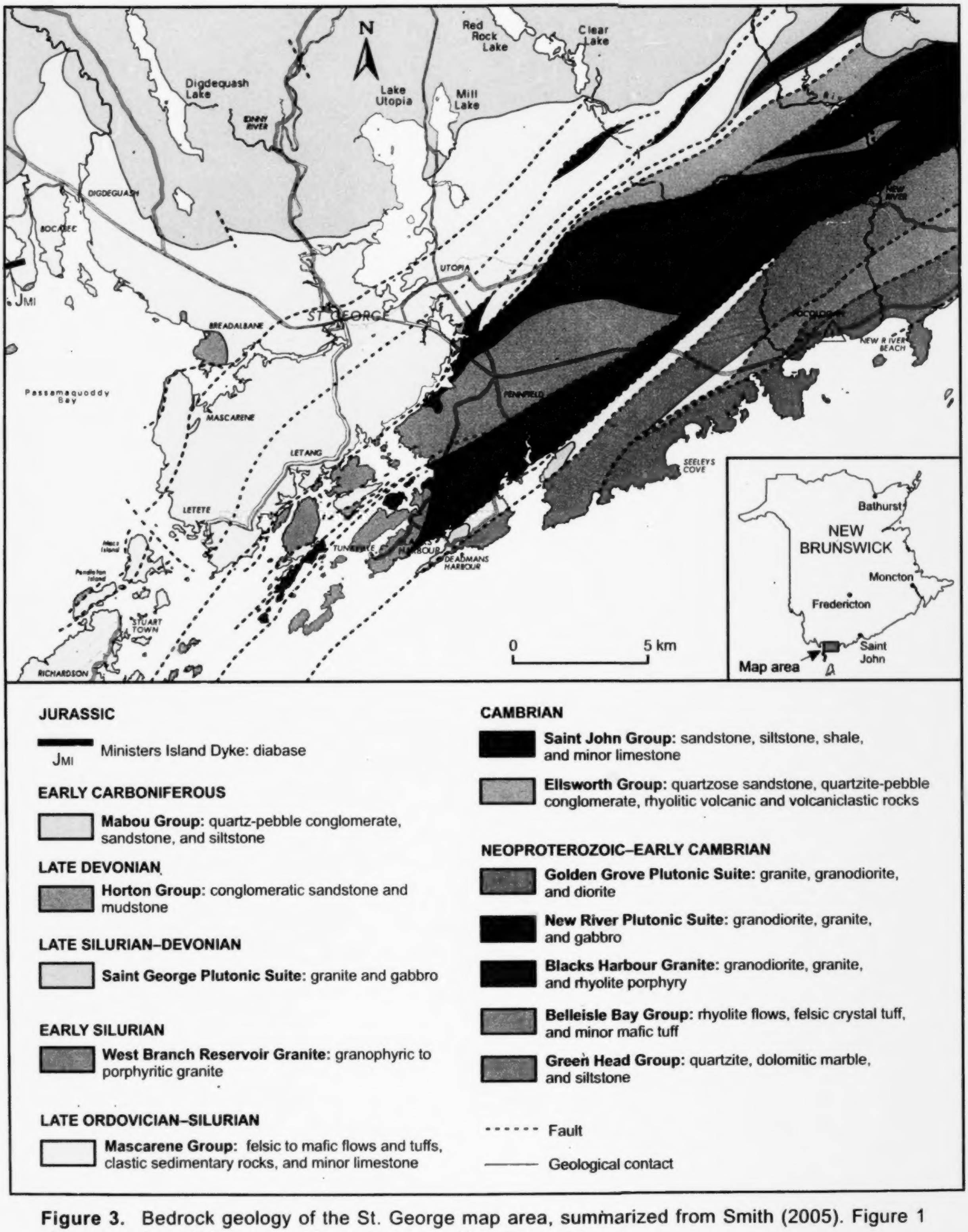
N
Red Rock Lake
Clear Lake
Digdequash Lake
Lake Utopia
Mill Lake
DIGDEQUASH
BOCABEC
JMI
BREADALBANE
ST GEORGE
UTOPIA
Passamaquoddy Bay
MASCARENE
LETANG
LETETE
PENNFIELD
POCOLOGAN
NEW RIVER
NEW RIVER BEACH
SEELEYS COVE
HARBOUR
DEADMANS HARBOUR
STUART TOWN
RICHARDSON
0
5 km
NEW BRUNSWICK
Bathurst
Moncton
Fredericton
Saint John
Map area
JURASSIC
JMI Ministers Island Dyke: diabase
EARLY CARBONIFEROUS
Mabou Group: quartz-pebble conglomerate, sandstone, and siltstone
LATE DEVONIAN
Horton Group: conglomeratic sandstone and mudstone
LATE SILURIAN–DEVONIAN
Saint George Plutonic Suite: granite and gabbro
EARLY SILURIAN
West Branch Reservoir Granite: granophyric to porphyritic granite
LATE ORDOVICIAN–SILURIAN
Mascarene Group: felsic to mafic flows and tuffs, clastic sedimentary rocks, and minor limestone
CAMBRIAN
Saint John Group: sandstone, siltstone, shale, and minor limestone
Ellsworth Group: quartzose sandstone, quartzite-pebble conglomerate, rhyolitic volcanic and volcaniclastic rocks
NEOPROTEROZOIC–EARLY CAMBRIAN
Golden Grove Plutonic Suite: granite, granodiorite, and diorite
New River Plutonic Suite: granodiorite, granite, and gabbro
Blacks Harbour Granite: granodiorite, granite, and rhyolite porphyry
Belleisle Bay Group: rhyolite flows, felsic crystal tuff, and minor mafic tuff
Green Head Group: quartzite, dolomitic marble, and siltstone
Fault
Geological contact

Figure 3. Bedrock geology of the St. George map area, summarized from Smith (2005). Figure 1 shows location of this map area in southwestern New Brunswick.

rocks spanning an area of approximately 2 000 km^2 in southwestern New Brunswick. Rocks of the Late Ordovician–Late Silurian Mascarene Group (Fig. 3) underlie much of the central and southwestern parts of the map area, where they consist of felsic to mafic flows and tuffs, and clastic sedimentary rocks with minor limestone. The Jurassic Ministers Island Dyke (diabase) intrudes rocks of the Mascarene Group south of Bocabec on the western boundary of the map area.

The remainder of the report area is underlain primarily by Neoproterozoic–Cambrian felsic to mafic extrusive rocks with associated sedimentary rocks, and various intrusive rocks (granite, granodiorite, gabbro, and diorite). From oldest to youngest, these lithologies represent the Green Head Group, Belleisle Bay Group, Blacks Harbour Granite, New River Plutonic Suite, Golden Grove Plutonic Suite, Ellsworth Group, and Saint John Group. Small areas of Late Devonian–Early Carboniferous sedimentary and metasedimentary rocks of the Horton and Mabou groups are restricted to a few coastal exposures in the western half of the map area.

SURFICIAL GEOLOGY

The recently compiled 1:50 000 scale surficial geology map of the St. George map area (Allard 2007b) was based on the work of Gadd (1968) and Pronk et al. (2004), and on fieldwork by the author in 2005 (Allard 2007a). The current report provides a summarized version of that map (Fig. 4) and detailed descriptions of the map units (see below). Figure 4 also shows most of the place names cited in the following text.

Pre-Quaternary

Undifferentiated Bedrock

Exposed bedrock is pervasive in coastal areas and is often overlain by thin wave-washed patches of till or glaciofluvial/glaciomarine debris. Bedrock surfaces are typically glacially scoured and polished, often exhibiting stoss-and-lee features indicative of glacial flow. In upland areas, bedrock overlain by minor till, soil, and colluvium is widespread. In these regions, striae as well as larger scale erosional features such as flutings and roche moutonnée are commonly encountered. Figure 5 shows striae mapped by Seaman et al. (1993), Pronk et al. (2004), and the author (field season 2005).

Pleistocene

Till Deposits

Basal till and ablation till appear as a single unit in Figure 4; however, they are shown as two individual units on the larger scale map of Allard (2007b), and are described separately below.

Basal Till Deposits (Early–Middle Wisconsinan)

Basal till occurs locally throughout the report area. Unlike the extensive till blankets found in

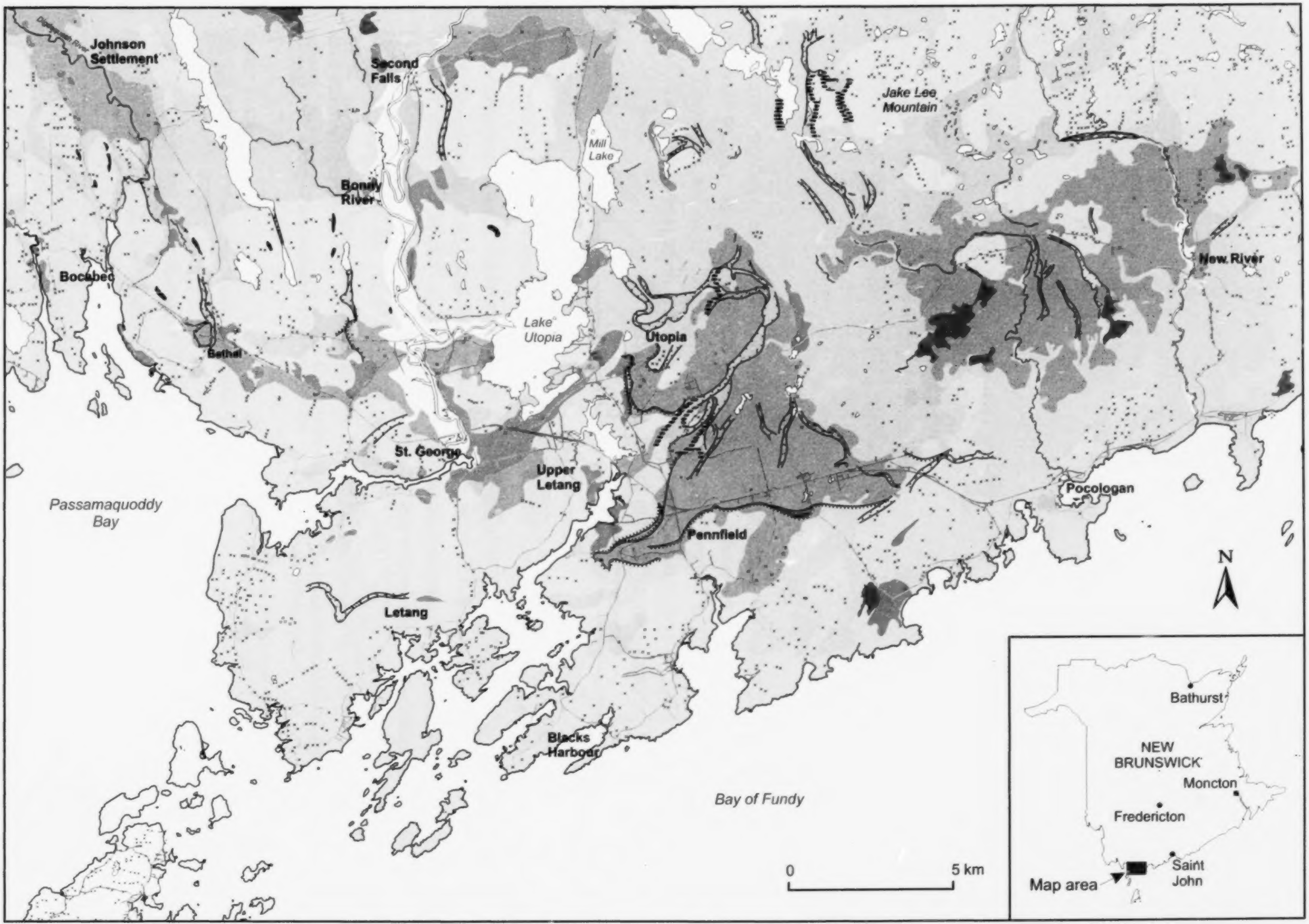
Johnson Settlement
Second Falls
Jake Lee Mountain
Mill Lake
Bonny River
New River
Bocabec
Lake Utopia
Utopia
Bethel
St. George
Upper Letang
Pocologan
Passamaquoddy Bay
Pennfield
N
Letang
Bathurst
NEW BRUNSWICK
Blacks Harbour
Moncton
Bay of Fundy
Fredericton
0
5 km
Saint John
Map area

Figure 4. Surficial geology of the St. George map area, simplified from Allard (2007b). Map legend appears on facing page. Figure 1 shows location of the map area in southwestern New Brunswick.

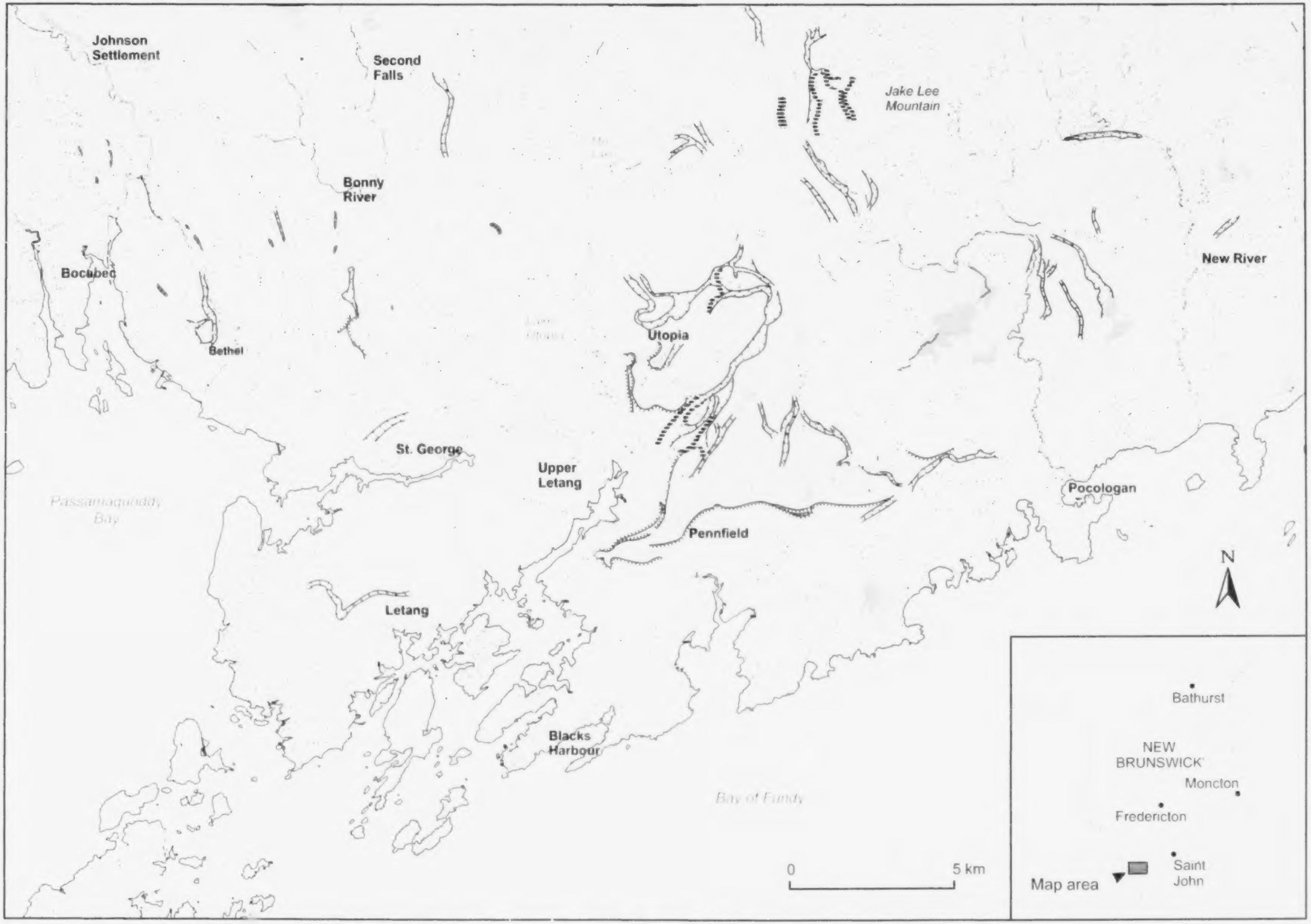
Johnson Settlement
Second Falls
Jake Lee Mountain
Bonny River
Bocabec
New River
Bethel
Lake Utopia
Utopia
St. George
Upper Letang
Passamaquoddy Bay
Pocologan
Pennfield
N
Letang
Bathurst
NEW BRUNSWICK
Moncton
Fredericton
Saint John
Map area
Blacks Harbour
Bay of Fundy
0
5 km

Figure 4. Surficial geology of the St. George map area, simplified from Allard (2007b). Map legend appears on facing page. Figure 1 shows location of the map area in southwestern New Brunswick.

QUATERNARY

HOLOCENE (nonglacial environment)

□ **Alluvial Deposits**
Sand and silt with minor clay and gravel; deposited by modern streams

▩ **Organic Deposits**
Peat and muck; 1–5 m thick

■ **Colluvial Deposits**
Fractured bedrock or reworked glacial deposits; indicated by slopes with > 20% grade

PLEISTOCENE (Wisconsinan glacial environment)

▒ **Glaciomarine Delta Deposits**
Sand, gravel, and cobbles; 1–30 m thick

░ **Glaciomarine Beach and Basin Deposits**
Medium- to coarse-grained sand and gravel (minor cobbles) or massive to stratified clay and silt with minor sand; often thin and discontinuous

▒ **Undifferentiated Glaciolacustrine/Glaciomarine Deposits**
Silt, clay, and sand

░ **Glaciofluvial Outwash Deposits**
Sand, gravel, cobbles; generally well sorted and stratified; 1–10 m thick

▓ **Glaciofluvial Ice-Contact Stratified Drift Deposits**
Well to poorly sorted sand and gravel- to boulder-sized material; varied amounts of silt, clay, and till; glaciotectonic deformation is common, as are abrupt changes in grain size

░ **Till Deposits**
Coarse, unsorted diamicton and sometimes crudely stratified gravel and sand (ablation till); varied amounts of basal till; discontinuous and typically thicker in low-lying areas

PRE-QUATERNARY

░ **Undifferentiated Bedrock**
May contain patches of till, marine, and glaciofluvial debris; is glacially scoured and polished

X Bedrock outcrop

Abandoned glaciofluvial channel

Escarpment

Figure 4 *(cont'd)*. Surficial geology of the St. George map area (legend for map on facing page).

many regions of New Brunswick, basal till deposits in the St. George region are discontinuous, being the remnants of previously larger landforms that were eroded and reworked by late-stage glacial processes such as glaciomarine erosion. Basal till here generally ranges in thickness from 0.5 m to 1 m, but at some sites (mainly on the lee side of topographic highs) can reach about 5 m. Elsewhere, the unit forms a veneer measuring only a few decimetres.

The basal till unit comprises lodgment till and/or basal melt-out till. Typically, only a single member is present at a given locality. However, some exposures display basal melt-out till

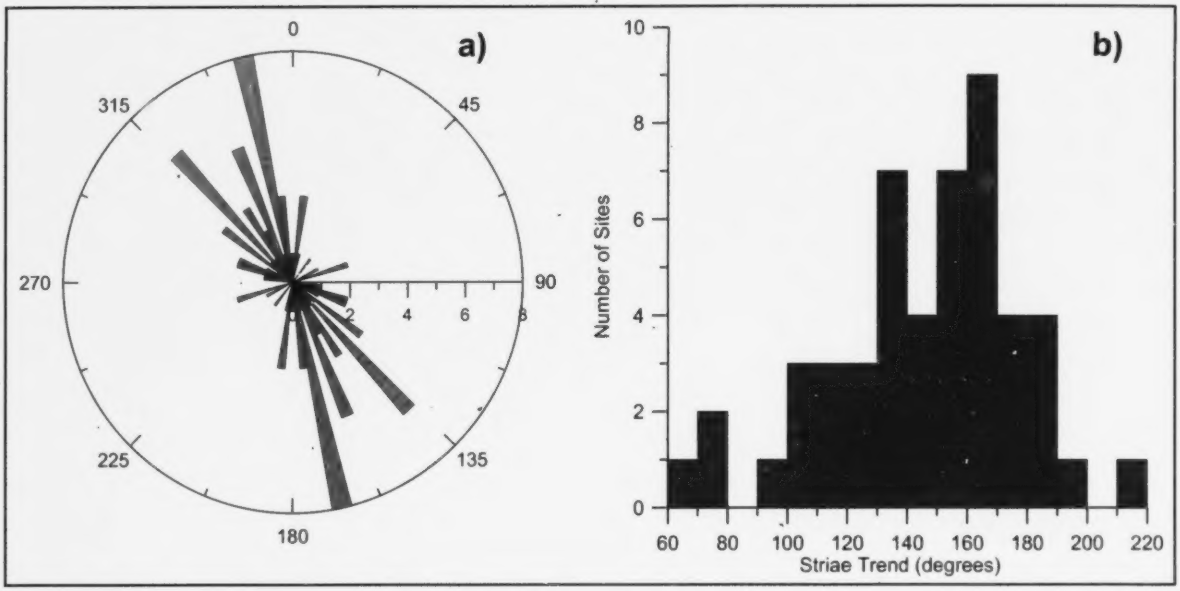

Figure 5. Diagrams showing glacial striae directions in the report area. The rose diagram (Figure 5a) indicates a bidirectional trend; the histogram (Figure 5b) displays frequency of the inferred trend.

grading downward into lodgment till. Basal till deposits commonly reflect the texture, lithology, and colour of local bedrock. Yellowish brown to olive-brown till with a sandy loam or loam texture is common. Stone content of the till varies from 30% to 60% (Pronk et al. 2004).

Grain-size analyses of 82 basal till samples demonstrated that the matrix component (< 2 mm fraction) averages 57.8% sand, 31.9% silt, and 10.3% clay (Pronk et al. 2004). Analysis of the clast component showed an average lithological composition of 39.9% intrusive clasts, 35.6% sedimentary clasts, 17.4% extrusive clasts, 6.2% metasedimentary clasts, and 0.9% other lithotypes (Pronk et al. 2004). In terms of aggregate application, basal till typically is used only as fill material. However, basal till with a substantial clay fraction is sufficiently impermeable to be suitable for liner or capping material.

Ablation Till Deposits (Late Wisconsinan)

Ablation till deposits consist of material that ranges from coarse, unsorted diamicton to crudely stratified gravel and sand. They occur extensively throughout the north-central and northwestern parts of the report area. As expected, texture of the ablation till here is substantially coarser and less compact than that of the basal till. Unit thickness varies markedly from a 10 cm veneer to at least 3 m. The terrain surface of some ablation till deposits is often hummocky and is characterized by small (1–3 m high) ridges with no preferred orientation.

Grain-size analyses of 25 ablation till samples showed that the matrix component averages 69.7% sand, 25.0% silt, and 5.3% clay (Pronk et al. 2004). As Rampton et al. (1984) observed, it is unclear whether the coarse texture is original or is secondary as a result of the fine material having been removed by meltwater action. An analysis of the clast component demonstrated a locally derived lithological composition averaging 58.1% intrusive clasts, 19.5% sedimentary clasts, 17.1% extrusive clasts, 4.8% metasedimentary clasts, and 0.5% other lithotypes (Pronk et al. 2004).

Ablation till does not undergo a high degree of abrasion during its glacial transport in the englacial and supraglacial debris load, nor during its deposition stage, which involves ice stagnation and little meltwater transport. This lack of abrasion allows unsound clasts to be preserved, and the minimal water transport results in a fairly high silt and clay content. Thus, the potential of ablation till for aggregate use is often limited by a large percentage of unsound clasts and a high concentration of fines.

Glaciofluvial Ice-Contact Stratified Drift Deposits (Late Wisconsinan)

Ice-contact stratified drift deposits are found throughout the report area (Fig. 4). They consist of well to poorly sorted sand and gravel- to boulder-sized material with varied amounts of silt, clay, and sometimes till inclusions. Glaciotectonic deformation is common in these sediments, as are abrupt changes in grain size. Both phenomena are the result of deposition on or adjacent to a glacier, and of the subsequent ice wasting. Geomorphologically, these deposits occur as end moraines, kames, or esker segments.

The St. George end moraine traverses the town of St. George and dams the south end of Lake Utopia. It is approximately 20 m thick (Gadd 1973) and represents the largest accumulation of ice-contact stratified drift *(sensu stricto)* in the report area. Kame deposits occur sporadically throughout the district and are often flanked by glaciofluvial outwash deposits.

Ice-contact stratified drift deposits are usually considered to have economic significance. They consist of material that was transported by water and thus are commonly purged of excess fine material and unsound clasts. Because the distance of meltwater transport is highly variable, however, some deposits may contain excessive fines. Eskers are usually excellent sources of clean gravel. Conversely, the varied grain-size distributions in kame and end moraine deposits mean that aggregate from these deposit types tends to be used for more low-end applications or requires beneficiation to upgrade quality.

Glaciofluvial Outwash Deposits (Late Wisconsinan)

Glaciofluvial outwash deposits occur extensively throughout the report area (Fig. 4) and vary significantly in composition from planar-bedded sand to massive, coarse-grained gravel sheets. Deposits typically are well sorted and stratified and occur as plains, fans, or channel infill. All facies associated with fluvial deposition can be expected (see Brodzikowski and Van Loon 1987). Thicknesses range from 1 m to more than 5 m.

Notable deposits of glaciofluvial outwash lie west of Lake Utopia and west of the community of Bonny River, in close association with Magaguadavic River. Extensive deposits also occur in the northeastern part of the map area flanking Jake Lee Mountain. South of Jake Lee Mountain, coarse, clast-supported gravels containing abundant cobbles and boulders have been observed with thicknesses greater than 3 m.

Small, isolated, and generally discontinuous deposits of glaciofluvial sediment are commonly found in coastal areas that otherwise are characterized by marine-wave-washed surfaces and bare rock. Glaciofluvial channels cut into underlying sediment or bedrock indicate Late Wisconsinan spillways. Glaciofluvial lag deposits typically occur in these abandoned channels.

Glaciofluvial outwash deposits are usually excellent sources of aggregate material, as they have undergone extensive meltwater transport prior to deposition, which results in winnowing of fines and comminution of unsound clasts. Various deposits throughout the map area have been exploited for quality aggregate material (see Finamore and Seaman 1988).

Undifferentiated Glaciolacustrine/Glaciomarine Deposits (Late Wisconsinan)

Undifferentiated (see below) glaciolacustrine/glaciomarine deposits occur in the northwestern corner of the report area in association with Digdeguash River, west of Lake Utopia, and north of Mill Lake (Fig. 4). Deposits flanking Digdeguash River consist of planar-bedded sand and silt, and type exposures can be seen along Highway 760 near Johnson Settlement. Deposits associated with the Mill Lake and Lake Utopia area comprise planar-bedded silt with minor clay, commonly interbedded with thin horizons of fine sand. South of Johnson Settlement, undifferentiated glaciolacustrine/glaciomarine sediment occurs as a veneer draped over ablation till.

Gadd (1968) originally mapped these deposits as glaciolacustrine. However, he subsequently (1973) designated them as moraine or glaciofluvial outwash, or incorporated them within his "marine basin deposits" unit. With respect to the latter interpretation, he noted that "[l]acustrine sediments of probably glacial origin have a very limited surface distribution in the vicinity of Lake Utopia and St. George" (Gadd 1973, p. 15) but presented no evidence to support a glaciolacustrine origin. On the adjacent map sheet (NTS 21 G/03), Thibault (1982) mapped related deposits as glaciomarine on the basis of their geomorphology and setting. Observations made during recent investigations (Allard 2007a) yielded no conclusive evidence to support classifying these deposits as either glaciomarine or glaciolacustrine. However, textural differences can be observed between deposits mapped as glaciolacustrine by Gadd (1968) and those mapped as glaciomarine.

Glaciomarine Beach and Basin Deposits (Late Wisconsinan)

Glaciomarine beach and basin deposits appear extensively along the coast and inland to a maximum elevation of approximately 85 m (Fig. 4). The 85 m contour roughly defines the maximum level of post-glacial submergence along this part of the Bay of Fundy.

Glaciomarine beach deposits in the report area consist of well sorted, medium- to coarse-grained sand and gravel with minor small cobbles. Inland beach ridges reflect past sea levels. Extensive beach deposits can be found in the New River district, where they cover an area that extends about 2 km inland from the coast, and south of the St. George moraine near the community of Utopia. Glaciomarine beach deposits are sometimes used as a source of granular aggregate. Deposits that presumably have been reworked from glaciofluvial outwash or ice-contact stratified drift are generally of good quality. However, the fact that most of these deposits occur in ecologically sensitive coastal areas limits their exploitability. Private pits have been established in glaciomarine beach deposits near the community of Upper Letang, south of St. George, and along Highway 1 east of the community of Bethel.

Glaciomarine basin deposits in the report area consist of massive to stratified clay and silt with minor sand. Extensive blankets of this material occur north of the community of Pocologan and south of the Pennfield–Utopia Delta Complex near Pennfield and Upper Letang. At the latter locale, sections up to 4 m thick have been documented. The approximate age of these deposits at Pocologan is ca. 12.5 ka B.P. (Seaman et al. 1993, p. 83).

Ice-dropped debris, ranging from small pebbles to large cobbles, is commonly found within basin deposits. In some cases, the large quantity of such debris gives the material an almost till-like appearance. One distinguishing feature is that the matrix of the glaciomarine diamicton is almost unimodal and lacks the range of grain sizes expected in till matrix. Some of these deposits were previously mapped as basal till (Gadd 1968, 1973) but have recently been reassigned to the glaciomarine facies (Allard 2007a).

Considerable wave-washing and marine erosion took place in coastal areas of the report area during Late Wisconsinan sea-level fluctuations. Often, wave-washing has eroded pre-existing deposits, leaving exposed bedrock or a veneer (< 1 m thick) of glaciomarine material of highly variable composition. This unit usually occurs as sandy silt infilling depressions along undulating bedrock surfaces. Ice-dropped material is commonly encountered, as are patches of reworked till veneer and glaciofluvial debris.

Glaciomarine Delta Deposits (Late Wisconsinan)

Major glaciomarine delta deposits are situated near the coast in the eastern half of the report area (Fig. 4), where they form blankets of sand, gravel, and cobbles 1 m to 35 m thick. The deposits typically take the form of a Gilbert-style delta with a well defined topset, foreset, and bottomset configuration. Topsets are up to 5 m thick and comprise outwash gravel, cobbles, and sand (Fig. 6). Foresets consist of bedded sand and fine gravel and were deposited in the subaqueous environment; bottomsets consist of silt and clay.

The largest of these glaciomarine delta deposits — the Pennfield–Utopia Delta Complex and the Pocologan Delta (Fig. 1, 7) — are spectacular landforms, occurring as extensive sand and gravel plains that stand as high as 89 m, well above current sea level. The Pennfield–Utopia deposit covers an area of about 39 km^2, while the Pocologan deposit spans nearly 40 km^2. Total thicknesses for these deposits have not yet been accurately determined, but stream incision in the Pocologan deposit has revealed depths exceeding 15 m. Preliminary geophysical data collected during the 2007 field season indicate thicknesses of up to 35 m.

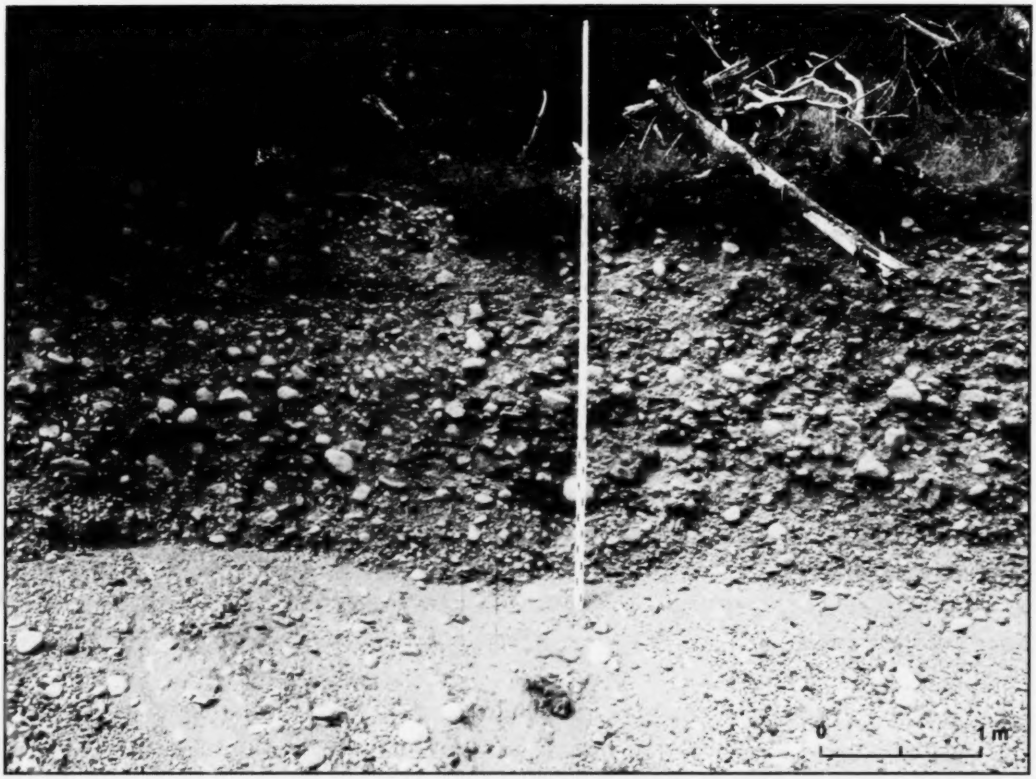

Figure 6. Exposed glaciomarine delta topsets from the southeastern district of the Utopia deposit (Pennfield–Utopia Delta Complex).

On the basis of 1) recent seismic studies conducted by the New Brunswick Department of Natural Resources (NBDNR) in partnership with the University of New Brunswick, 2) earlier seismic investigations (Chandra 1976), and 3) deposit morphology (see deposit descriptions below, under *Evolution of Pennfield–Utopia Delta* and *Evolution of Pocologan Delta*), it is reasonable to assume that many sections of the Pennfield–Utopia and Pocologan deposits exceed 10 m thick. By implication, these sand and gravel deposits represent a tremendous potential source of unconsolidated granular aggregate materials.

To obtain more comprehensive data on the quantity and quality of aggregate resources in the deposits, the author recently conducted a program of sample collection, testing, and analysis of Crown land aggregate resources on and near the two delta deposits. Results of the tests and analyses are detailed in Allard (2007a) and are summarized below.

Geotechnical Tests and Petrographic Analyses
In 2005 the author collected granular aggregate bulk samples from 30 sites on Crown land in the St. George map area, concentrating on areas with presumed high potential for quality aggregate (Allard 2007a). Twenty samples were collected from the Pocologan Delta, four samples were collected from the Pennfield–Utopia Delta Complex, and six samples were collected from glaciofluvial outwash or ice-contact stratified drift deposits adjacent to the delta deposits (Fig. 7). Each bulk sample consisted of approximately 40 kg of unsorted aggregate with a maximum clast size of 7.5 cm.

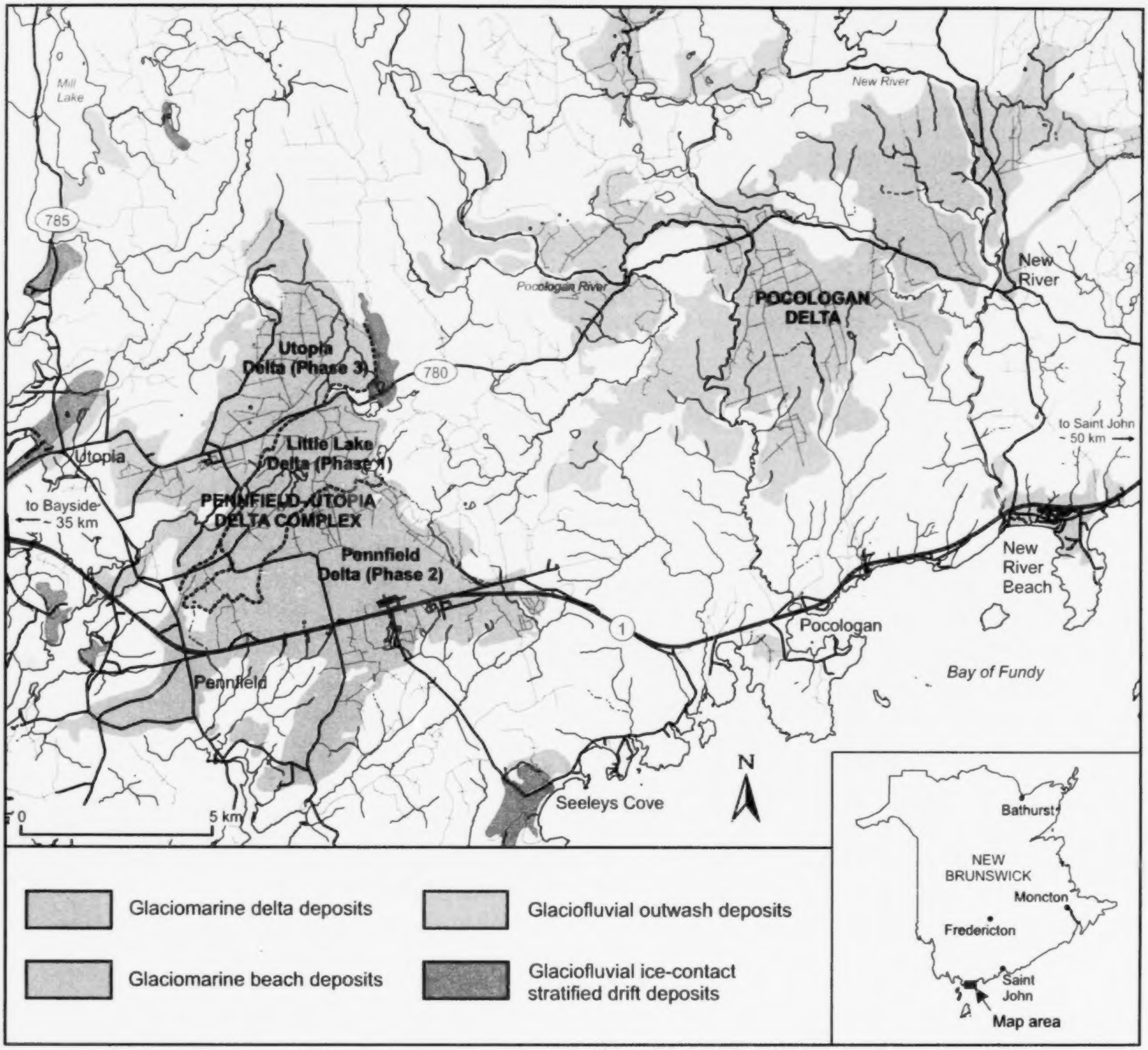
Mill Lake
New River
785
Pocologan River
POCOLOGAN DELTA
New River
Utopia Delta (Phase 3)
780
Little Lake Delta (Phase 1)
Utopia
to Saint John ~ 50 km
to Bayside ~ 35 km
PENNFIELD-UTOPIA DELTA COMPLEX
Pennfield Delta (Phase 2)
New River Beach
1
Pocologan
Bay of Fundy
Pennfield
N
Seeleys Cove
0
5 km
Glaciomarine delta deposits
Glaciofluvial outwash deposits
Glaciomarine beach deposits
Glaciofluvial ice-contact stratified drift deposits
Bathurst
NEW BRUNSWICK
Moncton
Fredericton
Saint John
Map area

Figure 7. Major aggregate deposits in the St. George map area, showing location of the Pennfield–Utopia Delta Complex and Pocologan Delta.

Selected samples from or near the two delta deposits were subjected to various geotechnical tests and analyses pertinent to current industry specifications (Table 1, 2). In general, the test results demonstrated that aggregate from both deposits potentially could satisfy the requirements for high-end applications such as Portland cement concrete and bituminous concrete. As well, preliminary geotechnical testing of the fine aggregate fraction indicated that material from some locations may be suitable for concrete or road sand (Table 2).

One of the geotechnical tests, the Accelerated Mortar Bar (AMB) test (see Note 1 in Table 3), was performed on a representative sample from each deposit to assess the potential for deleterious alkali-aggregate reactivity in concrete applications (see Note 2 in Table 3). The

Table 1. Geotechnical test results for coarse aggregate samples from the St. George map area, New Brunswick. Tests were conducted by Gemtec Limited of Fredericton, New Brunswick.

Sample No.	Finer Than 75 µm % ASTM C117	Low-Density Particles % ASTM C123	Mg Sulphate Soundness % Loss ASTM C88	Micro-Deval % Loss MTO LS-618	Los Angeles Abrasion % Loss ASTM C131	Unconfined Freeze-Thaw % Loss MTO LS-614	Relative Density Dry g/cm^3 ASTM C127	Relative Density (SSD) g/cm^3 ASTM C127	Absorption % ASTM C127
SA01	1.1	0.29	0.64	6.5	26.2	0.98	2.597	2.622	0.98
SA02	0.6	0.06	0.93	9.8	24.0	0.58	2.593	2.619	1.03
SA04	1.1	0.05	1.23	7.0	na	2.56	2.635	2.664	1.11
SA06	0.7	0.21	0.80	5.9	na	1.06	2.588	2.614	1.02
SA07	1.0	0.09	0.87	7.0	25.8	0.90	2.594	2.621	1.03
SA08	0.9	0.19	0.81	6.1	23.7	2.09	2.585	2.612	1.03
SA09	0.8	0.03	0.73	6.7	na	1.11	2.588	2.613	0.95
SA10	1.9	0.24	0.99	8.5	24.4	1.47	2.588	2.616	1.08
SA13	3.0	0.10	1.12	6.9	27.8	1.12	2.565	2.594	1.13
SA14	0.9	0.11	1.91	9.2	20.7	1.89	2.645	2.671	1.00
SA16	2.5	0.04	1.68	7.6	25.3	1.26	2.638	2.661	0.87
SA17	1.2	0.00	1.62	8.8	na	1.56	2.615	2.642	1.04
SA18	1.0	0.23	0.71	7.6	25.6	0.93	2.592	2.621	1.14
SA19	0.8	0.04	0.70	5.4	22.2	1.89	2.597	2.620	0.91
SA24	1.2	0.15	0.80	5.8	25.2	0.88	2.583	2.603	0.97
SA26	4.2	0.11	2.26	8.2	24.8	0.98	2.592	2.620	1.07
SA27	1.2	0.17	0.78	6.0	26.0	1.15	2.584	2.609	0.97
Mean	1.42	0.12	1.09	7.24	24.75	1.32	2.599	2.62	1.02
Minimum	0.6	0.0	0.6	5.4	20.7	0.6	2.565	2.6	0.9
Maximum	4.2	0.3	2.3	9.8	27.8	2.6	2.645	2.7	1.1

Table 2. Geotechnical test results for fine aggregate samples from the St. George map area, New Brunswick. Tests were conducted by Gemtec Limited of Fredericton, New Brunswick.

Sample No.	Low-Density Particles % ASTM C123	Mg Sulphate Soundness % Loss ASTM C88	Micro-Deval % Loss MTO LS-619	Relative Density (Dry) g/cm^3 ASTM C127	Relative Density (SSD) g/cm^3 ASTM C127	Absorption % ASTM C127
SA01	0.01	2.25	9.6	2.511	2.568	2.18
SA06	0.11	1.36	9.9	2.539	2.575	1.42
SA07	0.06	3.08	11.0	2.534	2.578	1.73
SA13	0.08	2.53	13.6	2.482	2.633	2.06
SA17	0.05	2.8	10.0	2.550	2.590	1.22
Mean	0.062	2.404	10.82	2.5232	2.5888	1.722
Minimum	0.01	1.36	9.6	2.482	2.568	1.22
Maximum	0.11	3.08	13.6	2.55	2.633	2.18

ASTM = American Society for Testing and Materials
MTO = Ministry of Transportation of Ontario

two samples yielded expansions of greater than 0.20% at 16 days (Table 3). American Society for Testing and Materials (ASTM) specifications (ASTM 2003) state that expansions exceeding 0.20% at 16 days may indicate deleterious expansion and that further testing or field performance records would be required to confirm the result. Moreover, DeMerchant et al. (2000) demonstrated that AMB test results are not consistently reliable, particularly when applied to granular aggregate deposits from New Brunswick. Thus, additional testing should be conducted to verify that expansion actually resulted from excessive alkali-silica reaction.

Table 3. Alkali-aggregate reactivity test results (ASTM C1260) for granular aggregate from the St. George map area, New Brunswick. Tests were conducted by Gemtec Limited of Fredericton.

Sample No. SA14: from the Pennfield–Utopia deposit							
Age (days)	**Reading 1**	**Reading 2**	**Reading 3**	**% Elong. 1**	**% Elong. 2**	**% Elong. 3**	**Mean Elong. %**
0	0.2440	1.8850	0.1260	0.0000	0.0000	0.0000	0.0000
4	0.2530	1.8960	0.1370	0.0035	0.0043	0.0043	0.0041
7	0.4430	2.0910	0.3250	0.0783	0.0811	0.0783	0.0793
12	0.8640	2.5070	0.7220	0.2441	0.2449	0.2346	0.2412
14	0.9950	2.6380	0.8470	0.2957	0.2965	0.2839	0.2920
21	1.3530	2.9930	1.2050	0.4366	0.4362	0.4248	0.4325
28	1.5720	3.2040	1.1460	0.5226	0.5193	0.5079	0.5167
Sample No. SA18: from the Pocologan deposit							
Age (days)	**Reading 1**	**Reading 2**	**Reading 3**	**% Elong. 1**	**% Elong. 2**	**% Elong. 3**	**Mean Elong. %**
0	-0.1900	0.1480	-0.3460	0.0000	0.0000	0.0000	0.0000
4	-0.1840	0.1510	-0.3270	0.0024	0.0012	0.0075	0.0037
7	-0.0530	0.2810	-0.1970	0.0539	0.0524	0.0587	0.0550
12	0.2220	0.5470	0.0630	0.1622	0.1571	0.1610	0.1601
14	0.3150	0.6460	0.1530	0.1988	0.1961	0.1965	0.1971
21	0.6120	0.9420	0.4540	0.3157	0.3126	0.3150	0.3144
28	0.7910	1.1250	0.6290	0.3862	0.3846	0.3839	0.3849

Notes: 1. The Accelerated Mortar Bar test is a quick screening method used to help predict whether aggregate for use in concrete applications is susceptible to deleterious internal expansion caused by excessive alkali-silica reaction (ASTM 2003). **2**. Alkali-aggregate reactivity is a chemical reaction between cryptocrystalline quartz (commonly found in fine-grained highly siliceous rock types) in the aggregate clasts, and hydroxyl ions associated with alkalis in the cement. The reaction product is a gel that absorbs water, causing concrete to expand and crack.

The 2005 sampling program of Allard (2007a) also involved collecting a pebble sample from 24 of the 30 sites to use for petrographic analysis. Analyses showed that the pebble samples average 89% clasts with good to excellent soundness, 9% clasts with fair soundness, 2.5% clasts with poor soundness, and less than 0.3% clasts with deleterious indicators. Petrographic numbers for the 24 pebble samples range from 103 to 174, giving a mean value of 132, which is well within industry specifications (Table 4).

Lithological composition of the pebble samples averages 61.5% plutonic clasts, 17% metasedimentary clasts, 11.5% volcanic clasts, 9% sedimentary clasts, and 1% other

Table 4. Clast soundness and petrographic numbers of pebble samples from granular aggregate in the St. George map area, New Brunswick. Analyses and calculations were performed by NBDNR.

Sample No.	% Good	% Fair	% Poor	% Deleterious	Petrographic No. (after MTO LS-609)
SA01	73.42	20.04	6.54	0.00	173
SA02	93.78	2.45	3.77	0.00	124
SA03	93.32	5.99	0.68	0.00	115
SA04	98.92	0.56	0.51	0.00	104
SA05	88.27	6.18	5.55	0.00	140
SA06	95.14	4.86	0.00	0.00	110
SA07	92.02	6.42	1.57	0.00	121
SA08	94.67	5.33	0.00	0.00	111
SA09	90.71	7.03	2.26	0.00	125
SA10	81.43	15.40	3.17	0.00	147
SA12	93.60	4.85	1.55	0.00	117
SA13	94.00	6.00	0.00	0.00	112
SA14	87.50	12.03	0.47	0.00	126
SA15	74.24	21.12	4.64	0.00	165
SA16	66.72	30.74	2.54	0.00	174
SA17	89.99	10.01	0.00	0.00	120
SA18	95.55	3.69	0.76	0.00	111
SA19	96.06	3.84	0.00	0.10	109
SA20	94.91	2.92	2.13	0.04	117
SA22	83.54	10.14	5.72	0.61	154
SA24	85.57	8.17	0.00	6.26	173
SA25	84.57	7.80	7.63	0.00	154
SA29	98.67	1.33	0.00	0.00	103
SA30	81.90	9.08	9.02	0.00	163
Mean	88.69	8.58	2.44	0.29	**132**
Minimum	66.72	0.56	0.00	0.00	**103**
Maximum	98.92	30.74	9.02	6.26	**174**

Note: A petrographic number (PN) below 180 indicates potential suitability for use in concrete, whereas a higher PN indicates poorer quality material (Canadian Standards Association 2004).

lithotypes. Prevalent plutonic lithotypes include granite, granitic porphyry, and granodiorite, with some gabbro and diabase. Dominant volcanic lithotypes include rhyolite, porphyritic rhyolite, and dacite, with some andesite and basalt. Primary bedrock sources of these clasts are the Saint George Plutonic Suite, Mascarene Group, New River Plutonic Suite, and Ellsworth Group (Fig. 3; NBDNR 2007). A small percentage of gravel clasts, mainly those that are well rounded and resistant, are interpreted to have derived from more distal bedrock sources in southwestern and west-central New Brunswick, and in adjacent Maine.

Opportunities to develop granular aggregate from the Pennfield–Utopia Delta Complex are restricted, given that only 15% of the deposit occurs on Crown land. The Pocologan Delta offers greater development potential, as approximately 66% of the deposit is situated on Crown land. Recent estimates indicate that more than 80% of the Pocologan deposit comprises sand and very fine- to fine-grained gravel; the remainder consists of coarse gravel and cobbles (Allard 2007a). Thick foreset beds of stratified sand and fine gravel with development potential occur throughout the Pocologan deposit, especially in lobes extending from the southern margin.

Coarse gravel and cobbles have been observed in thicknesses exceeding 4 m at numerous sites throughout the deposit, and coarse aggregate development opportunities exist in the northeastern and central districts. However, it is difficult to predict where areas of coarse gravel occur. Geophysical methods or extensive boring/excavation work would be required to accurately map thicknesses of the topset unit containing the coarse aggregate material.

Holocene

Colluvial Deposits

Colluvial debris consists of weathered/fractured bedrock or reworked glacial deposits affected by slope processes, and it is commonly found in elevated areas. Escarpments shown in Figure 4 indicate slopes with a grade exceeding 20%; such areas are especially susceptible to mass-wasting events.

Organic Deposits and Wetlands

Organic deposits composed primarily of peat and muck up to 5 m thick occur consistently in poorly drained topographic depressions across the report area (Fig. 4). Thibault (1992) described several organic deposits in the southeastern district. The most significant bogs (> 1 m thick) are shown in Figure 4. They lie proximal to the Pocologan deposit, along the Little Pocologan Stream, and locally near southern extremities of the Pocologan deposit. These bogs are 2 m to 4 m thick, ombrotrophic, and consist primarily of sphagnum peat. Fens and emergent wetlands with less organic deposition (< 1 m thick) are not shown in Figure 4, but are delineated on the St. George surficial geology map (Allard 2007b).

Alluvial Deposits

An extensive blanket of alluvium borders southern reaches of Magaguadavic River from the community of Second Falls to St. George (Fig. 4). The unit is up to 1 km wide and consists of sand, gravel, and minor silt or clay. These terrace and floodplain deposits are generally stratified and moderately sorted, and sometimes are overlain by a thin colluvial veneer or organic deposits. Unlike the silty alluvium usually found along lower courses of lowland streams approaching sea level, alluvium along this section is fairly coarse, due to the reworking of previously deposited glaciofluvial outwash deposits. Magaguadavic River and its alluvial plain bisect a 5 km wide blanket of glaciofluvial outwash that extends from west of Dawson Mountain to Lake Utopia. Minor alluvial deposits large enough to map at the 1:50 000 scale also appear here along southern reaches of Bocabec River and New River.

Alluvial deposits are sometimes used as aggregate sources. However, their proximity to watercourses and typical association with high water tables often impede any development of large-scale aggregate operations.

GLACIAL HISTORY WITH PARTICULAR REFERENCE TO GLACIOMARINE DELTAS

No evidence of pre-Wisconsinan glaciation has been documented in the St. George map area, although the district presumably was glaciated numerous times during the geological past. Effects of Wisconsinan glaciation thus appear to have been sufficient to completely obliterate earlier surficial deposits.

Wisconsinan Glaciation

During the Early–Middle Wisconsinan Caledonia Phase of glaciation (Rampton et al. 1984; Seaman 2004), the report area was blanketed with an ice sheet that emanated from western and northern Maine and extended over the Bay of Fundy into Nova Scotia (Stea et al. 1998). The Caledonia Phase (Table 5) is interpreted to comprise an Early Wisconsinan (ca. 100–50 ka B.P.) east-southeast erosional period, followed by a Middle Wisconsinan (ca. 50–20 ka B.P.) southeasterly depositional flow event (Rampton et al. 1984; Stea et al. 1998; Seaman 2004). Major erosional events occurred during this phase, and a basal till layer was deposited.

After its initial deposition, the single till unit underwent extensive reworking during a series of Late Wisconsinan ice-flow phases (Stea and Finck 2001; Allard and Pronk 2003; Seaman 2003). These phases (Fig. 8; Table 5) represent shifts in outflow orientation within a regional ice sheet, rather than multiple advances and retreats by local ice domes (Seaman 2004). Just northwest of the report area, for instance, Allard (2003) interpreted some till dispersal patterns and palimpsest landforms as being related to a Late Wisconsinan ice-flow event that followed the south-southwest Chignecto Phase flow trajectory.

Table 5. Wisconsinan ice-flow chronology for southwestern New Brunswick, depicting an interpretation of ice-flow chronology in the region. Data are based on striae crosscutting relationships and limited stratigraphy (Seaman 2004; Seaman, pers. comm. 2006).

Reference No. in Figure 8	Phase	Flow Trajectory	Inferred Age
11	Pollett River	55°–70°	Late Wisconsinan
10	Kent	70°–90°	Late Wisconsinan
9	Tuadook–Renous	90°–100°	Late Wisconsinan
8	Passamaquoddy	100°–135°	Late Wisconsinan
7	St. Martins	185°–195°	Late Wisconsinan
6	Port Elgin	220°–240°	Late Wisconsinan
5	Chignecto	205°–220°	Late Wisconsinan
4	Tantramar–Norton–Oromocto	175°–185°	Late Wisconsinan
3	Woodstock	155°–175°	Late Wisconsinan
2	Late Caledonia	135°–155°	Middle Wisconsinan
1	Early Caledonia	110°–120°	Early Wisconsinan

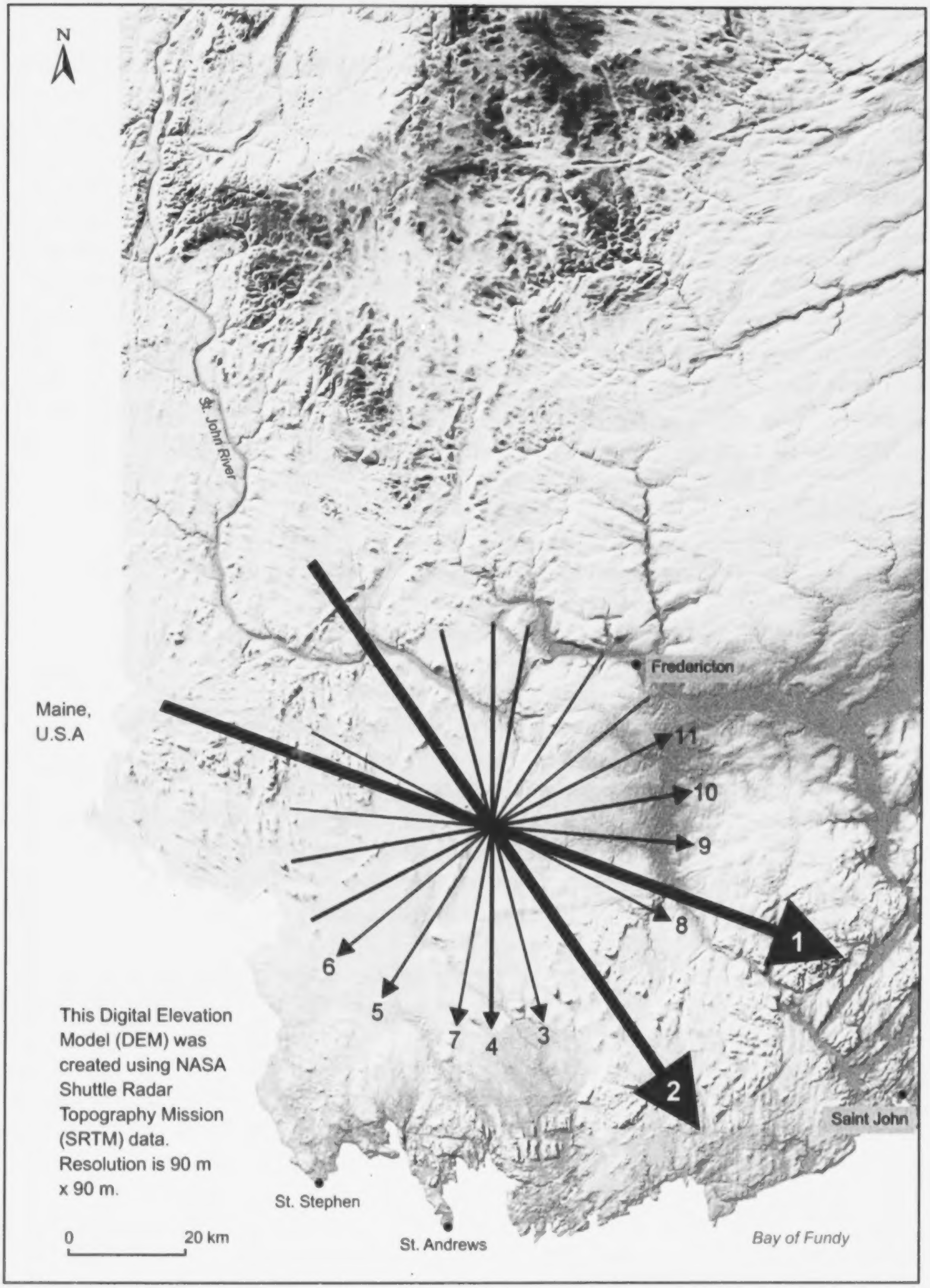
N
St. John River
Maine,
U.S.A
Fredericton
11
10
9
8
1
2
3
4
7
5
6
This Digital Elevation Model (DEM) was created using NASA Shuttle Radar Topography Mission (SRTM) data. Resolution is 90 m x 90 m.
Saint John
St. Stephen
St. Andrews
Bay of Fundy
0
20 km

Figure 8. Wisconsinan ice-flow trajectories across southwestern New Brunswick, depicting an interpretation of ice-flow chronology in the region. Data are based on striae crosscutting relationships and limited stratigraphy (Seaman 2004; Seaman, pers. comm. 2006). Numbers 1 to 11 refer to reference numbers in Table 5.

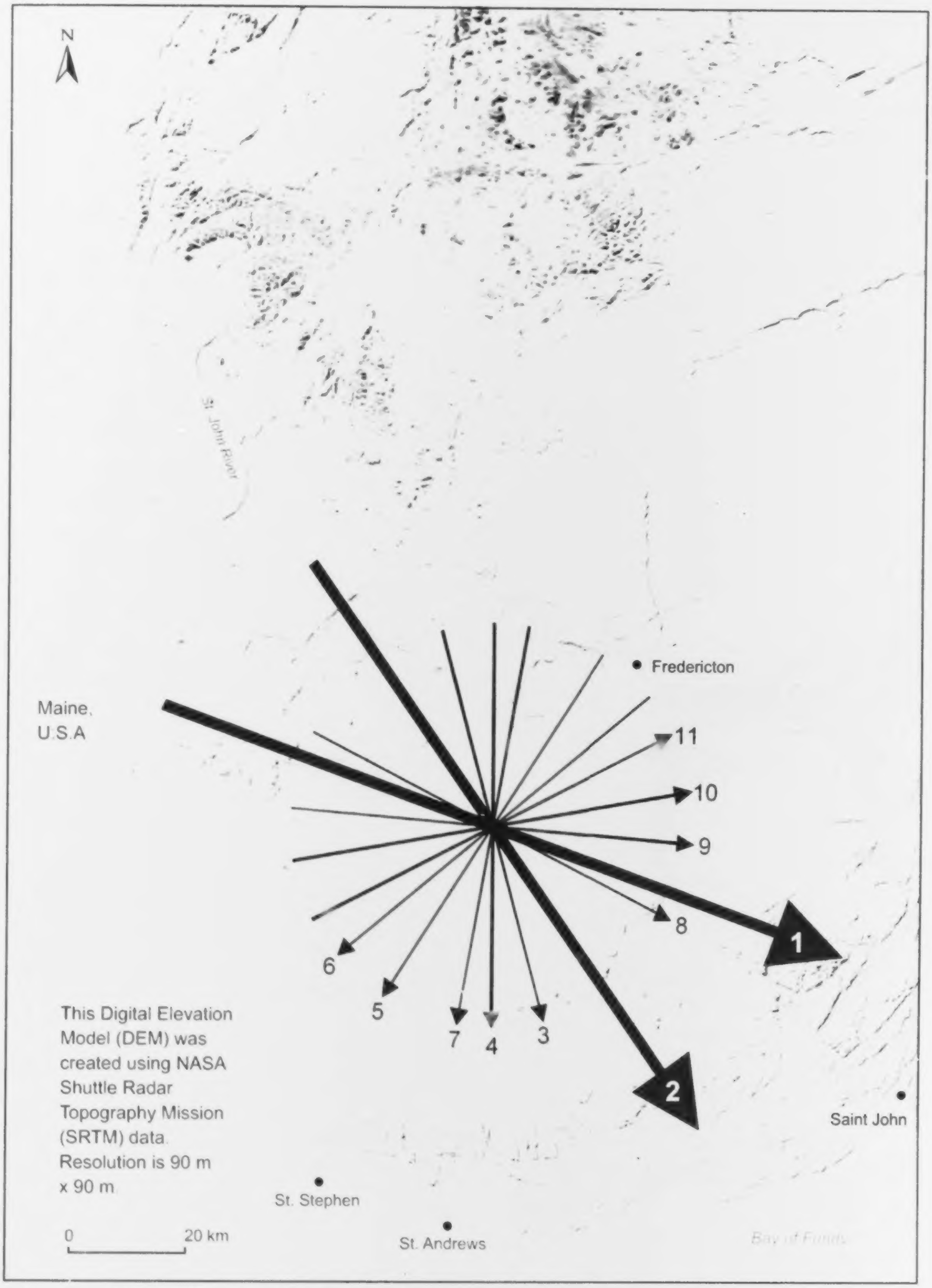
N
St. John River
Fredericton
Maine,
U.S.A
11
10
9
8
1
6
5
7
4
3
2
This Digital Elevation Model (DEM) was created using NASA Shuttle Radar Topography Mission (SRTM) data. Resolution is 90 m x 90 m.
Saint John
St. Stephen
0
20 km
St. Andrews
Bay of Fundy

Figure 8. Wisconsinan ice-flow trajectories across southwestern New Brunswick, depicting an interpretation of ice-flow chronology in the region. Data are based on striae crosscutting relationships and limited stratigraphy (Seaman 2004; Seaman, pers. comm. 2006). Numbers 1 to 11 refer to reference numbers in Table 5.

Unlike the Early–Middle Wisconsinan Caledonia Phase, the Late Wisconsinan ice-flow phases were fairly "weak." They added striae to exposed bedrock surfaces but did not produce new till deposits. Instead, these variations in outflow orientation (phases) caused physical properties of pre-existing till to be altered through increased homogenization, minor redistribution of till components, and re-alignment of clast fabric. The resulting deposit is a hybrid till with characteristics inherited from the multiple phases within one glacial episode (Allard and Pronk 2003; Seaman 2003). The complex erosional landforms and striae patterns observed in the report area and elsewhere throughout southwestern New Brunswick record these Late Wisconsinan dynamics and attest to the high degree of glacial complexity (Seaman 2004).

Late Wisconsinan Deglaciation

It is not known precisely when deglaciation began in coastal areas in southwestern New Brunswick. A radiocarbon date on marine shells (*Hiatella arctica*) collected from a diamicton overlain by marine sediments and underlain by glaciofluvial sediments just east of the report area (Rampton et al. 1984) suggests that deglaciation started here ca. 13.9 ka B.P. (see Table 2 of Rampton et al. 1984). However, deglaciation more likely began earlier, following development of a calving bay in the Bay of Fundy. The oldest reported radiocarbon date indicating Late Wisconsinan coastal submergence in southwestern New Brunswick is 14.4 ka B.P. (Lowdon and Blake 1979; Rampton and Paradis 1981).

Deglaciation proceeded through ice stagnation and downwasting (Seaman 2004), not by ice-marginal retreat, as was originally proposed by Gadd (1973) and expanded on by Rampton et al. (1984). As downwasting took place across the report area, ablation till melted out of the englacial and supraglacial sediment load and was deposited more or less in situ. The widespread but presumably thin blanket of ablation till situated east of Lake Utopia and between the Pennfield–Utopia and Pocologan deposits (Fig. 4) locally exhibits characteristics common to ice-contact stratified drift deposits. However, the unit more likely represents a gradation between ice-contact and ablation material, having undergone varied degrees of meltwater interaction.

The term "disintegration moraine" has been used (Gauthier 1982) to describe similar deposits observed elsewhere in New Brunswick. Rampton et al. (1984) suggested that such features signified the gradual downwasting of ice blocks severed from the source glacier in the final stages of decay. Indeed, decaying remnant ice could have occupied the Musquash Lowlands east of Lake Utopia (Fig. 2) during Late Wisconsinan deglaciation. With increasing downwasting, a substantial ice block could have been separated from the source glacier through excessive ice thinning over the Bocabec Hills immediately to the north (Fig. 2). If such an event took place, however, ablation till deposition would have occurred before the Late Wisconsinan coastal submergence around 14 ka B.P.; otherwise, seawater would have inundated the area and floated the remnant ice mass.

Ice withdrawal from coastal zones during the Late Wisconsinan was likely enhanced by drawdown effects of the (by then) largely ice-free Bay of Fundy. The withdrawal caused seawater to inundate coastal regions to a maximum elevation of 85 m above sea level, after which the rate of isostatic uplift began to exceed the rate of eustatic sea level rise, leading to net land emergence (see below).

Throughout the period of land submergence and re-emergence, and as Late Wisconsinan climate warming and downwasting continued, a widespread subglacial/englacial meltwater network known as the Pennfield–Pocologan glacial drainage system (Allard 2007c) developed in the ice mass across southwestern New Brunswick (Fig. 1). The system flushed huge volumes of sediment continuously from the glacier toward the Bay of Fundy, and it was this sedimentary material that gave rise to the massive Pennfield–Utopia and Pocologan glaciomarine deposits (Fig. 1, 7).

Evolution of Pennfield–Utopia Delta Complex

The Pennfield–Utopia Delta Complex refers collectively to the Little Lake, Pennfield, and Utopia deltas or deposits (Fig. 7). The deposits represent three distinct deltaic phases that record the gradually falling sea levels following the Late Wisconsinan marine submergence.

Little Lake Deposit (Phase 1)

The first delta to form in this environment was the Little Lake deposit. It exhibits a heavily kettled terrain surface with an average elevation of about 89 m. Many kettles reach depths of 10 m or more, and some contain small lakes. Although organic material at the base of the Little Lake deposit was dated at 16.5 ka years B.P. (Mott 1975), the date was considered invalid (anomalously old) after being compared with pollen profiles from similar sites in southwestern New Brunswick.

The unusual appearance of the Little Lake deposit has led to differing interpretations of its origin. It has been variously designated as an outwash deposit by Gadd (1973), an ice-contact stratified drift deposit by Finamore (1977), and a glaciomarine delta by Stea et al. (1987). Poor exposure of the deposit impedes verification of the actual mode of deposition. However, deposit morphology and setting suggest that it likely originated as a grounding-line fan (subaqueous fan) during the Late Wisconsinan glacial retreat when glacial ice was in direct contact with the Bay of Fundy. Meltwater exited the ice mass directly into deep water through englacial and subglacial tunnels, resulting in rapid deposition of sediment load. With ice and sea maintaining a steady state for a considerable time, sediment levels aggraded to the water level, and an ice-contact delta formed.

The abundant kettle holes mark subaerial deposition of ice blocks proximal to the ice margin and provide evidence for the formation of an ice-contact delta. Internal structure of the deposit presumably conforms somewhat with that of a Gilbert-type delta, although the deposit likely has been deformed by faulting and collapse following ice melting. Under this scenario, the contact between topsets and foresets in the deposit would define the maximum level of marine submergence during the Late Wisconsinan. Although the contact cannot be observed, topset thickness for the deposit is assumed to be about 4 m, similar to that of adjacent glaciomarine deltas. This interpretation would suggest a maximum Late Wisconsinan marine submergence of about 85 m above sea level along this part of the Bay of Fundy.

Pennfield Deposit (Phase 2)

With continued ice retreat and wasting during Late Wisconsinan global warming, the rate of isostatic uplift began to exceed the rate of eustatic sea level rise, resulting in net land emergence. Scott et al. (1987) postulated that the shift took place ca. 14 ka B.P. The differential led to development of the Pennfield Delta just south of the Little Lake Delta. The contact between these two deltas is marked by a gradual transition in elevation and a dramatic reduction in kettle landforms. The Little Lake and Pennfield deposits thus can be considered as one evolving delta, although, in terms of delta genesis, it is useful to discuss each as a separate deltaic phase.

The Pennfield Delta forms a roughly triangular fan ranging in elevation from 60 m near the southern toe to more than 80 m at its northern margin. Pits in the deposit expose a classic Gilbert-type delta sequence. Topsets locally reach 3 m to 4 m thick and comprise coarse gravel, sand, and cobbles of glaciofluvial origin. Topsets may have been substantially reworked near the delta toe. Shells collected from the delta toe (Gadd 1973) returned an uncorrected radiocarbon date of about 13 ka B.P. Seaman et al. (1993) describe surface planation of the delta's southwestern arm by wave action. A 5 m high scarp in this area provides evidence of a coastal erosion period (Stea et al. 1987; Seaman et al. 1993), possibly coeval with the later deltaic phase that gave rise to the Utopia Delta.

Utopia Deposit (Phase 3)

Falling sea levels and continued glacial retreat resulted in formation of the Utopia Delta adjacent to, but in the rear of, the Little Lake Delta. The extremely flat terrain of the Utopia Delta surface ranges from 67 m to 73 m above sea level, and kettle holes are strewn sporadically across the deposit. Like the Pennfield deposit, the Utopia deposit exhibits a classic Gilbert-type delta structure. Topsets of very coarse, cobble-rich outwash gravels are up to 4 m thick at some localities. Foresets generally dip steeply toward the coast and comprise bedded sand and fine gravel.

Evolution of Pocologan Delta

The Pocologan Delta was the last large-scale, glacier-fed delta to form along the Bay of Fundy coast in the report area. The deposit ranges in elevation from 50 m to 70 m and exhibits a typical Gilbert-type configuration. The topset unit essentially represents a subaerial outwash deposit and varies greatly in thickness and composition across the deposit. In the northwestern and central districts, topsets consist of coarse gravel containing abundant cobbles with minor sand. The eastern district is characterized by thinner topsets with compositions that range from fine- to medium-grained sandy gravel to gravelly sand. Lobes extending from the southern margin of the deposit generally have little topset material, although some hand-dug excavations reveal thin topset units consisting of fine- to medium-grained gravel and sand. Overall, topset material becomes finer toward the south and east.

In addition to the foregoing larger scale trends, localized fluctuations in topset composition also occur. As is common in deposits of fluvial origin, a variety of sedimentary facies can be observed. Scour and channel-fill deposition, overbank deposition, lag deposition, and fluctuations in flow intensity — all characteristics of bifurcating streams — have given rise to a range of sedimentary structures.

Foreset units of the Pocologan deposit typically comprise gravelly sand or sand, and they slope toward the delta toe farther south. Stream incision of thick foreset beds along the southern deposit margin has formed several distinct lobes. The lobes are composed almost entirely of clean sand with minor gravel and are up to 30 m thick. As mentioned earlier, they have excellent development potential as a high-quality sand resource.

CONCLUSIONS

- The complex surficial geology of the St. George map area is largely the result of Early–Middle Wisconsinan glacial erosion and deposition, reworking of till deposits by Late Wisconsinan regional ice-flow events, and Late Wisconsinan deglaciation through downwasting. Land submergence followed by emergence during the Late Wisconsinan added to this complex scenario by facilitating marine erosion, deposition, and reworking of deposits in coastal areas.
- Morphology of the large, multiphase glaciomarine deltas in the report area (the Pennfield–Utopia and Pocologan deposits) indicates that their deposition took place during a period of net land emergence caused by post-glacial isostatic rebound. Holocene deposits in the region include accumulated colluvial and organic material, as well as alluvial deposits caused by extreme downcutting and channel meandering.
- Recent investigations in the report area (Allard 2007a, 2007b) provide new information pertinent to assessing the area's granular aggregate potential. The recent reports describe and map the Utopia–Pennfield and Pocologan deposits, concluding that the deposits represent a massive, high-quality resource of granular aggregate materials. The two deposits are currently under-exploited and potentially could support valuable extraction operations close to tidewater for domestic and export aggregate markets.
- Results of geotechnical testing show that coarse aggregate from the Utopia–Pennfield and Pocologan deposits may be suitable for Portland cement concrete or bituminous concrete production. However, additional work would be required to locate areas with sufficient volumes of coarse aggregate to warrant large-scale development. Portions of these deposits, especially the southern portion of the Pocologan Delta, also represent a tremendous resource of fine aggregate (sand) that may be suitable for concrete or road sand applications.

ACKNOWLEDGEMENTS

The author recognizes Jillian Craig, Holly Stewart, and Will Gilmore for their considerable assistance with fieldwork. Will Gilmore conducted petrographic analysis of all aggregate samples. Discussions with Allen Seaman provided insight into the glacial history of southwestern New Brunswick. Tim Webb, Allen Seaman, and Rex Boldon aided the author with field logistics.

REFERENCES

Allard, S. 2003. Geochemistry, lithology and depositional history of the Rollingdam map area till (21 G/06), southwestern New Brunswick. New Brunswick Department of Natural Resources and Energy; Minerals and Energy Division, Open File 2003-2, 218 p.

Allard, S. 2007a. Granular aggregate resources and surficial geology of the St. George map area (NTS 21 G/02), southwestern New Brunswick. New Brunswick Department of Natural Resources; Minerals, Policy and Planning Division, Mineral Resource Report 2007-2, 74 p.

Allard, S. 2007b. Surficial geology of the St. George map area (NTS 21 G/02), Charlotte County. New Brunswick Department of Natural Resources; Minerals, Policy and Planning Division, Plate 2007-10.

Allard, S. 2007c. Geotechnical and petrographic data for granular aggregate samples from the Pokiok Esker, Canterbury map area (NTS 21G/14), west-central New Brunswick. New Brunswick Department of Natural Resources; Minerals, Policy and Planning Division, Open File 2007-7, 90 p.

Allard, S., and Pronk, A.G. 2003. Glacial history of southwestern New Brunswick: challenges to drift prospecting. *In* Current Research 2002. *Edited by* B.M.W. Carroll. New Brunswick Department of Natural Resources; Minerals, Policy and Planning Division, Mineral Resource Report 2003-4, p. 1–11.

American Society for Testing and Materials (ASTM). 2003. Standard specification for concrete aggregates (C33-03). Publication by ASTM International. URL < http://www.astm.org >

Barr S.M., and White, C.E. 2001a. Bedrock geology 21 G/2b, part of 21 G/2c and g, Seeleys Cove area, Charlotte County. New Brunswick Department of Natural Resources and Energy; Minerals and Energy Division, Plate 2001-34.

Barr S.M., and White, C.E. 2001b. Bedrock geology 21 G/2h, part of 21 G/2a, New River Beach area, Charlotte County. New Brunswick Department of Natural Resources and Energy; Minerals and Energy Division, Plate 2001-35.

Bostock, H.S. 1970. Physiographic regions of Canada. Geological Survey of Canada, Map 1254A (with marginal notes).

Brodzikowski, K., and Van Loon, A.J. 1987. A systematic classification of glacial and periglacial environments, facies, and deposits. Earth-Science Reviews, **24**, p. 297–381.

Canadian Standards Association (CSA). 2004. Concrete materials and methods of concrete construction/methods of test and standard practices for concrete (CAN/CSA-A23.1-04/A23.2-04). Publication by the Canadian Standards Association, 10th edition, 526 p.

DeMerchant, D.P., Fournier, B., and Strang, F. 2000. Alkali-aggregate research in New Brunswick. Canadian Journal of Civil Engineering, **37** (4), p. 212–225.

Chandra, J. 1976. Seismic surveys carried out in Camp Utopia, Pennfield Ridge, Pocologan Station, Blagdon (Nerepis) and Rocky Brook (Pabineau) areas of New Brunswick in 1975 for the purpose of determining sand and gravel thickness. New Brunswick Department of Natural Resources; Mineral Resources Branch, Topical Report 76-7, 35 p.

Finamore, P.F. 1977. Granular resources in parts of the St. George (21 G/2) and McDougall Lake (21 G/7) map-areas. New Brunswick Department of Natural Resources; Mineral Resources Branch, Topical Report 77-1, 145 p.

Finamore, P.F., and Seaman, A.A. 1988. Granular aggregate resources, St. George (NTS 21 G/02) map area, New Brunswick. New Brunswick Department of Natural Resources and Energy; Minerals and Energy Division, Open File Report 88-2, 105 p.

Fyffe, L.R. 1998. Geology of the Jake Lee Mountain area (NTS 21 G/02g), Charlotte County, New Brunswick. New Brunswick Department of Natural Resources and Energy; Minerals and Energy Division, Plate 98-70, revised May 2004.

Gadd, N.R. 1968. Surficial geology of the St. George (NTS 21 G/02) map area. New Brunswick Department of Natural Resources and Energy; Minerals and Energy Division, Plate 96-4.

Gadd, N.R. 1973. Quaternary geology of southwest New Brunswick with particular reference to Fredericton area. Geological Survey of Canada, Paper 71-34, 31 p.

Gauthier, R.C. 1982. Surficial deposits, northern New Brunswick. Geological Survey of Canada, Open File 856, 9 maps.

Lowdon, J.A., and Blake, W., Jr. 1979. Geological Survey of Canada radiocarbon dates XIX. Geological Survey of Canada, Paper 79-7, 58 p.

McLeod, M.J., Johnson, S.C., Barr, S.M., and White, C.E. 2005. Bedrock geology of the St. George area (NTS 21 G/02), Charlotte County, New Brunswick. New Brunswick Department of Natural Resources; Minerals, Policy and Planning Division, Plate 2005-27.

Mott, R.J. 1975. Palynological studies of lake sediment profiles from southwestern New Brunswick. Canadian Journal of Earth Sciences, **12**, p. 273–288

New Brunswick Department of Natural Resources and Energy. 1987. Atlas of granular aggregate resources, New Brunswick. Mineral Resources Division, Miscellaneous Report 6, 90 p.

New Brunswick Department of Natural Resources. 2007. Lexicon of the bedrock nomenclature of New Brunswick. < http://www1.gnb.ca/0078/GeoscienceDatabase/Lexicon/GeoSearch-e.asp >

Pronk, A.G., Allard S., and Boldon, G.R. 2004. Till geochemistry of the St. George (NTS 21 G/02) map area, Charlotte County, New Brunswick. New Brunswick Department of Natural Resources; Minerals, Policy and Planning Division, Open File 2004-5, 67 p.

Rampton, V.N., and Paradis, S. 1981. Quaternary geology of the Amherst map area (21 H), New Brunswick. New Brunswick Department of Natural Resources; Mineral Resources Branch, Map Report 81-3.

Rampton, V.N., Gauthier, R.C., Thibault, J., and Seaman, A.A. 1984. Quaternary geology of New Brunswick. Geological Survey of Canada, Memoir 416, 77 p.

Scott, D.B., Boyd, E., and Medioli, F.S. 1987. Relative sea-level changes on a former glacial margin: observed level and sedimentological changes vs. theoretical models. *In* Selected Papers of the International Symposium on Sea-level Changes and Quaternary Shorelines, July 7–14, 1986, Sao Paulo, Brazil. *Edited by* K. Suguio, L. Martin, and J. Rabassa. Quaternary of South America and Antarctic Peninsula, **4**, p. 311–332. A.A. Balkema, Rotterdam.

Seaman, A.A. 1989a. Glacial striae trends in New Brunswick: a compilation. New Brunswick Department of Natural Resources and Energy; Mineral and Energy Division, Open File Report 89-34, 136 p.

Seaman, A.A. 1989b. Quaternary stratigraphy: York, Sunbury, and Charlotte counties, New Brunswick. *In* Project Summaries for 1989: Fourteenth Annual Review of Activities. *Edited by* S.A. Abbott, New Brunswick Department of Natural Resources and Energy; Minerals and Energy Division, Information Circular 89-2, p. 44–51.

Seaman, A.A. 2003. Follow-up till geochemistry, Coldstream (NTS 21 J/06) map area and part of the adjacent Napadogan (NTS 21 J/07) map area, York and Carleton counties, New Brunswick. New Brunswick Department of Natural Resources; Minerals, Policy and Planning Division, Open File 2003-11, 103 p.

Seaman, A.A. 2004. Late Pleistocene history of New Brunswick, Canada. *In* Quaternary Glaciations — Extent and Chronology, Part II: North America. *Edited by* J. Ehlers and P.L. Gibbard. Developments in Quaternary Science, Volume 2b, p. 151–167. Elsevier, Amsterdam.

Seaman, A.A., Broster, B.E., Cwynar, L.C., Lamothe, M., Miller, R.F., and Thibault, J.J. 1993. Field guide to the Quaternary geology of southwestern New Brunswick. New Brunswick Department of Natural Resources and Energy; Mineral Resources, Open File Report 93-1, 102 p.

Smith, E.A. 2005. Bedrock geology of southwestern New Brunswick (NTS 21 G, part of 21 B). New Brunswick Department of Natural Resources; Minerals, Policy and Planning Division, Map NR-5 (Second Edition).

Stea, R.R., and Finck, P.W. 2001. An evolutionary model of glacial dispersal and till genesis in Maritime Canada. *In* Drift Exploration in Glaciated Terrain. *Edited by* M.B. McClenaghan, P.T. Bobrowsky, G.E.M. Hall, and S.J. Cook. Geological Society of London, Special Publications 185, p. 237–265.

Stea, R.R., Scott, D.B., Kelly, J.T., Kelley, A.R., Wightman, D.M., Finck, P.W., Seaman, A., Nicks, L., Bleakney, S., Boyd, R., and Douma, M. 1987. Quaternary glaciations, geomorphology and sea-level changes: Bay of Fundy region. *In* NATO ASI-IGCP Project 200: Late Quaternary Sea-Level Correlations and Applications, July 20–26, 1987, Halifax, Nova Scotia. Field Trip Guidebook, 79 p.

Stea, R.R., Piper, D.J.W., Fader, G.B.J., and Boyd, R. 1998. Wisconsinan glacial and sea-level history of Maritime Canada and the adjacent continental shelf: a correlation of land and sea events. Geological Society of America Bulletin, **110**, p. 821–845.

Thibault, J.J. 1982. Granular aggregate resources of Rollingdam (NTS 21 G/6) and St. Stephen (NTS 21 G/3). New Brunswick Department of Natural Resources; Mineral Resources Division, Open File Report 82-15, 88 p.

Thibault, J.J. 1992. The New Brunswick peatland database. New Brunswick Department of Natural Resources and Energy; Minerai Resources Division, Mineral Resource Report 6, 84 p.

CHEAVER LAKES EAST OCCURRENCE: SETTING OF PORPHYRY-DYKE-RELATED CU–ZN–SN–W–MO MINERALIZATION, NORTH-CENTRAL NEW BRUNSWICK

JAMES A. WALKER

Geological Surveys Branch, New Brunswick Department of Natural Resources,
P.O. Box 50 Bathurst, New Brunswick, CANADA E2A 3Z1 *(jim.walker@gnb.ca)*

Walker, J.A. 2007. Cheaver Lakes East occurrence: setting of porphyry-dyke-related Cu–Zn–Sn–W–Mo mineralization, north-central New Brunswick. New Brunswick Department of Natural Resources; Minerals, Policy and Planning Division, Mineral Resources Report 2007-1, p. 49–86.

The Cheaver Lakes East Cu–Zn–Sn–W–Mo occurrence in north-central New Brunswick is one of several disseminated-sulphide and vein-sulphide occurrences that are spatially related to main and/or late-stage phases of the Late Silurian–Early Devonian North Pole Stream Granite in the Long Lake–Cheaver Lakes area (NTS 21 O/2 W). The Cheaver Lakes East occurrence consists of semi-massive- to massive-sulphide veins that cut amphibolites and sedimentary rocks of the Ordovician Trousers Lake Complex. Mineralization comprises pyrrhotite and sphalerite; subordinate chalcopyrite, pyrite, and galena; and elevated levels of granophile elements (e.g., Sn, W, Mo, U). Quartz–feldspar porphyry dykes occur in spatial association with the Cheaver Lakes East mineralized veins and are considered to be genetically related to that mineralized system. Similar porphyry dykes and associated mineralization cut the main phase of the North Pole Stream Granite near Long Lake, which suggests the possibility of a fairly large mineralizing porphyry system at depth.

Several lithogeochemical indicators suggest that the porphyry dykes are the product of extreme fractionation from a felsic melt. Specifically, the dykes have atypically low values for ΣREE (< 10 ppm), Zr/Hf (16–24), La_n/Lu_n (1.2–7.6), and Nb/Ta (< 7.5); and high contents for Nb (18–28 ppm), Ta (2.6–7 ppm), and granophile elements (Sn–W–Mo). Many of these geochemical characteristics are exhibited by high-level granitic rocks associated with the Late Devonian Mount Pleasant Sn–W–Mo porphyry system in southwestern New Brunswick.

Lithogeochemical data and petrographic observations allow the construction of a metallogenetic model for the Cheaver Lakes East occurrence, in which a zoned magma chamber of granitic composition undergoes continuous fractional crystallization to produce porphyry dykes and sulphide mineralization. This model suggests that the dykes are not related to the main phase of the North Pole Stream Granite but instead are associated with a magmatic system coeval with the Mount Pleasant caldera complex.

La venue de Cu–Zn–Sn–W–Mo des lacs Cheaver Est, dans le centre-nord du Nouveau-Brunswick, représente l'une de plusieurs venues de sulfures en filons ou disséminées spatialement apparentées aux phases principales ou tardives du granite du Siluro–Dévonien tardif du ruisseau North Pole, dans le secteur des lacs Long–Cheaver (SNRC 21 O/2 ouest). La minéralisation est constituée de filons de sulfures semi-massifs à massifs dans lesquels prédomine la pyrrhotite, accompagnée de quantités secondaires de pyrite et de sphalérite, et à teneur élevée en éléments granophiles (p. ex. Sn, W, Mo, U). Les filons recoupent des roches sédimentaires et de l'amphibolite du complexe ordovicien du lac Trousers et ils sont spatialement apparentés à des dykes de porphyre quartzo-feldspathique. Des dykes de porphyre similaires et une minéralisation connexe recoupent la phase principale du granite du ruisseau North Pole près du lac Long et sont considérés comme génétiquement apparentés au système minéralisateur des lacs Cheaver Est. Ces observations permettent de supposer la possibilité de la présence d'un système porphyrique minéralisé passablement vaste en profondeur.

Plusieurs indicateurs lithogéochimiques laissent supposer que les dykes de porphyre proviennent d'une cristallisation fractionnée extrême d'un magma felsique. Les dykes présentent plus précisément des concentrations exceptionnellement basses d'ΣÉTR (< 10 ppm), de Zr/Hf (16 à 24), de Lan/Lun (1,2 à 7,6) et de Nb/Ta (< 7,5) ainsi que des concentrations élevées de Nb (18 à 28 ppm), de Ta (2,6 à 7 ppm) et d'éléments granophiles (Sn–W–Mo). Nombre de ces caractéristiques géochimiques transparaissent dans les roches granitiques de faible profondeur associées au système porphyrique de Sn–W–Mo du Dévonien tardif du mont Pleasant, dans le Sud-Ouest du Nouveau-Brunswick.

Les données lithogéochimiques et les observations pétrographiques permettent la construction d'un modèle métallogénique de la venue des lacs Cheaver Est dans lequel une chambre magmatique zonée à composition granitique subit une cristallisation fractionnée continue pour produire des dykes porphyriques et une minéralisation de sulfures. Ce modèle permet de supposer que les dykes ne sont pas apparentés à la phase principale du granite du ruisseau North Pole, mais qu'ils sont plutôt associés à un système magmatique du même âge que le complexe de caldeira du Dévonien tardif du mont Pleasant.

INTRODUCTION

The area northeast of Long Lake in the Miramichi Highlands, northern New Brunswick (Fig. 1), has seen sporadic mineral exploration since the mid-1950s. Exploration activities resulted in the discovery of several mineral occurrences, including U–base-metal sulphides at Long Lake, and base-metal sulphides at nearby Cheaver Lakes and Cheaver Lakes East (Fig. 2). The widespread mineralization near Long Lake, coupled with recent price increases for metals such as U, Mo, W, Sn, and Zn, has renewed exploration interest in the vicinity of Long Lake–Cheaver Lakes and prompted further examination of mineralization in the area.

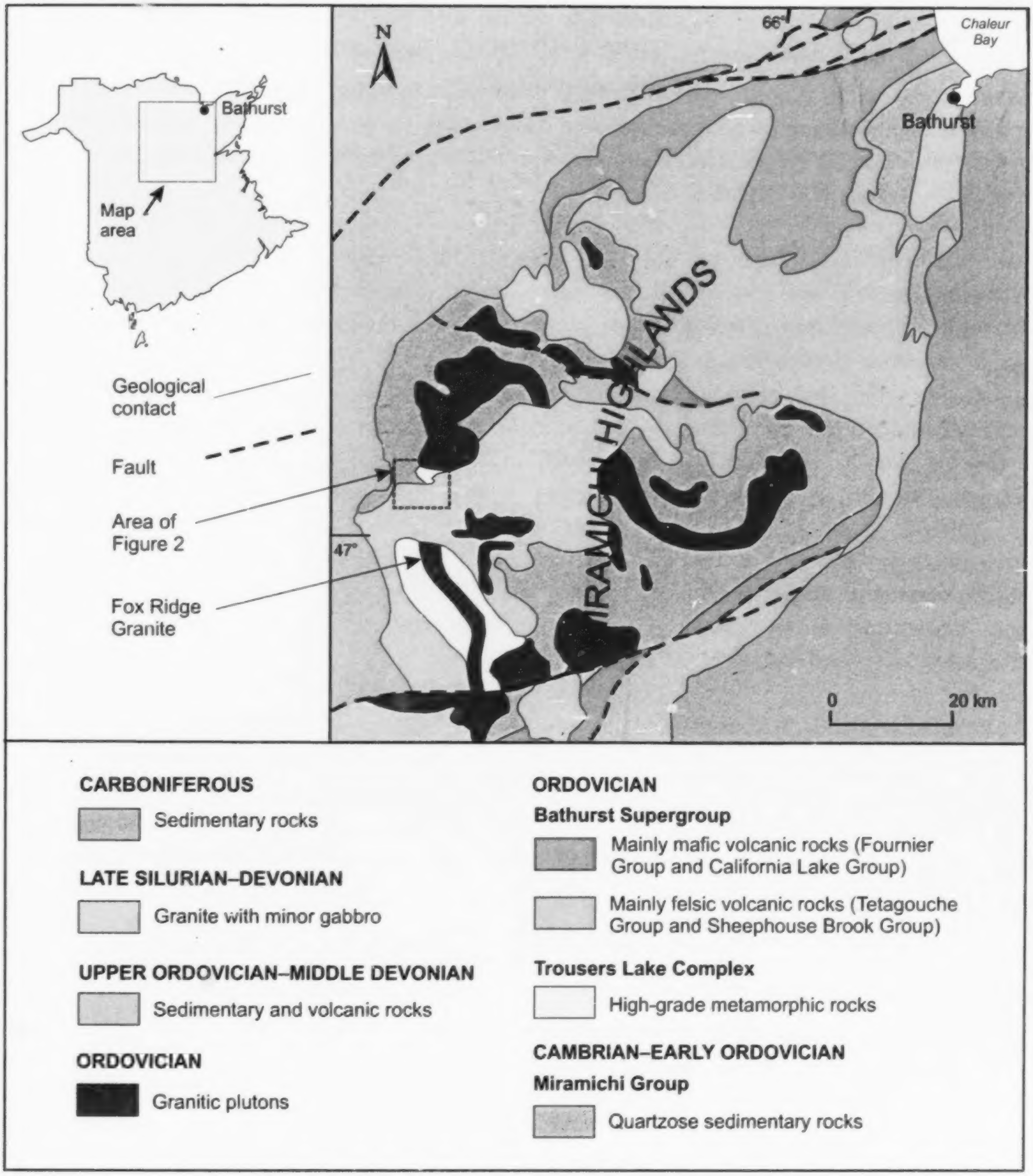
Bathurst
Map area
Geological contact
Fault
Area of Figure 2
Fox Ridge Granite
N
66°
Chaleur Bay
Bathurst
MIRAMICHI HIGHLANDS
47°
0
20 km
CARBONIFEROUS
Sedimentary rocks
LATE SILURIAN–DEVONIAN
Granite with minor gabbro
UPPER ORDOVICIAN–MIDDLE DEVONIAN
Sedimentary and volcanic rocks
ORDOVICIAN
Granitic plutons
ORDOVICIAN
Bathurst Supergroup
Mainly mafic volcanic rocks (Fournier Group and California Lake Group)
Mainly felsic volcanic rocks (Tetagouche Group and Sheephouse Brook Group)
Trousers Lake Complex
High-grade metamorphic rocks
CAMBRIAN–EARLY ORDOVICIAN
Miramichi Group
Quartzose sedimentary rocks

Figure 1. Regional geology of northern New Brunswick, showing location of the Long Lake–Cheaver Lakes area. Geology is from New Brunswick Department of Natural Resources and Energy (2000).

The Cheaver Lakes East Cu–Zn–Sn–W–Mo occurrence (Fig. 2) has been selected for the present, detailed investigation because 1) it is representative of mineralized systems in the area, and 2) drill core from previous exploration work is available at the New Brunswick Department of Natural Resources core repository at Madran, northeastern New Brunswick. The research aim here is to document mineralization style and related hydrothermal alteration at the occurrence, and to formulate a genetic model that will aid future exploration.

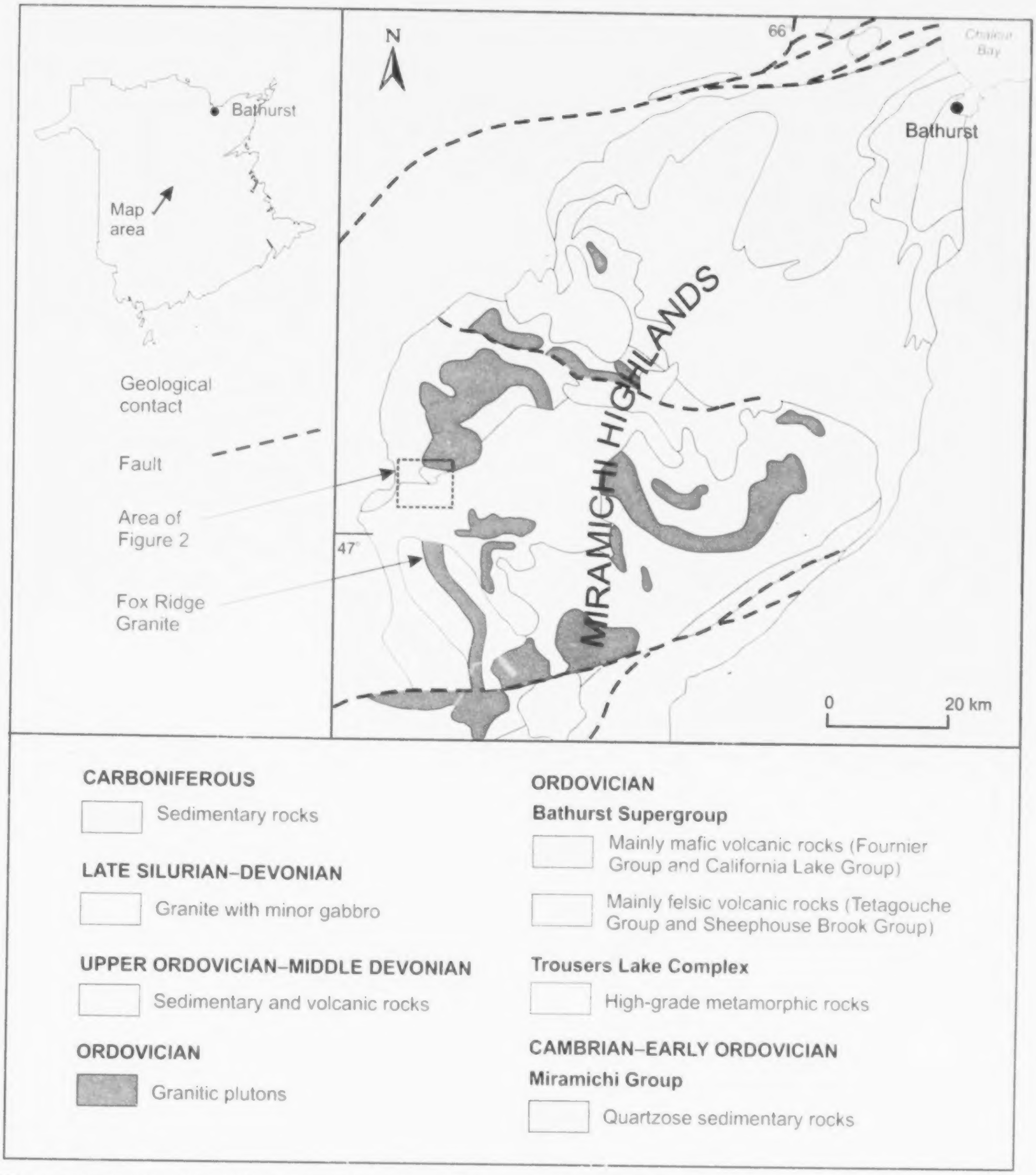
N
66
Chaleur Bay
Bathurst
Bathurst
Map area
Geological contact
Fault
Area of Figure 2
Fox Ridge Granite
47°
MIRAMICHI HIGHLANDS
0
20 km
CARBONIFEROUS
Sedimentary rocks
LATE SILURIAN–DEVONIAN
Granite with minor gabbro
UPPER ORDOVICIAN–MIDDLE DEVONIAN
Sedimentary and volcanic rocks
ORDOVICIAN
Granitic plutons
ORDOVICIAN
Bathurst Supergroup
Mainly mafic volcanic rocks (Fournier Group and California Lake Group)
Mainly felsic volcanic rocks (Tetagouche Group and Sheephouse Brook Group)
Trousers Lake Complex
High-grade metamorphic rocks
CAMBRIAN–EARLY ORDOVICIAN
Miramichi Group
Quartzose sedimentary rocks

Figure 1. Regional geology of northern New Brunswick, showing location of the Long Lake–Cheaver Lakes area. Geology is from New Brunswick Department of Natural Resources and Energy (2000).

The Cheaver Lakes East Cu–Zn–Sn–W–Mo occurrence (Fig. 2) has been selected for the present, detailed investigation because 1) it is representative of mineralized systems in the area, and 2) drill core from previous exploration work is available at the New Brunswick Department of Natural Resources core repository at Madran, northeastern New Brunswick. The research aim here is to document mineralization style and related hydrothermal alteration at the occurrence, and to formulate a genetic model that will aid future exploration.

PREVIOUS WORK

Several exploration programs have been conducted in the Long Lake–Cheaver Lakes area, including combinations of geochemical and geophysical surveys, trenching, and drilling. This section summarizes only the more significant of these activities. Numbered drillholes referred to below are shown on Figure 2.

The first exploration work in the area included a 33-hole drilling program conducted immediately south and east of Cheaver Lakes (Anthonian Mining Corporation 1957, 1963). Drilling was conducted primarily to test electromagnetic anomalies, most of which were the result of minor disseminated and fracture-filling sulphide minerals (chalcopyrite, galena, sphalerite, pyrite, and pyrrhotite) and magnetite encountered in a variety of host rocks that included greywacke, porphyritic rhyolite, and altered granite. The best assay results gave 1.19% Cu over 0.76 m in drillhole 9; and 0.28% Cu, 2.55% Zn, and 20 ppm Ag over 0.91 m in drillhole 18.

Consolidated Mining and Smelting (Shewman 1964) conducted soil sampling and electromagnetic surveys and completed drillhole AT-3 (Fig. 2) south of Cheaver Lakes. The hole intersected biotite granite containing sparse sphalerite, galena, and chalcopyrite mineralization associated with epidote and chlorite veins.

Canadian Occidental Petroleum Ltd. drilled two holes (L-1 and L-2) that intersected highly fractured, silicified, and kaolinized granite and quartz porphyry containing stringers and fracture fillings of pyrite with traces of chalcopyrite and sphalerite. Assay results on the drill core yielded up to 2690 ppm Cu, 400 ppm Mo, and 1.3% Zn (Saracoglu 1973). The company subsequently acquired ground to cover stream sediment uranium and coincident base-metal anomalies immediately north of Long Lake (Hauseux 1980, 1981). There, it completed drillholes 80-1 through 80-5, from which the best assays gave 1.88% Cu over 0.3 m in drillhole 80-1; and 0.2% Pb and 15.3% Zn over 0.3 m in drillhole 80-3. A granite boulder exposed during trenching on the south side of Cheaver Lakes returned up to 2868 ppm Sn, and an assay from the trench gave 3.38% Zn over 0.61 m (Hauseux 1980).

Brunswick Mining and Smelting staked its “Sears Lake” property (Mann 1985), which covered the Cheaver Lakes and Cheaver Lakes East occurrences, to follow up on stream sediment sampling that showed highly anomalous lead and zinc contents (Davies 1982). The company focused on two areas, one situated 7 km northeast of the Cheaver Lakes East occurrence and the other just northeast of the area covered in Figure 1. The work independently reproduced the anomalous silt geochemistry of Davies (1982), obtaining Zn values of up to 6000 ppm and Pb values of up to 7560 ppm in stream silt samples from a site just (1–2 km) east of Cheaver Lakes (Fig. 2). Soil samples yielded up to 10 000 ppm Pb and 4400 ppm Zn.

Fyffe and Pronk (1985) investigated bedrock and surficial geology in the area. They interpreted a glacial transport direction toward the east-southeast (~ 100°) and concluded that base-metal soil geochemical anomalies southeast of Cheaver Lakes most likely were due to transport from the Long Lake U–base-metal occurrence (Fig. 2).

When NovaGold Resources Inc. acquired ground in the Long Lake–Cheaver Lakes area, it 1) conducted ground and airborne magnetic, EM, and VLF-EM surveys, and 2) sunk drillholes 91-36-1 to 91-36-3 (Fig. 2) northeast of the Cheaver Lakes East occurrence (Giggie 1990, 1991). A few years later, the company drilled five additional holes (93-36-4 to 93-36-8) to test coincident geochemical and geophysical anomalies over a 1500 m by 300 m area (Burton 1993). The current investigation is based on data obtained from core associated with these five most recent drillholes.

REGIONAL GEOLOGY

The Long Lake–Cheaver Lakes area (Fig. 1, 2) is underlain by greenschist-grade clastic sedimentary rocks of the Cambrian–Early Ordovician Miramichi Group and a sequence of amphibolite-grade mafic and associated sedimentary rocks of the Trousers Lake Complex (Fyffe and Pronk 1985; Fyffe et al. 1988; van Staal et al. 2003). These rocks have been intruded by Ordovician and Late Silurian–Devonian granitic plutons (Whalen 1993). The contact between the Trousers Lake Complex and Miramichi Group is unexposed in the report area; however, south of the North Pole Stream Granite (Fig. 2), the contact has been placed (Fyffe et al. 1988) at the gradational zone between the Miramichi Group and sillimanite-bearing migmatitic rocks of the Trousers Lake Complex.

South of the report area, rocks of the Trousers Lake Complex are interleaved with Ordovician felsic intrusive rocks that can be correlated with the Fox Ridge Granite (Crouse 1978; Fyffe et al. 1988). The Fox Ridge Granite (Fig. 1) is a pink to orangish-pink, medium-grained, foliated granite that commonly contains ovoid megacrysts of alkali feldspar, and it has returned a U–Pb zircon age of 451 +15/-1 Ma (Fyffe et al. 1988).

The Serpentine River Granite (Fig. 2) crops out approximately 700 m north of the Cheaver Lakes East occurrence, where it intrudes the Trousers Lake Complex (Whalen 1993). This pluton consists of dark pink, orange, and red, fine- to medium-grained, weakly to strongly foliated, equigranular to locally porphyritic granite. The granite has returned a U–Pb zircon age of 466 ± 2 Ma (McNicoll et al. 2003). Thus, the Trousers Lake amphibolites can be no younger than Middle Ordovician, which makes them coeval with the Flat Landing Brook Formation (Fig. 1) of the Tetagouche Group (van Staal et al. 2003) in the Bathurst area.

Trace-element analyses of the amphibolites indicate a mixed protolith of intercalated volcanic-arc and within-plate tholeiitic basalts that are compositionally similar to some mafic volcanic rocks in the Tetagouche Group (Fig. 1; Fyffe et al. 1988). Given the regional metamorphic grade, some Trousers Lake amphibolites may have originated as dykes that intruded

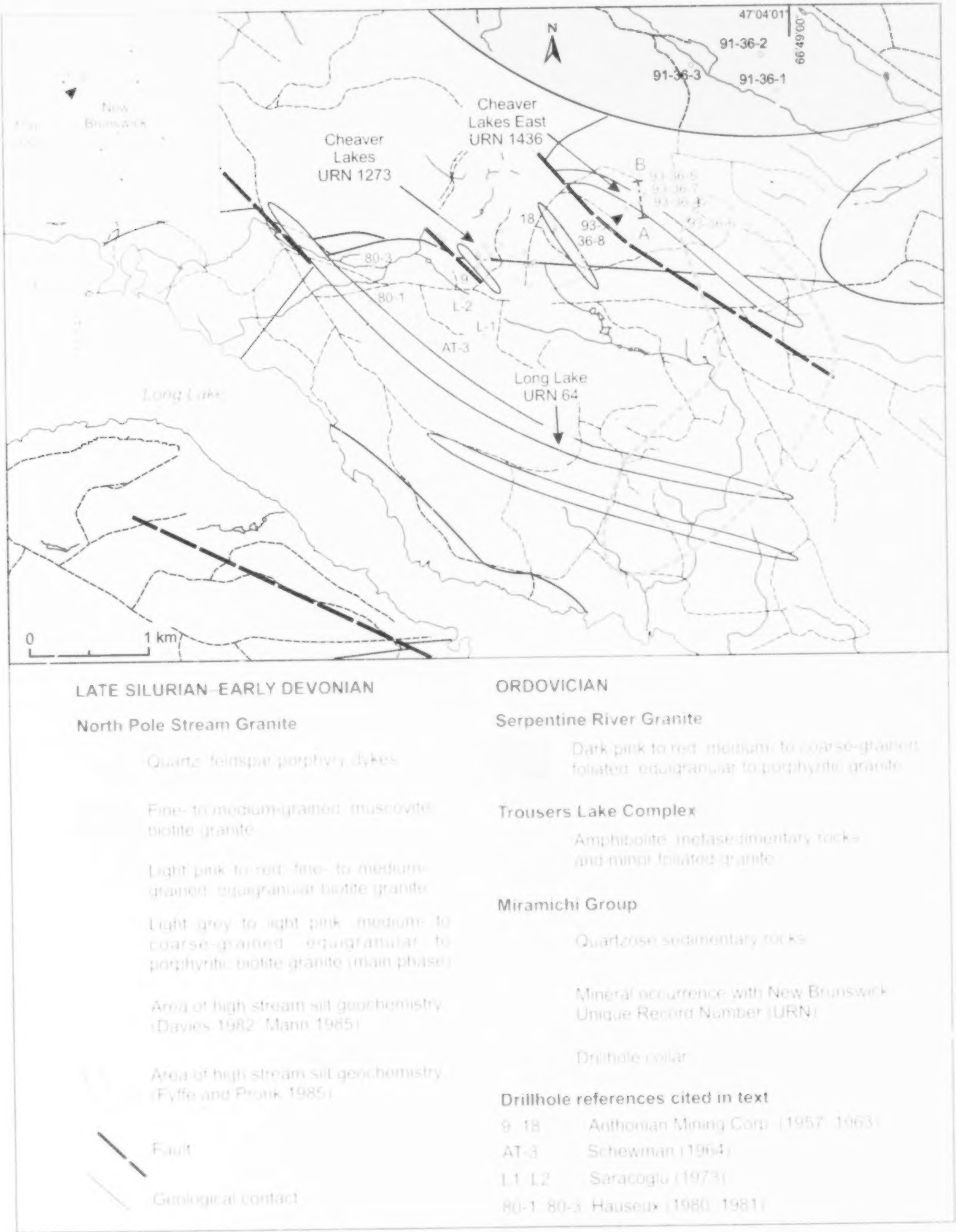
47°04'01"
66°49'00"
N
91-36-2
91-36-3
91-36-1
New Brunswick
Cheaver Lakes East URN 1436
Cheaver Lakes URN 1273
B
93-36-5
93-36-7
93-36-4
93-36-6
18
93-36-8
A
80-3
9
80-1
L-2
L-1
AT-3
Long Lake URN 64
Long Lake
0
1 km
LATE SILURIAN–EARLY DEVONIAN
North Pole Stream Granite
Quartz-feldspar porphyry dykes
Fine- to medium-grained, muscovite-biotite granite
Light pink to red, fine- to medium-grained, equigranular biotite granite
Light grey to light pink, medium- to coarse-grained, equigranular to porphyritic biotite granite (main phase)
Area of high stream silt geochemistry (Davies 1982; Mann 1985)
Area of high stream silt geochemistry (Fyffe and Pronk 1985)
Fault
Geological contact
ORDOVICIAN
Serpentine River Granite
Dark pink to red, medium- to coarse-grained, foliated, equigranular to porphyritic granite
Trousers Lake Complex
Amphibolite, metasedimentary rocks and minor foliated granite
Miramichi Group
Quartzose sedimentary rocks
Mineral occurrence with New Brunswick Unique Record Number (URN)
Drillhole collar
Drillhole references cited in text
9, 18 Anthonian Mining Corp. (1957, 1963)
AT-3 Schewman (1964)
L1, L2 Saracoglu (1973)
80-1, 80-3 Hauseux (1980, 1981)

Figure 2. General geology near Cheaver Lakes East occurrence, compiled and modified from Fyffe and Pronk (1985) and Whalen (1993). Drillhole locations are compiled from Anthonian Mining Corp. (1957, 1963), Giggie (1991), and Burton (1993). Cross-section A–B is shown in Figure 3.

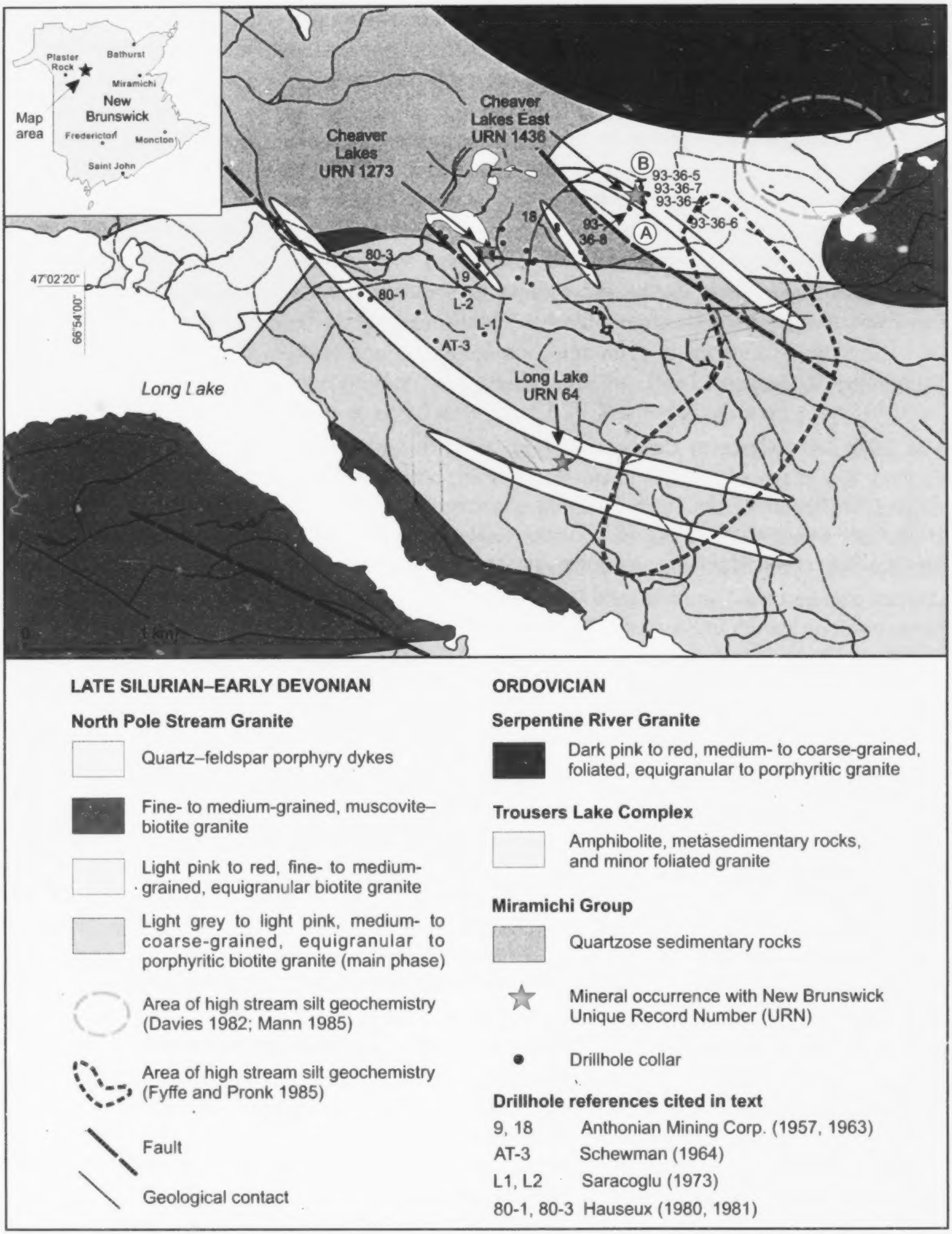
Plaster Rock
Bathurst
Miramichi
New Brunswick
Map area
Fredericton
Moncton
Saint John
Cheaver Lakes East URN 1436
Cheaver Lakes URN 1273
B
93-36-5
93-36-7
93-36-4
93-36-6
A
93-36-8
18
80-3
9
80-1
L-2
L-1
AT-3
47°02'20"
66°54'00"
Long Lake
Long Lake URN 64
0
1 km
LATE SILURIAN–EARLY DEVONIAN
North Pole Stream Granite
Quartz–feldspar porphyry dykes
Fine- to medium-grained, muscovite–biotite granite
Light pink to red, fine- to medium-grained, equigranular biotite granite
Light grey to light pink, medium- to coarse-grained, equigranular to porphyritic biotite granite (main phase)
Area of high stream silt geochemistry (Davies 1982; Mann 1985)
Area of high stream silt geochemistry (Fyffe and Pronk 1985)
Fault
Geological contact
ORDOVICIAN
Serpentine River Granite
Dark pink to red, medium- to coarse-grained, foliated, equigranular to porphyritic granite
Trousers Lake Complex
Amphibolite, metasedimentary rocks, and minor foliated granite
Miramichi Group
Quartzose sedimentary rocks
Mineral occurrence with New Brunswick Unique Record Number (URN)
Drillhole collar
Drillhole references cited in text
9, 18 Anthonian Mining Corp. (1957, 1963)
AT-3 Schewman (1964)
L1, L2 Saracoglu (1973)
80-1, 80-3 Hauseux (1980, 1981)

Figure 2. General geology near Cheaver Lakes East occurrence, compiled and modified from Fyffe and Pronk (1985) and Whalen (1993). Drillhole locations are compiled from Anthonian Mining Corp. (1957, 1963), Giggie (1991), and Burton (1993). Cross-section A–B is shown in Figure 3.

sedimentary rocks of the Miramichi Group (Fig. 1) and fed stratigraphically higher volcanic units (Fyffe et al. 1988). Intrusive contacts between amphibolites and sedimentary rocks could have been obscured during post-emplacement deformation and metamorphism, which would have resulted in apparently conformable contacts.

Younger intrusions in the report area are represented by phases of the Late Silurian–Early Devonian North Pole Stream Granite (Whalen 1993). The main phase occurs approximately 600 m south of the Cheaver Lakes East occurrence (Fig. 2) and comprises light grey to light pink, medium- to coarse-grained, equigranular to porphyritic biotite granite. It contains alkali feldspar and plagioclase phenocrysts up to 3 cm long, and hornblende is present locally. One minor phase consists of light pink to red, fine- to medium-grained, equigranular biotite granite and lies west of Cheaver Lakes. Other minor phases comprise fine- to medium-grained muscovite–biotite granite; they occur east and southwest of Cheaver Lakes (Whalen 1993) and appear to intrude the main phase of the North Pole Stream Granite (Fig. 2).

A wide range of radiometric ages has been reported from the North Pole Stream Granite, indicating a protracted history of emplacement and cooling (Whalen 1993, and references therein). A U–Pb monazite age of 417 ± 1 Ma was obtained from the main biotite granite phase at a location 25 km east of the report area (Whalen 1993). Rb–Sr and K–Ar ages ranging from 425 Ma to 381 Ma were obtained from the apparently younger muscovite–biotite phase of the North Pole Stream Granite. These ages include Rb–Sr dates of 425 ± 4 Ma on muscovite and 397 ± 4 Ma on biotite from a site within the report area, immediately south of Long Lake; and a Rb–Sr date of 414 ± 5 Ma and a K–Ar date of 381 ± 4 Ma on muscovite from a site about 15 km northeast of Long Lake (Whalen 1993).

Quartz–feldspar porphyry dykes (Fig. 2) intrude the main phase of the North Pole Stream Granite near the Long Lake U–base-metal occurrence, and also cut amphibolites of the Trousers Lake Complex at the Cheaver Lakes East occurrence. West of Cheaver Lakes, another porphyry dyke apparently intrudes the contact between light pink to red biotite granite and muscovite–biotite granite (Fig. 2). While drilling south and east of Cheaver Lakes, Anthonian Mining Corporation intersected similar dykes that were associated with mineralization. The fact that porphyry dykes are the youngest intrusions in the area and are associated with mineralization is highly significant to the present investigation and is discussed in detail later in this report.

CHEAVER LAKES EAST OCCURRENCE

Geology

The Cheaver Lakes East occurrence is situated approximately 45 km northeast of the village of Plaster Rock and 1.5 km east of Cheaver Lakes (Fig. 2). The property lies on freehold ground controlled by Fraser Papers Inc. and is easily accessible from the northwest end of Long Lake via a well developed network of logging roads.

Due to thick overburden in the area, the present investigation relied entirely on diamond drill core from NovaGold Resources Inc., using material from drillholes 93-36-4 through 93-36-8 (Fig. 2). (Core from drillholes 80-1 through 80-5 of Canadian Occidental Petroleum Ltd. is intact but has a small diameter and is in poorer condition than the NovaGold material.) The most interesting core in terms of mineralization is from drillhole 93-36-4, which intersected 1) an intercalated sequence of amphibolites and sedimentary rocks, 2) deformed and foliated alkali-feldspar-phyric intrusive rocks, and 3) undeformed quartz–feldspar porphyry dykes (Fig. 2, 3). These rocks, and their lithogeochemical analyses, are described below in this and the following section.

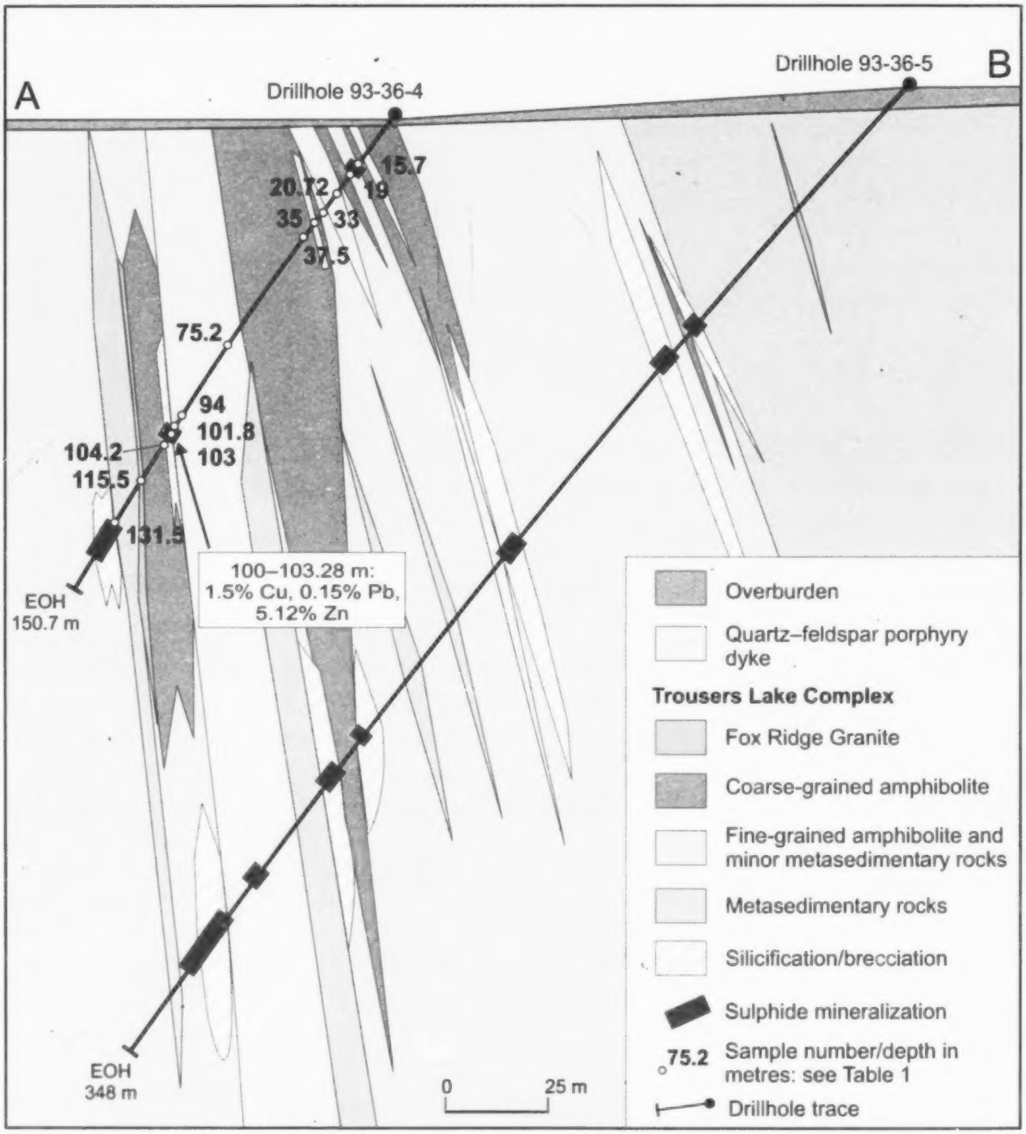
A
Drillhole 93-36-4
Drillhole 93-36-5
B
15.7
20.72
19
35
33
37.5
75.2
94
101.8
103
104.2
115.5
131.5
100–103.28 m:
1.5% Cu, 0.15% Pb,
5.12% Zn
EOH
150.7 m
EOH
348 m
0
25 m
Overburden
Quartz–feldspar porphyry dyke
Trousers Lake Complex
Fox Ridge Granite
Coarse-grained amphibolite
Fine-grained amphibolite and minor metasedimentary rocks
Metasedimentary rocks
Silicification/brecciation
Sulphide mineralization
75.2 Sample number/depth in metres: see Table 1
Drillhole trace

Figure 3. Geological cross-section through the Cheaver Lakes East occurrence, modified from data in Burton (1993). Lithogeochemical sample numbers in Table 1 are plotted here with respect to geology. Line of cross-section A–B is shown in Figure 2.

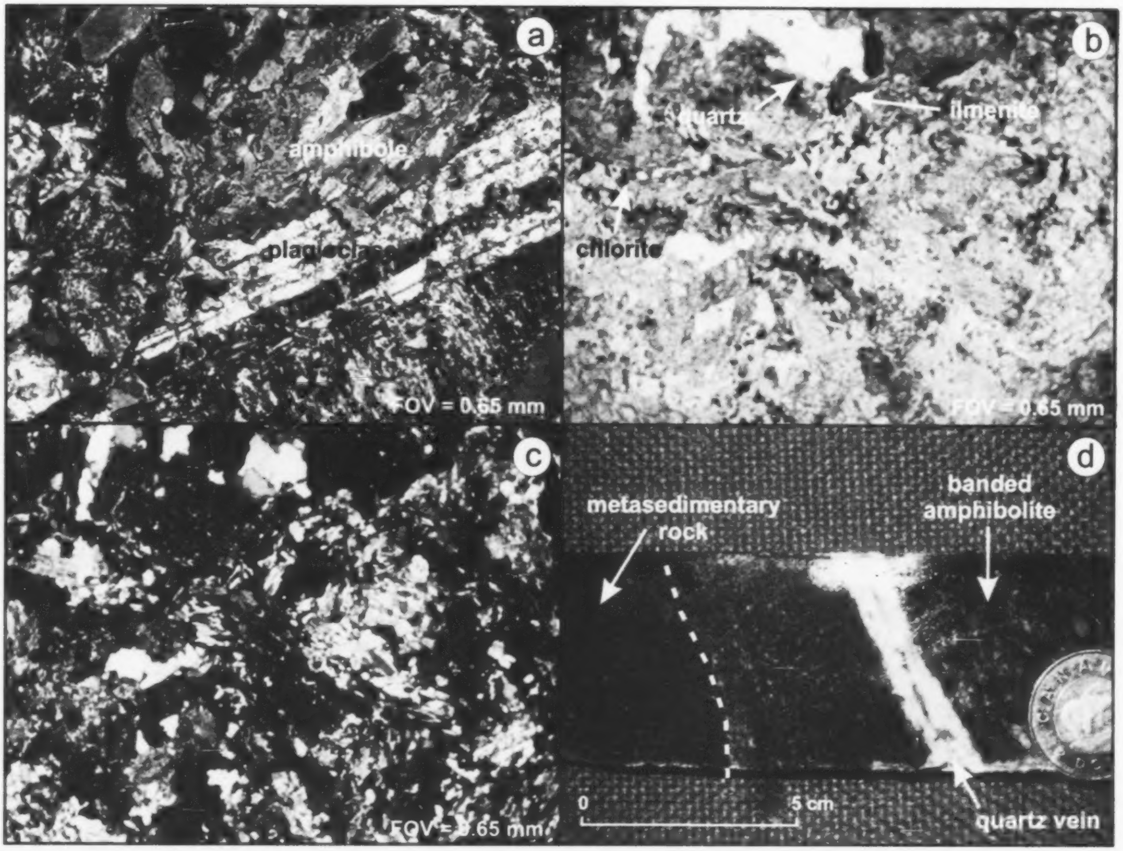

Figure 4. Host rocks from the Trousers Lake Complex at Cheaver Lakes East, observed in core from drillhole 93-36-4. a) Photomicrograph of amphibolite from 19 m shows amphibole and plagioclase under crossed polars. b) Photomicrograph of amphibolite from 19 m shows chlorite-altered zones in plane polarized light. c) Same as in Figure 4b but under crossed polars. d) Core sample from 9.5 m shows metasedimentary rock in contact with banded amphibolite.

The amphibolites range from fine grained (possibly volcanic rocks) to coarse grained (possibly dykes) and consist of amphibole and plagioclase in roughly equal proportions (Fig. 4a). Sericitization of plagioclase phenocrysts is weakly developed locally, and iron oxides and titanium oxides together constitute 1% to 2% of the rock. In some thin sections, amphibolite adjacent to the porphyry dykes shows evidence of biotite (1–10%) replacing amphibole; as well, chlorite (≤ 5%) alteration is weakly developed locally (Fig. 4b, 4c). These observations suggest that water-dominated fluids interacted with amphibolite adjacent to the porphyry dykes. Sedimentary rocks interlayered with the amphibolite consist mainly of rounded quartz and mica with less abundant, variably altered feldspar (Fig. 4d).

A narrow (< 2 m) interval of foliated alkali-feldspar-phyric granite interleaved with amphibolite was intersected in drillhole 93-36-4 at a depth of 115 m and has been assigned to the Fox Ridge Granite (Fig. 1, 3). Foliation in the granitic interval parallels the dominant foliation in adjacent sedimentary rocks (Fig. 5), implying a similar metamorphic history for both rocks. In thin section, about 30% of the granite consists of irregular aggregates of quartz and K-

Due to thick overburden in the area, the present investigation relied entirely on diamond drill core from NovaGold Resources Inc., using material from drillholes 93-36-4 through 93-36-8 (Fig. 2). (Core from drillholes 80-1 through 80-5 of Canadian Occidental Petroleum Ltd. is intact but has a small diameter and is in poorer condition than the NovaGold material.) The most interesting core in terms of mineralization is from drillhole 93-36-4, which intersected 1) an intercalated sequence of amphibolites and sedimentary rocks, 2) deformed and foliated alkali-feldspar-phyric intrusive rocks, and 3) undeformed quartz–feldspar porphyry dykes (Fig. 2, 3). These rocks, and their lithogeochemical analyses, are described below in this and the following section.

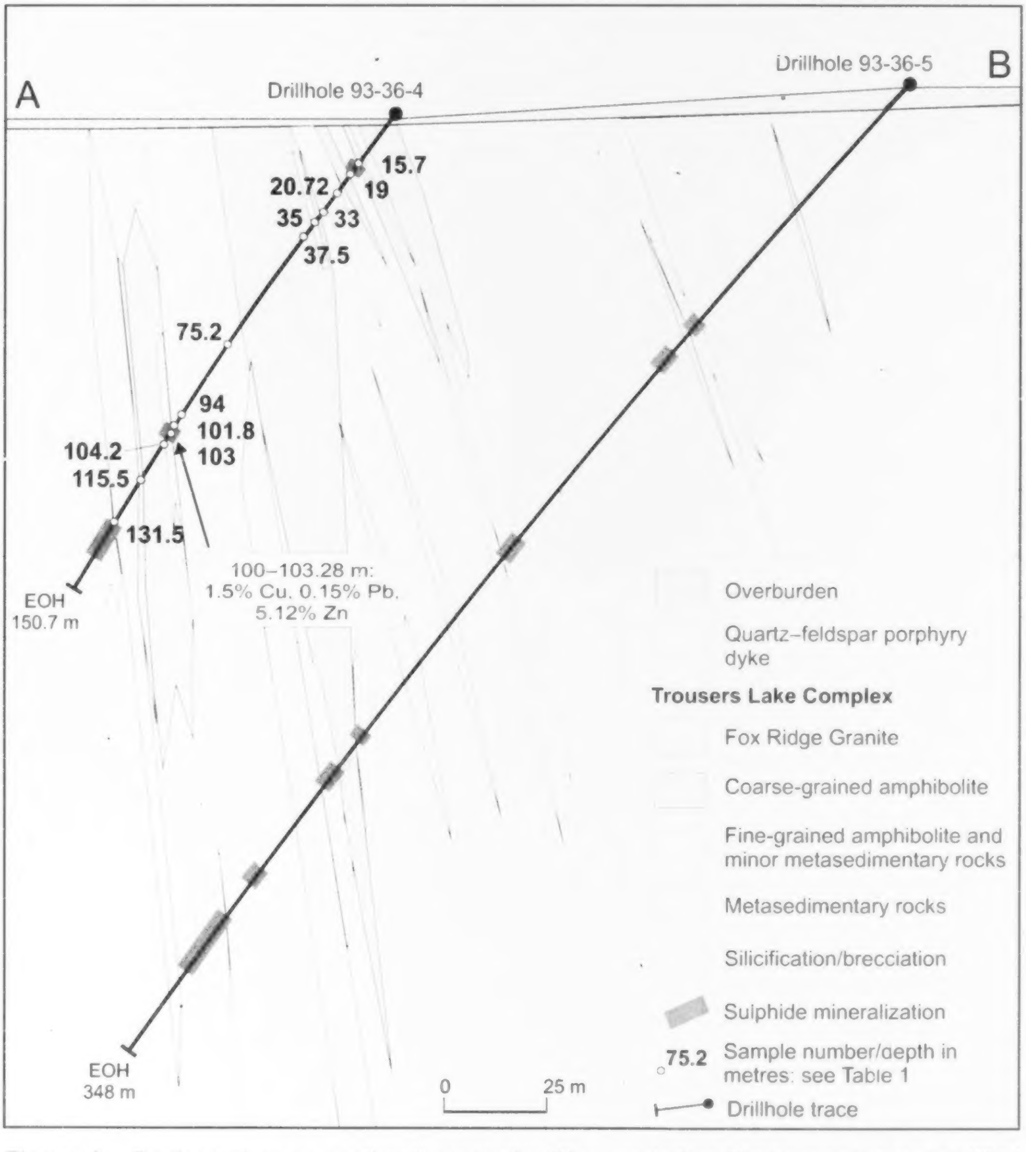
A
Drillhole 93-36-4
Drillhole 93-36-5
B
15.7
20.72
19
35
33
37.5
75.2
94
101.8
103
104.2
115.5
131.5
100–103.28 m:
1.5% Cu, 0.15% Pb,
5.12% Zn
EOH
150.7 m
EOH
348 m
0
25 m
Overburden
Quartz–feldspar porphyry dyke
Trousers Lake Complex
Fox Ridge Granite
Coarse-grained amphibolite
Fine-grained amphibolite and minor metasedimentary rocks
Metasedimentary rocks
Silicification/brecciation
Sulphide mineralization
75.2 Sample number/depth in metres: see Table 1
Drillhole trace

Figure 3. Geological cross-section through the Cheaver Lakes East occurrence, modified from data in Burton (1993). Lithogeochemical sample numbers in Table 1 are plotted here with respect to geology. Line of cross-section A–B is shown in Figure 2.

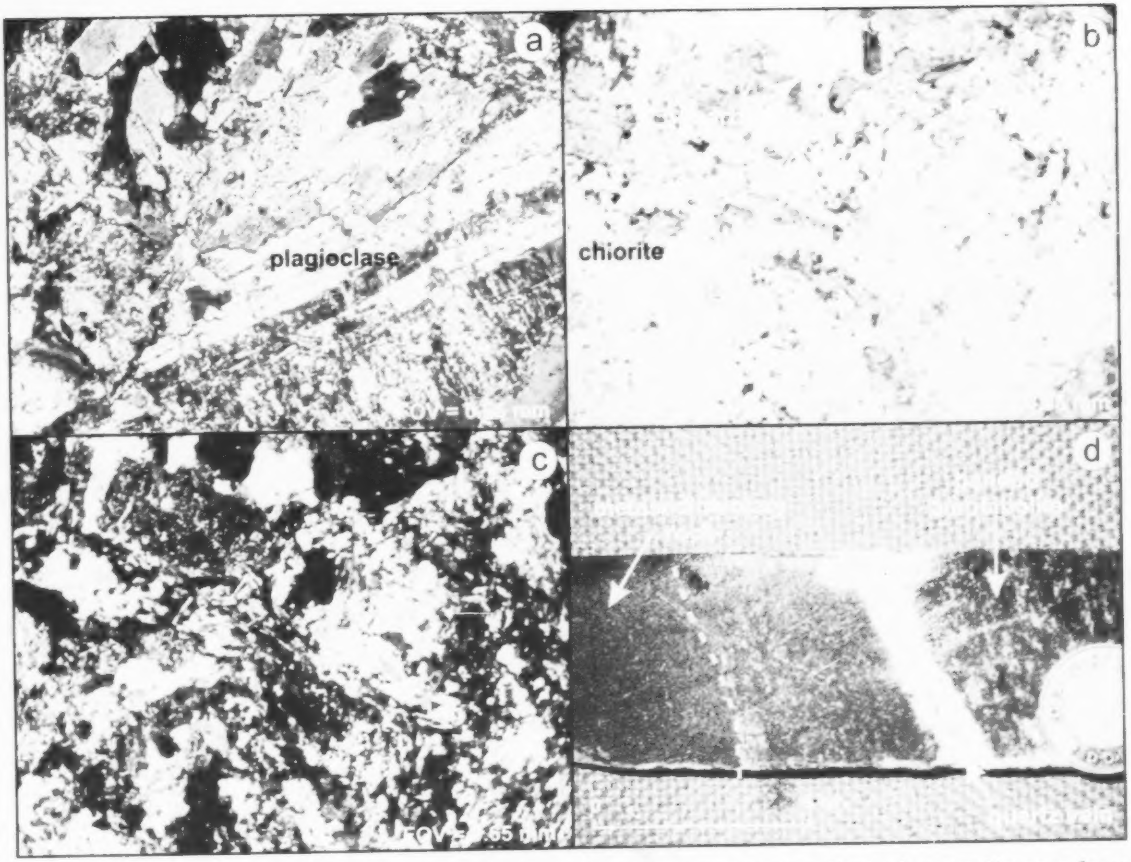

Figure 4. Host rocks from the Trousers Lake Complex at Cheaver Lakes East, observed in core from drillhole 93-36-4. a) Photomicrograph of amphibolite from 19 m shows amphibole and plagioclase under crossed polars. b) Photomicrograph of amphibolite from 19 m shows chlorite-altered zones in plane polarized light. c) Same as in Figure 4b but under crossed polars. d) Core sample from 9.5 m shows metasedimentary rock in contact with banded amphibolite.

The amphibolites range from fine grained (possibly volcanic rocks) to coarse grained (possibly dykes) and consist of amphibole and plagioclase in roughly equal proportions (Fig. 4a). Sericitization of plagioclase phenocrysts is weakly developed locally, and iron oxides and titanium oxides together constitute 1% to 2% of the rock. In some thin sections, amphibolite adjacent to the porphyry dykes shows evidence of biotite (1–10%) replacing amphibole; as well, chlorite (≤ 5%) alteration is weakly developed locally (Fig. 4b, 4c). These observations suggest that water-dominated fluids interacted with amphibolite adjacent to the porphyry dykes. Sedimentary rocks interlayered with the amphibolite consist mainly of rounded quartz and mica with less abundant, variably altered feldspar (Fig. 4d).

A narrow (< 2 m) interval of foliated alkali-feldspar-phyric granite interleaved with amphibolite was intersected in drillhole 93-36-4 at a depth of 115 m and has been assigned to the Fox Ridge Granite (Fig. 1, 3). Foliation in the granitic interval parallels the dominant foliation in adjacent sedimentary rocks (Fig. 5), implying a similar metamorphic history for both rocks. In thin section, about 30% of the granite consists of irregular aggregates of quartz and K-

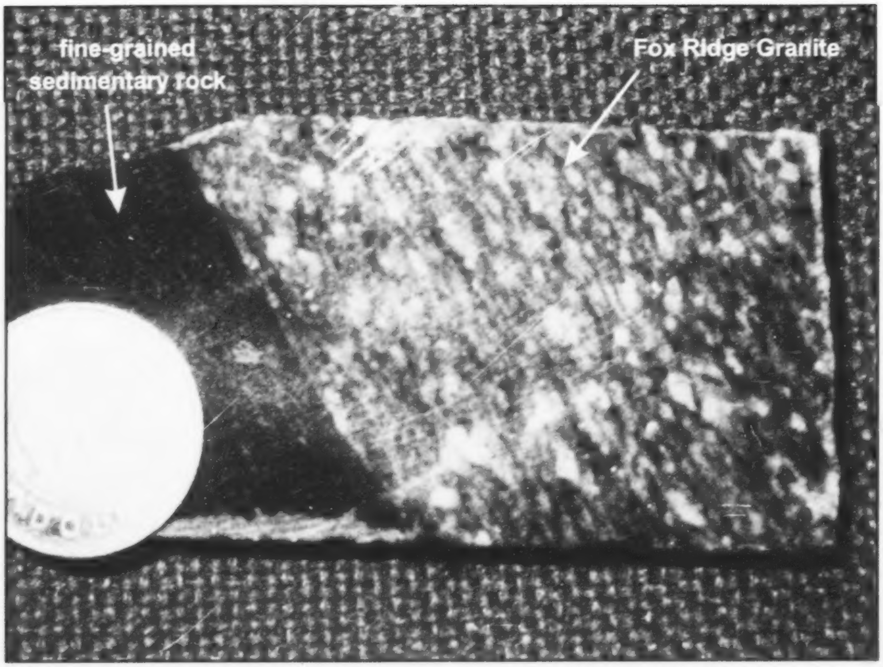

Figure 5. Fox Ridge Granite in tectonic contact with fine-grained sedimentary rock. Core is from 115.5 m in drillhole 93-36-4 at Cheaver Lakes East.

feldspar. The quartz commonly displays undulatory extinction, which signifies deformation. Fine-grained white mica is the next most abundant phase and occurs interstitially to the quartz.

The porphyry dyke samples range from grey to pink and have a very fine-grained groundmass of quartz and white mica with minor disseminated sulphides (Fig. 6a–e). Phenocrysts of quartz, plagioclase, alkali feldspar, and biotite constitute from 5% to 20% of the rock and range in size from < 0.5 mm to 5 mm; the feldspar phenocrysts (plagioclase and alkali feldspar) are variably altered and, in part, replaced by intergrowths of white mica and quartz (Fig. 6b, 6c). Bands containing higher concentrations of white mica can be identified and are interpreted to represent zones of higher relative fluid flow resulting in localized K-metasomatism. In some instances, small biotite phenocrysts are partially replaced by sulphides (Fig. 6d); Fe- and Ti-bearing minerals are all but absent.

The existence of biotite crystals (hydrous phase) as inclusions in quartz phenocrysts (Fig. 6e) indicates that the melt from which the porphyry dykes crystallized contained some water. The presence of zircon inclusions within biotite phenocrysts reveals that the parent melt was saturated in zircon before dyke emplacement, a fact critical to calculating zircon-saturation temperatures (see *Temperature–Pressure–Composition Constraints on Porphyry Dykes*, below). Some quartz phenocrysts are mantled by a thin layer of muscovite. The space required for mica crystallization may have been provided by the volume decrease of quartz phenocrysts as they transitioned from high-temperature β-quartz to low-temperature α-quartz.

Mineralization

Mineralization at Cheaver Lakes East occurs as massive-sulphide veins (≤ 5 cm in width) and veinlets (Fig. 3), in which the main sulphide minerals are pyrrhotite and sphalerite,

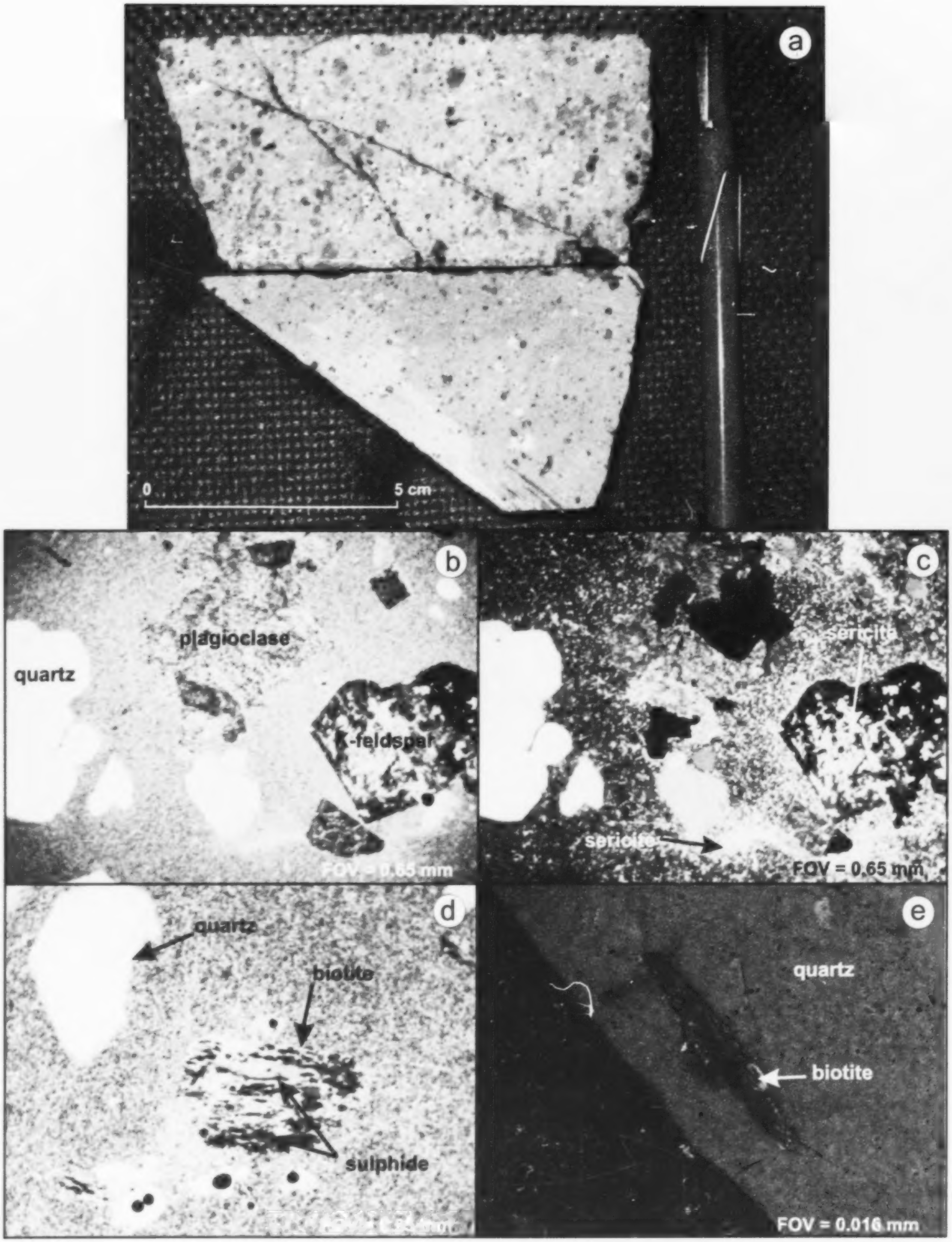
a
0
5 cm
b
plagioclase
quartz
K-feldspar
FOV = 0.65 mm
c
sericite
sericite
FOV = 0.65 mm
d
quartz
biotite
sulphide
e
quartz
biotite
FOV = 0.016 mm

Figure 6. Porphyry dykes at Cheaver Lakes East, observed in core from drillhole 93-36-4. a) Porphyry dyke from 15.7 m (upper core) and from 20.72 m (lower core). b) Photomicrograph of porphyry dyke, under plane polarized light. c) Same as in Figure 6b but under crossed polars. d) Photomicrograph showing biotite crystal replaced by white mica and minor sulphides, under plane polarized light. e) Photomicrograph showing biotite crystal inclusion in quartz, under plane polarized light. Samples for Figures 6b– e are from 75.2 m.

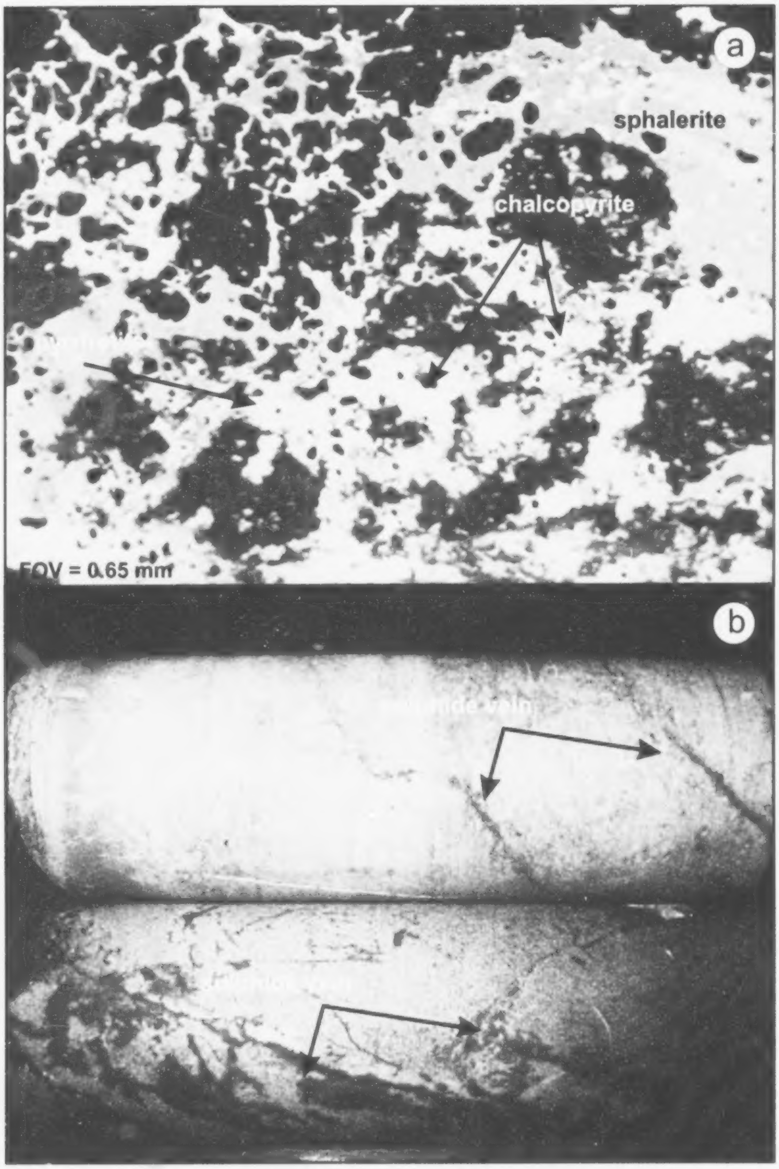

Figure 7. Mineralization at Cheaver Lakes East in core from drillhole 93-36-4. a) Photomicrograph of sample from 101.8 m; shows pyrrhotite–sphalerite intergrowths and minor chalcopyrite in plane polarized light. b) Upper core sample from 35 m shows sulphide veins cutting porphyry dyke. Lower core from about 104 m shows sulphide veins cutting sedimentary rock. Diameter of each core is 4.7 cm.

accompanied by minor pyrite, chalcopyrite, and galena (Fig. 7a). Less commonly, sulphides occur in quartz-dominated veins. In drillhole 93-36-4, sulphide veins crosscut the amphibolites and sedimentary host rocks near the porphyry dykes. Sulphide veins also intersect the porphyry dykes themselves (Fig. 7b), albeit to a lesser extent than in the amphibolites or sedimentary rocks. The similarity in metal content of dykes and sulphide veins suggests a close temporal relationship between dyke emplacement and mineralization. Minor pyrite–

pyrrhotite mineralization is disseminated in amphibolite at a distance from the porphyry dykes. It is unknown whether this phenomenon represents primary sulphides in the mafic protolith or mineralization imparted to the rocks after amphibolitization.

The abundance of magnetic (hexagonal) pyrrhotite associated with sphalerite, chalcopyrite, and minor galena suggests that mineralization was probably emplaced at ≥ 300°C from fluids that had low O_2 and S_2 fugacities. Cation transport in such a system was likely accomplished by complexing with HS^- ligands, which can readily transport sufficient (> 1 ppm) Cu and Zn but not Pb at temperatures in the range of 250°C to 300°C (Lydon 1988).

In addition to containing elevated levels of Cu and Zn, the mineralized zones are enriched in elements commonly associated with granite-related deposits, namely Sn, W, and Mo. Most analyzed samples, including some of the amphibolite collected adjacent to the porphyry dykes, also have elevated Sn, W, and Mo contents. Amphibolite Sample No. 93-36-4-19, for instance, yielded significant Sn and W contents of 85 ppm and 28 ppm, respectively, as well as 4515 ppm Zn (Table 1).

LITHOGEOCHEMISTRY

For the current investigation, 13 core samples from drillhole 93-36-4 were subjected to lithogeochemical analysis. The selected rock types consisted of amphibolite (n = 4), foliated granite (n = 1), quartz–feldspar porphyry dyke (n = 5), massive sulphides (n = 1), and sedimentary rock (n = 2). Figure 3 shows the location of these samples with respect to downhole geology. All analyses were conducted by Acme Analytical Laboratories Ltd. of Vancouver, British Columbia, and the data are summarized in Table 1.

This paper compares geochemical data from the 13 core samples with data from different phases of the North Pole Stream Granite, as reported by Whalen (1993). The various phases consist of medium- to coarse-grained biotite granite (the main phase); fine- to medium-grained biotite granite; muscovite–biotite granite; granodiorite; and mafic intrusive rocks.

Major-Element Chemistry

Major-element chemistry involving some combination of K_2O, $Na_2O + K_2O$, and SiO_2 has typically been used to characterize igneous rock types (Pearce and Cann 1973; Pearce et al. 1984) and is applied here.

On the $Na_2O + K_2O$ vs SiO_2 discrimination diagram, porphyry dykes show SiO_2 contents ranging from 72.0 wt % to 75.8 wt % (Fig. 8a). These numbers fall within the rhyolite field, as do most geochemical data from the North Pole Stream Granite, and collectively the data more or less follow a subalkaline/tholeiitic trend. The Fox Ridge Granite sample of foliated alkali-feldspar-phyric granite analyzes at 72 wt % SiO_2 and 8.4 wt % ($Na_2O + K_2O$), and plots along the same subalkaline/tholeiitic trend. On the K_2O vs SiO_2 diagram (Fig. 8b), the Fox Ridge Granite

Table 1. Lithogeochemical data from drillhole 93-36-4 at the Cheaver Lakes East sulphide occurrence.

Sample No. (ending with drillhole depth in metres)			93-36-4-15.7	93-36-4-19	93-36-4-20.72	93-36-4-33	93-36-4-35	93-36-4-37.5	93-36-4-75.2
	Detection Limit	Method / Rock Type	Pink quartz-feldspar porphyry	Chloritic amphibolite	Grey feldspar +/- quartz porphyry	Fresh amphibolite	Pink aphyric rhyolite	Deformed amphibolite	Quartz–feldspar porphyry cut by sulphide vein
SiO_2	0.01	XRF	75.8	47.8	73.7	51.5	73.4	51.2	73.8
Al_2O_3	0.01	XRF	12.3	14.8	12.2	15.1	12.4	15.1	11.1
Fe_2O_3	0.01	XRF	1.18	14.5	1.84	10.1	1.47	10.5	5.71
MgO	0.01	XRF	0.12	6.55	0.15	6.86	0.17	6.86	0.12
CaO	0.01	XRF	0.07	5.42	0.17	10.2	0.85	9.69	0.12
Na_2O	0.01	XRF	1.06	1.36	0.4	2.41	2.97	2.42	0.18
K_2O	0.01	XRF	7.87	2.86	8.65	1.05	6.21	1.51	5.01
TiO_2	0.01	XRF	0.09	1.20	0.09	1.11	0.03	1.18	0.07
P_2O_5	0.01	XRF	< 0.01	0.11	< 0.01	0.12	0.1	0.11	< 0.01
MnO	0.01	XRF	0.02	0.66	0.02	0.29	0.08	0.37	0.03
LOI			0.84	3.42	1.14	1.19	0.94	1.46	3.27
Sum			99.4	98.7	98.3	99.9	98.5	100.5	99.3
Ag	0.5	AR / ICP-MS	< .5	< .5	< .5	< .5	< .5	< .5	< .5
As	1	AR / ICP-MS	2	4	4	1	< 1	1	1
Ba	0.1	ICP-MS	322.2	110.9	132.5	139.5	159.1	108.7	81.7
Bi	0.1	AR / ICP-MS	4.3	11.1	10.6	< .5	0.8	1.9	56.7
Cd	0.1	AR / ICP-MS	2.4	21.9	0.7	0.9	54.5	0.3	0.2
Co	0.1	ICP-MS	1.3	36.7	0.9	34.5	5	32.8	7.6
Cs	0.1	ICP-MS	4.9	23	6.2	6.3	6.8	11.3	5.5
Cu		AR / ICP-MS	98	134	120	74	24	89	631
Ga	0.1	ICP-MS	17.6	24.7	15.3	15.6	17.5	17.1	23.2
Hf	0.1	ICP-MS	2.5	3	3.5	3	1.4	2.8	2.3
Mo	0.1	AR / ICP-MS	2.6	4.1	3.1	0.8	2.2	0.8	4.5
Nb	0.1	ICP-MS	23.8	6.1	20.5	5.5	28.4	6.1	18.5
Ni	1	AR / ICP-MS	2	56	2	33	2	32	2
Pb	1	AR / ICP-MS	11	14	19	14	8	4	15
Rb	0.1	ICP-MS	471.2	402.3	501.4	80.8	352.6	155.8	382.8
Sb	0.5	AR / ICP-MS	< .5	< .5	< .5	< .5	< .5	< .5	< .5
Sn	1	ICP-MS	17	85	24	5	24	14	54
Sr	0.1	ICP-MS	45.3	99.2	37.4	153.1	26.7	161.8	11.1
Ta	0.1	ICP-MS	3.4	0.3	2.9	0.4	6.9	0.3	2.6
Th	0.1	ICP-MS	26.3	3.8	21.1	3	5.4	3.2	21.9
Tl	0.1	AR / ICP-MS	1.7	1.8	2.2	0.7	1.2	0.9	1
U	0.1	ICP-MS	15.3	1.4	11.6	1	23.4	0.9	13.2
V	5	ICP-MS	< 5	243	5	208	6	223	< 5
W	1	ICP-MS	16	28	10	< 1	2	9	20
Y	0.1	ICP-MS	25.7	38.3	31.5	30.5	20.7	30	40
Zn	1	AR / ICP-MS	26	4515	115	128	9373	116	69
Zr	0.1	ICP-MS	58.7	100.8	56.5	100.4	23.4	89.2	48.2
La	0.1	ICP-MS	6.2	16.3	7.3	12	10.5	11.7	12.7
Ce	0.1	ICP-MS	14.1	31.6	18.9	24.9	16.6	25.1	28.8
Pr	0.01	ICP-MS	1.82	3.66	2.28	3.11	1.83	2.97	3.58
Nd	0.1	ICP-MS	6.9	19.1	9.1	15.4	6.7	13.6	14.8
Sm	0.1	ICP-MS	2.6	4.5	2.9	3.9	2.6	3.4	4.7
Eu	0.01	ICP-MS	0.34	1.64	0.26	1.05	0.7	1.22	0.31
Gd	0.01	ICP-MS	2.55	6.48	4.23	4.66	2.59	4.61	5.19
Tb	0.01	ICP-MS	0.67	1	0.7	0.84	0.47	0.8	0.86
Dy	0.01	ICP-MS	3.95	6.11	4.76	5.3	2.83	4.85	5.95
Ho	0.01	ICP-MS	0.88	1.21	0.96	1	0.55	1.01	1.19
Er	0.01	ICP-MS	2.84	3.6	3.21	3.06	1.5	3.06	3.5
Tm	0.01	ICP-MS	0.49	0.6	0.52	0.45	0.23	0.39	0.52
Yb	0.01	ICP-MS	3.13	3.14	3.36	2.69	1.75	2.74	3.42
Lu	0.01	ICP-MS	0.53	0.54	0.53	0.45	0.23	0.4	0.56

Notes: 1. Major oxides and their detection limits are in wt %. 2. Trace elements and REE, and their detection limits, are in ppm. 3. Values preceded by ">" are above detection limit. 4. **ICP-MS** = lithium metaborate/tetraborate fusion and nitric acid digestion followed by inductively coupled mass spectrometry. **AR / ICP-MS** = Aqua Regia digestion followed by inductively coupled mass spectrometry. **XRF** = X-ray fluorescence.

Table 1 *(cont'd)*. Lithogeochemical data from drillhole 93-36-4 at the Cheaver Lakes East sulphide occurrence.

Drillhole No. (ending with drillhole depth in metres)			93-36-4-94	93-36-4-101.8	93-36-4-103	93-36-4-104.2	93-36-4-115.5	93-36-4-131.5
	Detection Limit	Rock Type / Method	Feldspar phyric rhyolite	Po, ccp, gn, sph, py vein	Altered amphibolite heavy po	Metasediment with disseminated py and po	Sheared Fox Ridge Granite	Pyrrhotite vein in metasediment
SiO_2	0.01	XRF	74.7	7.1	52.7	62.4	72	55.3
Al_2O_3	0.01	XRF	12.7	5.35	15.8	13.5	12.3	12.2
Fe_2O_3	0.01	XRF	1.08	49.1	13.6	8.47	3.18	19
MgO	0.01	XRF	0.11	0.73	1.55	1.61	0.45	0.71
CaO	0.01	XRF	0.58	0.34	0.68	2.99	0.73	0.43
Na_2O	0.01	XRF	3.03	6.21	0.93	1.72	1.33	0.2
K_2O	0.01	XRF	5.99	0.78	4.82	3.89	7.18	4.01
TiO_2	0.01	XRF	0.09	0.09	1.67	1.27	0.36	1.01
P_2O_5	0.01	XRF	< 0.01	< 0.01	0.34	0.3	0.07	0.24
MnO	0.01	XRF	0.03	0.6	0.27	0.32	0.13	0.09
LOI			0.85	12.9	4.59	2.09	1.03	5.16
Sum			99.1	83.3	97	98.6	98.7	98.4
Ag	0.5	AR / ICP-MS	< .5	185.5	3	< .5	0.6	0.7
As	1	AR / ICP-MS	1	2	2	3	2	1
Ba	0.1	ICP-MS	73.1	26.1	227.1	500.4	505.4	139.6
Bi	0.1	AR / ICP-MS	0.7	422.8	9.9	3.6	1	9.6
Cd	0.1	AR / ICP-MS	0.5	1306.6	147	2.1	1.2	24
Co	0.1	ICP-MS	0.7	19.6	13.6	12.6	5.4	31.9
Cs	0.1	ICP-MS	2.6	1	15.6	10.5	4.7	3.1
Cu		AR / ICP-MS	19	26139	1189	103	250	2329
Ga	0.1	ICP-MS	18.4	15.1	24.2	20	14.2	20.7
Hf	0.1	ICP-MS	3.6	< .5	9.1	9.6	6.3	8.8
Mo	0.1	AR / ICP-MS	1.8	373	3.7	1.7	3.5	1.6
Nb	0.1	ICP-MS	22.9	2.2	21.2	19.6	11.8	18
Ni	1	AR / ICP-MS	3	46	7	12	4	15
Pb	1	AR / ICP-MS	9	2053	14	8	13	4
Rb	0.1	ICP-MS	265.4	49.1	368.9	261	281.4	298.2
Sb	0.5	AR / ICP-MS	< .5	< .5	< .5	< .5	< .5	< .5
Sn	1	ICP-MS	7	61	108	21	11	67
Sr	0.1	ICP-MS	47.9	1.8	6	126.8	73.9	5.9
Ta	0.1	ICP-MS	3.5	< .1	1.3	1.3	1	1.3
Th	0.1	ICP-MS	25.6	0.9	14.7	8.7	13.9	10.4
Tl	0.1	AR / ICP-MS	0.9	0.5	0.9	1	1	0.4
U	0.1	ICP-MS	15	0.3	3.7	2.8	5.3	2.8
V	5	ICP-MS	< 5	55	85	87	21	65
W	1	ICP-MS	7	7	43	17	3	60
Y	0.1	ICP-MS	50.4	7.9	69.8	57.2	37.1	60.5
Zn	1	AR / ICP-MS	118	> 99999	22606	485	213	3934
Zr	0.1	ICP-MS	58.3	18.1	350.8	319.5	226.6	289.6
La	0.1	ICP-MS	13.9	1.2	47.3	34.1	37	75.3
Ce	0.1	ICP-MS	32.7	3.3	94.9	69.8	71.8	147.8
Pr	0.01	ICP-MS	4.14	0.36	11.44	8.44	7.55	16.72
Nd	0.1	ICP-MS	18.9	1.2	47	37.5	30.4	68
Sm	0.1	ICP-MS	6.2	0.4	10.7	8.4	5.9	16.2
Eu	0.01	ICP-MS	0.35	0.11	1.77	2.23	1.02	1.79
Gd	0.01	ICP-MS	6.53	0.67	11.31	9.65	5.59	14.8
Tb	0.01	ICP-MS	1.19	0.16	1.81	1.53	0.99	1.99
Dy	0.01	ICP-MS	7.41	1.09	10.78	9.32	6.39	11.03
Ho	0.01	ICP-MS	1.45	0.27	2.31	1.84	1.19	1.93
Er	0.01	ICP-MS	4.36	0.78	7.16	5.86	3.86	5.98
Tm	0.01	ICP-MS	0.65	0.11	1.11	0.84	0.56	0.85
Yb	0.01	ICP-MS	4.7	0.66	6.56	4.56	3.39	5.39
Lu	0.01	ICP-MS	0.71	0.12	1.16	0.8	0.5	0.89

Notes *(cont'd)*: 5. Ccp = chalcopyrite, gn = galena, po = pyrrhotite, py = pyrite, sph = sphalerite. 6. All analyses were conducted at Acme Analytical Laboratories Ltd., Vancouver, British Columbia.

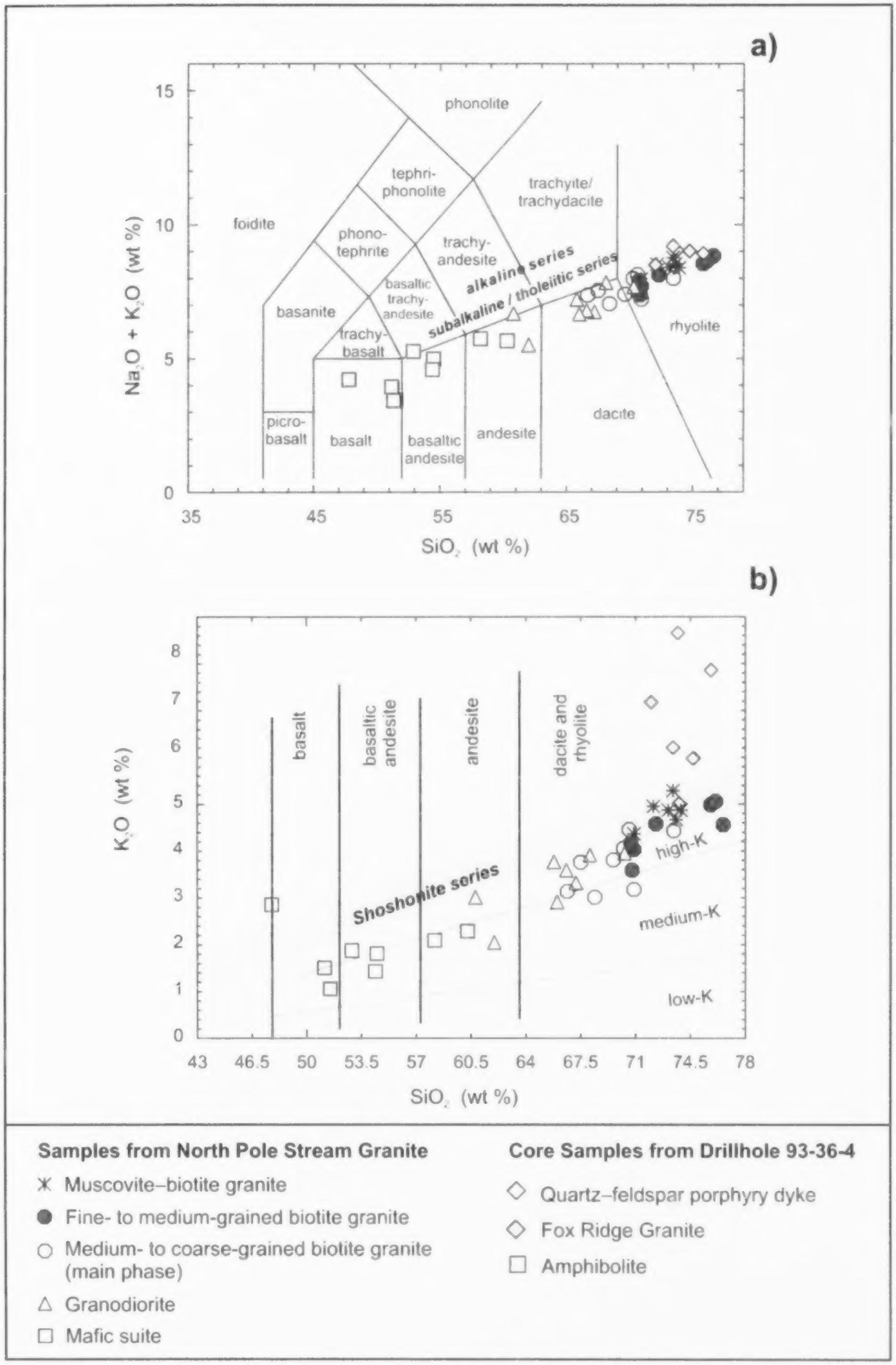

Figure 8. Major-element lithogeochemical discrimination diagrams for Cheaver Lakes East samples. a) $Na_2O + K_2O$ vs SiO_2. Yellow line separating alkaline and subalkaline/tholeiitic series is from Irvine and Baragar (1971). b) K_2O vs SiO_2. Field boundaries in both diagrams are from Le Maitre et al. (1989), and shoshonite series is from Rickwood (1989). Data for North Pole Stream Granite are from Whalen (1993).

sample plots in the high-K dacite and rhyolite field, well above the shoshonitic series of Rickwood (1989). Most felsic samples from Whalen (1993) lie within the dacite and rhyolite field and plot on or near the high-K trend line (Fig. 8b), but others plot higher, into the shoshonitic series. Although the porphyry dyke samples show Na_2O contents of 0.4 wt % to 6.21 wt % (avg. 2.73 wt %), their elevated K_2O contents (5–7.9 wt %) cause them to plot well above the trend for North Pole Stream Granite samples (Fig. 8b). The high K_2O content is not surprising, given the dominance of fine-grained white mica in the groundmass of the more altered porphyry dyke samples. Despite their atypically high K_2O, the samples are strongly peraluminous, having Al_2O_3 / (K_2O + Na_2O + CaO) values of > 1.1.

The amphibolite samples fall in the basalt field on both the Na_2O + K_2O vs SiO_2 and K_2O vs SiO_2 diagrams (Fig. 8a, 8b), which supports a tholeiitic basalt protolith for the Trousers Lake Complex, as suggested by Fyffe et al. (1988). Two of these samples have low (< 1.5 wt %) K_2O contents, whereas a third sample has a K_2O content of about 3 wt % and shows evidence of sericitized plagioclase in thin section. (A fourth sample with significant sulphide mineralization was not included in the diagrams.)

Alkali (Na_2O + K_2O) contents of the amphibolites are generally low, in keeping with the presumed unaltered derivation (from tholeiitic basalt) of these rocks. However, the paucity of alkali is unexpected, given the amphibolites' degree of deformation and the high mobility of alkali elements during hydrothermal alteration and deformation. These low values suggest that amphibolitization took place under conditions characterized by closed systems with respect to alkali elements.

Trace-Element Chemistry

Figure 9a presents primitive-mantle-normalized, trace-element spider diagrams for samples of the porphyry dykes and of the main phase (medium- to coarse-grained biotite granite) of the North Pole Stream Granite. Compared with the main phase of the granite, the porphyry dykes are depleted in Ba, Sr, Nd, Ti, Hf, light rare-earth elements (LREE), Zr, and Eu; and are enriched in Rb, Th, U, K, and Nb. The most useful of these elements for petrogenetic discrimination and fractionation are the high-field-strength elements Ti, Hf, Zr, Nb, and Ta, which are relatively immobile, even under conditions of hydrothermal alteration.

The Nb/Ti vs Zr/Ti plot (Fig. 9b) depicts two fractionation trends for samples from the North Pole Stream Granite. The trend on the left shows a slight increase in Nb/Ti with increasing Zr/Ti in the mafic and granodiorite samples of Whalen (1993). The trend on the right shows a marked increase in Nb/Ti with increasing Zr/Ti, as the trend progresses from the main granite phase to the more evolved phases (fine- to medium-grained biotite granite and muscovite–biotite granite). Porphyry dykes samples have slightly higher Nb/Ti and Zr/Ti values than do most North Pole Stream samples (Fig. 9b). However, Zr and Ti contents for the porphyry dyke samples are considerably lower than for most Whalen (1993) samples, suggesting that, if the two rock groups were related, the porphyry dykes would have to represent a more highly fractionated part of the North Pole Stream Granite.

When normalized to Y, Zr and Ti values for most granitic samples from the North Pole Stream Granite plot along a line with slope (m) = 14, whereas those for the porphyry dyke samples and three of the fine- to medium-grained biotite granite samples plot along a line with m = 9 (Fig. 9c). Samples that plot along a line of constant Zr/Ti are generally considered to have undergone a similar fractionation history (Barrett and MacLean 1994). The three atypical granite samples fall on a Ti/Y vs Zr/Y trajectory unlike that of other North Pole Stream granitic samples and thus may have a different, possibly unrelated, crystallization history.

The North Pole Stream Granite samples yield Zr and Hf contents of 222 ppm and 7.6 ppm, respectively. On a plot of Zr/Hf vs TiO_2, Zr/Hf ranges from 26 to 36, typical of crustal values (Fig. 9d). For the three fine- to medium-grained granite samples (discussed above), Zr/Hf is 14 to 24, lower than for the main phase of the North Pole Stream Granite. Similarly, Zr/Hf for the porphyry dyke samples ranges between 16.1 and 23.5 (avg. 18.7), which is low relative to crustal values (Fig. 9d).

Zr/Hf systematics are important to understanding the genesis of the porphyry dykes. In most magmatic systems, the isovalent (+ 4) high-field-strength elements Hf and Zr behave similarly (Dostal and Chatterjee 2000). Zr is incompatible in fractionating felsic melts with SiO_2 contents ≤ 67 wt % (Watson and Harrison 1983); however, at higher (≥ 70 wt %) SiO_2 contents, Zr becomes highly compatible and rapidly crystallizes in the form of zircon as temperatures decrease. In magmas that have undergone extensive zircon fractionation, Zr/Hf may be used as a gauge of extreme fractionation (Claiborne 2006, and references therein). Most igneous rock shows Zr/Hf close to mantle values of 25 to 35. The ratio remains constant even at lower (< 100 ppm) Zr concentrations. However, during extreme fractionation of high-silica magmas — i.e., at a point where Zr solubility is very low — zircon crystallization consumes Hf at a decreased rate, even though the partition coefficient of Hf in zircon relative to the melt is a very high 3193 (Mahood and Hildreth 1983). This causes Zr/Hf of the melt to drop below 20. The decrease in Zr/Hf at low Zr content is due to the limited number of zircon crystals in which Hf can substitute and ultimately fractionate.

On a Pb–Cu–Zn ternary diagram (Fig. 9e), samples from the North Pole Stream Granite display a typical trend, in which Pb contents move from low to high, and Zn/Cu slightly decreases, with increasing fractionation. This trend reflects incorporation of Pb into K-feldspar with a partition coefficient of 2.473 (Nash and Crecraft 1985). Porphyry dykes do not fall along the same fractionation trend as do rocks of the North Pole Stream Granite. Instead, they plot along a line that is adjacent and parallel to the Zn–Cu axis, showing variable Zn/Cu and low Pb. It is possible that the low Pb in these samples is due simply to Pb loss during feldspar-destructive alteration. However, given that the porphyry dyke samples are variably altered, their consistent deviation toward low Pb may be due, not to alteration, but rather to low Pb in the parent melt, resulting from extreme fractionation of K-feldspar and, with it, most of the Pb.

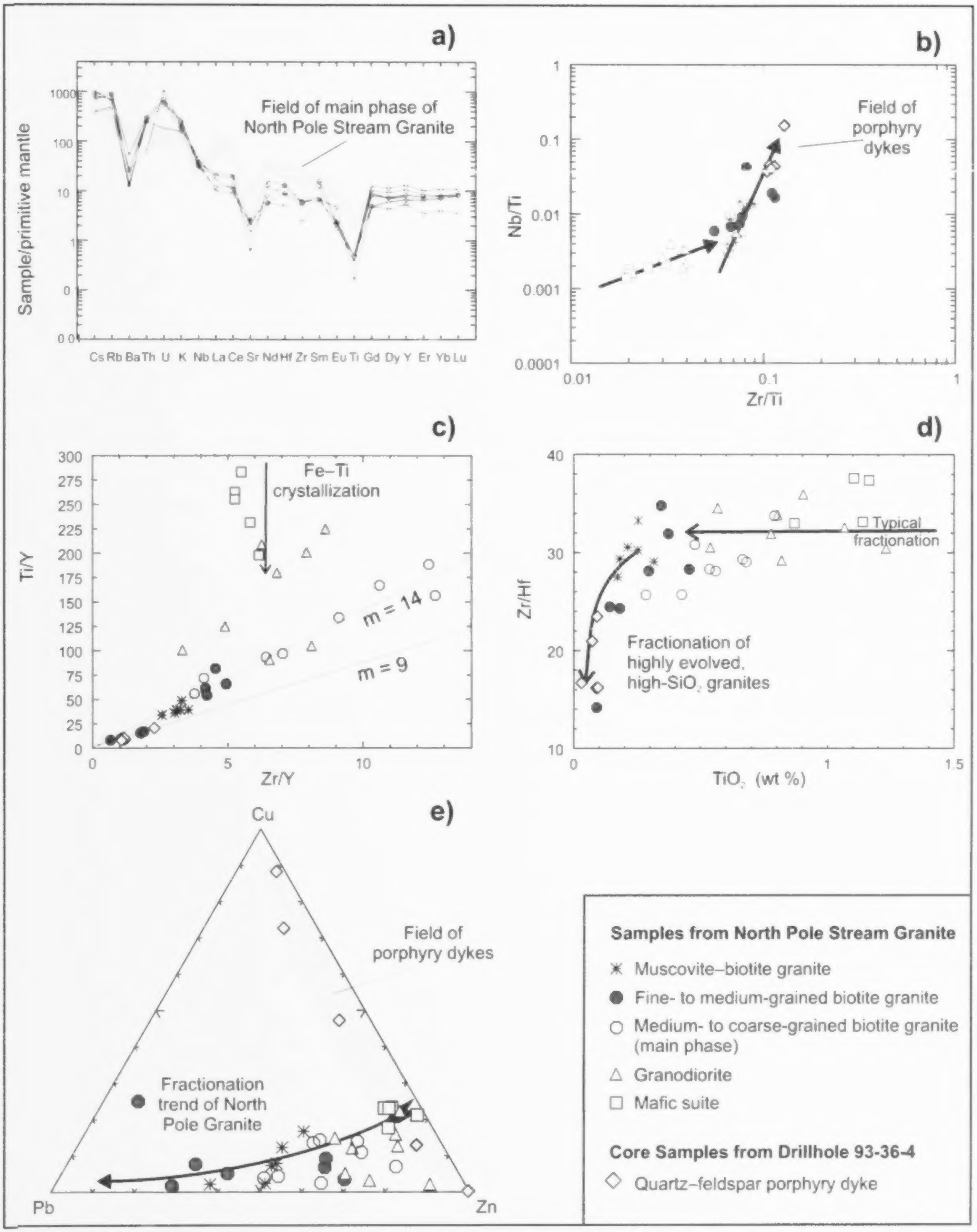

Figure 9. Trace-element lithogeochemical diagrams of porphyry dyke samples from Cheaver Lakes East. a) Primitive-mantle-normalized spider diagram, using normalization factors of Taylor and McLennan (1985). b) Nb/Ti vs Zr/Ti diagram. c) Ti/Y vs Zr/Y diagram. d) Zr/Hf vs TiO$_2$ diagram. e) Pb–Cu–Zn ternary diagram. Data for North Pole Stream Granite are from Whalen (1993).

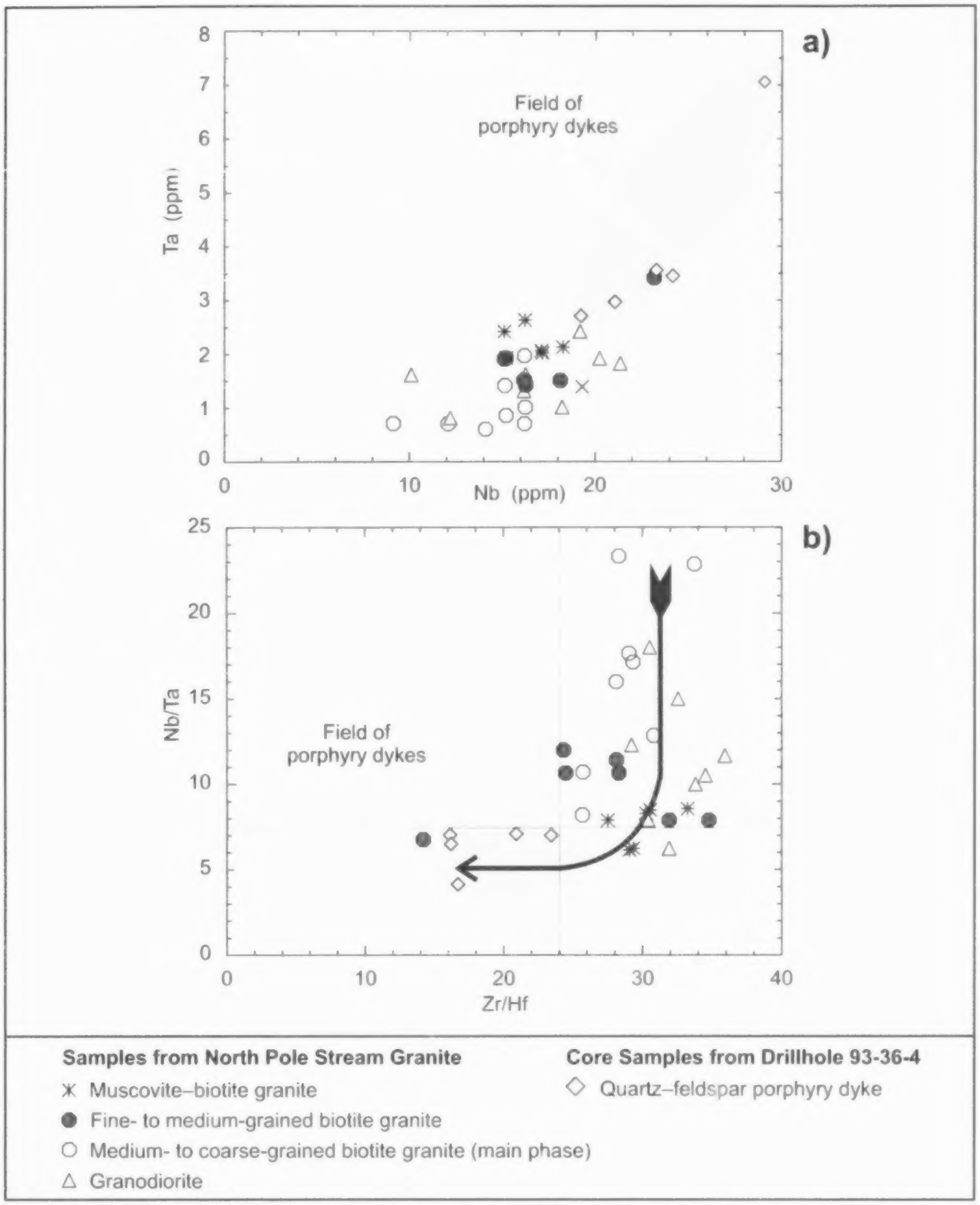

Figure 10. High-field-strength-element discrimination diagrams for porphyry dyke samples from Cheaver Lakes East. Data for North Pole Stream Granite are from Whalen (1993). a) Ta vs Nb. b) Nb/Ta vs Zr/Hf.

Nb and Ta are highly incompatible in magmatic systems, as partition coefficients of these elements are low for most silicate phases. However, accessory minerals such as rutile, cassiterite, and columbite–tantalite have high partition coefficients for Nb and Ta (Brennan et al. 1994), as does titanite (Green and Pearson 1987). Concentrations of Nb and Ta in the North Pole Stream Granite samples rise with increasing degree of fractionation, whereas Nb/Ta decreases with increasing fractionation (Fig. 10a, 10b). Porphyry dyke samples have

Nb contents ranging between 18.5 ppm and 28.4 ppm, which overall are higher than in the North Pole Stream Granite samples. Ta content of the porphyry dyke samples (2.6–6.9 ppm) is also higher than in the granitic samples. Nb/Ta for the porphyry dyke samples ranges from 4.1 to 7.1 (avg. 5.1), well below values for various phases of the North Pole Stream Granite (Fig. 10b).

Fractional crystallization of accessory minerals such as rutile could cause Nb/Ta to decrease in fractionated granitic rocks (Green 1995); however, this should lead to a decreased concentration of both Nb and Ta in the remaining melt. Such is not the case with porphyry dyke samples from Cheaver Lakes East. Instead, their Nb and Ta concentrations are higher, and their Nb–Ta ratios are lower, than in almost all North Pole Stream Granite samples (Fig. 10a, 10b). Although Nb/Ta could change if fractional crystallization of a mineral phase preferentially partitions Nb over Ta (or vice versa), that process clearly could not account for increased Nb and Ta concentrations in the remaining melt.

Rare-Earth-Element Chemistry

Rare-earth-element (REE) data for the 13 core samples are listed in Table 1 and graphically represented in Figure 11. In the following discussion, the Eu anomaly is defined as $Eu_n/Eu^* = Eu_n / \sqrt{(Sm_n \times Gd_n)}$. Unless otherwise stated, the normalization factors (n) are from Evensen et al. (1978).

The five porphyry dyke samples are characterized by very low ΣREE, which ranges from 10.4 ppm to 103 ppm (avg. 53.7 ppm). The profiles are flat (Fig. 11a), as La_n/Lu_n values are 1.2 to 7.6 (avg. 2.9). Four of the samples have pronounced negative Eu anomalies (Fig. 11a), with Eu/Eu* values of 0.192 to 0.62 (avg. 0.35). The remaining sample shows almost no Eu anomaly (Eu/Eu* = 0.94) and has a slightly lower heavy-rare-earth-element (HREE) content. Such Eu-depleted profiles are consistent with a magma that has undergone extensive feldspar fractionation. Samples from the main phase of the North Pole Stream Granite show higher LREE contents than do the porphyry dyke samples. The Fox Ridge Granite sample (not depicted in Fig. 11) has a ΣREE of 176 ppm, shows a moderately negative Eu anomaly (Eu/Eu* = 0.62), and is characterized by LREE enrichment, as indicated by a La_n/Lu_n of 7.7. Overall, the Fox Ridge Granite and North Pole Stream Granite profiles are similar.

The amphibolite samples are characterized by ΣREEs of 76 to 255 (avg. 130) and have relatively flat Eu profiles (Eu/Eu* = 0.56–1.07 (avg. 0.88); Fig. 11b). These rocks show LREE enrichment and have gently to moderately sloping profiles, with La_n/Lu_n at 2.8 to 4.4 (avg. 3.6). The two sedimentary rock samples have positively sloping North American Shale Composite (NASC)-normalized REE profiles; for both, La_n/Lu_n is close to 0.5 (Fig. 11c). The absence of a negative Eu anomaly implies nonexistent to minimal hydrothermal input, whereas the lack of a positive Ce anomaly is interpreted to represent deposition in a reducing water column (Toyoda and Masuda 1991).

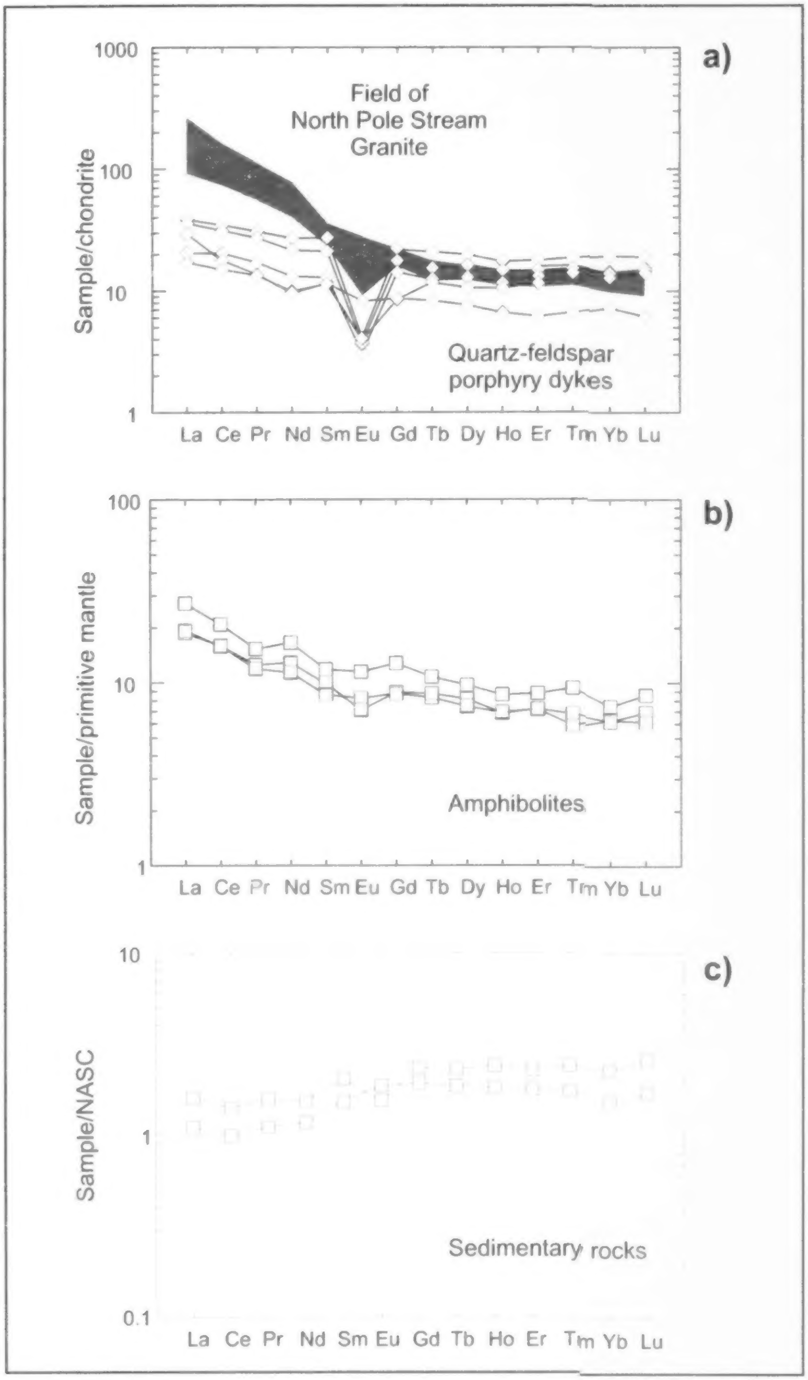

Figure 11. Normalized REE diagrams for rocks collected from drillhole 93-36-4. a) Chondrite-normalized REE diagram for porphyry dyke samples; normalization factors are from Evensen et al. (1978). b) Primitive-mantle-normalized REE diagram for amphibolite samples; normalization factors are from Taylor and McLennan (1985). c) NASC-normalized REE diagram for sedimentary samples; normalization factors are from Gromet et al. (1984).

The one sample of massive-sulphide vein analyzed during this investigation (not plotted on Fig. 11) has a very low REE content, a ΣREE of 10.4 ppm, and a relatively flat REE profile (La_n/Lu_n = 1.03). The sample also shows a slight depletion of middle REE (Nd, Sm, Eu, and Gd). Low ΣREE is expected here for two reasons: 1) hydrothermal sulphide has a low ability to incorporate REE (Graf 1977), and 2) no REE-hosting trace-mineral phases such as carbonate are present.

TECTONIC SETTING

A previous report on amphibolite-grade rocks in the Miramichi Highlands area (Fyffe et al. 1988) indicated that two types of amphibolites — striped and unstriped — may extend into the Cheaver Lakes East area. Such amphibolites found south of the report area were interpreted to have formed from mafic volcanic and related sedimentary rocks showing affinities with volcanic-arc and within-plate basalts, respectively (Fyffe et al. 1988).

Amphibolite samples from the current investigation plot on the tholeiitic trend on the $Na_2O + K_2O$–FeO–MgO diagram (Fig. 12a), and confirm the subalkalic/tholeiitic affinity suggested by the $Na_2O + K_2O$ vs SiO_2 diagram (Fig. 8a). On the Zr–Ti–Sr and Zr–Ti–Y diagrams, the amphibolites plot in the ocean-floor-basalt field (Fig. 12b, 12c). The use of Sr as a discriminator is commonly restricted to unaltered rocks because Sr, which normally resides in feldspar, is mobile under conditions of feldspar-destructive hydrothermal alteration (Pearce and Cann 1973). However, the Zr–Ti–Sr diagram is used here for two reasons: 1) there is an apparent conservation of alkali elements in the amphibolites (Fig. 8a, 8b), and 2) all amphibolite samples fall in the same field (ocean-floor basalt) on the Zr–Ti–Y diagram.

The relationship of amphibolites in the Trousers Lake Complex to mafic volcanic rocks in the Bathurst Supergroup of northeastern New Brunswick is poorly understood (Fig. 1). Alkali and tholeiitic basalts of the Tetagouche, California Lake, and Sheephouse Brook groups of the Bathurst Supergroup are interpreted to represent ensimatic to transitional back-arc crust that formed in the Tetagouche–Exploits back-arc basin (van Staal et al. 2003). The volcanic-arc and within-plate nature of some Trousers Lake amphibolites is consistent with such a tectonic setting (Fyffe et al. 1988).

Several discrimination diagrams based on trace elements are used to fingerprint the tectonic setting of felsic intrusive rocks. On the Rb vs Y + Nb diagram (Fig. 13a), the porphyry dyke samples plot within the S-type granite field. Most North Pole Stream Granite rocks plot in the I-type granite field, although a few samples fall within the A-type granite field. Trends for partial melting and fractional crystallization of different source areas (from Christiansen and Keith 1996) have been superimposed in Figure 13a. Comparison of these trends with geochemical data from the current investigation and Whalen (1993) suggests that the porphyry dykes were derived from magma generated from an accretionary prism that underwent post-generation contamination, whereas the North Pole Stream Granite originated from a less contaminated parent magma. On a Rb vs Rb/Nb diagram, most porphyry dyke

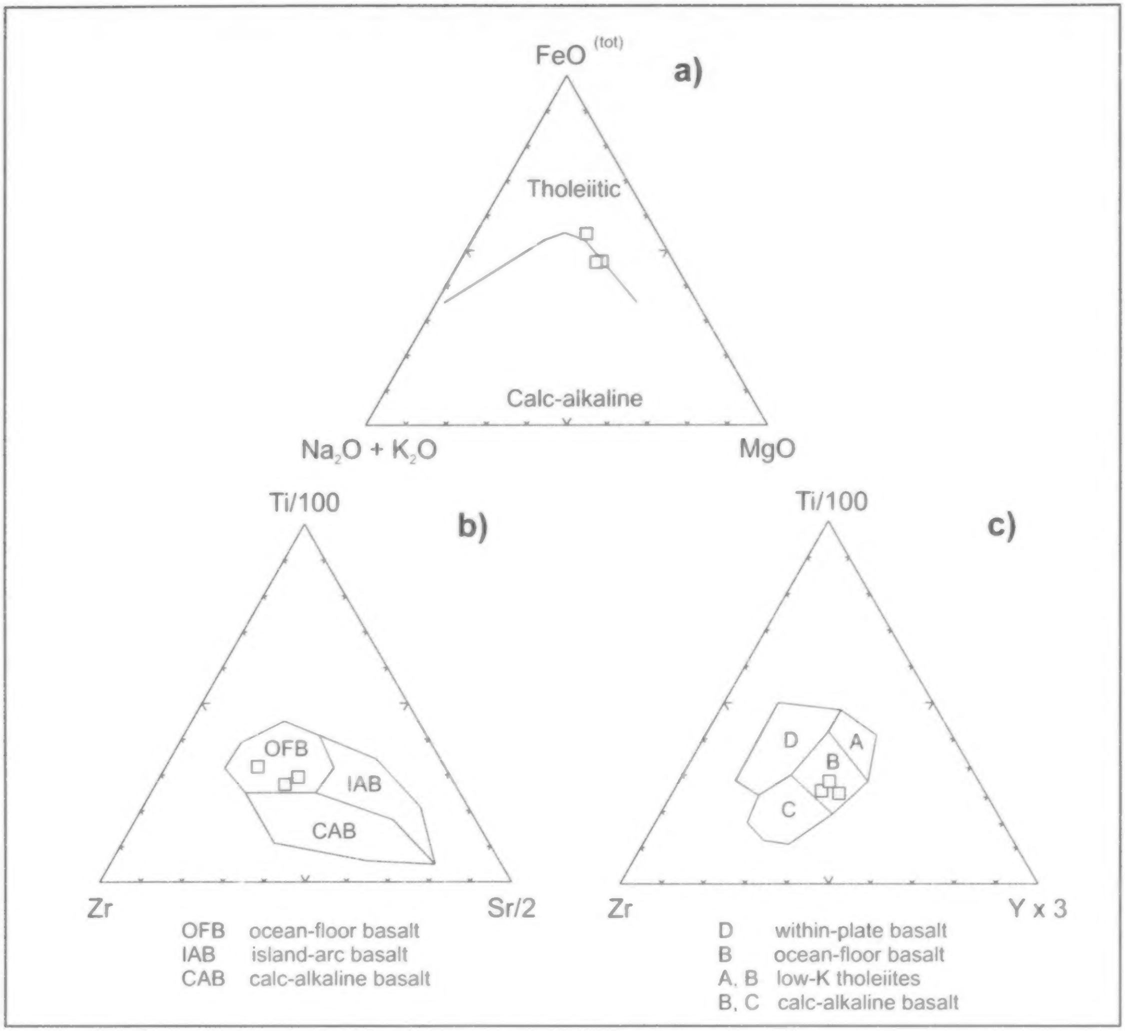

Figure 12. Tectonic discrimination diagrams for mafic volcanic rocks as applied to amphibolite rocks from the Cheaver Lakes East area. a) $Na_2O + K_2O–FeO^{(tot)}–MgO$; diagram from Irvine and Baragar (1971). b) Zr–Ti/100–Sr/2; diagram from Pearce and Cann (1973). c) Zr–Ti/100–Y x 3; diagram from Pearce and Cann (1973). Data for North Pole Stream Granite are from Whalen (1993).

samples plot in the S-type granite field, whereas the North Pole Stream Granite samples plot in the I-type and A-type granite fields (Fig. 13b). The porphyry dykes display chemical characteristics of S-type intrusions: they are peraluminous, depleted in Na, enriched in K, and have low ΣREE. Recognition of these dykes as S-type granitoids is significant from an economic standpoint, as Sn–W–base-metal deposits are commonly associated with S-type intrusions (Christiansen and Keith 1996).

On a Y–Nb–Ce diagram, most data for the porphyry dykes and several phases of the North Pole Stream Granite fall within the A2 (crustally derived) magma field (Fig. 13c). On the Th/Ta vs Yb diagram (Fig. 13d), North Pole Stream Granite data are evenly distributed across the active-continental-margin field. Most porphyry dyke samples plot in the active-continental-margin field but lie closer to its boundary with the within-plate volcanic zone field.

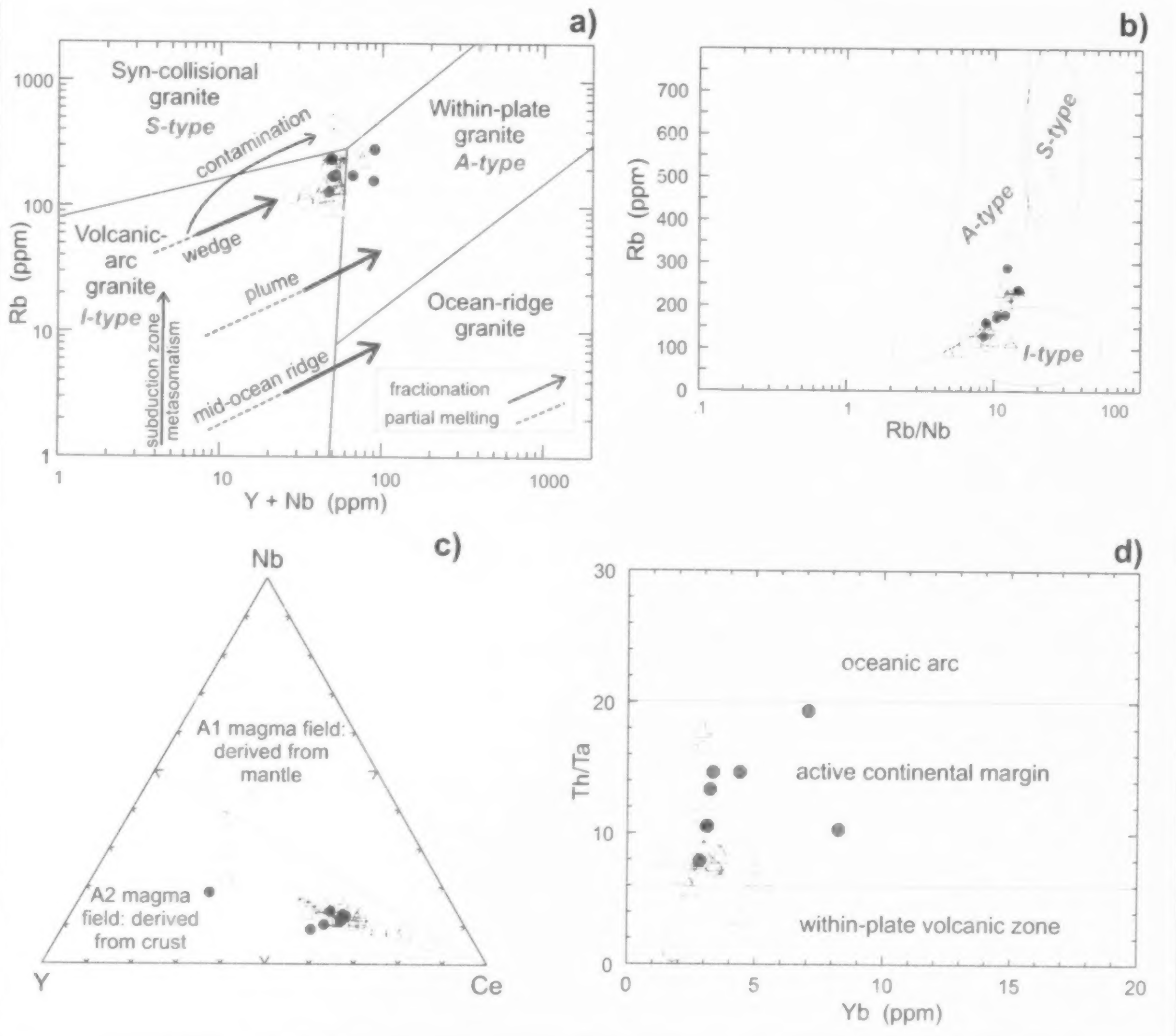

Samples from North Pole Stream Granite

- ⋇ Muscovite–biotite granite
- ● Fine- to medium-grained biotite granite
- ○ Medium- to coarse-grained biotite granite (main phase)
- △ Granodiorite
- ☐ Mafic suite

Core Samples from Drillhole 93-36-4

- ◇ Quartz–feldspar porphyry dyke

Figure 13. Tectonic discrimination diagrams for porphyry dykes from the Cheaver Lakes East area. a) Rb vs Y + Nb diagram from Pearce et al. (1984). Granitoid nomenclature (in red italics) and melting and fractionation vectors are from Christiansen and Keith (1996). b) Rb vs Rb/Nb diagram from Christiansen and Keith (1996). c) Y–Nb–Ce diagram from Eby (1992). d) Th/Ta vs Yb diagram from Gorton and Schandl (2000). Data for North Pole Stream Granite are from Whalen (1993).

DISCUSSION

As just described, mineralization (Zn, Cu, Sn, W, Mo, and U) at the Cheaver Lakes East occurrence is spatially and temporally related to quartz–feldspar porphyry dykes. Macroscopically similar dykes and related granophile-element mineralization have been observed at nearby Long Lake and Cheaver Lakes, which suggests that mineralization at all three locales may be part of a larger system. The following discussion highlights critical points concerning the evolution of this system, including timing of dyke emplacement, and pressure–temperature–composition constraints on the porphyry dykes.

Timing of Dyke Emplacement

Given that porphyry dykes cut Ordovician sedimentary and amphibolitized mafic volcanic rocks at Cheaver Lakes East and also cut main-phase rocks of the North Pole Stream Granite at Long Lake, dyke emplacement could have taken place during three possible times: 1) coevally with emplacement of the Late Silurian–Early Devonian North Pole Stream Granite, 2) coevally with volcanism of the Early Devonian Tobique Group (ca. 412 Ma), or 3) coevally with a Late Devonian intrusion, similar to those observed elsewhere in New Brunswick (see below).

If the porphyry dykes are genetically related to the North Pole Stream Granite, they must be late dykes sourced from a deeper, more highly differentiated part of the magma chamber (Burnham 1997). However, no apparent link exists between the porphyry dykes at Cheaver Lakes East and the main phase of the North Pole Stream Granite, apart from their spatial proximity. In fact, the porphyry dyke and North Pole Stream Granite samples show substantial variation in their Nb and Ta contents and Nb/Ta, suggesting that the two sample groups were derived from different source magmas. At present, the age of mineralization at Cheaver Lakes East can be only loosely constrained to having occurred after emplacement of the main phase of the North Pole Stream Granite at 417 ± 1 Ma.

The porphyry dykes are unlikely to have been feeder dykes for Early Devonian volcanic rocks of the Tobique Group farther west (Fig. 1), as their trace-element systematics have no recognizable analogue in either the felsic volcanic or hypabyssal intrusions of that group (Walker 2005, and references therein). The Tobique Group hosts several base-metal occurrences of volcanogenic massive-sulphide affinity such as those at Sewell Brook (Wilson 1992), Mount Costigan (Fyffe and Pronk 1985), and Shingle Gulch East. At least one of these occurrences (Shingle Gulch East) resulted from hydrothermal fluids with an inferred magmatic component (Walker 2005) that possibly is analogous to fluids responsible for mineralization at Cheaver Lakes East. However, the base-metal content at Cheaver Lakes East shows Zn + Cu with little or no Pb. Conversely, deposits hosted by the Tobique Group are rich in Zn + Pb and have only minor Cu. Moreover, the Cheaver Lakes East occurrence is enriched in Sn, W, U, Th, and Mo; deposits hosted by the Tobique Group show no such enrichment.

The third and most plausible age of dyke emplacement and coincident mineralization at Cheaver Lakes East is Late Devonian or about 385 Ma to 359 Ma (see time scale of Gradstein et al. 2004). Such a time frame would be consistent with the ages of other significant, post-orogenic Sn–W–Mo mineralized systems related to felsic intrusions in New Brunswick. Ages for these systems are fairly tightly constrained: ca. 381 Ma for Burnthill (MacLellan et al. 1990), 376 ± 4 Ma for Dungarvon (MacLellan et al. 1990), and ca. 360 Ma for Mount Pleasant (Sinclair et al. 1988).

Although the Cheaver Lakes East dykes have yet to be age-dated, mineralized rocks related to similar dykes at the Long Lake U occurrence (Fig. 1) will be undergoing geochronological analysis as part of a research project at the University of New Brunswick in Fredericton.

Temperature–Pressure–Composition Constraints on Porphyry Dykes

The temperature and composition of the magma from which the porphyry dykes crystallized can be constrained by a combination of zircon-saturation temperatures and petrographic evidence. The zircon-saturation temperature is calculated using the following equation from Watson and Harrison (1983):

$$\ln D^{Zr,\ zircon/melt} = \{ -3.8 - [0.85(M-1)]\} + 12\ 900/T$$

where ln = natural log of; $M = [(Na + K + 2Ca) / Al \times Si]$, all in mole fractions; $D^{Zr,\ zircon/melt}$ is the ratio of Zr concentration in ppm in zircon (476 000) to that in the saturated melt; and T = temperature in degrees kelvin.

Rearranging the equation to yield T_{Zr} gives:

$$T_{Zr} = 12\ 900 / [2.95 + 0.85M + \ln (496\ 000/Zr_{melt})]$$

This equation is applicable to a wide range of melt compositions and conditions (Watson and Harrison 1983). Zircon solubility is insensitive to pressure and deviates from the calculated values only at very low H_2O contents (≤ 1.5 wt % H_2O). These data indicate that the porphyry dykes were emplaced at 680°C to 790°C, within the temperature range of Cold Granites, as defined by Miller et al. (2003). Figure 14a shows the calculated zircon-saturation temperatures from Cheaver Lakes East, plotted with respect to pressure and temperature. For temperatures in the foregoing range, the water-saturated granite solidus translates to a H_2O content of 2 wt % to 6 wt %.

Recognizing the porphyry dykes as Cold Granites has two important implications with respect to tectonic setting and emplacement.

- The generation of granitoid magmas is generally attributed to dehydration reactions, in which water is obtained from the breakdown of muscovite, biotite, or Ca-amphibole at temperatures higher than 800°C. To form melts at temperature lower than 800°C requires an influx of water from outside the melt region (Miller et al. 2003). Such fluids could ascend into the melting zone following dehydration of underthrust sedimentary rocks or hydrous mafic silicates in mafic or ultramafic rocks. Therefore, Cold Granites are generated in tectonic settings that do not reach high temperatures and where fluid influx is high.

- At the calculated melt temperature of about 750°C, mafic minerals and calcic plagioclase are highly insoluble; therefore, the melt is near the albite–orthoclase–quartz minimum melt composition. This suggests that the dykes carried a 5% to 25% volume of crystals from the source magma (Miller et al. 2003). The low temperature and high crystal content would slow magma ascent and inhibit the magma from erupting (Miller et al. 2003). This factor is important in terms of deposit generation, as magma eruption implies a loss of fluid and reduced potential for deposit formation.

According to work by Naney (1983) on phase equilibria of Fe–Mg silicates in synthetic felsic melts, the phenocryst assemblage preserved in the porphyry dykes can be used to define limits on the temperature and water content of the parent melt. The melt compositions of Naney (1983) represent granite and granodiorite at pressures of 200 MPa and 800 MPa; both melts could produce the phenocryst assemblage of porphyry dykes at Cheaver Lakes East.

Phenocryst mineralogy of the porphyry dykes can be delineated on phase relationship diagrams for the two synthetic melts (Fig. 14b, 14c). Fields containing pyroxene or amphibole are not pertinent to the Cheaver Lakes East dykes, but those containing quartz–K-feldspar–plagioclase, and biotite may approximate P_{H_2O} conditions of the parent melt when dykes were emplaced. In the synthetic granite system (Fig. 14b), the phenocryst assemblage (quartz–K-feldspar–plagioclase–biotite) is stable between 720°C and 680°C and 0 wt % to < 4 wt % H_2O. In the synthetic granodiorite system (Fig. 14c), the same phenocryst assemblage is stable over a larger (~ 670–850°C) temperature range and somewhat narrower (~ 1.5–4 wt %) H_2O range.

Magma Fractionation

Low Zr/Hf (avg. 18.7) of the Cheaver Lakes East porphyry dyke samples indicates the degree of fractionation undergone by the parent magma of the dykes. It is interesting to note that granitic intrusions related to the polymetallic Mount Pleasant deposit in southern New Brunswick give similarly low Zr–Hf ratios of 16 to 22 (Inverno and Hutchinson 2006).

The degree of fractionation may also be considered in terms of Nb–Ta systematics. In comparison with samples from the North Pole Stream Granite, porphyry dyke samples from Cheaver Lakes East have atypically high Nb (17–30 ppm) and Ta (2.5–7 ppm) contents and low Nb/Ta (avg. 7.3) values that are typical of highly evolved felsic intrusions. Samples of the

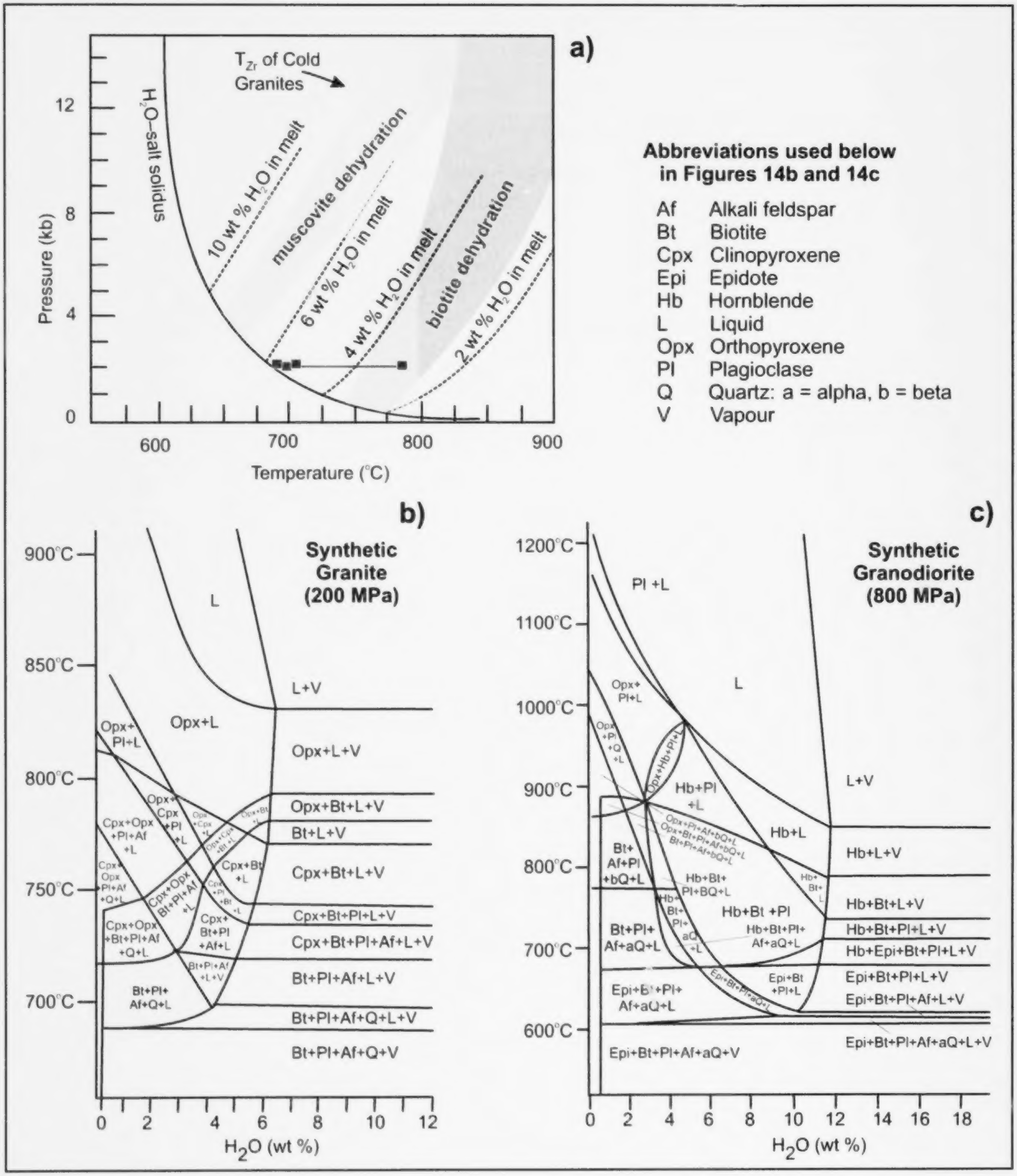

Abbreviations used below in Figures 14b and 14c

Af	Alkali feldspar
Bt	Biotite
Cpx	Clinopyroxene
Epi	Epidote
Hb	Hornblende
L	Liquid
Opx	Orthopyroxene
Pl	Plagioclase
Q	Quartz: a = alpha, b = beta
V	Vapour

Figure 14. a) Zircon-saturation temperatures calculated for porphyry samples (shown by red line and squares) from Cheaver Lakes East, plotted against field of Cold Granites as constrained by temperature and pressure. Diagram is modified from Miller et al. (2003). b) Phase relationships in the synthetic granite system at 200 MPa. c) Phase relationships in the synthetic granodiorite system at 800 MPa. Yellow fields in Figures 14b and 14c correspond to mineralogy preserved in the porphyry dyke samples. Diagrams for Figures 14 b and 14c are modified from Naney (1983).

Davis Lake Pluton associated with the East Kemptville Sn deposit in Nova Scotia show similar Nb–Ta covariation (Dostal and Chaterjee 2000). The Davis Lake data have been interpreted to reflect fractionation of Ta, Rb, and Li (and, to a lesser extent, Nb) into a fluid with high fluorine activity (Dostal and Chaterjee 2000).

Fluorine-rich fluids are commonly invoked as being key to mineralization in evolved felsic magmatic systems. Thus, it is suggested here that a Ta-rich (and fluorine-rich?) fluid phase of the porphyry dykes at Cheavers Lakes East may have been responsible for the lower Nb/Ta and high granophile-element content of the porphyry dykes.

GENETIC MODEL

The intimate association of porphyry dykes with Sn–W–Mo–base-metal mineralization at Cheaver Lakes East implies that the mineralization is magmatically derived. Under such systems, evolution and cooling of the parent magma directly influences the generation and nature of dykes and mineralizing fluids. High-level, chemically evolved dykes such as those at Cheaver Lakes East commonly represent the top or first-erupted part of a magma chamber. Such dykes are known to occur in the hanging wall of the Mount Pleasant Sn–W–Mo deposit in southwestern New Brunswick (McCutcheon 1990). Given the foregoing, the following genetic model (Fig. 15) is proposed for fractionation of the parent melt leading to porphyry dyke formation.

1. In this model, the parent magma was generated via partial melting of a pelitic sedimentary protolith at moderate temperatures (800–900°C) and an initial H_2O content of less than 4 wt %. The parent melt fit the category of S-type granite generated in a tectonic setting, transitional between active-continental-margin and within-plate-volcanic zones. Magma generation could have taken place via the mechanism proposed in the subduction/overthrust model of Schoonmaker et al. (2005). Once the magma ascended to a point in the crust where neutral buoyancy precluded further ascent, cooling and crystallization became the dominant controls on the system.

2. Under the proposed model, the fractionation of feldspar, Fe- and Ti-bearing minerals, and minerals such as apatite likely played a critical role in influencing melt chemistry. Plagioclase crystallization caused a general decrease in ΣREE and development of a strongly negative Eu anomaly. Plagioclase fractionation reduced Sr content of the residual melt, given the high partition coefficient for Sr in plagioclase (Nash and Crecraft 1985). Fractionation of K-feldspar was considerable, as evidenced by the low Pb content of dyke samples and high partition coefficient of Pb in K-feldspar (Nash and Crecraft 1985). Pb uptake by K-feldspar began fairly early in crystallization history of the intrusion and continued after magma chamber segregation. Figure 15a shows the proposed relative timing of crystallization for these minerals and their control on residual melt chemistry.

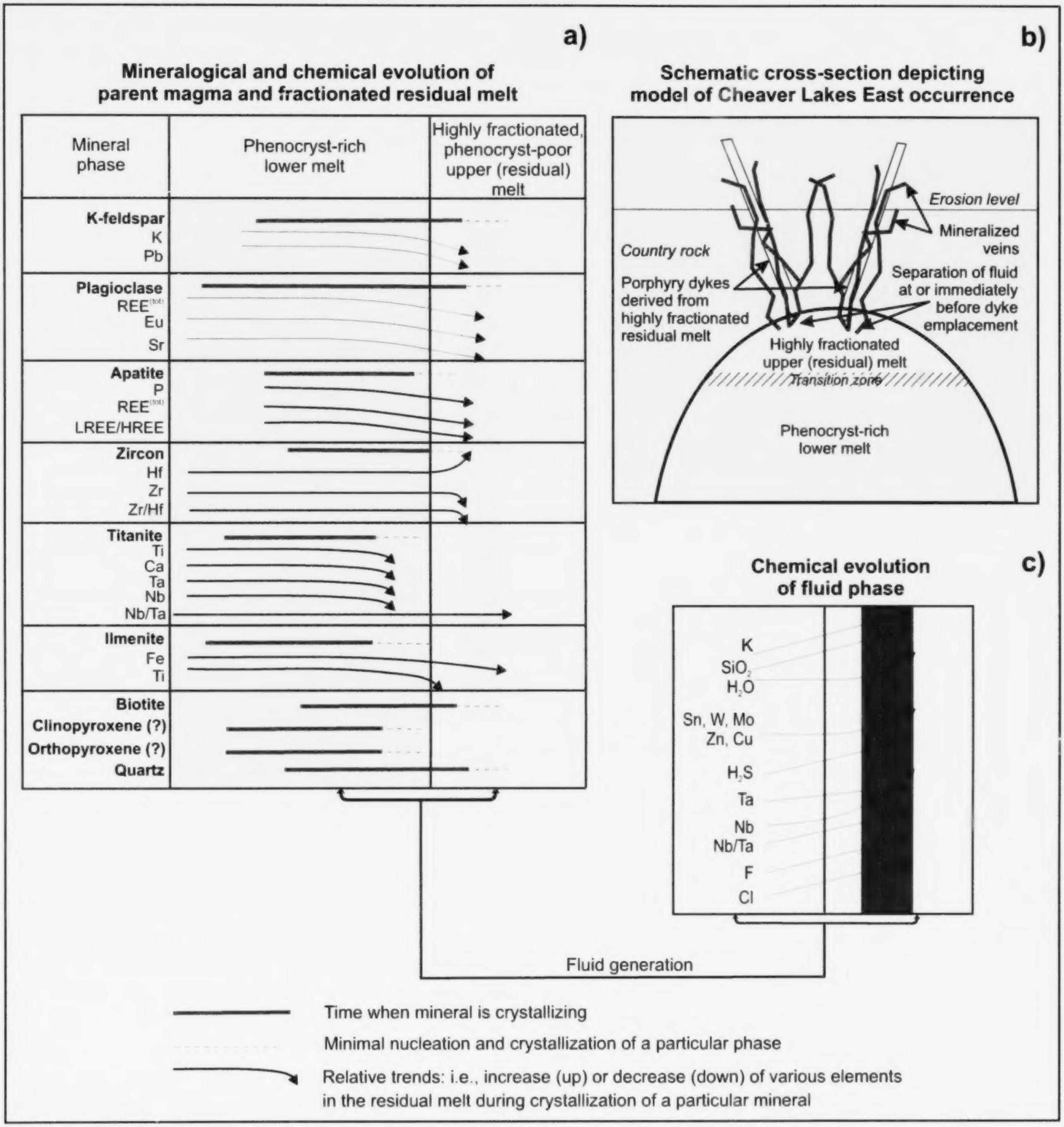
a)
Mineralogical and chemical evolution of parent magma and fractionated residual melt
Mineral phase
Phenocryst-rich lower melt
Highly fractionated, phenocryst-poor upper (residual) melt
K-feldspar
K
Pb
Plagioclase
REE(tot)
Eu
Sr
Apatite
P
REE(tot)
LREE/HREE
Zircon
Hf
Zr
Zr/Hf
Titanite
Ti
Ca
Ta
Nb
Nb/Ta
Ilmenite
Fe
Ti
Biotite
Clinopyroxene (?)
Orthopyroxene (?)
Quartz
b)
Schematic cross-section depicting model of Cheaver Lakes East occurrence
Erosion level
Mineralized veins
Country rock
Porphyry dykes derived from highly fractionated residual melt
Separation of fluid at or immediately before dyke emplacement
Highly fractionated upper (residual) melt
Transition zone
Phenocryst-rich lower melt
c)
Chemical evolution of fluid phase
K
SiO2
H2O
Sn, W, Mo
Zn, Cu
H2S
Ta
Nb
Nb/Ta
F
Cl
Fluid generation
Time when mineral is crystallizing
Minimal nucleation and crystallization of a particular phase
Relative trends: i.e., increase (up) or decrease (down) of various elements in the residual melt during crystallization of a particular mineral

Figure 15. Genetic model depicting crystallization sequence and chemical evolution of porphyry dykes and mineralizing fluid at Cheaver Lakes East. a) Magma evolution chart shows mineralogical and chemical changes in the lower, dominant, phenocryst-rich melt and in the upper, highly evolved, phenocryst-poor, residual melt. b) Cross-section shows porphyry dyke emplacement and mineralization. c) Evolution of fluid phase shows enrichment/depletion in selected elements. Yellow shaded area in Figures 15a and 15b indicates state of melt at time of porphyry dyke emplacement. Red shaded area in Figure 15c represents fluid at time of mineralization.

3. Concurrent crystallization of Fe- and Ti-bearing minerals such as ilmenite and titanite had the overall effect of lowering Fe, Ti, Nb, and Ta contents in the residual melt. Ilmenite has partition coefficients for LREE to HREE in the range of 7.8 to 3.6, respectively; its crystallization lowered the residual melt in ΣREE and also lowered LREE/HREE (see Nash and Crecraft 1985). Given the differing partition coefficients of Ta (16.5) and Nb (6.3) in titanite, crystallization of this phase lowered Nb/Ta of the remaining melt. Limiting factors on the crystallization of ilmenite and titanite were the availability of Fe and Ti (for ilmenite) and Ca and Ti (for titanite). Orthopyroxene and clinopyroxene may have crystallized at this point, but no evidence of either mineral has been preserved in the porphyry dykes.

4. Fractional crystallization of minerals such as apatite lowered the ΣLREE of the parent magma, with a preferential decrease in LREE relative to HREE, thereby imparting the flat REE profile with low ΣREE (Rollinson 1993). In the porphyry dykes, apatite microphenocrysts appear as inclusions in biotite phenocrysts; however, apatite seems absent as an accessory mineral in the dyke groundmass. This observation is supported by chemical analyses (Table 1) that show P_2O_5 values below detection limits (< 0.01 wt %) for all but one porphyry dyke. Apatite crystallization thus may have occurred early in the melt history and then ceased, probably because the melt became depleted of available P_2O_5, a critical component of apatite.

   At this point in magma fractionation, the magma chamber became segregated into an upper part and a lower part (Fig. 15b). The larger, lower part was a phenocryst-rich melt characterized by major minerals (plagioclase, K-feldspar, quartz), minor minerals (apatite, titanite, ilmenite), and a subordinate fluid phase. Fractionation left the upper, residual part of the melt phenocryst-poor. Its bulk composition was depleted in ΣREE, Fe, and Ti; had low La_n/Lu_n; and was elevated in Si, Sn, Zr, Hf, W, Mo, Cu, Zn, and HS^-. After the magma chamber segregated and crystallization of accessory Fe–Ti minerals ceased, Nb and Ta were fractionated into the fluid phase. As the degree of crystallization increased, there was a rise in Nb and Ta contents but not in Nb/Ta.

5. With further magma evolution, and as feldspar fractionation proceeded, zircon and biotite fractionation became important. Continued fractionation of feldspars caused SiO_2 content of the residual melt to increase to ≥ 67 wt %, at which point zircon became highly insoluble and began to crystallize. Given the high (> 73 wt %) SiO_2 content of the porphyry dykes, zircon crystallization likely continued for an extended time, resulting in almost complete removal of Zr from the melt fraction and development of an atypically low Zr/Hf. Such a scenario would explain why zircon microphenocrysts appeared in biotite phenocrysts but not in the porphyry dyke groundmass.

   Biotite crystallization commenced once the temperature dropped below 800°C, beneath the orthopyroxene–clinopyroxene–biotite stability line (Fig. 14a, 14b). As shown by experiments using synthetic granite (Fig. 14b), the facts that 1) biotite is stable, and 2) the dykes reveal no evidence for separation of a vapour phase together constrain H_2O content of the residual melt to less than 4 wt %. Likewise, in experiments using synthetic granodiorite (Fig. 14c), the absence of hornblende constrains the melt to less than 4% H_2O content except at temperatures lower than 700°C, during which the H_2O content may approach 6 wt %. Given these constraints and the high partition coefficient of Rb in biotite, there likely was a coincident reduction of Rb content (Nash and Crecraft 1985). Temperatures in the upper part of the magma chamber were 680°C to 790°C, according to calculations of the zircon-saturation temperatures.

At this fractionation stage, the upper part of the magma chamber contained Na-plagioclase, K-feldspar, quartz, and subordinate biotite phenocrysts that together accounted for about 20% of the magma volume. The fluid phase (Fig. 15c) was depleted in ΣREE, Zr, Hf, and Pb; had atypically low Zr/Hf and Nb/Ta; and was enriched in Si, K, Nb, Ta, Cu, Zn, Mo, Sn, W, and U. As well, it may have held a small fraction of an immiscible sulphide liquid. The fluid phase might have contained Cl and F, given the presence of same in many similar, highly evolved mineralizing systems. Cl and F are both important for deposit generation, as they enhance cation transport and lower the solidus in felsic melts.

6. According to the proposed model, dyke emplacement occurred when the upper magma chamber was tapped off into the surrounding rocks, possibly as the result of overpressuring due to separation of a fluid phase (Fig 15b). Disequilibrium between the phenocryst assemblage and highly evolved mineralizing fluids resulted in deuteric alteration of feldspar phenocrysts and formation of a fine-grained muscovite–quartz groundmass. For some time after dyke emplacement, magma in the upper chamber continued to undergo cooling and crystallization. This increased the crystal content and concentrated incompatible elements such as Cu, Zn, Fe, Sn, Mo, and S in the fluid phase. Eventual separation of the fluid phase from the crystal mush likely generated the hydrothermal fluids that subsequently formed the mineralized sulphide veins.

CONCLUSIONS

- In the Long Lake–Cheaver Lakes area, country rocks include greenschist-grade sedimentary rocks of the Cambrian–Early Ordovician Miramichi Group (the basal unit of the Bathurst Supergroup) and a sequence of amphibolite-grade mafic volcanic and sedimentary rocks of the Trousers Lake Complex. The Trousers Lake sequence is Middle Ordovician or older, as constrained by crosscutting relationships with the Serpentine River Granite. Sedimentary rocks of the Miramichi Group underlie the Bathurst Supergroup, whereas the mafic rocks are tholeiitic basalts that may have counterparts in the Flat Landing Brook Formation of the Bathurst Supergroup.
- Major- and trace-element (Na_2O, K_2O, SiO_2, Zr, Ti, Y, and Sr) chemistry of the Trousers Lake amphibolites are typical of tholeiitic basalts, indicating that amphibolitization must

have occurred within closed systems with respect to these elements.

- Mineralization in the Cheaver Lakes East area is spatially and genetically related to highly fractionated quartz–K-feldspar–plagioclase–biotite porphyritic dykes with S-type granite affinity.
- The chemical signature of porphyry dykes from the report area does not resemble chemical profiles of the Early Devonian Tobique Group, or those of major phases of the North Pole Stream Granite. A genetic model using a zoned granitic magma chamber is suggested to explain chemical composition of the porphyry dykes.
- The porphyry dykes are no older than the main phase of the North Pole Stream Granite, which has been dated at 417 ± 1 Ma. However, their absolute age is unknown and may be as young as Late Devonian, which would be consistent with the age of other New Brunswick felsic intrusions associated with Sn–W–Mo mineralization.
- The magmatic component of the Cheaver Lakes East mineralization, including elevated U, Zn, Mo, Cu, W, and Bi contents, is similar to that at the Cheaver Lakes and Long Lake occurrences. Thus, mineralization in the Long Lake–Cheaver Lakes area may be genetically and temporally linked to a larger intrusion at depth. Such an intrusion may contain associated polymetallic deposits similar to those in the Late Devonian Mount Pleasant porphyry system. Although indium was not tested for during the present investigation, indium analysis should be undertaken in the report area, as magmatic systems such as those at Mount Pleasant are known potential sources of this metal.

ACKNOWLEDGEMENTS

Thanks to Jennifer German for her assistance at the core shed, to Cyndie Pitre for drillhole digitization, and to E.A. Brooks (the former property holder) for interesting discussions on the area. This manuscript has benefited greatly from critical reviews by S.R. McCutcheon, M.J. McLeod, and R.A. Wilson.

REFERENCES

Anthonian Mining Corp. 1957. Report of work on the Long Lake Group. Department of Natural Resources; Minerals, Policy and Planning Division, Mineral Assessment Report # 470791.

Anthonian Mining Corp. 1963. Report of work on the Long Lake Group. Department of Natural Resources; Minerals, Policy and Planning Division, Mineral Assessment Report # 470792.

Barrett, T.J., and MacLean, W.H., 1994. Chemostratigraphy and hydrothermal alteration in exploration for VHMS deposits in greenstones and younger volcanic rocks. *In* Alteration and Alteration Processes Associated with Ore-forming Systems. *Edited by* D.R. Lentz. Geological Association of Canada, Short Course Notes, **11**, p. 433–467.

Brennan, J.M., Shaw, H.F., Phinney, D.L., and Ryerson, F.J. 1994. Rutile–aqueous fluid partitioning of Nb, Ta, Hf, Zr, U and Th: implications for high field strength element depletions in island-arc basalts. Earth and Planetary Science Letters, **128**, p. 327–339.

Burnham, C.W. 1997. Magmas and hydrothermal fluids. *In* Geochemistry of Hydrothermal Ore

Deposits, 3rd Edition. *Edited by* H.L. Barnes. John Wiley and Sons Inc., New York, 992 p.

Burton, D.M. 1993. Report of diamond drilling, Sears Lake claim group for NovaGold Resources Inc. New Brunswick Department of Natural Resources; Minerals, Policy and Planning Division, Mineral Assessment Report # 474392.

Christiansen, E.H., and Keith, J.D. 1996. Trace element systematics in silicic magmas: a metallogenic perspective. *In* Trace Element Geochemistry of Volcanic Rocks: Application for Massive Sulphide Exploration. *Edited by* D.A. Wyman. Geological Association of Canada, Short Course Notes, **12**, p. 115–151.

Claiborne, L.L. 2006. Tracking magmatic processes through Zr/Hf ratios in rocks and Hf and Ti zoning in zircons: an example from the Spirit Mountain Batholith Nevada. Unpublished M.Sc. thesis, Vanderbilt University, Nashville, Tennessee, U.S.A, 286 p.

Crouse, G.W. 1978. Geology of head of Clearwater Brook, map-area K-13. New Brunswick Department of Natural Resources; Mineral Resources Branch, Map Report 77-1, 16 p.

Davies, J.L. 1982. Geochemistry of Serpentine Lake (NTS 21 O/02), zinc content of stream and spring sediments. New Brunswick Department of Natural Resources; Minerals, Policy and Planning Division, Plate 83-33. Scale 1:50,000.

Dostal, J., and Chatterjee, A.K. 2000. Contrasting behaviour of Nb/Ta and Zr/Hf ratios in a peraluminous granitic pluton (Nova Scotia, Canada). Chemical Geology, **16**, p. 207–218.

Eby, N.G. 1992. Chemical subdivision of the A-type granitoids: petrogenetic and tectonic implications. Geology, **20**, p. 641–644.

Evensen, N.M., Hamilton, P.J., and O'Nions, R.K. 1978. Rare earth abundances in chondritic meteorites. Geochimica et Cosmochimica Acta, **42**, p. 1199–1212.

Fyffe, L.R., and Pronk, T. 1985. Bedrock and surficial geology: rock and till geochemistry in the Trousers Lake area, Victoria County, New Brunswick. New Brunswick Department of Natural Resources; Minerals Policy and Planning Division, Report of Investigation 20, p. 74.

Fyffe, L., Barr, S.M., and Bevier, M.L. 1988. Origin and U–Pb geochronology of amphibolite-facies metamorphic rocks, Miramichi Highlands, New Brunswick. Canadian Journal of Earth Sciences, **25**, p. 1674–1686.

Giggie, K.V. 1990. Report of work on the Sears Lake claim group, NTS 21 O/02W. New Brunswick Department of Natural Resources and Energy; Minerals, Policy and Planning Division, Mineral Assessment Report # 473955.

Giggie, K.V. 1991. Report of work on the Sears Lake claim group, NTS 21 O/02W. New Brunswick Department of Natural Resources and Energy; Minerals, Policy and Planning Division, Mineral Assessment Report # 474110.

Gorton, M.P., and Schandl, E.S. 2000. From continents to island arcs: a geochemical index for tectonic setting for arc-related and within-plate felsic to intermediate volcanic rocks. Canadian Mineralogist, **38**, p. 1065–1076.

Gradstein, F.M., Ogg, J.G., Smith, A.G. Bleeker, W., and Lourens, L.J. 2004. A new geologic time scale, with special reference to Precambrian and Neogene. Episodes, **27**, p. 83–100.

Graf, J.L. 1977. Rare earth elements as hydrothermal tracers during the formation of massive sulphide deposits in volcanic rocks, **72**, p. 527–548.

Green, T.H. 1995. Significance of Nb/Ta as an indicator of geochemical processes in the crust-mantle system. Chemical Geology, **120**, p. 347–359.

Green, T.H., and Pearson, N.J. 1987. An experimental study of Nb and Ta partitioning between Ti-rich minerals and silicate liquids at high pressure and temperature. Geochimica et Cosmochimica Acta, **51**, p. 55–62.

Gromet, L.P., Dymek, R.F., Haskin, L.A., and Korotev, R.L. 1984. The "North American Shale Composite": its compilation, major and trace element characteristics. Geochimica et Cosmochimica Acta, **48**, p. 2469–2482.

Hauseux, M. 1980. Report of work on the Long Group. New Brunswick Department of Natural Resources and Energy; Minerals, Policy and Planning Division, Mineral Assessment Report # 473155.

Hauseux, M. 1981. Report of work on the Long Group. New Brunswick Department of Natural Resources and Energy; Minerals, Policy and Planning Division, Mineral Assessment Report # 472695.

Inverno, C.M.C., and Hutchinson, R.W. 2006. Petrochemical discrimination of evolved granitic intrusions associated with Mount Pleasant deposits, New Brunswick, Canada. Applied Earth Science Transactions of the Australian Institute of Mining and Metallurgy, **115**, p. 23–39.

Irvine, T.N., and Baragar, W.R.A. 1971. A guide to the chemical classification of the common volcanic rocks. Canadian Journal of Earth Sciences, **8**, p. 523–548.

Le Maitre, R.W., Bateman, P., Dudek, A., Keller, J., Lameyre Le Bas, M.J., Sabine, P.A., Schmid, R., Sorensen, H., Streckeisen, A., Wolley, A.R., and Zanettin, B. 1989. A classification of igneous rocks and glossary of terms. Blackwell, Oxford, 193 p.

Lydon, J.W. 1988. Volcanogenic massive sulphide deposits: part 2 – genetic models. *In* Geoscience Canada Reprint Series 3. *Edited by* R.G. Roberts and P.A. Sheahan. Geoscience Canada, **11**, p. 155–181.

MacLellan, H.E., Taylor, R.P., and Gardiner, W.W. 1990. Geology and geochemistry of Middle Devonian Burnthill Brook granites and related tin-tungsten deposits, York and Northumberland counties, New Brunswick. New Brunswick Department of Natural Resources and Energy; Minerals and Energy Division, Mineral Resource Report 4, 95 p.

Mahood, G., and Hildreth, W. 1983. Large partition coefficients for trace elements in high silica rhyolites. Geochemica Cosmochemica Acta, **47**, p. 11–30.

Mann, R. 1985. Report of work on the Sears Lake claim group for Brunswick Mining and Smelting. New Brunswick Department of Natural Resources and Energy; Minerals, Policy and Planning Division, Mineral Assessment Report # 473154.

McCutcheon, S.R. 1990. The Late Devonian Mount Pleasant Caldera complex: stratigraphy, mineralogy, geochemistry and geological setting of a Sn–W deposit in southwestern New Brunswick. Unpublished Ph.D. thesis, Dalhousie University, Halifax, Nova Scotia, Canada, 609 p.

McNicoll, V.J., Whalen, B.J., and Stern, R.A. 2003. U–Pb geochronology of Ordovician plutonism, Bathurst Mining Camp, New Brunswick. *In* Massive Sulphide Deposits of the Bathurst Mining Camp, New Brunswick and Northern Maine. *Edited by* W.D. Goodfellow, S.R. McCutcheon, and J.M. Peter. Economic Geology Monograph 11, p. 203–218.

Miller, C.F., McDowell, S.M., and Mapes, R.W. 2003. Hot and cold granites? Implications of Zircon saturation temperatures and preservation of inheritance. Geology, **31**, p. 529–532.

Naney, M.T. 1983. Phase equilibria of rock-forming ferromagnesian silicates in granitic systems. American Journal of Science, **283**, p. 993–1033

Nash, W.P., and Crecraft, H.R. 1985. Partition coefficients for trace elements in silicic magmas. Geochimica et Cosmochimica Acta, **49**, p. 2309–2322.

New Brunswick Department of Natural Resources and Energy (NBDNRE). 2000. Bedrock geology of New Brunswick. New Brunswick Department of Natural Resources and Energy; Minerals and Energy Division, Map NR-1 (2000 edition). Scale 1:500 000.

Pearce, J.A., and Cann, J.R. 1973. Tectonic setting of basic volcanic rocks determined using trace element analysis. Earth and Planetary Science Letters, **19**, p. 290–300.

Pearce, J.A., Harris, N.B.W., and Tindle, A.G. 1984. Trace element discrimination for the tectonic interpretation of granitic rocks. Journal of Petrology, **25**, p. 15–32.

Rickwood, P.C. 1989. Boundary lines within petrologic diagrams which use oxides of major and minor elements. Lithos, **22**, p. 247–263.

Rollinson, H. 1993. Using geochemical data: evaluation, presentation, interpretation. Longman, London, 352 p.

Saracoglu, N. 1973. Report of work on the Long Group. New Brunswick Department of Natural Resources and Energy; Minerals, Policy and Planning Division, Mineral Assessment Report # 473002.

Schoonmaker, A., Kidd, W.S.F., and Bradley, D.C. 2005. Foreland–forearc collisional granitoid and mafic magmatism caused by lower plate lithospheric slab breakoff: the Acadian of Maine and other orogens. Geology, **33**, p. 961–964.

Shewman, R.W. 1964. Report of work on the Cheaver Group. New Brunswick Department of Natural Resources and Energy; Minerals, Policy and Planning Division, Mineral Assessment Report # 470800.

Sinclair, W.D., Kooiman, G.J.A., and Martin, D.A. 1988. Geological setting of granites and related tin deposits in the North Zone, Mount Pleasant, New Brunswick. *In* Current Research, Part B, Geological Survey of Canada, Paper 88-1B, p. 201–208.

Taylor, S.R., and McLennan, S.M. 1985. The continental crust: its composition and evolution, an examination of the geochemical record preserved in sedimentary rocks. Blackwell Scientific Publications, Oxford, 312 p.

Toyoda, K., and Masuda, A. 1991. Chemical leaching of pelagic sediments: identification of the carrier of Ce anomaly. Geochemical Journal, **25**, p. 95–119.

van Staal, C.R., Wilson, R.A., Rogers N., Fyffe, L.R., Langton, J.P., McCutcheon, S.R., McNicoll, V., and Ravenhurst, C.E. 2003. Geology and tectonic history of the Bathurst Supergroup, Bathurst Mining Camp, and its relationships to coeval rocks in southwestern New Brunswick and adjacent Maine — a synthesis. *In* Massive Sulphide Deposits of the Bathurst Mining Camp, New Brunswick and Northern Maine. *Edited by* W.D. Goodfellow, S.R. McCutcheon, and J.M. Peter. Economic Geology Monograph 11, p. 37–60.

Walker, J.A. 2005. Petrogenesis and tectonic setting of Devonian volcanic and related rocks and their control on mineralization at the Shingle Gulch East Zn–Pb–Ag sulphide deposit, northwest New Brunswick. Unpublished Ph.D. thesis, University of New Brunswick, Fredericton, New Brunswick, Canada, 403 p.

Watson, E.B., and Harrison, T.M. 1983. Zircon saturation revisited: temperature and composition effects in a variety of crustal magma types. Earth and Planetary Science Letters, **64**, p. 295–304.

Whalen, J.B. 1993. Geology, petrography, and geochemistry of Appalachian granites in New Brunswick and Gaspésie, Quebec. Geological Survey of Canada, Bulletin 436, p. 124.

Wilson, R.A. 1992. Petrographic features of Siluro–Devonian felsic volcanic rocks in the Riley Brook area, Tobique Zone, New Brunswick: implications for base metal mineralization at Sewell Brook. Atlantic Geology, **28**, p. 115-135.

STRUCTURAL STYLES IN LATE DEVONIAN–EARLY CARBONIFEROUS ROCKS ALONG THE SOUTHERN MARGIN OF THE MONCTON SUBBASIN: CALEDONIA MOUNTAIN TO ELGIN, SOUTHEASTERN NEW BRUNSWICK

ADRIAN F. PARK [1], CLINTON J. ST. PETER [2], AND DAVID G. KEIGHLEY [3]

[1] Department of Geology, University of New Brunswick,
P.O. Box 4400, Fredericton, New Brunswick, CANADA E3B 5A3 *(apark@unb.ca)*
[2] Geological Surveys Branch, New Brunswick Department of Natural Resources,
P.O. Box 6000, Fredericton, New Brunswick, E3B 5H1 *(Clint.St.Peter@gnb.ca)*
[3] Department of Geology, University of New Brunswick,
P.O. Box 4400, Fredericton, New Brunswick, CANADA E3B 5A3 *(keig@unb.ca)*

Park, A.F., St. Peter, C.J., and Keighley, D.G. 2007. Structural styles in Late Devonian–Early Carboniferous rocks along the southern margin of the Moncton Subbasin: Caledonia Mountain to Elgin, southeastern New Brunswick. *In* Geological Investigations in New Brunswick for 2006. *Edited by* G.L. Martin. New Brunswick Department of Natural Resources; Minerals, Policy and Planning Division, Mineral Resource Report 2007-1, p. 87–125.

Late Devonian (Famennian) and Early Carboniferous (Tournaisian) terrestrial strata of the Horton and Sussex groups along the southern margin of the Moncton Subbasin lie within an end-Tournaisian inversion zone. The eastern part of the zone comprises a fold-thrust belt that has been transported over crystalline basement of the Caledonia Uplift. The fold-thrust belt follows the trace of the basement-bounding Caledonia Fault and is offset in several places by northwest-trending structures that define sidewall ramps. These features coincide with older structures that influenced deposition of the Horton and Sussex groups, the most striking of which is the overstep of the Sussex Group onto the Caledonia basement. The westernmost sidewall structure lies immediately west of Prosser Brook village and demarks the termination of the fold-thrust belt.

West of the Prosser Brook sidewall structure, the inversion zone comprises a strike-slip duplex with right-lateral shear sense. Exhumation of the Horton and Sussex groups in this duplex is related to movement along the northeast-trending Gordon Falls, Pollett River, and Lee Brook faults. Significant differences exist in thickness, stratigraphic succession, and facies of deposition within the Horton and Sussex groups between the eastern (fold-thrust zone) and western (strike-slip duplex) parts of the inversion zone.

Inversion structures in the Horton and Sussex groups pre-date, and are partly concealed beneath, the unconformity of the undisturbed Hillsborough Formation (Visean), which indicates that the fold-thrust belt and strike-slip duplex developed contemporaneously. Both sets of structures are compatible with basin inversion at the end of the Tournaisian and imply development in a regional, right-lateral, transpressive tectonic regime. The older

northwest-trending sidewall structures became reactivated at least once after the end-Tournaisian inversion, influencing deposition of the Visean Hillsborough Formation. The end-Tournaisian fold-thrust belt is itself a reactivation of a basin-controlling structure, that being the Caledonia Fault. Later movement on the northeast-trending Prosser Brook Fault (post-Visean and pre-Bashkirian) subsequently offset the basement margin.

Des strates terrestres du Dévonien tardif (Famennien) et du Carbonifère précoce (Tournaisien) des groupes de Horton et de Sussex le long de la limite méridionale du sous-bassin de Moncton sont présentes à l'intérieur d'une zone d'inversion de la fin du Tournaisien. La partie orientale de la zone comporte une ceinture à pli chevauchant ayant été transportée au-dessus du socle cristallin du soulèvement de Caledonia. La ceinture à pli chevauchant suit la trace de la faille délimitant le socle de Caledonia et elle est décalée en plusieurs endroits par des structures orientées vers le nord-ouest qui définissent les pentes des parois latérales. Ces caractéristiques coïncident avec des structures plus âgées ayant influé sur la sédimentation des groupes de Horton et de Sussex, dont la plus saisissante est la formation transgressive du groupe de Sussex recouvrant le socle de Caledonia. La structure latérale la plus à l'ouest se trouve immédiatement à l'ouest du village de Prosser Brook et marque la fin de la ceinture à pli chevauchant.

À l'ouest de la structure latérale de Prosser Brook, la zone d'inversion comporte un duplex à décrochement à cisaillement dextre. L'exhumation des groupes de Horton et de Sussex dans ce duplex est apparentée au déplacement survenu le long des failles orientées vers le nord-est des chutes Gordon, de la rivière Pollett et du ruisseau Lee. Il existe des différences marquées dans l'épaisseur, la succession stratigraphique et les faciès de sédimentation à l'intérieur des groupes de Horton et de Sussex, entre les parties orientale (zone du pli chevauchant) et occidentale (duplex à décrochement) de la zone d'inversion.

Les structures d'inversion dans les groupes de Horton et de Sussex sont dissimulées sous la discordance de la Formation non remaniée de Hillsborough (viséenne), ce qui révèle que la ceinture à pli chevauchant et le duplex à décrochement se sont développés vers la même époque. Les deux ensembles de structures sont compatibles avec l'inversion du bassin de la fin du Tournaisien et laissent supposer un développement dans un régime tectonique transpressif, dextre et régional. Les structures latérales orientées vers le nord-ouest plus âgées sont redevenues actives au moins une fois après l'inversion de la fin du Tournaisien, exerçant une influence sur la sédimentation de la Formation viséenne de Hillsborough. La ceinture à pli chevauchant de la fin du Tournaisien constitue elle-même une réactivation de la structure de contrôle du bassin, c'est-à-dire la faille de Caledonia. Un déplacement ultérieur sur la faille orientée vers le nord-est du ruisseau Prosser (post-viséenne et prébashkirienne) a par la suite décalé la limite du socle.

INTRODUCTION

The Moncton Subbasin (Fig. 1) is one of several subbasins of the Late Devonian–Carboniferous Maritimes Basin in southeastern New Brunswick (Williams 1974). The subbasins are defined as containing thick sequences of the first two depositional cycles of the Late Devonian–Carboniferous succession, those being the unconformity-bounded Horton and Sussex groups (Fig. 2). The subbasins are separated by uplifted areas of pre-Late Devonian basement rocks, over which the Horton and/or Sussex successions are either absent or condensed (St. Peter 2001).

The southern margin of the Moncton Subbasin impinges against basement rocks of the Caledonia Uplift, a tract dominated by metamorphosed Late Precambrian–Cambrian metavolcanic and metasedimentary rocks intruded by a variety of mafic to felsic plutons (Barr and White 1996). Between the Albert Mines area and Prosser Brook (Fig. 3a), the southern margin is marked by the Caledonia Fault (St. Peter and Johnson 1997). West of Prosser Brook, other faults complicate the picture, and the unconformity between rocks of the basement and Horton Group is locally undisturbed.

The current report presents a structural analysis of Late Devonian (Famennian)–Early Carboniferous (Tournaisian) rocks of the Horton and Sussex groups along the southern margin of the Moncton Subbasin from Caledonia Mountain to Elgin (Fig. 1, 3a, 3b). This investigation is a continuation of mapping conducted farther east along the same subbasin margin in the Hillsborough–Albert Mines area (Fig. 3a), work that identified a major fold-thrust belt related to end-Tournaisian basin inversion (Park and St. Peter 2005). In the Albert Mines area, much of the deformation along the Caledonia Fault can be related to folds and thrusts of this fold-thrust belt, which in part are concealed beneath the unconformity at the base of the Hillsborough Formation (Fig. 2, 3a, 3b).

The primary objective of the present investigation was to establish how far west the fold-thrust belt extends and to identify how structural features influenced the change in stratigraphy west of Prosser Brook. This report has relied heavily on detailed lithostratigraphic mapping in the area (e.g., St. Peter 1989; St. Peter and Johnson 1997). In addition, it has incorporated 1) data from several palynological studies (Dolby 1991, 1993, 1994, 2000a, 2000b, 2005, 2006a, 2006c), and 2) minor stratigraphic revisions.

REGIONAL STRATIGRAPHY

Horton Group

The Horton Group in the report area is represented by the Memramcook, McQuade Brook, and Albert formations (Fig. 2). All three formations are exhumed west of Prosser Brook, whereas only the Albert Formation is exposed east of the brook (St. Peter 2006).

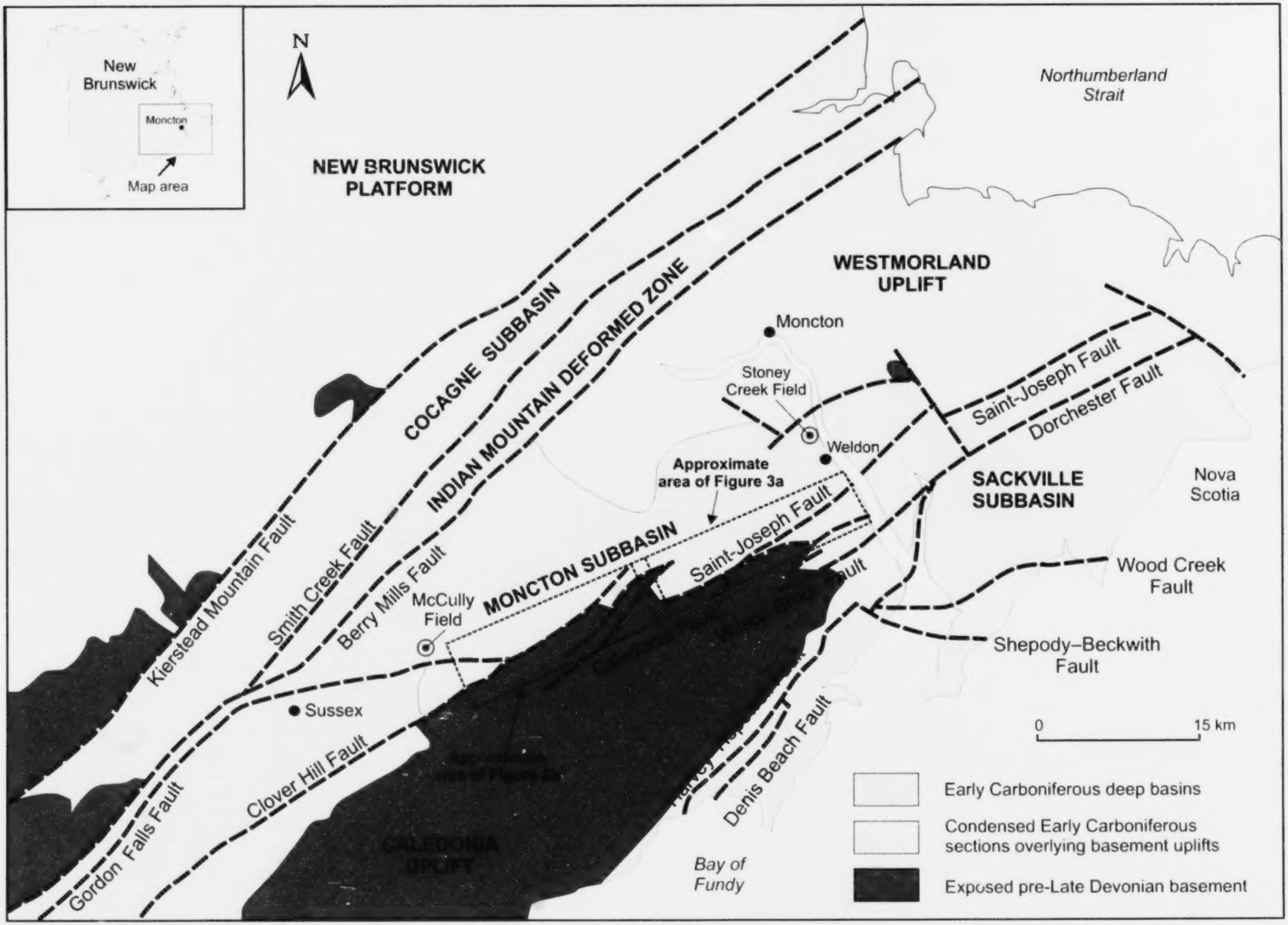
New Brunswick
Moncton
Map area
N
NEW BRUNSWICK PLATFORM
Northumberland Strait
WESTMORLAND UPLIFT
COCAGNE SUBBASIN
INDIAN MOUNTAIN DEFORMED ZONE
Moncton
Stoney Creek Field
Weldon
Saint-Joseph Fault
Dorchester Fault
SACKVILLE SUBBASIN
Nova Scotia
Approximate area of Figure 3a
Saint-Joseph Fault
MONCTON SUBBASIN
Kierstead Mountain Fault
Smith Creek Fault
Berry Mills Fault
McCully Field
Caledonia Fault
Wilson Brook Fault
Wood Creek Fault
Shepody–Beckwith Fault
Sussex
Clover Hill Fault
Approximate area of Figure 3b
Harvey–Hopewell Fault
Denis Beach Fault
0
15 km
Gordon Falls Fault
CALEDONIA UPLIFT
Bay of Fundy
Early Carboniferous deep basins
Condensed Early Carboniferous sections overlying basement uplifts
Exposed pre-Late Devonian basement

Figure 1. Geological map showing the Early Carboniferous subbasins of southwestern New Brunswick (after St. Peter 2001).

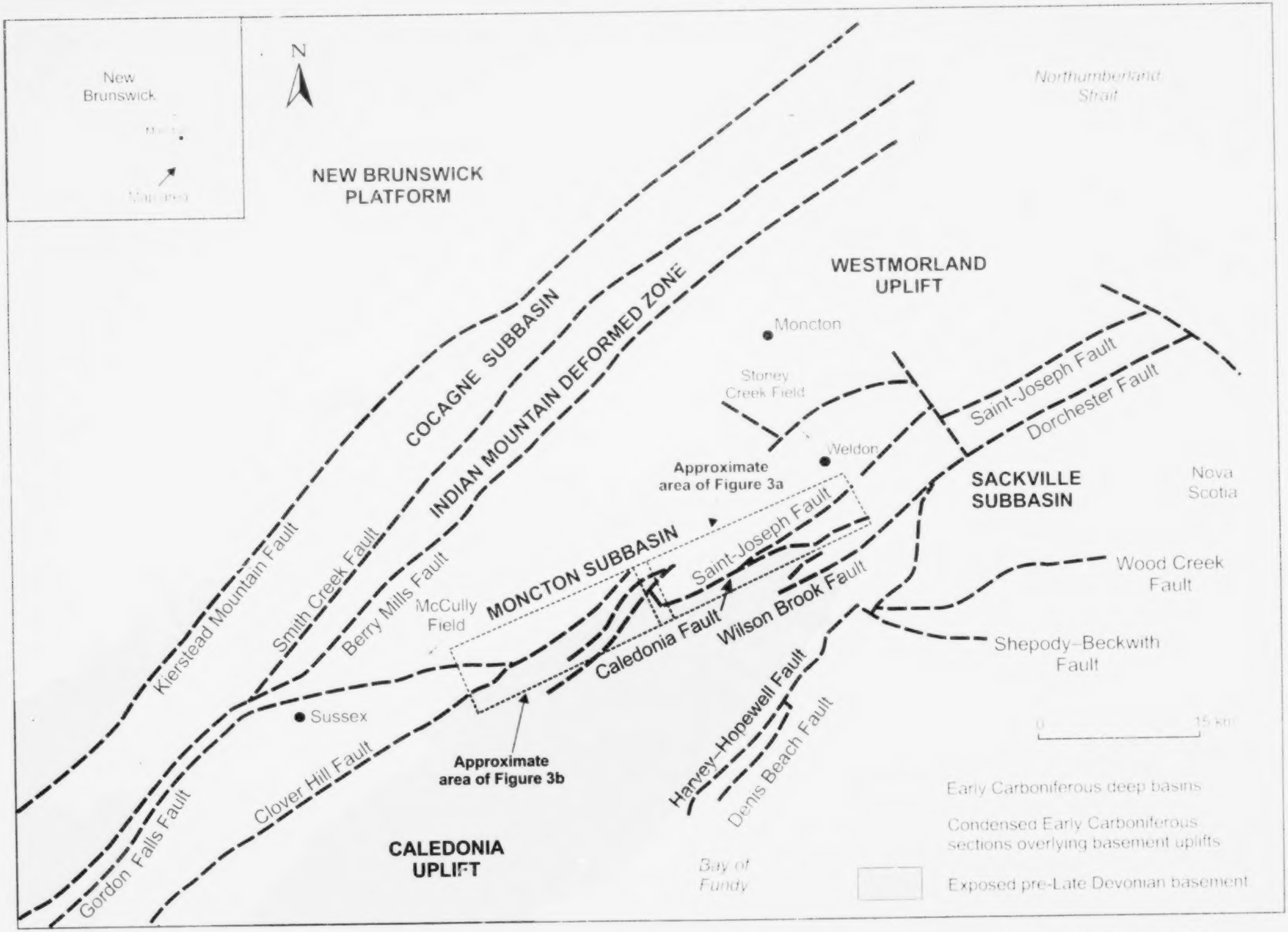
New Brunswick
Map area
N
NEW BRUNSWICK PLATFORM
Northumberland Strait
WESTMORLAND UPLIFT
COCAGNE SUBBASIN
INDIAN MOUNTAIN DEFORMED ZONE
Moncton
Storey Creek Field
Weldon
Saint-Joseph Fault
Dorchester Fault
Approximate area of Figure 3a
SACKVILLE SUBBASIN
Nova Scotia
MONCTON SUBBASIN
Saint-Joseph Fault
Wood Creek Fault
Kierstead Mountain Fault
Smith Creek Fault
Berry Mills Fault
McCully Field
Caledonia Fault
Wilson Brook Fault
Shepody–Beckwith Fault
Sussex
Harvey–Hopewell Fault
Denis Beach Fault
0
15 km
Clover Hill Fault
Approximate area of Figure 3b
Gordon Falls Fault
CALEDONIA UPLIFT
Bay of Fundy
Early Carboniferous deep basins
Condensed Early Carboniferous sections overlying basement uplifts
Exposed pre-Late Devonian basement

Figure 1. Geological map showing the Early Carboniferous subbasins of southwestern New Brunswick (after St. Peter 2001)

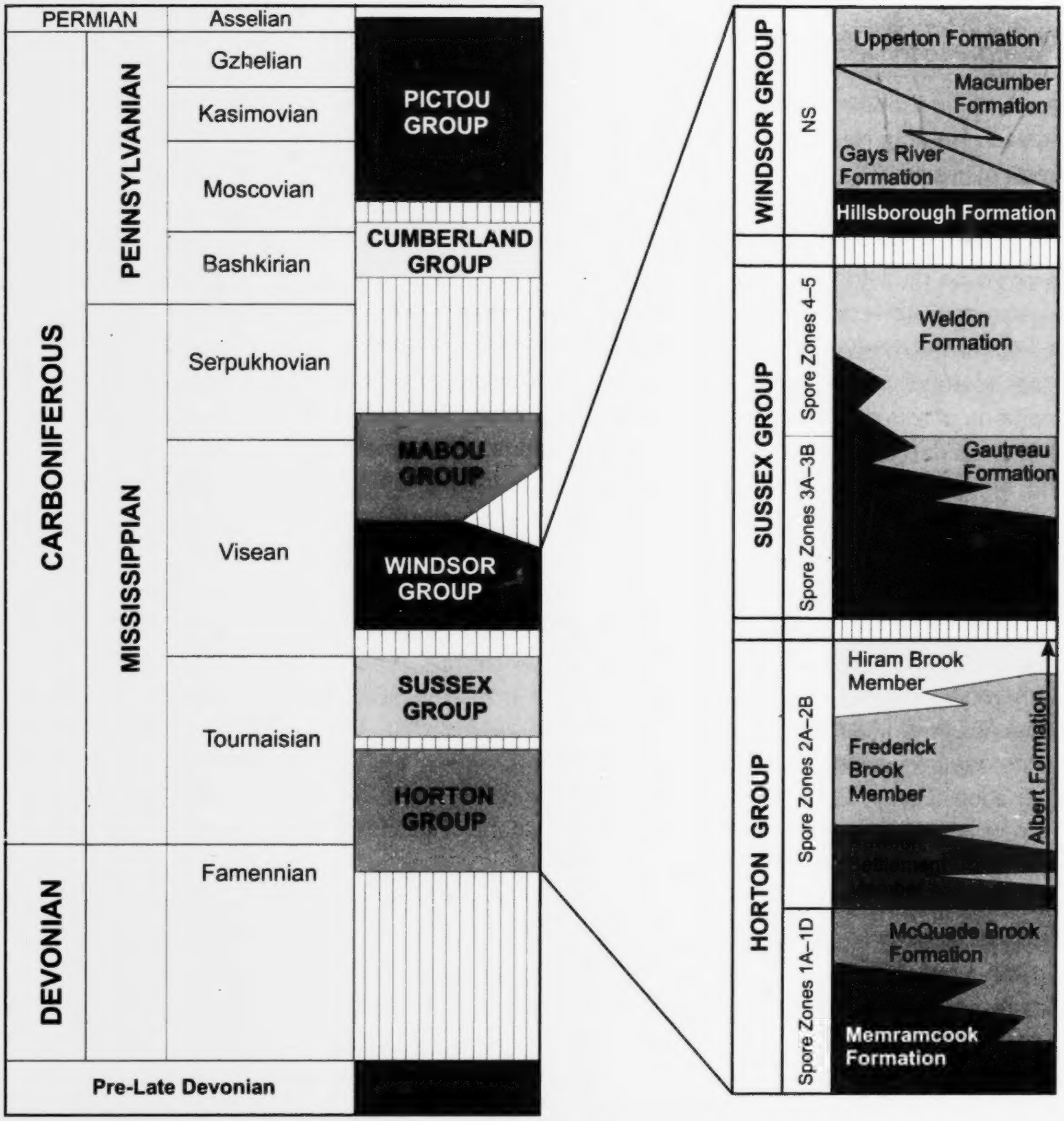
PERMIAN
Asselian
CARBONIFEROUS
PENNSYLVANIAN
Gzhelian
Kasimovian
Moscovian
Bashkirian
MISSISSIPPIAN
Serpukhovian
Visean
Tournaisian
DEVONIAN
Famennian
Pre-Late Devonian
PICTOU GROUP
CUMBERLAND GROUP
MABOU GROUP
WINDSOR GROUP
SUSSEX GROUP
HORTON GROUP
WINDSOR GROUP
NS
Upperton Formation
Macumber Formation
Gays River Formation
Hillsborough Formation
SUSSEX GROUP
Spore Zones 4–5
Spore Zones 3A–3B
Weldon Formation
Gautreau Formation
HORTON GROUP
Spore Zones 2A–2B
Spore Zones 1A–1D
Hiram Brook Member
Frederick Brook Member
Settlement
Albert Formation
McQuade Brook Formation
Memramcook Formation

Figure 2. Summary of Carboniferous stratigraphy in the Moncton Subbasin of the Caledonia Mountain–Elgin area. Spore zone designations for the Horton and Sussex groups are after Dolby (2006a). Spore zone designation (NS) for the Windsor Group is after Utting (1987).

The lower part of the Horton Group begins with a polymictic, coarse to very coarse, conglomerate-dominated sequence of the Memramcook Formation. It lies with marked angular unconformity directly on pre-Late Devonian crystalline basement and is dominated by clasts of local basement rock types, especially granitoids. Palynological data (Carr 1968; McGregor 1983a, 1983b) suggest that the lowest part of the Memramcook Formation is Late Devonian (Famennian); most of the sequence is earliest Tournaisian or Zone 1A age (Utting et al. 1989). The Memramcook Formation is conformably overlain by a redbed sequence dominated by red, purple, and brown shale, siltstone, and fine-grained sandstone with minor conglomerate of the McQuade Brook Formation (St. Peter 2006).

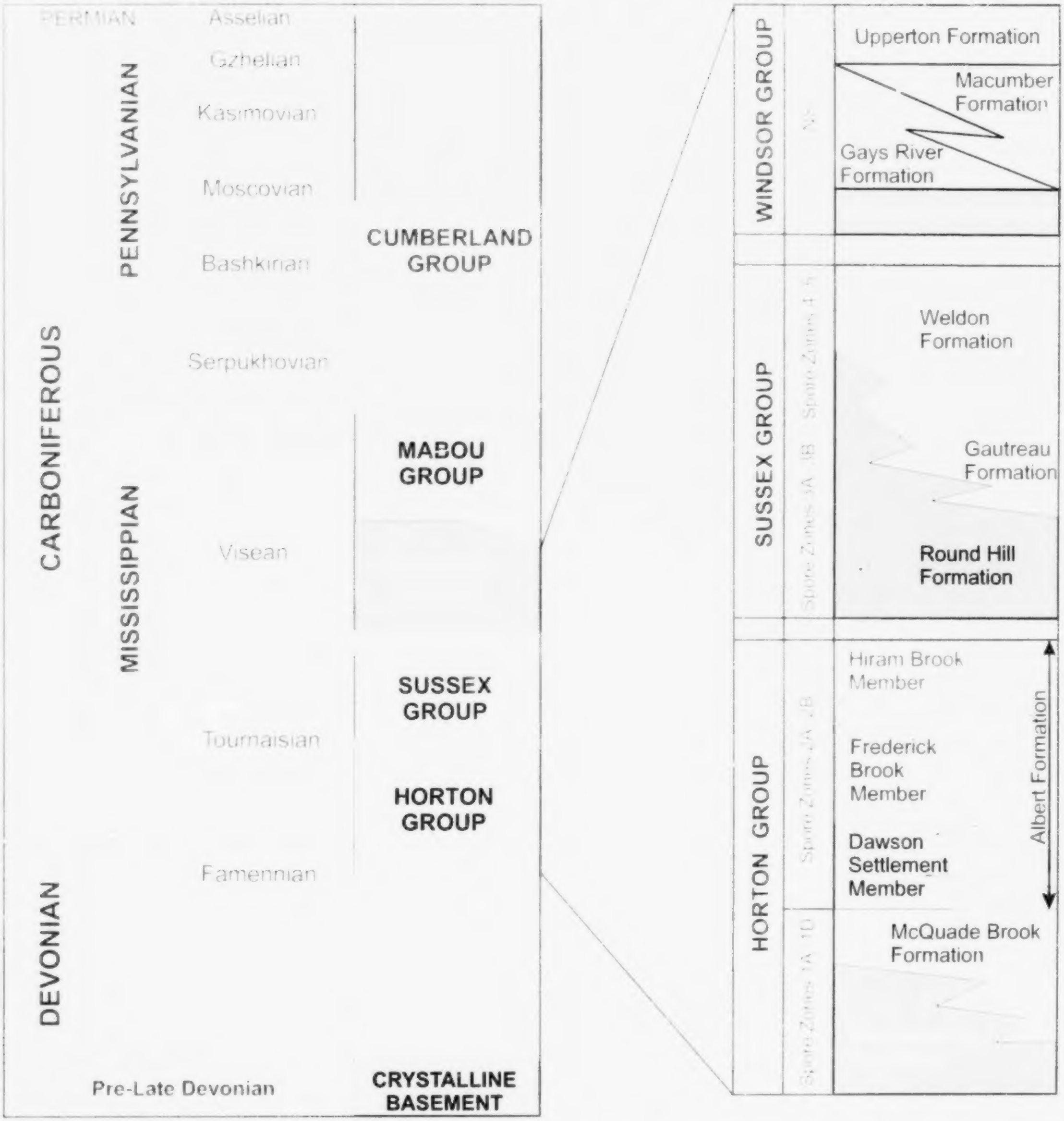
PERMIAN
Asselian
Gzhelian
PENNSYLVANIAN
Kasimovian
Moscovian
Bashkirian
CUMBERLAND GROUP
CARBONIFEROUS
Serpukhovian
MABOU GROUP
MISSISSIPPIAN
Visean
SUSSEX GROUP
Tournaisian
HORTON GROUP
DEVONIAN
Famennian
Pre-Late Devonian
CRYSTALLINE BASEMENT
WINDSOR GROUP
NS
Upperton Formation
Macumber Formation
Gays River Formation
SUSSEX GROUP
Spore Zones 3A, 3B
Spore Zones 4, 5
Weldon Formation
Gautreau Formation
Round Hill Formation
HORTON GROUP
Spore Zones 2A, 2B
Hiram Brook Member
Frederick Brook Member
Dawson Settlement Member
Albert Formation
Spore Zones 1A, 1D
McQuade Brook Formation

Figure 2. Summary of Carboniferous stratigraphy in the Moncton Subbasin of the Caledonia Mountain–Elgin area. Spore zone designations for the Horton and Sussex groups are after Dolby (2006a). Spore zone designation (NS) for the Windsor Group is after Utting (1987).

The lower part of the Horton Group begins with a polymictic, coarse to very coarse, conglomerate-dominated sequence of the Memramcook Formation. It lies with marked angular unconformity directly on pre-Late Devonian crystalline basement and is dominated by clasts of local basement rock types, especially granitoids. Palynological data (Carr 1968; McGregor 1983a, 1983b) suggest that the lowest part of the Memramcook Formation is Late Devonian (Famennian); most of the sequence is earliest Tournaisian or Zone 1A age (Utting et al. 1989). The Memramcook Formation is conformably overlain by a redbed sequence dominated by red, purple, and brown shale, siltstone, and fine-grained sandstone with minor conglomerate of the McQuade Brook Formation (St. Peter 2006).

Rocks of the McQuade Brook Formation pass upward into the Albert Formation, a thick sequence of lacustrine and fluvial sediments dominated by grey sandstone, dark grey and brown kerogenous mudstone and shale, and lesser conglomerate with minor limestone. The Albert Formation has been divided into the Dawson Settlement, Frederick Brook, and Hiram Brook members (Fig. 2).

The Dawson Settlement Member (Greiner 1962) comprises sandstone, siltstone, and minor kerogenous mudstone, shale, and limestone. In the western Moncton Subbasin, exposures of this member adjacent to the Caledonia basement contain abundant polymictic conglomerate and coarse-grained lithic sandstone (St. Peter 2002; Hinds and St. Peter 2006). The Frederick Brook Member contains dolomitic, kerogenous mudstone and shale (including oil shale) with interbeds of siltstone, and minor sandstone and limestone. The Hiram Brook Member consists of interbedded sandstone alternating with siltstone, mudstone, shale, kerogenous mudstone, and kerogenous shale. Like the Dawson Settlement Member, the Hiram Brook Member adjacent to the Caledonia basement includes intervals of polymictic conglomerate. Spore assemblages have been dated for many samples of the Albert Formation in the Moncton Subbasin. The better assemblages yield Tournaisian Zones 1 and 2 ages (Dolby 1991, 1993, 1994, 1995a, 1995b, 2000a, 2000b, 2001a–c, 2002a, 2002b, 2003, 2004, 2005, 2006a–d).

Commercial oil and gas fields have been discovered in the Moncton Subbasin at Stoney Creek south of Moncton and at McCully east of Sussex (Fig. 1). The fields are situated within sandstone reservoirs in the Hiram Brook and Dawson Settlement members of the Albert Formation (Foley 1989; Wilson 2005; Hinds and St. Peter 2006). The petroleum source is interpreted to be mainly organic shale of the Frederick Brook Member (Chowdhury et al. 1991; Chowdhury and Noble 1992; Chowdhury 1995).

Sussex Group

The Sussex Group overlies the Horton Group with angular unconformity and locally oversteps Horton rocks to rest directly on underlying crystalline basement (St. Peter 1993; St. Peter and Johnson 1997; Park and St. Peter 2005; St. Peter 2006). In the report area, the Sussex Group is represented by the Round Hill, Gautreau, and Weldon formations (Fig. 2).

Along the southern margin of the Moncton Subbasin, the Round Hill Formation is a coarse to very coarse, red-brown breccia conglomerate with minor coarse-grained sandstone and red mudstone (McLeod 1980; St. Peter and Johnson 1997; Park and St. Peter 2005). The Round Hill Formation is overlain by the Gautreau Formation, a thin sequence of grey, green, and red shale and mudstone with abundant desiccation features. Boreholes a few kilometres north of the subbasin margin indicate that the Gautreau Formation thickens northward and includes the evaporites halite, anhydrite, glauberite, and hydroglauberite (Greiner 1962, 1974; St. Peter 1992). Concomitant with thickening of the Gautreau Formation, the Round Hill Formation thins to the north, away from the southern subbasin margin, suggesting that the two formations are partly contemporaneous. Both units are overlain by the Weldon Formation, a fine-grained redbed sequence consisting mostly of red mudstone and shale with fine-grained sandstone and siltstone (Park and St. Peter 2005).

Windsor Group

The Hillsborough Formation is a red-brown sequence of polymictic conglomerate and sandstone that overlies the Sussex Group with marked angular unconformity; it represents the first unit of the Visean depositional cycle (Fig. 2). The Hillsborough Formation traditionally has been included with limestone and overlying marine sediments in the Windsor Group (McLeod 1980; St. Peter and Johnson 1997; Park and St. Peter 2005), and this practice is continued here (Fig. 2).

The Windsor Group in the report area is represented by the Hillsborough, Gays River, and Macumber formations (Fig. 2, 3a). From east of Caledonia Mountain to the Prosser Brook Fault (Fig. 3a), the Hillsborough Formation unconformably overlies, and cuts downsection from, the Sussex Group (Weldon Formation) in the east to the Caledonia basement in the west. The Hillsborough Formation varies considerably in thickness: the New Brunswick Gas and Oilfields Ltd. Well No. 127 near Baltimore (Fig. 3a: Location H) intersected about 700 m of Hillsborough strata (Fig. 4: Section H), but along Pollett River and at Lee Brook north of Elgin (Fig. 3b), the surface section of the formation is only a few metres or tens of metres thick (Fig. 4: Section C). (Lee Brook, not shown on Figure 3b, is an eastward-draining tributary of Pollett River.)

Marine limestone concordantly overlies the Hillsborough Formation at Berryton (Fig. 3a) and along Lee Brook (Fig. 3b). At Berryton, this Windsor limestone is light grey, laminated and/or massive (Hamilton 1965) and is characterized by irregular, stacked lensoidal mounds of algal boundstone intercalated with thinly bedded intermound wackestone and packstone (Webb 1997). McCutcheon (1981) assigned similar limestone dominated by algal mounds to the Gays River Formation of the Windsor Group (Fig. 2). On the north bank of Lee Brook, an exposure of Windsor limestone shows grey flaggy laminated beds containing shelly fossils (Hamilton 1965). McCutcheon (1981) assigned the limestone at Lee Brook to the Macumber Formation (Fig. 2). Limestones of the Gays River and Macumber formations are succeeded by anhydrite and gypsum of the Upperton Formation (Fig. 2), which is not exposed in the report area but is known from boreholes to exist in the subsurface a few kilometres farther north in the Moncton Subbasin.

Mabou Group

At Lee Brook, the Late Mississippian Mabou Group unconformably oversteps limestone of the Windsor Group. Southwest of there, just south of Goshen, it unconformably oversteps rocks of the Sussex Group (Fig. 3b). The Mabou Group comprises red-brown or locally grey-green coarse polymictic conglomerate and lithic sandstone with minor interbeds of red siltstone and mudstone.

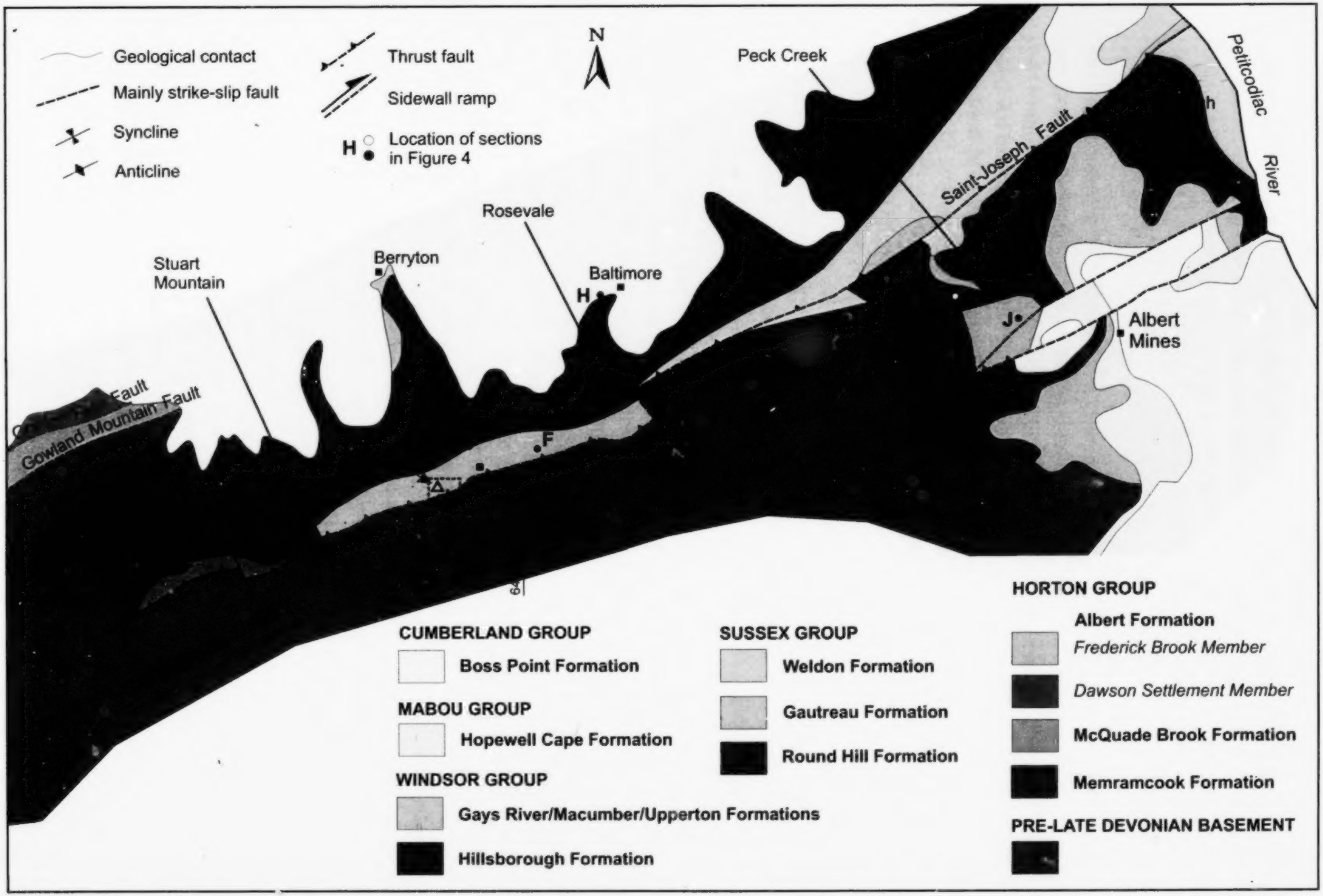
Geological contact
Mainly strike-slip fault
Syncline
Anticline
Thrust fault
Sidewall ramp
H
Location of sections in Figure 4
N
Peck Creek
Petitcodiac River
Saint-Joseph Fault
Rosevale
Berryton
Baltimore
H
Stuart Mountain
Fault
Gowland Mountain Fault
F
J
Albert Mines
CUMBERLAND GROUP
Boss Point Formation
MABOU GROUP
Hopewell Cape Formation
WINDSOR GROUP
Gays River/Macumber/Upperton Formations
Hillsborough Formation
SUSSEX GROUP
Weldon Formation
Gautreau Formation
Round Hill Formation
HORTON GROUP
Albert Formation
Frederick Brook Member
Dawson Settlement Member
McQuade Brook Formation
Memramcook Formation
PRE-LATE DEVONIAN BASEMENT

Figure 3. a) Geological map (eastern half) of the Caledonia Mountain–Elgin area on the southern margin of the Moncton Subbasin, after St. Peter (1989). Map shows 1) the distribution of thrust faults and sidewall ramps in the fold-thrust belt between Albert Mines and Prosser Brook, and 2) strike-slip faults northwest of Prosser Brook. See Park and St. Peter (2005) for details east of Caledonia Mountain. Figure 1 shows location of this map in southeastern New Brunswick.

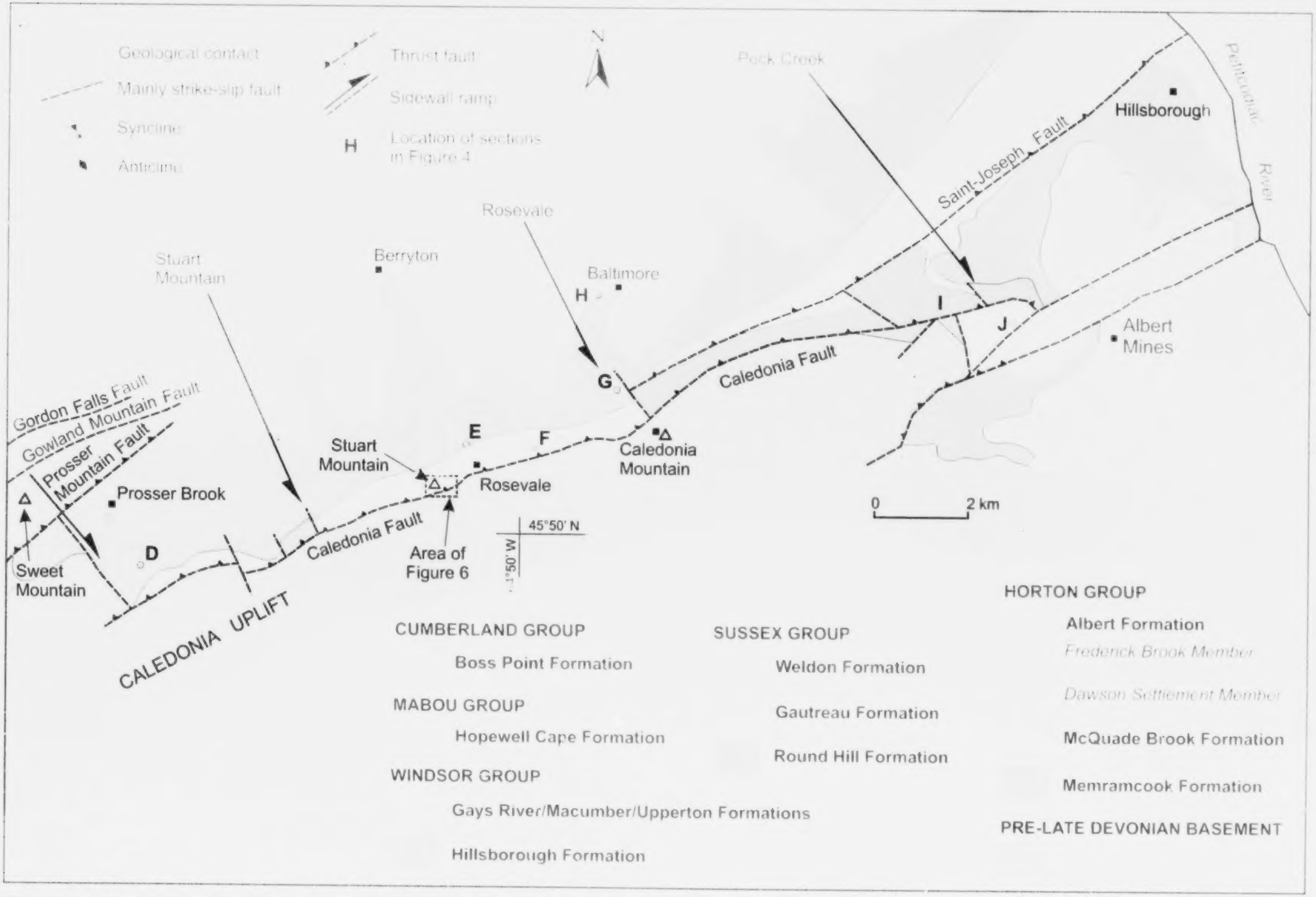
Geological contact
Mainly strike-slip fault
Syncline
Anticline
Thrust fault
Sidewall ramp
H
Location of sections in Figure 4
N
Rock Creek
Hillsborough
Petitcodiac River
Saint-Joseph Fault
Rosevale
Berryton
Stuart Mountain
Baltimore
H
I
J
Albert Mines
G
Caledonia Fault
Gordon Falls Fault
Gowland Mountain Fault
Prosser Mountain Fault
E
F
Stuart Mountain
Caledonia Mountain
Rosevale
Prosser Brook
Sweet Mountain
D
Caledonia Fault
Area of Figure 6
45°50' N
.1°50' W
0
2 km
CALEDONIA UPLIFT
CUMBERLAND GROUP
Boss Point Formation
MABOU GROUP
Hopewell Cape Formation
WINDSOR GROUP
Gays River/Macumber/Upperton Formations
Hillsborough Formation
SUSSEX GROUP
Weldon Formation
Gautreau Formation
Round Hill Formation
HORTON GROUP
Albert Formation
Frederick Brook Member
Dawson Settlement Member
McQuade Brook Formation
Memramcook Formation
PRE-LATE DEVONIAN BASEMENT

Figure 3. a) Geological map (eastern half) of the Caledonia Mountain–Elgin area on the southern margin of the Moncton Subbasin, after St. Peter (1989). Map shows 1) the distribution of thrust faults and sidewall ramps in the fold-thrust belt between Albert Mines and Prosser Brook, and 2) strike-slip faults northwest of Prosser Brook. See Park and St. Peter (2005) for details east of Caledonia Mountain. Figure 1 shows location of this map in southeastern New Brunswick.

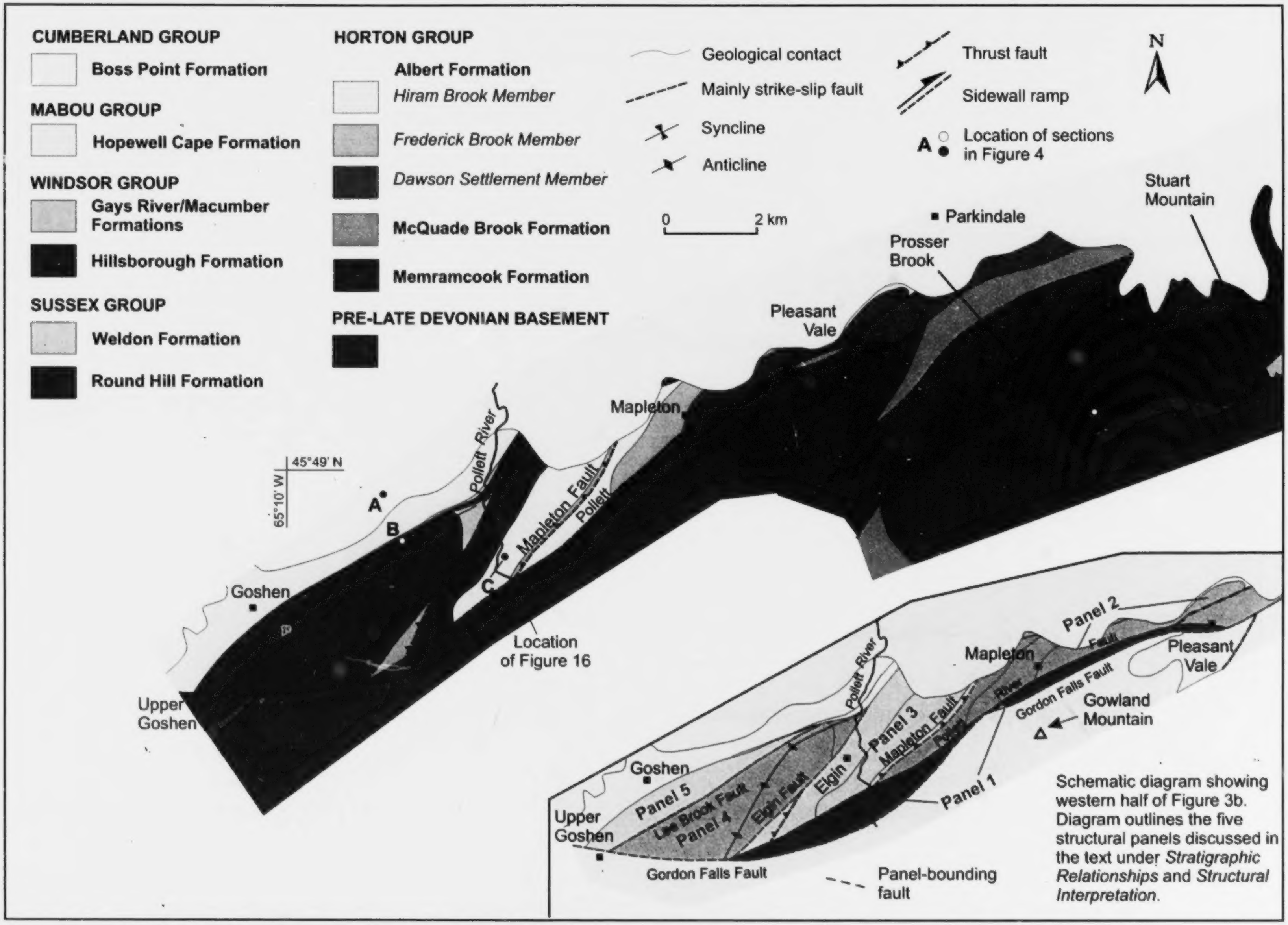
CUMBERLAND GROUP
Boss Point Formation
MABOU GROUP
Hopewell Cape Formation
WINDSOR GROUP
Gays River/Macumber Formations
Hillsborough Formation
SUSSEX GROUP
Weldon Formation
Round Hill Formation
HORTON GROUP
Albert Formation
Hiram Brook Member
Frederick Brook Member
Dawson Settlement Member
McQuade Brook Formation
Memramcook Formation
PRE-LATE DEVONIAN BASEMENT
Geological contact
Mainly strike-slip fault
Syncline
Anticline
Thrust fault
Sidewall ramp
A Location of sections in Figure 4
N
0
2 km
Parkindale
Stuart Mountain
Prosser Brook
Pleasant Vale
Mapleton
Pollett River
45°49' N
65°10' W
A
B
C
Mapleton Fault
Pollett
Goshen
Location of Figure 16
Upper Goshen
Panel 2
Fault
Pleasant Vale
Mapleton
River
Gordon Falls Fault
Gowland Mountain
Pollett River
Panel 3
Mapleton Fault
Pollett
Panel 1
Elgin
Goshen
Panel 5
Lee Brook Fault
Elgin Fault
Panel 4
Upper Goshen
Gordon Falls Fault
Panel-bounding fault
Schematic diagram showing western half of Figure 3b. Diagram outlines the five structural panels discussed in the text under *Stratigraphic Relationships* and *Structural Interpretation*.

Figure 3 *(cont'd)*. b) Geological map (western half) of the Caledonia Mountain–Elgin area on the southern margin of the Moncton Subbasin, after St. Peter (1989). Map shows 1) the distribution of thrust faults and sidewall ramps in the fold-thrust belt east of Prosser Brook, and 2) strike-slip faults between Prosser Brook and Elgin. Figure 1 shows location of this map in southeastern New Brunswick.

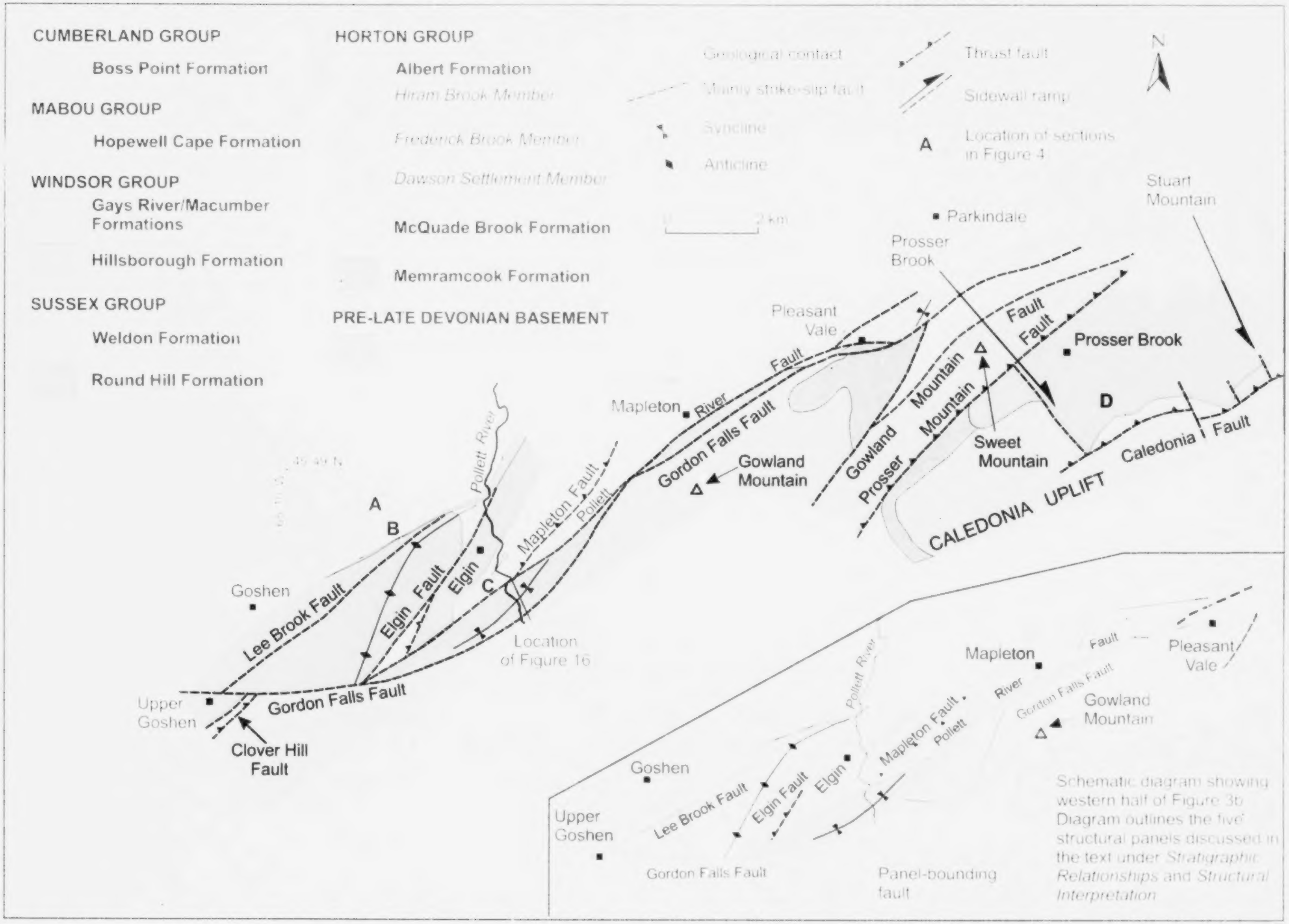
CUMBERLAND GROUP
Boss Point Formation
MABOU GROUP
Hopewell Cape Formation
WINDSOR GROUP
Gays River/Macumber Formations
Hillsborough Formation
SUSSEX GROUP
Weldon Formation
Round Hill Formation
HORTON GROUP
Albert Formation
Hiram Brook Member
Frederick Brook Member
Dawson Settlement Member
McQuade Brook Formation
Memramcook Formation
PRE-LATE DEVONIAN BASEMENT
Geological contact
Mainly strike-slip fault
Syncline
Anticline
0
2 km
Thrust fault
Sidewall ramp
A
Location of sections in Figure 4
N
Parkindale
Stuart Mountain
Prosser Brook
Pleasant Vale
Fault
Fault
Prosser Brook
Mapleton
River
Fault
Gordon Falls Fault
Gowland Mountain
Gowland Mountain
Prosser Mountain
Sweet Mountain
D
Caledonia Fault
CALEDONIA UPLIFT
45 49 N
A
B
C
Pollett River
Mapleton Fault
Pollett
Elgin
Elgin Fault
Goshen
Lee Brook Fault
Location of Figure 16
Upper Goshen
Gordon Falls Fault
Clover Hill Fault
Mapleton
Fault
Pleasant Vale
River
Gordon Falls Fault
Gowland Mountain
Pollett River
Mapleton Fault
Pollett
Elgin
Goshen
Upper Goshen
Lee Brook Fault
Elgin Fault
Gordon Falls Fault
Panel-bounding fault

Schematic diagram showing western half of Figure 3b Diagram outlines the five structural panels discussed in the text under *Stratigraphic Relationships* and *Structural Interpretation*

Figure 3 *(cont'd)* b) Geological map (western half) of the Caledonia Mountain–Elgin area on the southern margin of the Moncton Subbasin, after St Peter (1989) Map shows 1) the distribution of thrust faults and sidewall ramps in the fold-thrust belt east of Prosser Brook, and 2) strike-slip faults between Prosser Brook and Elgin. Figure 1 shows location of this map in southeastern New Brunswick

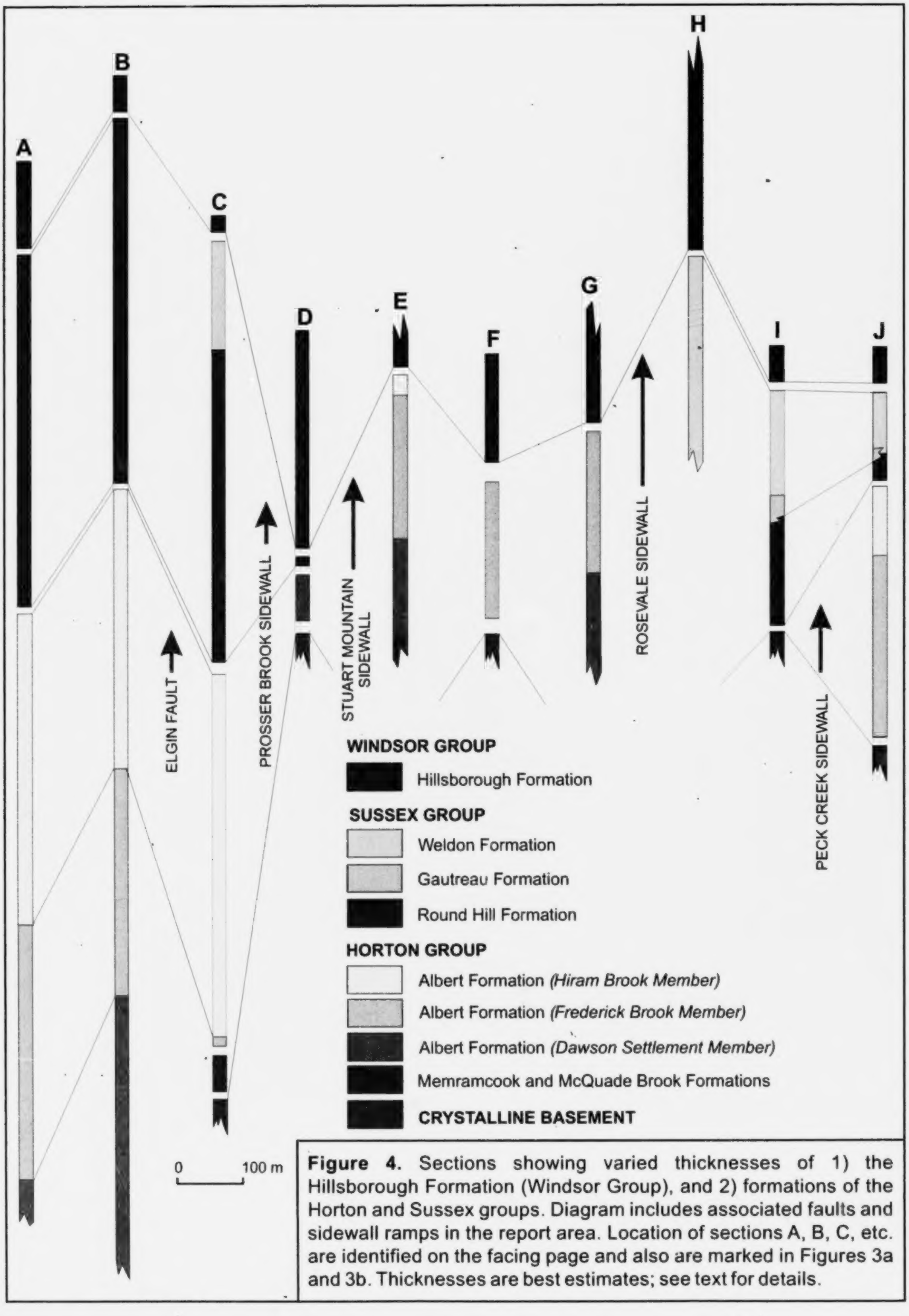
A
B
C
D
E
F
G
H
I
J
ELGIN FAULT
PROSSER BROOK SIDEWALL
STUART MOUNTAIN SIDEWALL
ROSEVALE SIDEWALL
PECK CREEK SIDEWALL
WINDSOR GROUP
Hillsborough Formation
SUSSEX GROUP
Weldon Formation
Gautreau Formation
Round Hill Formation
HORTON GROUP
Albert Formation (Hiram Brook Member)
Albert Formation (Frederick Brook Member)
Albert Formation (Dawson Settlement Member)
Memramcook and McQuade Brook Formations
CRYSTALLINE BASEMENT
0
100 m

Figure 4. Sections showing varied thicknesses of 1) the Hillsborough Formation (Windsor Group), and 2) formations of the Horton and Sussex groups. Diagram includes associated faults and sidewall ramps in the report area. Location of sections A, B, C, etc. are identified on the facing page and also are marked in Figures 3a and 3b. Thicknesses are best estimates; see text for details.

Rocks lithologically similar to the Mabou Group overlie the Albert Formation northeast of Pleasant Vale (Fig. 3b). Mabou strata in the Caledonia Mountain–Elgin area are assigned to the Hopewell Cape Formation of the Mabou Group (Fig. 2, 3a, 3b). Under this interpretation, they are analogous to Hopewell Cape rocks near Hillsborough in the eastern Moncton Subbasin, where the Hopewell Cape Formation unconformably overlies Windsor and older strata.

Cumberland Group

The most significant unconformity in the Carboniferous section in the report area lies at the base of the Cumberland Group. The basal unit, the Boss Point Formation (Fig. 2, 3a, 3b), is a sequence of buff quartz-pebble conglomerate, quartzose sandstone, and minor red and grey siltstone and mudstone. Palynomorph assemblages from many samples of the Boss Point Formation give an Early Pennsylvanian (late Bashkirian) age (Fig. 2).

The overstep of the sub-Cumberland unconformity is clearly demonstrated by the fact that beds of the Boss Point Formation lie on the Mabou Group from Goshen to Pollett River, on the Horton Group from Pollett River to Parkindale, on basement north-northeast of Prosser Brook, and on the Windsor Group (Hillsborough Formation) from Prosser Brook to east of Baltimore (Fig. 3a).

A Note on Stratigraphic Terminology

Stratigraphic terminology in this report follows the usage of St. Peter and Johnson (1997), Park and St. Peter (2005), and St. Peter (2006) with respect to the following points.

1. The names *Round Hill Formation* and *Weldon Formation* do not appear in maps of St. Peter (1989). Instead, coarse-grained and fine-grained clastic rocks representing the Round Hill and Weldon formations, respectively, were included in the Moncton Formation (now abandoned) of the Horton Group. The Round Hill and Weldon formations are currently recognized as units within the Sussex Group (St. Peter and Johnson 1997).

2. The Lee Brook Formation of St. Peter (1989) is a conglomerate-dominated unit in the Elgin area; it lies unconformably on the Sussex Group and is now seen to be equivalent to the Hillsborough Formation, as mapped elsewhere in the Moncton Subbasin. The Hillsborough Formation has nomenclatural precedence (Norman 1941), and therefore the name *Lee Brook Formation* has been abandoned.

Figure 4 *(cont'd).* Sections A, B, and C lie in the Elgin area, west of the fold-thrust belt. Sections D, E, F, G, I, and J lie adjacent to the Caledonia Fault between Prosser Brook and Albert Mines. Section H lies within the Moncton Subbasin, away from the Caledonia Fault.

A	Corridor/Columbia Will DeMille Well No. 1
B	Irving/Chevron Lee Brook Well No. 1
C	Elgin area: based on outcrops 1) along Pollett River, 2) east of Elgin, and 3) along Lee Brook north of Elgin
D	Prosser Brook area: based on surface exposures
E	New Brunswick Gas and Oilfields Turtle Creek Well No. 59
F	Stuart Mountain to Rosevale area: based on exposed sections in Bray Brook and Stuart Brook
G	Canadian Occidental Petroleum Rosevale Well No. 1
H	New Brunswick Gas and Oilfields Baltimore Well No. 127
I	Peck Creek: for measured section, see Park and St. Peter (2005) and St. Peter and Park (2006)

STRATIGRAPHIC RELATIONSHIPS ON SOUTHERN MARGIN OF THE MONCTON SUBBASIN

The following section examines stratigraphic relationships among rocks of the Horton and Sussex groups along the southern margin of the Moncton Subbasin between Caledonia Mountain and Elgin (Fig. 3a, 3b). The section is divided into three consecutive transects that occur roughly from east to west: 1) Caledonia Mountain to Prosser Brook, 2) Prosser Brook to Parkindale, and 3) Parkindale to Elgin. As detailed later under *Structural Interpretation*, the eastern Caledonia Mountain–Prosser Brook transect lies within a fold-thrust belt, whereas the western Parkindale–Elgin transect lies within a strike-slip duplex. The intervening Prosser Brook–Parkindale transect crosses a basement block that separates these two regions of distinctive deformational style.

Caledonia Mountain–Prosser Brook Transect

The widespread outcropping of Horton and Sussex rocks in the fold-thrust belt of the Hillsborough–Albert Mines area (Park and St. Peter 2005) narrows significantly westward along the southern margin of the Moncton Subbasin toward Prosser Brook (Fig. 3a). The narrowing is due in part to the overstepping trend of the unconformity beneath the Hillsborough Formation, and in part to thinning of the Horton and Sussex groups west of Albert Mines (Fig. 3a, 3b).

Horton Group

The oldest exposed Carboniferous strata along the southern margin of the Moncton Subbasin between Caledonia Mountain and Prosser Brook are assigned to the Albert Formation (Wright 1922; Gussow 1953; Brown and Whaley 1986; St. Peter 1989; St. Peter and Johnson 1997). Between Caledonia Mountain and Stuart Mountain (Fig. 3a), Albert beds are dominantly brown, dolomitic, kerogenous mudstone and shale (oil shale) with subordinate to minor interbeds of siltstone, sandstone, and conglomerate. In this section are beds of unusual boulder conglomerate containing contorted shale and oil shale clasts (Fig. 5a–d). Some beds display an upper part comprising a fining-upward mud-matrix conglomerate or breccia overlying a lower part of massive mud-matrix boulder conglomerate or breccia. Shale clasts are found only in the lower part, and their size is comparable with commingled boulders of basement granite (up to 0.4 m diameter). The shale clasts are contorted and commonly wrapped around the granite boulders or distorted into the interclast interstices. Conglomerate or breccia of this type is considered to be talus or debris flow proximal to the scarp defining the southern margin of the lacustrine basin of the Albert Formation.

On Stuart Mountain, two slices of crystalline basement occur within the Albert Formation on the hanging walls of small thrusts (Fig. 6). One slice is exposed in the roadbed on Stuart Mountain (Park and St. Peter 2005), and the other is visible in clearings near the summit of Stuart Mountain. Rocks of the Albert Formation are exposed in creek sections structurally below these slices, separating the slices from the main basement mass to the south. Outcrop here is poor, but local mapping suggests these basement slices are lenticular in section and plan, and are rootless (see *Structural Interpretation* for details).

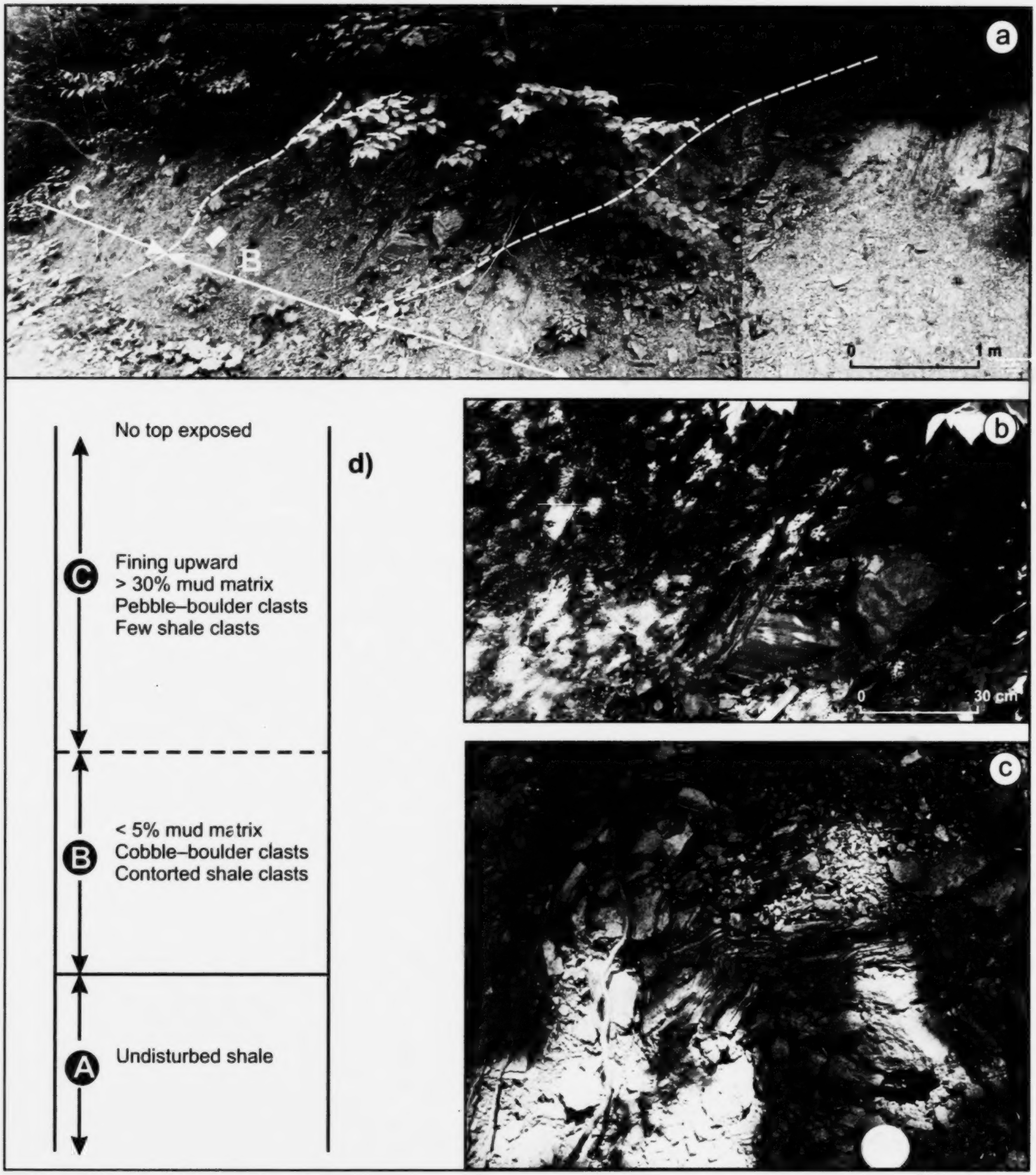
a
C
B
A
0
1 m
No top exposed
d)
C
Fining upward
> 30% mud matrix
Pebble–boulder clasts
Few shale clasts
B
< 5% mud matrix
Cobble–boulder clasts
Contorted shale clasts
A
Undisturbed shale
b
0
30 cm
c

Figure 5. a) Overview of conglomerate in the Frederick Brook Member, Albert Formation, along the Prosser Brook Road (GPS N45°50.637'; W64°52.539'). Yellow letters A, B, and C refer to the layers delineated in Figure 5d. b) Detail of granite boulders in Layer B of conglomerate in Figure 5a. c) Detail of contorted shale clasts and granite boulders in Layer B of conglomerate in Figure 5a. Coin (quarter) for scale. d) Schematic section through conglomerate in Figure 5a.

Immediately west of Stuart Mountain, outcrops of the Albert Formation along Stuart Brook and Prosser Brook Road reveal a succession comprising intervals of fine-grained strata (oil shale and siltstone) interstratified with coarse-grained intervals of pebble to boulder conglomerate and granular sandstone. Both the fine- and coarse-grained intervals range from beds a few centimetres thick to amalgamated sections up to 10 m in thickness. Shale beds within conglomerate-dominated intervals are commonly seen to be the locus of shear zones, many of which are marked by brown limonitic gouge (Fig. 7). Such shear zones, which are typically subparallel to bedding, demonstrate the continued westward presence of the fold-thrust belt documented to the east (Park and St. Peter 2005).

It is difficult to estimate thickness of the Albert Formation between Caledonia Mountain and Stuart Mountain. Bedding-parallel or near-parallel slip surfaces observed in many outcrops imply structural thickening. Disregarding such thickening, the best exposed section, along Bray Brook, suggests about 250 m of strata in that area (Fig. 4: Section F). (Bray Brook, not shown on Figure 3a, is a tributary of Turtle Creek between Caledonia Mountain and Rosevale.)

The dominance of grey shale, kerogenous mudstone and shale, and minor associated coarser clastic rocks suggests that Albert beds in the Caledonia Mountain–Stuart Mountain section can be assigned to the Frederick Brook Member (Fig. 3a). Five palynological assemblages from these beds yield either Tournaisian Zones 1 to 2 dates (two samples) or Tournaisian Zones 1D to 2 dates (three samples), thus supporting assignment of the beds to the Frederick Brook Member (Fig. 2).

The Albert Formation is exposed south of Prosser Brook village in a narrow belt bounded 1) on the south by basement rocks along the Caledonia Fault, 2) on the north by the unconformably overlying Hillsborough Formation (Fig. 8), 3) on the east by a northwest-trending fault against the Round Hill Formation, and 4) on the west by the overstepping Hillsborough Formation and a northwest-trending fault against the basement (Fig. 3a). This significant northwest-trending fault appears to terminate the major fold-thrust belt that extends eastward from the fault, and through the Albert Mines area to the Belliveau–Boudreau area on the east side of Petitcodiac River (see *Structural Interpretation* below). The same northwest-trending fault was previously interpreted as also terminating the Hillsborough Formation (St. Peter 1989), but new outcrops (GPS N45°49.843'; W64°58.143') along Beaman Road just west of Prosser Brook village reveal Hillsborough strata resting directly on crystalline basement, demonstrating that the unconformity at the base of the Hillsborough Formation cuts out the entire Tournaisian section in this area.

South of Prosser Brook, the Albert Formation consists mainly of polymictic conglomerate, lithic sandstone, and minor grey fine-grained quartzose sandstone, grey mudstone, and kerogenous shale. Because these Albert beds have not been sampled for spore determination, their stratigraphic position within the formation is uncertain. The preponderance of coarse clastic rocks suggests assigning the beds to the Dawson Settlement Member (Fig. 3a).

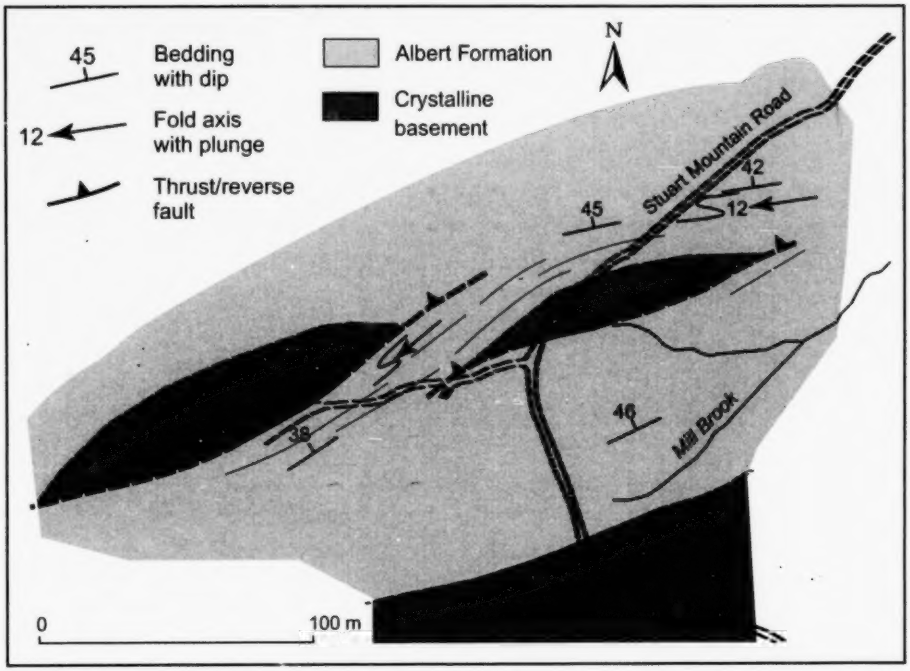
45
Bedding with dip
12
Fold axis with plunge
Thrust/reverse fault
Albert Formation
Crystalline basement
N
Stuart Mountain Road
42
12
45
38
46
Mill Brook
0
100 m

Figure 6. Geological map of the Stuart Mountain summit area, showing basement slices in the hanging walls of thrusts in the Albert Formation. Park and St. Peter (2005) provide details of the section along Stuart Mountain Road. Map location is shown in Figure 3a.

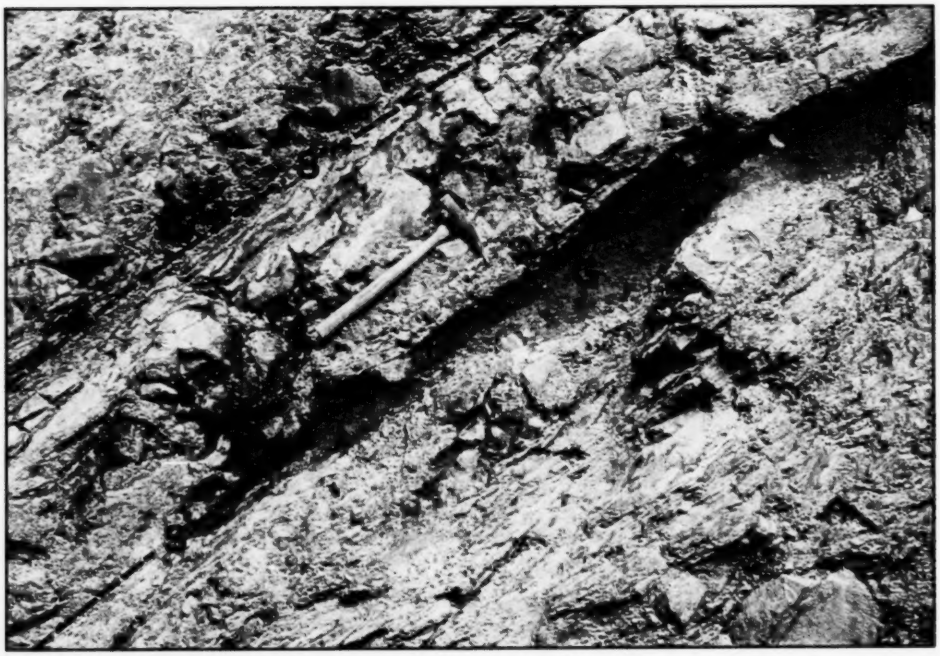

Figure 7. Strata of the Albert Formation along Prosser Brook Road near Stuart Brook, showing beds of pebble to boulder conglomerate (upper left, behind hammer, and lower right) interstratified with kerogenous fissile shale. Shale beds are commonly the focus of shear zones (S), some of which are marked by limonitic gouge (G). Hammer is 40 cm long.

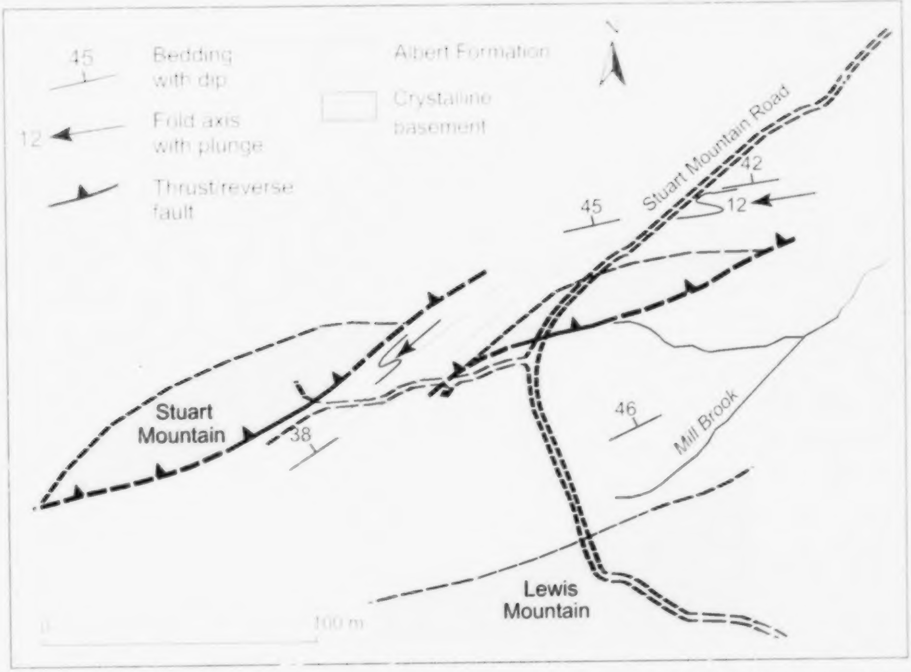
45
Bedding with dip
12
Fold axis with plunge
Thrust/reverse fault
Albert Formation
Crystalline basement
N
Stuart Mountain Road
42
12
45
Stuart Mountain
38
46
Mill Brook
Lewis Mountain
0
100 m

Figure 6. Geological map of the Stuart Mountain summit area, showing basement slices in the hanging walls of thrusts in the Albert Formation. Park and St. Peter (2005) provide details of the section along Stuart Mountain Road. Map location is shown in Figure 3a.

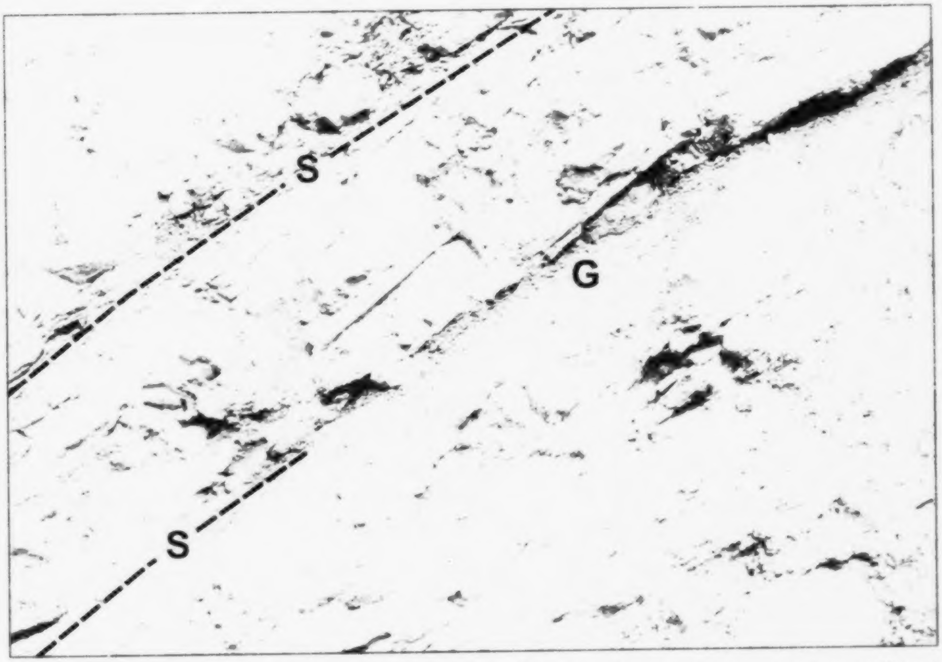

Figure 7. Strata of the Albert Formation along Prosser Brook Road near Stuart Brook, showing beds of pebble to boulder conglomerate (upper left, behind hammer, and lower right) interstratified with kerogenous fissile shale. Shale beds are commonly the focus of shear zones (S), some of which are marked by limonitic gouge (G). Hammer is 40 cm long.

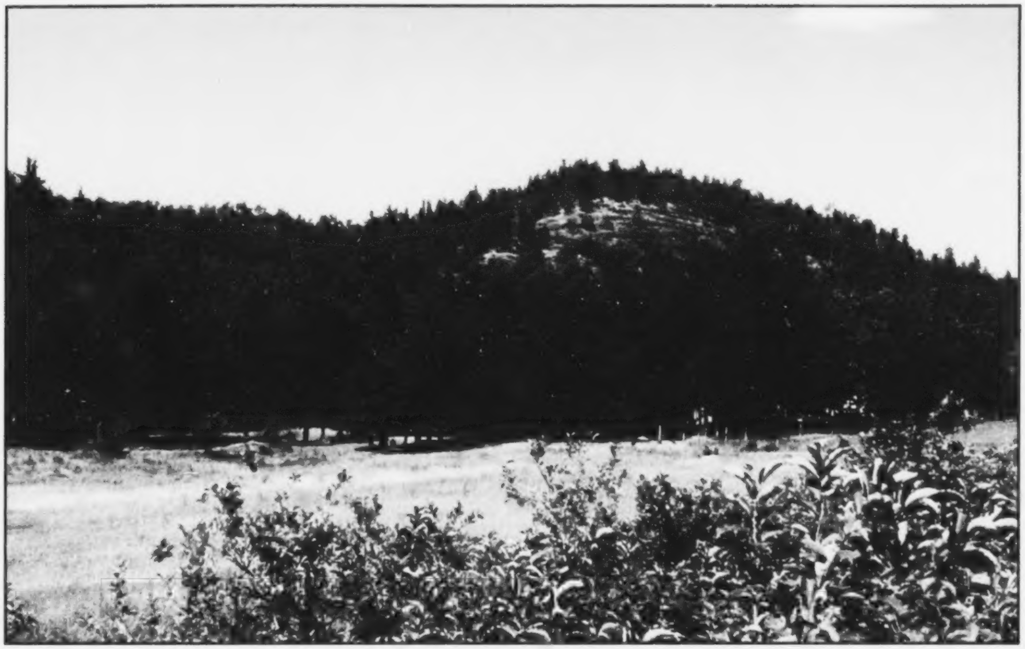

Figure 8. Conglomerate and sandstone of the Hillsborough Formation exposed on a hill about 1.6 km east of Prosser Brook village. The hillside consists of a 400 m thick section of shallowly dipping red-brown conglomerate and sandstone. View is from Prosser Brook Road.

Sussex Group

The Sussex Group is exposed in two places in the Caledonia Mountain–Prosser Brook transect: east of Caledonia Mountain and west of Stuart Mountain (Fig. 3a). North of Caledonia Mountain and from there 7 km eastward to Peck Creek (Fig. 3a; Fig. 2 in Park and St. Peter 2005), the Round Hill Formation dips shallowly to moderately north and lies directly against pre-Late Devonian crystalline rocks of the Caledonia Uplift in a faulted unconformity. Conglomerate and sandstone of the Round Hill Formation north and east of Caledonia Mountain are concordantly succeeded by fine-grained red sandstone and mudstone of the Weldon Formation. Just east of the report area, near Peck Creek (Fig. 3a) and northeast of there near Weldon (Fig. 1; in the axial part of the Moncton Subbasin), the Round Hill Formation is succeeded by the Gautreau Formation. At Peck Creek, grey mudrock of the Gautreau Formation has yielded late Tournaisian Zone 5 spores (Dolby 2004).

The contact between the Round Hill Formation and Albert Formation immediately north of Caledonia Mountain (Fig. 3a) is another significant northwest-trending fault. Movement along the fault is dominantly Tournaisian and shows only minor offset of the unconformably overlying Hillsborough Formation.

West of Stuart Mountain, the Sussex Group comprises a stacked sequence of fining-upward cycles of polymictic conglomerate, lithic sandstone, and minor siltstone and mudstone; consequently, these rocks are analogous to strata of the Round Hill Formation exposed east of Caledonia Mountain (Park and St. Peter 2005). Round Hill strata west of Stuart Mountain are 1) faulted against the Caledonia basement on the south, 2) unconformably succeeded by the Hillsborough Formation on the north, and 3) juxtaposed against the Albert Formation on the east and west by two northwest-trending cross-faults that delineate the boundaries of a Round Hill overstep onto basement rocks. Neither fault appears to offset the line of basement defined by the Caledonia Fault; however, outcrop control suggests that both cross-faults slightly displace the overlying Hillsborough boundary (Fig. 3a). The two cross-faults are interpreted as sidewall ramps associated with the end-Tournaisian fold-thrust event described later under *Structural Interpretation*.

Prosser Brook–Parkindale Transect

In the Caledonia Mountain–Prosser Brook transect just described, Horton and Sussex rocks of the fold-thrust belt and the unconformably overlying Windsor strata (Hillsborough Formation) are interrupted by crystalline basement rocks of the Sweet Mountain block west of Prosser Brook village (Fig. 3b). Foliated granodiorite, diorite, and amphibolite of this block are exposed in a roadcut at the Prosser Brook gorge north of the village (Fig. 9a). The basement block is bounded by the Prosser Mountain Fault on the southeast and the Gowland Mountain Fault on the northwest. Neither bounding fault is exposed, although the basement rocks are cut by numerous small faults and fractures.

Basement rocks at the south end of the gorge at Prosser Brook are intensely shattered and altered within 10 m of the projected trace of the Prosser Mountain Fault, and some fracture surfaces show an iron-rich clayey gouge. Northward through the gorge, a prominent fault set displays the same northeast trend as does the Prosser Mountain Fault and dips consistently 50° to 70° northwest (Fig. 9a, 9b). Slickensides associated with these faults plunge consistently west and show a shear sense of top-to-the-southeast or -east (Fig. 9c), suggesting that the Prosser Mountain Fault is a steep, northwest-dipping reverse fault with a strongly oblique right-lateral component of movement. A second set of faults appears to be conjugate to the Prosser Mountain Fault; these structures are also northeast-trending reverse faults but dip southeast (Fig. 9a, 9b).

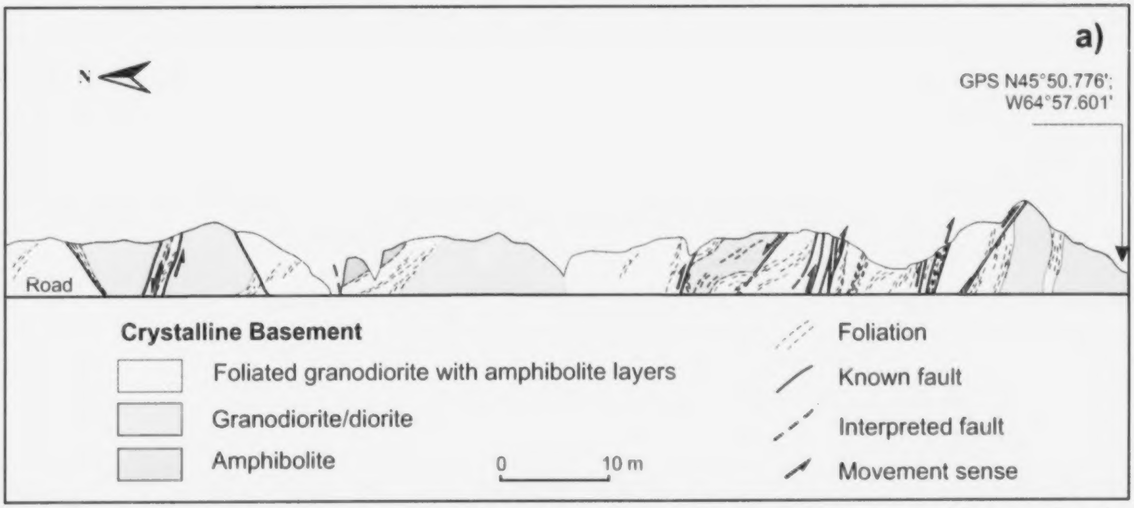

Figure 9. a) Detailed section along east side of the gorge at Prosser Brook, north of Prosser Brook village, showing faults cutting the pre-Late Devonian crystalline basement.

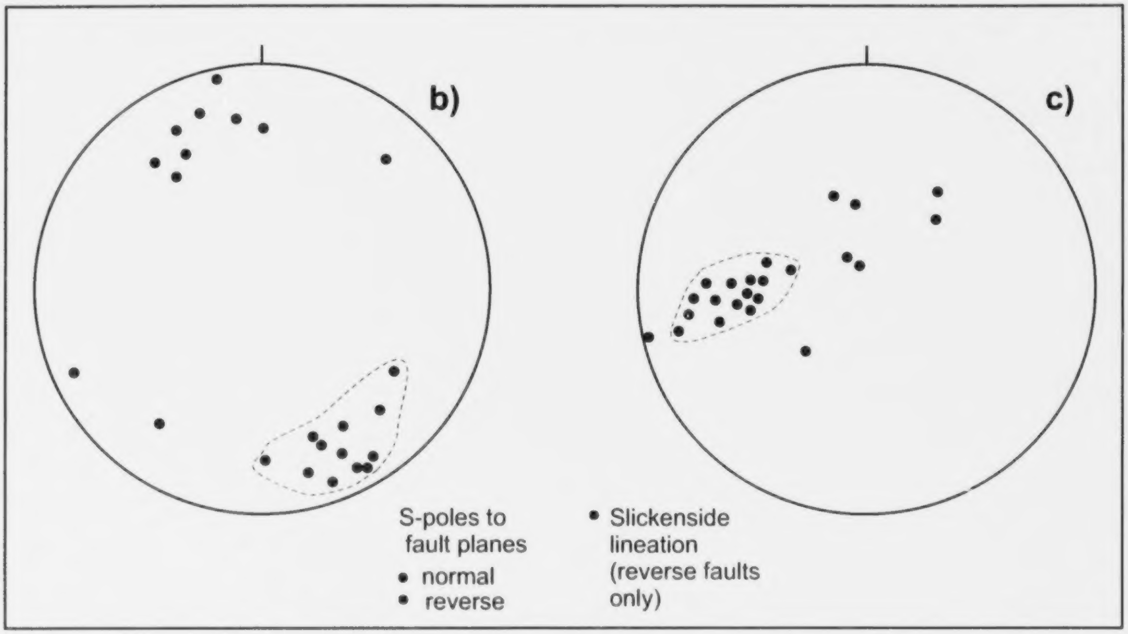

Figure 9 *(cont'd)*. Stereograms of structural elements in the pre-Late Devonian crystalline basement of the gorge section at Prosser Brook. b) S-poles to faults. c) Slickenside lineations from reverse faults. Points encircled by dashed lines represent structures parallel to the Prosser Mountain Fault. Figures 9b and 9c are both equal area projection, lower hemisphere.

The Prosser Mountain Fault can be traced northeast along the valley toward the high ground north of Prosser Brook village, where it is overstepped, without offset, by the Boss Point Formation (Fig. 10). Movement on the Prosser Mountain Fault therefore took place after deposition of the Hillsborough Formation but before deposition of the Boss Point Formation. Because the Boss Point Formation oversteps directly onto the Hillsborough Formation, cutting out the intervening succession, a more refined timing of movement is not possible. However, at nearby Berryton, St. Peter and Johnson (1997) mapped limestone of the Windsor Group in what should be the fault footwall, implying post-Windsor movement.

Geology on the northwestern margin of the Sweet Mountain block marks a fundamental change in character for rocks of the Horton Group. From this point westward, the Albert Formation is underlain by both the McQuade Brook and Memramcook formations, neither of which is present in surface exposures in the more easterly Caledonia Mountain–Prosser Brook transect.

The Gowland Mountain Fault separates the Sweet Mountain block from a steeply dipping, northwest-younging sequence of red shale, siltstone, and sandstone of the McQuade Brook Formation to the northwest (Fig. 3b). South of Parkindale, the Gordon Falls Fault juxtaposes these McQuade Brook redbeds against a north-younging sequence of conglomerate, lithic sandstone, minor mudstone, shale, and limestone of the Albert Formation (St. Peter and Johnson 1997). Exposures of the redbeds can be observed in road scrapes along Lane Road (GPS N45°51.183'; W64°57.531') to within 10 m of the Gordon Falls Fault trace. The generally coarse-grained lithofacies of the Albert Formation and its proximity to McQuade

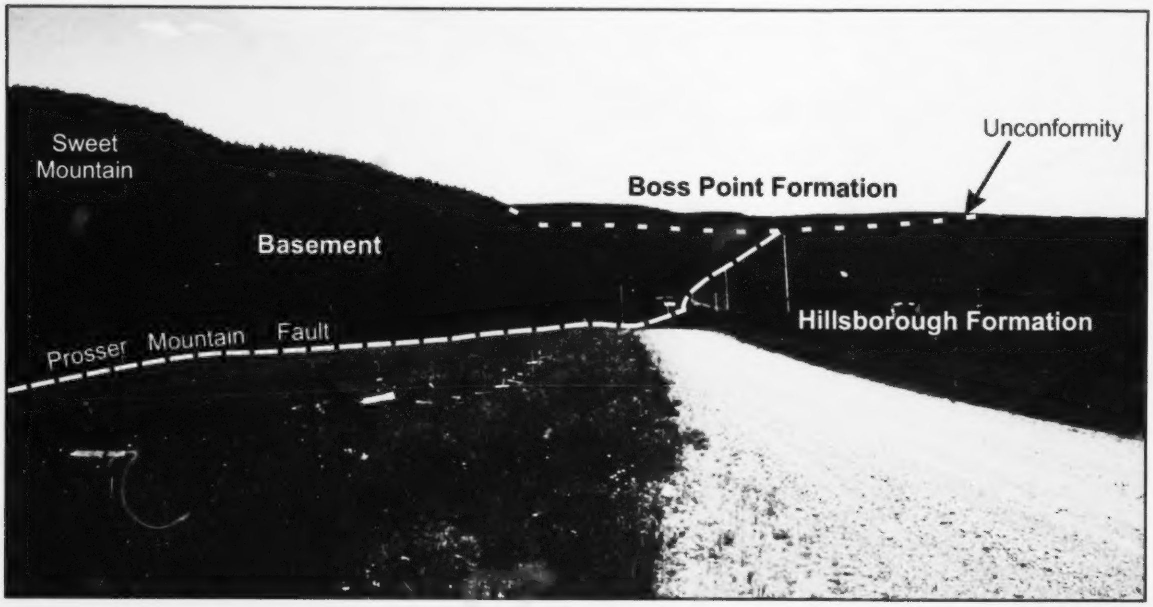

Figure 10. View from Beaman Road (GPS N45°49.843'; W64°58.143') looking northeast along the southern edge of the Sweet Mountain basement block. Basement rocks are in the hanging wall of the Prosser Mountain Fault, and Hillsborough rocks are in the footwall. The fault is truncated by the unconformity below the Boss Point Formation, shown along the background ridge.

Brook redbeds in this locale imply that Albert beds in the Parkindale area likely belong to the Dawson Settlement Member.

The Albert Formation in the Parkindale area forms the southern limb of a regional synclinal structure truncated by splays of the Gowland Mountain and Gordon Falls faults. Fold and fault splays run beneath the Boss Point Formation along the northern side of the valley east of Parkindale (St. Peter 1989; St. Peter and Johnson 1997).

Stratigraphic and fault relationships on the northwest side of the Sweet Mountain block imply a north-side downthrow on both the Gowland Mountain and Gordon Falls faults. An unknown thickness of the lower McQuade Brook Formation and underlying Memramcook Formation has been cut out on the north side of the Gowland Mountain Fault. Upper beds of the McQuade Brook Formation and lower beds of the Albert Formation are absent on the north side of the Gordon Falls Fault.

Parkindale–Elgin Transect

In the Parkindale–Elgin transect west of the Sweet Mountain block, rocks of the Horton and Sussex groups lie along the southern margin of the Moncton Subbasin. Stratigraphic sequences of both groups in this area have been disrupted and incorporated into a series of five fault-bounded panels during the formation of a strike-slip duplex. Panels cited in the following description (Panel 1, Panel 2, etc.) are shown schematically in Figure 3b (inset) and are delineated by their fault boundaries, as elaborated on under *Structural Interpretation*.

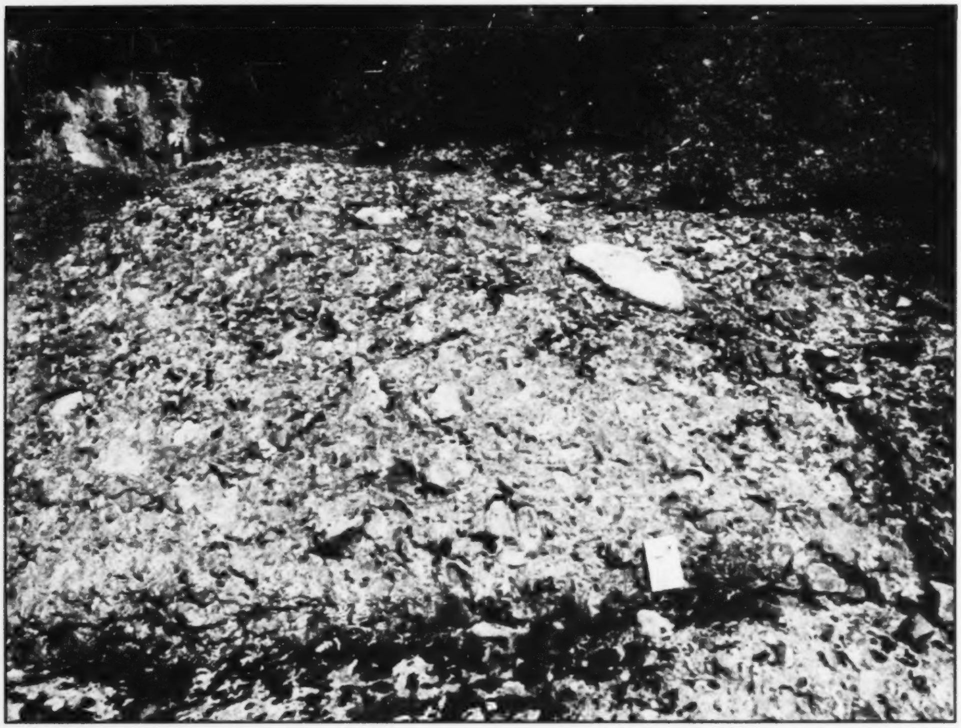

Figure 11. Boulder conglomerate of the Memramcook Formation in the Pollett River gorge, south of Elgin (GPS N45°47.464'; W65°5.993'). Notebook is 19 cm long.

Horton Group

The Memramcook Formation lies at the faulted base of the Carboniferous succession in the Elgin area (Panel 1). Its angular unconformity with crystalline basement rocks in the Gowland Mountain area can be observed south of Pleasant Vale (Fig. 3b). The coarse to very coarse polymictic conglomerate (with clasts up to boulders > 1 m diameter) that characterizes the formation is generally matrix-supported with angular to rounded clasts dominated by basement lithologies (Fig. 11). The Memramcook Formation is only a few tens of metres thick south of Pleasant Vale between the Gowland Mountain and Gordon Falls faults but is at least 100 m thick in the gorge at Pollett River, where neither top nor base are exposed (Fig. 3b).

The McQuade Brook Formation overlies the Memramcook Formation southwest of Pleasant Vale between the Gordon Falls and Pollett River faults (Panel 1), although only a few metres of the McQuade Brook Formation are preserved in this fault block. The McQuade Brook sequence there comprises red sandstone, siltstone, and shale; a spore assemblage from the section (Dolby 1991) dates the formation as earliest Tournaisian or Zone 1A (Fig. 2).

Between Elgin and Pleasant Vale, the Albert Formation is juxtaposed against the Memramcook and McQuade Brook formations along the Pollett River Fault (Panel 2; part of Panel 3); consequently, the base of the Albert section is not seen. In this area, the Albert Formation in a regional sense strikes northeast to north-northeast in a succession that youngs to the northwest and lies obliquely against the more easterly trending Pollett River Fault. The Albert Formation here was divided into lithological facies (St. Peter 1989, 1992), but lack of biostratigraphic control and inadequate understanding of structural detail prevented assigning the lithofacies to the three conventional stratigraphic members (Dawson Settlement, Frederick Brook, and Hiram Brook) as set out by Greiner (1962). Structural findings from the present investigation now allow this subdivision to be made.

The Dawson Settlement Member occurs from Mapleton through Pleasant Vale to just southwest of Parkindale (Panel 2). Southwest of Mapleton, the Frederick Brook and Hiram Brook members are located in the hanging wall of two northeast-trending reverse faults that are splays off the Pollett River Fault and that approximately follow the strike of bedding (Fig. 3b).

The more easterly of the reverse faults — the newly named Mapleton Fault (see below) — trends from Pollett River south of Elgin northeasterly towards Mapleton. Its hanging wall carries a very thin interval of organic shale of the Frederick Brook Member, overlain to the west by a thick unit of dominantly coarse clasts of the Hiram Brook Member (Panel 3). The more westerly, unnamed, splay lies southwest of Elgin in the Webster Brook area and is truncated by the Elgin Fault. (Webster Brook, not shown in Figure 3b, is a northeast-draining tributary of Pollett River.) This splay brings a fault-bounded wedge of organic mudrock of the Frederick Brook Member in its hanging wall to the west over coarse 'redbed' clastic rocks of the Round Hill Formation in the footwall to the east (southwest part of Panel 3). The following description of members of the Albert Formation in Panels 2 and 3 (Figure 3b inset) show the spatial variability of member lithology and demonstrates how structure influenced lithological distribution along these two northeast-trending splays of the Pollett River Fault.

The Dawson Settlement Member is not well exposed between Mapleton and Pleasant Vale, but small outcrops on the roadside and in streambeds reveal an interlayered sequence of grey polymictic conglomerate, lithic to feldspathic sandstone, and lesser grey siltstone and shale, the last of which may be locally kerogenous. At Pleasant Vale and farther northeast at Parkindale (Panel 2), the coarse conglomerate and sandstone sequence contains a 25 m thick limestone interval. The limestone beds comprise 1) grainstone carrying variable quantities of siliciclastic pebbles, granules and sand; and carbonate pellets and algal oncolites, 2) parallel-laminated quartzose and pelloidal packstone/grainstone, and 3) massive crystalline limestone (St. Peter 1992).

Thickness of the Dawson Settlement Member between Mapleton and the Parkindale area is difficult to estimate. As noted, basal beds are absent along the Pollett River Fault, and the basal depositional contact with the McQuade Brook Formation is not exposed. The section on the limbs of the minor syncline southwest of Parkindale (Fig. 3b) suggests a minimum thickness of 400 m (Panel 2). An additional indication of the thickness is given in Irving/Chevron Lee Brook Well No. 1 (Fig. 3b: Location B) drilled 2 km west of Elgin. There, 460 m of mainly coarse clastic rocks of the Dawson Settlement Member were encountered before drilling terminated at a 2100 m depth, still intersecting the member (Fig. 4: Section B). Only 46 m were drilled at

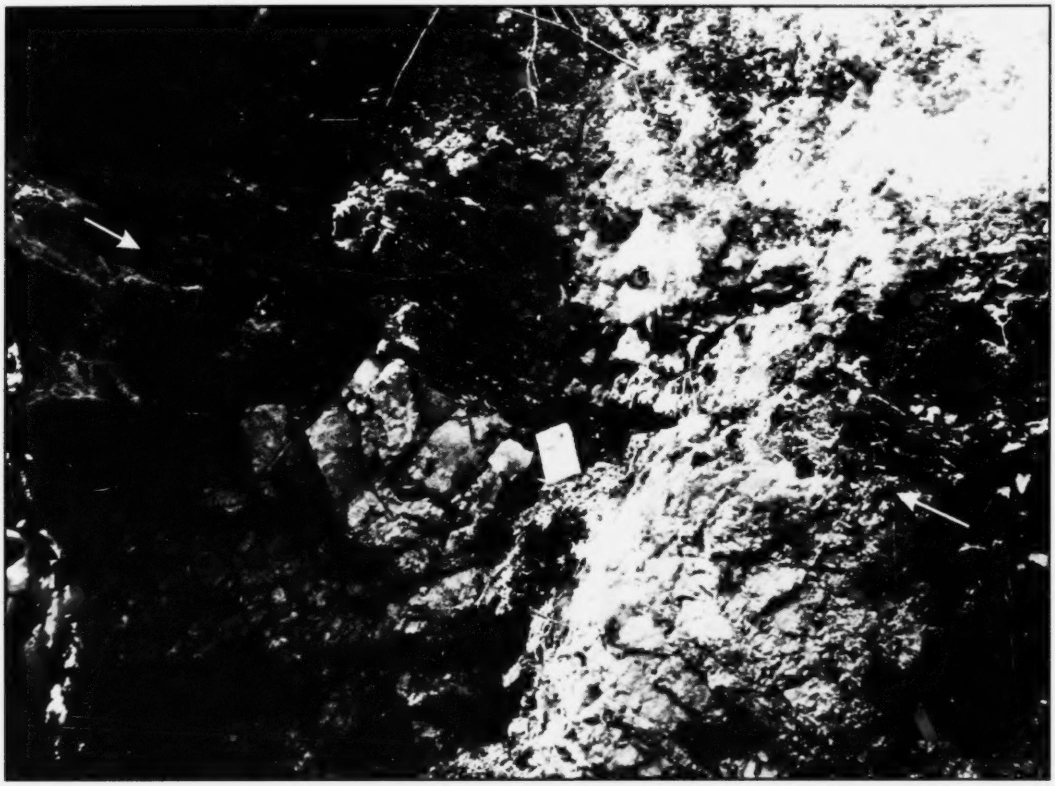

Figure 12. Limestone with slump structures overlain by kerogenous black shale and siltstone of the Frederick Brook Member of the Albert Formation, Horton Group. The outcrop is located in the bed of Popple Intervale Brook, Mapleton (GPS N 45° 49.271'; W 65° 3.341'). Yellow arrows indicate an erosion surface. Notebook is 19 cm long.

the top of the Dawson Settlement Member in the adjacent Corridor/Columbia Will DeMille Well No. 1 (Fig. 3b: Location A) before drilling ceased at 2644 m (Fig. 4: Section A).

The contact between the Dawson Settlement Member and overlying Frederick Brook Member is not exposed in the Mapleton area but appears from widely spaced outcrops to be gradational and conformable. The Frederick Brook Member is clearly observed along Popple Intervale Brook, a northward-draining tributary of Pollett River near Mapleton (Panel 2). There, the Frederick Brook Formation is dominated by dark grey calcareous and dolomitic mudstone with subordinate micritic limestone and kerogenous shale (oil shale); some of the limestone beds display slump structures (Fig. 12). The section shows an upward coarsening, and sandstone becomes more abundant to the northwest.

Thickness of the Frederick Brook Member at Popple Intervale Brook is estimated at 300 m. The estimate is based on the dip of bedding in brook exposures, and it assumes no faults or folds exist in concealed intervals that might offset thickness calculations. By way of comparison, the drilled (apparent) thickness of the Frederick Brook Member in Irving/Chevron Lee Brook Well No. 1 (Fig. 3b: Location B) is 438 m (Fig. 4: Section B) and in Corridor/Columbia Will DeMille Well No. 1 (Fig. 3b: Location A) is 512 m (Fig. 4: Section A).

The boundary with the overlying Hiram Brook Member is placed where sandstone begins to dominate the finer grained lithotypes of the underlying Frederick Brook Formation. The Hiram Brook Member in the section along Popple Intervale Brook (Panel 2) comprises grey, fine- to medium-grained sandstone that displays both wave ripples and current ripples. The coarser beds are commonly cross bedded; minor thin beds of grey siltstone and shale occur within the sandstone. Beds of coarse to granular sandstone and polymictic pebble and cobble conglomerate occur in the upper part of the section.

Along strike to the southwest of this section, the Hiram Brook Member consists of more abundant polymictic pebble and cobble conglomerate and interbeds of granular and coarse lithic sandstone. Fine-grained, ripple-laminated sandstone comprises only a minor part of the section near the Pollett River Fault, presumably in a location adjacent to the paleobasin margin.

The exposure of Hiram Brook strata at and southwest of Popple Intervale Brook (Panel 2) is overlain to the northwest by a thin interval (a few metres or tens of metres) of kerogenous mudrock and oil shale containing minor thin interbeds of sandstone and limestone (Panel 3). These beds are exposed along Pollett River and some tributary streams (St. Peter 1989) and are assigned to the Frederick Brook Member. Their contact with underlying beds of the Hiram Brook Member to the east (in Panel 2) is interpreted to be a reverse fault, herein named the Mapleton Fault (see *Structural Interpretation*).

Along Pollett River just south of Elgin (Panel 3), the Hiram Brook Member comprises a series of stacked, fining-upward cycles of grey polymictic pebble and cobble conglomerate (Fig. 13a, 13b), cross-bedded to massive, coarse to granular lithic sandstone, minor fine-grained sandstone, and dark grey mudstone, and rare kerogenous shale; the shale locally bears slump structures (Fig. 13c) and rare fish scales. The fining-upward cycles are up to 10 m in thickness (St. Peter 1992). Palynomorph assemblages from four samples of grey mudrock from the Hiram Brook Member in this area yield Tournaisian Zones 1C to 2A ages (Dolby 1991).

Thickness of the Hiram Brook Member along Pollett River south of Elgin is about 630 m. This is comparable with the 500 m of drilled thickness (Fig. 4: Section B) for the member in Irving/Chevron Lee Brook Well No. 1 (Fig. 3b: Location B) and the 550 m of drilled thickness (Fig. 4: Section A) in Corridor/Columbia Will DeMille Well No. 1 (Fig. 3b: Location A). These wells lie on the north side of the Elgin Fault (Fig. 3b) and northwest of the Hiram Brook section along Pollett River. The Hiram Brook Member in both wells contains significantly greater mudstone and shale and correspondingly less sandstone and conglomerate than it does in surface section along Pollett River. Such findings are consistent with the Pollett River section representing proximal beds adjacent to the basement, and the well sections representing more distal sequences.

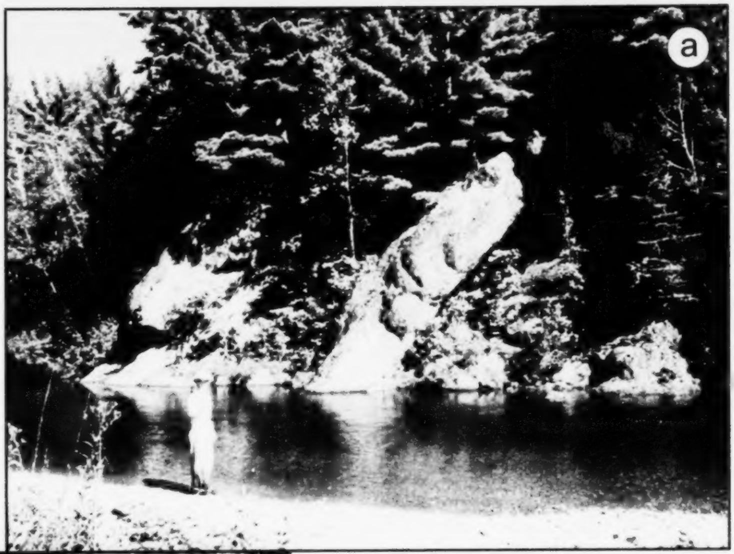

Figure 13. a) Large conglomerate unit of the Hiram Brook Member of the Albert Formation, Horton Group. Site is located on the east bank of Pollett River east of Elgin (GPS N45°47.984'; W65°6.134').

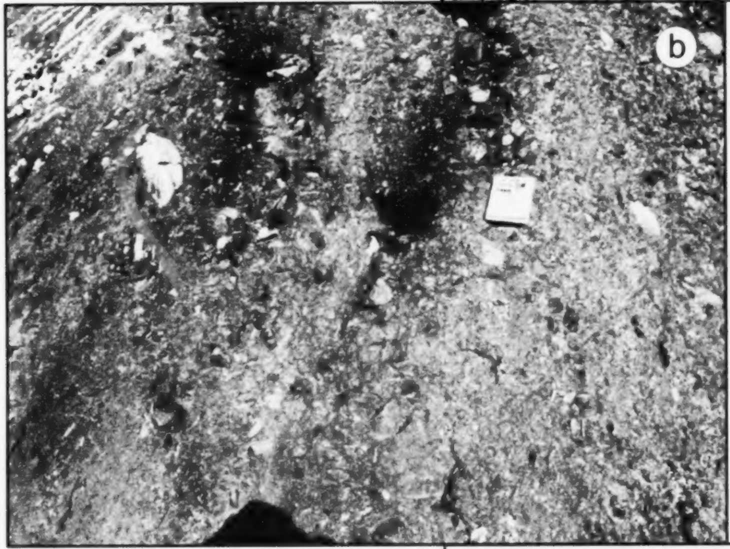

Figure 13. b) Boulder conglomerate unit of the Hiram Brook Member of the Albert Formation, Horton Group. Site is located on the east bank of Pollett River at the north end of the Pollett River gorge south of Elgin. Notebook is 19 cm long.

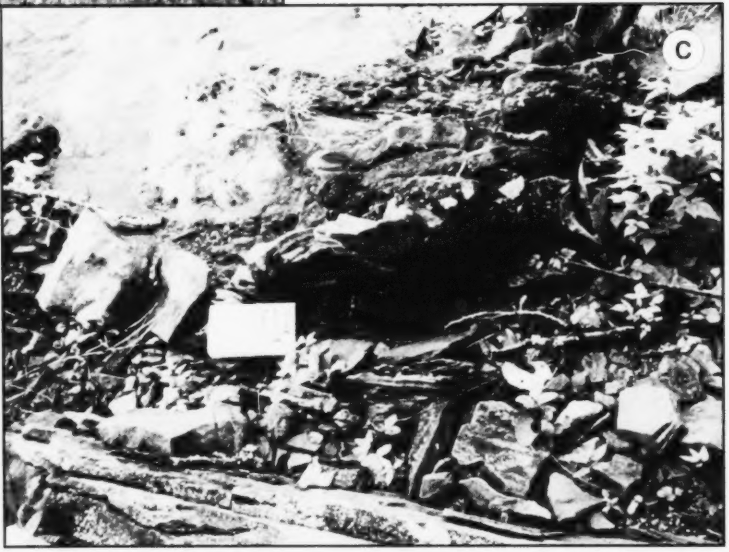

Figure 13. c) Sandstone with pebbly layers, shale partings, and slump structures (above notebook) in the Hiram Brook Member of the Albert Formation, Horton Group. Site is located along Pollett River east of Elgin (GPS N45°47.919'; W65°6.096'). Notebook is 19 cm long.

About 3 km southwest of Elgin (southwest part of Panel 3), kerogenous mudstone and kerogenous shale of the Albert Formation are exposed for nearly 1 km along Webster Brook (Fig. 3b). The section also has thin interbeds of fine-grained rippled sandstone and rare beds of gritty sandstone and dolostone. Thickness of this fault-bounded Albert section is unclear, due to the presence of abundant soft sediment deformation and later structures including shears, minor folds, and calcite veins. However, the rocks are assigned to the Frederick Brook Member on the basis of their lithological composition. A spore assemblage from the beds at Webster Brook and an assemblage from beds of the Frederick Brook Member at Popple Intervale Brook both yield Tournaisian Zone 1C ages (Dolby 1991).

On the south side of the Gordon Falls Fault near Upper Goshen (Fig. 3b), the Albert Formation consists primarily of grey to green polymictic pebble to boulder conglomerate with lesser fine- to coarse-grained feldspathic and lithic sandstone, and minor grey mudstone and kerogenous shale. These Albert rocks are tentatively assigned to the Dawson Settlement Member on the basis of their dominantly coarse lithotypes and proximity to basement.

Sussex Group

Where the Sussex Group overlies the Albert Formation in the Elgin area (Panel 3), the Round Hill Formation (Sussex Group) consists of fining-upward cycles of reddish-brown polymictic conglomerate, lithic sandstone, and lesser reddish-brown siltstone and mudstone (Fig. 3b). Excellent exposures of the Round Hill Formation occur along Pollett River at or near Elgin; its basal contact with the Albert Formation can be seen on the east bank of Pollett River about 270 m downstream from the bridge over the river at Elgin. The section of Round Hill strata along Pollett River is approximately 500 m thick from its contact with the Albert Formation to its upper contact against the Elgin Fault (Fig. 4: Section C).

Along Popple Intervale Brook just north of Mapleton (Fig. 3b), the Round Hill Formation overlies the Hiram Brook Member of the Albert Formation (Panel 2). The uppermost Hiram Brook beds comprise interbedded grey polymictic conglomerate, lithic sandstone, and minor grey mudstone and kerogenous shale. Round Hill strata immediately to the north are grey polymictic conglomerate with minor interbeds of lithic sandstone and fine-grained sandstone. The Round Hill Formation at this locale is distinguishable from the coarse Albert facies primarily by the former unit's absence of kerogenous mudstone or shale. Although the formational contact is not exposed, an angular unconformity is implied by the fact that Albert beds dip steeply to vertically, whereas Round Hill beds dip at 20° or less. It should be noted that rocks assigned here to the Round Hill Formation were previously included in the Albert Formation (see Gussow 1953; Greiner 1962; St. Peter 1989).

Immediately north of Elgin along the lower part of Lee Brook (Panel 4), sandstone, red siltstone, and red mudstone of the Weldon Formation (Sussex Group) succeed the Round Hill Formation (Fig. 3b). Here, about 200 m of Weldon Formation is preserved below the unconformity at the base of the Hillsborough Formation (Fig. 4: Section C).

STRUCTURAL INTERPRETATION

Caledonia Mountain–Prosser Brook Fold-Thrust Belt

An end-Tournaisian fold-thrust belt was recently defined in the Hillsborough–Albert Mines area just east of the report area (Park and St. Peter 2005), involving (among other structures) the Caledonia and Saint-Joseph faults. The current investigation demonstrates that the belt continues westward from Caledonia Mountain to Prosser Brook, following the Caledonia Fault. West of Albert Mines, however, the Saint-Joseph and Caledonia faults converge into a fairly narrow zone, possibly as a result of displacements along sidewall ramps (Fig. 3a). The actual width decrease of the fold-thrust belt west of Caledonia Mountain cannot be determined, because the belt is hidden beneath the unconformity at the base of the Hillsborough Formation.

Additional sidewall ramps occur between Caledonia Mountain and Prosser Brook, each coincident with the Sussex Group (Round Hill Formation) overstepping the Horton Group (Albert Formation) onto basement (Fig. 3a). All ramps seem to be northwest-trending features, although only the one immediately west of Prosser Brook could be observed directly in outcrop to verify this assumption. These northwest-trending structures on which sidewall ramps nucleated during the end-Tournaisian inversion had a fundamental influence on deposition of the Horton and Sussex groups. Along the entire section between Albert Mines and Elgin (Fig. 3a, 3b), the structures coincide with overstepped Sussex rocks, and with major changes in thickness and facies of the Albert Formation (Fig. 4).

The northwest-trending structures also appear to have been active during deposition of the Hillsborough Formation, causing a major change in geometry of that unit. Near Hillsborough, the formation is up to 100 m thick, as defined by outcrop; in hillsides north of Prosser Brook village, it is least 500 m thick (Fig. 8); and in the New Brunswick Gas and Oilfields Well No. 127 at Baltimore (Fig. 4: Section H), the formation has a true thickness of more than 700 m. Over the sidewall trace immediately west of Prosser Brook village, the Hillsborough Formation oversteps all older Carboniferous units directly onto basement but also undergoes a substantial reduction in thickness. This reduction is evident farther west around Elgin (Fig. 3b: Location C), where outcrops of the Hillsborough Formation are less than 50 m thick (Fig. 4: Section C).

The slices of basement rocks within the Albert Formation (Fig. 6) around Stuart Mountain (described under *Stratigraphic Relationships*) are anomalous. Nowhere else in the fold-thrust belt from Saint-Joseph to Prosser Brook are allochthonous masses of crystalline basement present, although this apparent absence may be a consequence of limited exposure. Where relief is sufficient to assess the shape of these bodies, the Stuart Mountain slices appear to be rootless: that is, they are not tips of basement material that enlarges with depth to become contiguous with a basement mass at depth. Instead, the phenomenon of rootless basement

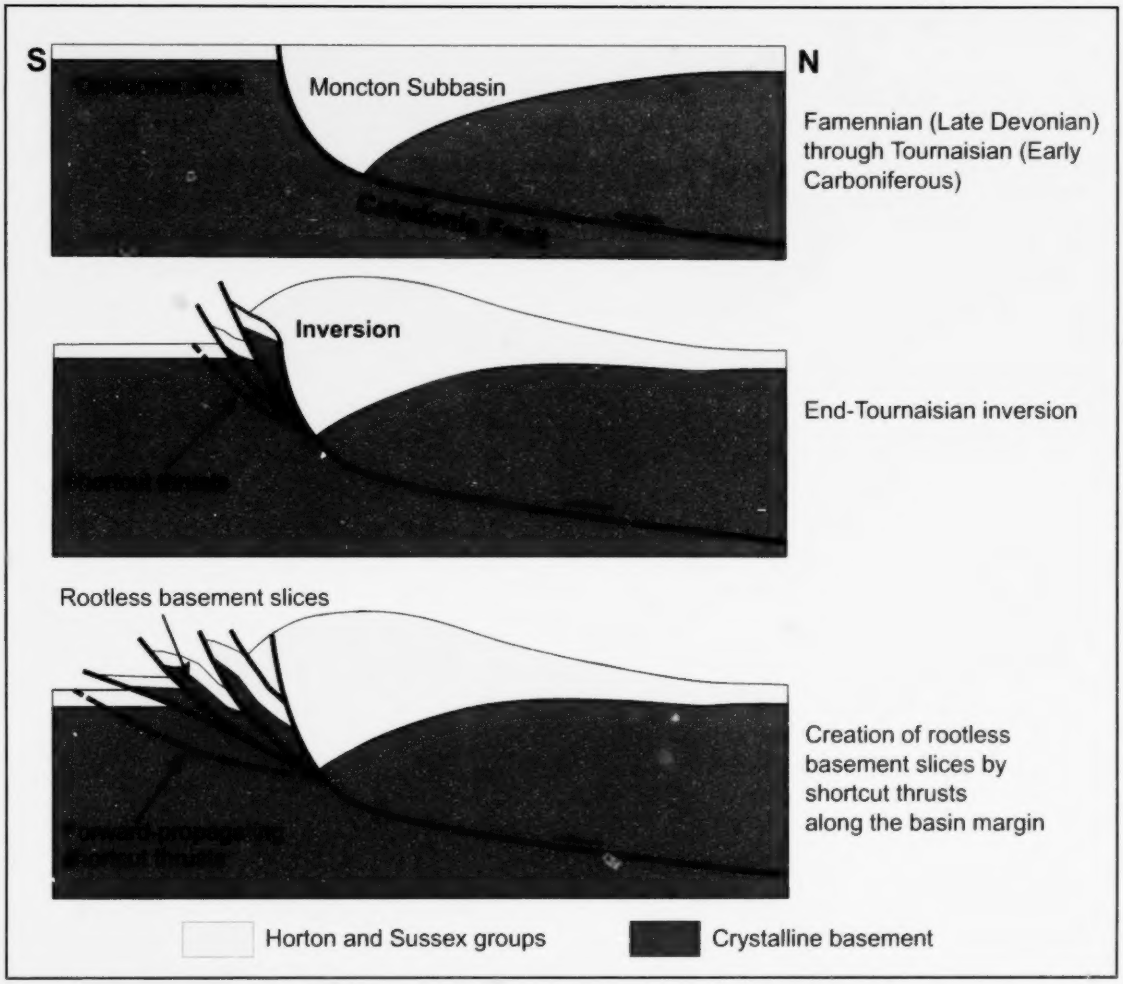
S
Moncton Subbasin
N
Famennian (Late Devonian) through Tournaisian (Early Carboniferous)
Caledonia Fault
Inversion
End-Tournaisian inversion
Shortcut thrusts
Rootless basement slices
Creation of rootless basement slices by shortcut thrusts along the basin margin
Forward-propagating shortcut thrusts
Horton and Sussex groups
Crystalline basement

Figure 14. Evolution of the Caledonia Fault from a basin-controlling extensional listric structure during deposition of the Horton and Sussex groups to a contractional structure at the time of post-Sussex (end-Tournaisian) inversion. The rootless basement slices (see text) could have been formed by 'shortcut' thrusts along the basin margin, as described in Hayward and Graham (1998) and McClay (1998). Any topographic deviation from a simple listric profile along the original fault can produce these rootless basement slices.

slices could be explained here by interpreting the Caledonia Fault as a pre-existing structure reactivated by the end-Tournaisian fold-thrust belt (Fig. 14).

Several workers have identified the Caledonia Fault as being either the southern bounding structure of the Moncton Subbasin, or located close to this margin (Gussow 1953; St. Peter 1993; Wilson and White 2006). The coarse, boulder conglomerate breccias in the Albert Formation along the line of the Caledonia Fault are consistent with a proximal relation to the basin margin. If the Albert Formation basin were a half-graben and the Caledonia Fault a larger structure in asymmetric profile, then thrust slices of basement such as those at Stuart Mountain could represent 'shortcut' structures (Fig. 14) generated when the half-graben underwent inversion (Hayward and Graham 1989; McClay 1998). Slices generated by such shortcut thrusts can be rootless and disconnected from autochthonous basement.

Parkindale–Elgin Strike-Slip Duplex

As discussed under *Stratigraphic Relationships*, rocks of the Horton and Sussex groups between Parkindale and Elgin are contained in five structural panels within a strike-slip duplex (Fig. 3b). These fault-bounded panels are delineated by their fault boundaries, as follows.

- **Panel 1** lies south of the Pollett River Fault, forming a long narrow block between the Pollett River and Gordon Falls faults. The panel consists entirely of Memramcook and McQuade Brook formations of the Horton Group.
- **Panels 2 to 5** lie on the north side of the Pollett River Fault between Upper Goshen and just east of Pleasant Vale. They are composed mainly of rocks of the Horton Group (Albert Formation) and Sussex Group (Round Hill and Weldon formations). The western boundary of **Panel 2** is the Mapleton Fault; from there, the panel reaches eastward to just east of Pleasant Vale. **Panel 3** is bounded by the Elgin Fault on the west and Mapleton Fault on the east. **Panel 4** is bounded by the Lee Brook Fault on the west and Elgin Fault on the east. The Lee Brook Fault forms the eastern boundary of **Panel 5**.

The Lee Brook, Elgin, and Mapleton faults are northeast- to north-northeast-striking structures that are splays off either the Gordon Falls Fault to the southwest or the Pollett River Fault to the northeast (Fig. 3b).

Panel Descriptions

Panel 1

Along Pollett River south of Elgin, the Memramcook Formation occurs in a doubly (northeast and southwest) plunging, open syncline (Fig. 3b, Fig. 15a). In contrast, immediately southwest of Pleasant Vale, between the Gordon Falls and Pollett River faults, a thin wedge of McQuade Brook strata is located in the trough of a steep, north-plunging syncline. In the latter area, the Memramcook and McQuade Brook formations lie in faulted contact with basement rocks that include bedded limestone and marble. The marble is unlike other basement rock types in the Caledonia Uplift in this area, more closely resembling marble units in the Brookville Terrane west of Sussex (Barr and White, pers. comm.).

Panel 2

Exhumed strata in the panel between the Mapleton and Pollett River faults consists mainly of moderately to steeply northwest-dipping, northwest-facing thick strata of the Albert Formation along the southern limb of a regional syncline (Fig. 15b). Some large-scale folds occur in siltstone and limestone along Popple Intervale Brook south of Highway 895 at Mapleton (Fig. 12), but these folds are bounded by parallel-bedding surfaces and appear to be analogous to the large soft-sediment structures in the Albert Formation in the southwestern part of the Moncton Subbasin near Sussex (Wilson 2004). Beds of the Sussex Group are exposed in this panel only north of Mapleton along Popple Intervale Brook, where a few metres of Round Hill Formation appear immediately below the overstepping unconformity at the base of the Boss Point Formation (Fig. 3b).

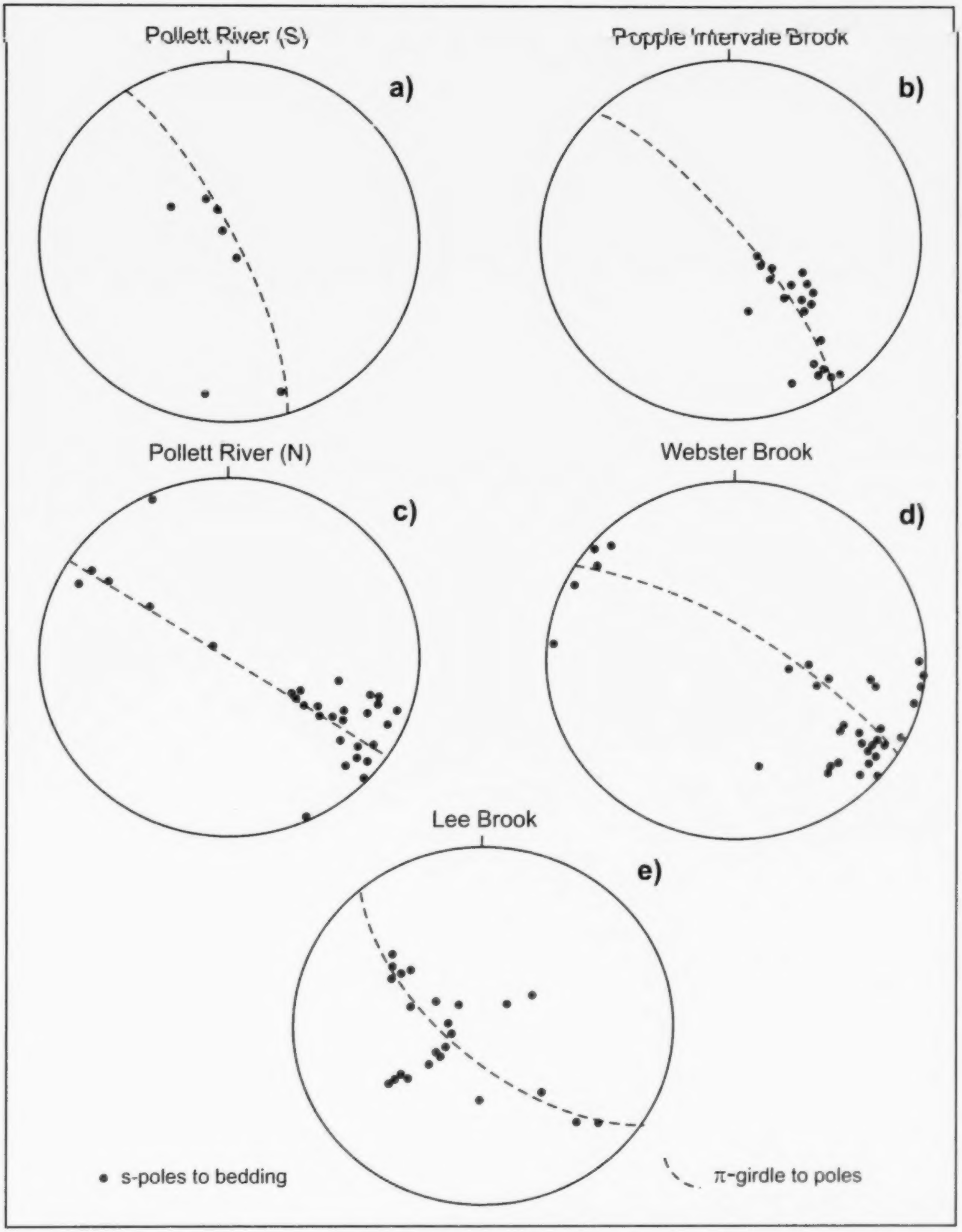

Figure 15. Stereograms of s-poles to bedding in domains of the Horton and Sussex groups between Parkindale and Upper Goshen. In domains north of the Pollett River Fault, evidence indicates that fold axes trend northeast. Between the Pollett River Fault and Gordon Falls Fault, folds trend east to east-northeast. All projections are equal area, lower hemisphere.

Panel 3

The panel between the Mapleton and Elgin faults comprises rocks of the Horton Group (Albert Formation) and Sussex Group (Round Hill Formation). The eastern part of the panel is a moderately to steeply dipping, northwest-facing sequence of Frederick Brook and Hiram Brook beds, overlain to the west by a steeply northwest-dipping section of the Round Hill Formation (Fig. 15c). In the southwest corner of the panel, the Round Hill section continues to young northwest and is interpreted to be in faulted contact with the wedge of Albert Formation (Frederick Brook Member) just west of it (Fig. 3b). Within those Frederick Brook beds, soft-sediment structures are common, especially in shale interbedded with dolomitic marlstone and grey limestone. The beds here show steep, vertical, and steeply overturned dips (Fig. 15d); younging indicators from ripples give a consistent regional northwest-facing direction.

Panel 4

Panel 4 is bounded by the Gordon Falls Fault on the south, Elgin Fault on the east, and Lee Brook Fault on the west. Rocks of the Sussex Group are exposed here along parts of Lee Brook, and the panel is characterized by a close to open, northerly plunging anticline (Fig. 15e). Beds of the Round Hill Formation appear on both fold limbs. Mudrock of the Weldon Formation is exposed to the northeast and on the downplunge end of the anticline along Lee Brook and Webster Brook.

Panel 5

The panel on the northwest side of the Lee Brook Fault is a moderately to steeply dipping, northwest-facing sequence of coarse Round Hill Formation.

Fault Exposures

Faults marking the boundaries of structural panels on the north side of the Gordon Falls Fault are not well exposed, and consequently their kinematic histories are incompletely understood.

Gordon Falls Fault

The Gordon Falls Fault crosses Pollett River in the gorge north of Gordon Falls (GPS N45°47.088'; W65°5.727') and at this locality is marked by a 50 m concealed interval between basement rocks and the Memramcook Formation. The only other outcrops adjacent to the Gordon Falls Fault occur in road scrapes and ditches between Elgin and Gowland Mountain (GPS N45°47.896'; W65°4.787'). In one outcrop, fabric in grey shaly gouge gives a dip-slip sense of motion with north-side down.

Pollett River Fault

The Pollett River Fault is exposed along the gorge at Pollett River, where conglomerate of the Memramcook Formation impinges on conglomerate of the Albert Formation (Hiram Brook Member). The fault trace is indicated by Memramcook beds that dip shallowly southeast, while Hiram Brook strata north of the fault dip subvertically and face northwest. Several discrete fault surfaces occur south of the fault in the Memramcook Formation, and much evidence exists of bedding-parallel slip in this unit. Kinematic indicators, however, are ambiguous. Many bedding-parallel slip surfaces in the Memramcook Formation indicate top-to-the-north with a dip-slip sense of motion. Fault surfaces discordant to bedding (generally near-vertical) record dip-slip and strike-slip motion, and roughness indicates all possible shear senses, including both left- and right-lateral.

Mapleton Fault

The Mapleton Fault merges with the Pollett River Fault on the east bank of Pollett River (Fig. 3b). In this locale, the Memramcook Formation on the south is juxtaposed against grey shale, siltstone, and limestone of the Albert Formation (Frederick Brook Member) on the north. Only 10 m of Frederick Brook beds are preserved here. The beds are disrupted by folding and boudinage of limestone layers and by an extensional duplex in sandstone–siltstone layers. Both features indicate strike-slip motion, but left- and right-lateral senses can be deduced (Fig. 16).

Elgin Fault

The location of the Elgin Fault west of Pollett River is indicated by 1) a dip reversal in the Round Hill Formation in outcrops along the lower part of Webster Brook, 2) west-facing Round

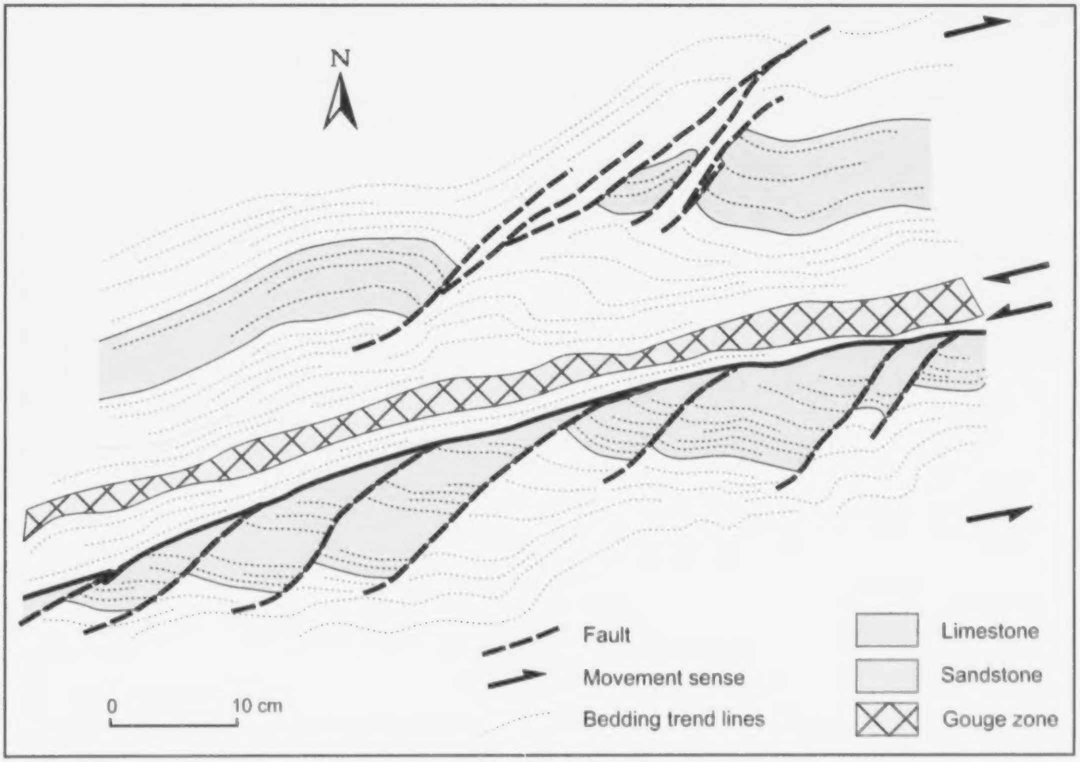

Figure 16. Sketch of kinematic indicators in deformed rocks of the Frederick Brook Member, Albert Formation, adjacent to the Mapleton and Pollett River faults. Drawing shows horizontal surface of an exposure on the east bank of Pollett River. Extension of the limestone layer north of the gouge zone suggests right-lateral motion. The extensional duplex in the sandstone layer south of the gouge zone is more ambiguous. Location of sketch is shown in Figure 3b.

Hill beds structurally below and in juxtaposition with steep, northwest-facing Albert beds along upper Webster Brook, and 3) shallowly north-dipping beds of the Weldon Formation against steeply northwest-facing Round Hill strata along the lower reaches of Webster Brook and Lee Brook. The fault surface is exposed nowhere along the actual interpreted fault trace.

Lee Brook Fault

The existence and approximate location of the Lee Brook Fault is shown along the upper part of Lee Brook, where shallowly dipping redbeds of the Round Hill Formation on the southeast side of the fault lie against steep to vertical northwest-younging Round Hill redbeds on the northwest side of the fault.

Fault Displacement

The latest phase of movement on the Gordon Falls Fault and faults bounding adjacent structural panels to the north can be deduced from the relationship of those structures to overstepping unconformities. For example, the Lee Brook and Elgin faults and the intervening anticline are covered by the Hillsborough Formation (Fig. 3b) and therefore are pre-Visean structures. The Gordon Falls Fault east of Parkindale and the Mapleton Fault west of Mapleton show no apparent displacement of the Cumberland Group (Boss Point Formation); thus, their latest movement was pre-Pennsylvanian (Bashkirian).

Northeast of Pleasant Vale, the location and distribution of the Mabou Group (Hopewell Cape Formation) relative to adjacent exposures of the Albert Formation strongly imply that the shallowly dipping Mabou beds are slightly displaced by the Pollett River Fault (Fig. 3b). The absence of exposures of the Boss Point Formation in this area prevents determination of whether this formation is displaced by the Pollett River Fault. In summary, it is concluded that fault structures defining the steeply dipping, folded panels of Horton and Sussex groups mainly pre-date deposition of the Hillsborough Formation. Such a conclusion permits the interpretation of a fault-related deformation that is end-Tournaisian, roughly contemporaneous with the pre-Hillsborough fold-thrust belt east of Prosser Brook.

The bedding-parallel slip surfaces and related folds with thrusts observed from east of Prosser Brook to Albert Mines and beyond (Fig. 7; see also Park and St. Peter 2005) have not been seen west of Prosser Brook. The Pleasant Vale–Upper Goshen area shows no evidence for continuation of the end-Tournaisian fold-thrust belt documented between Caledonia Mountain and Prosser Brook. Instead, the end-Tournaisian deformation between Pleasant Vale and Upper Goshen is manifested as a rotation of bedding into a series of en échelon, fault-bounded panels — a style not observed east of Prosser Brook. Geometry of the en échelon panels lying oblique to the Pollett River Fault suggests a strike-slip duplex between the Lee Brook and Gordon Falls faults (St. Peter 1992); the panel geometry also implies a right-lateral sense of movement (Fig. 17). The synclinal panel of the Memramcook Formation between the Gordon Falls and Pollett River faults (Fig 3b: Panel 1) is consistent with this synthesis.

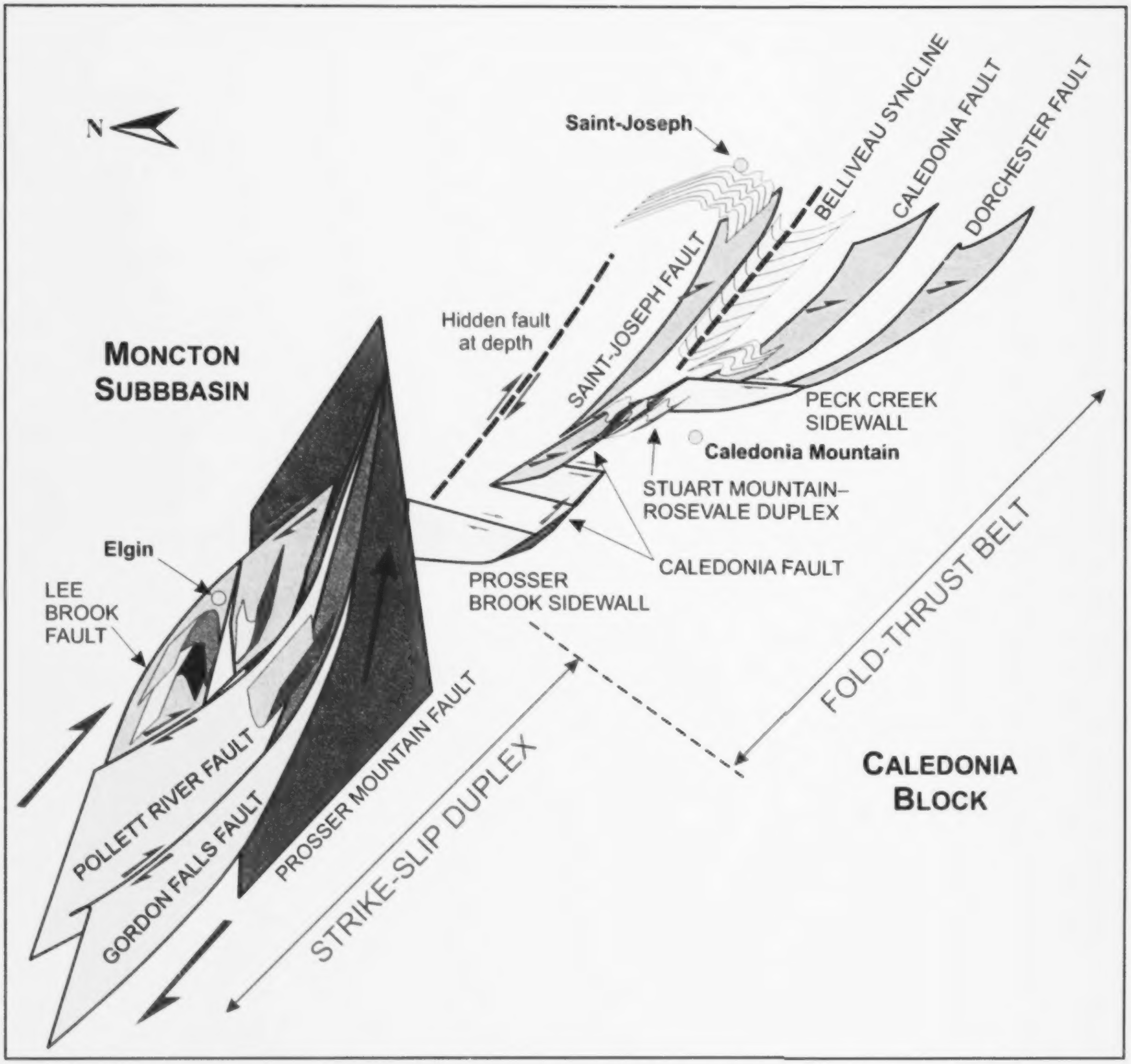
N
Saint-Joseph
BELLIVEAU SYNCLINE
CALEDONIA FAULT
DORCHESTER FAULT
SAINT-JOSEPH FAULT
Hidden fault at depth
MONCTON SUBBBASIN
PECK CREEK SIDEWALL
Caledonia Mountain
STUART MOUNTAIN–ROSEVALE DUPLEX
CALEDONIA FAULT
PROSSER BROOK SIDEWALL
Elgin
LEE BROOK FAULT
FOLD-THRUST BELT
CALEDONIA BLOCK
POLLETT RIVER FAULT
GORDON FALLS FAULT
PROSSER MOUNTAIN FAULT
STRIKE-SLIP DUPLEX

Figure 17. Schematic block diagram viewed from the east-southeast, depicting synoptic geometry of the end-Tournaisian inversion between Elgin and Saint-Joseph, southeastern New Brunswick. Diagram relates the 1) right-lateral, strike-slip duplex between the Gordon Falls and Lee Brook faults in the Elgin area to the 2) thrust-fold belt between Prosser Brook and Hillsborough as the structural framework to end-Tournaisian inversion along the southern margin of the Moncton Subbasin. See Park and St. Peter (2005) for details east of Caledonia Mountain.

The overall geometry of Horton–Sussex panels (Fig. 3b: Panels 2 to 5) between the Lee Brook and Pollett River faults and the enclosed oblique fold axes (Fig. 15b–e) strongly imply that the end-Tournaisian event had a transpressional, right-lateral strike-slip as the sense of movement. Because the movement would have involved elements of transpression or transtension, individual slip surfaces could record many related movement directions and senses (ignoring for the moment the effect of reactivation). Bedding-parallel slip surfaces appear in conglomerate of the Memramcook Formation along the Pollett River section in the south wall of the Pollett River Fault (Panel 1); they likely relate to formation of the syncline between the Pollett River and Gordon Falls faults (Fig. 15a). Such a supposition does not rule out the fold being a consequence of strike-slip motion with transpression, but neither does it prove the case. Both the pattern of folds and fault data gathered within the Parkindale–Elgin transect strongly suggest the overall geometry of a strike-slip duplex with right-lateral transpressive deformation.

CONCLUSIONS

- The end-Tournaisian fold-thrust belt related to basin inversion after deposition of the Sussex Group was initially recognized in the Hillsborough–Albert Mines area and can be traced westward through Caledonia Mountain to Prosser Brook. The belt appears to terminate against a northwest-trending structure immediately west of Prosser Brook village.
- The end-Tournaisian fold-thrust belt contains a number of sidewall ramps, one of which is the terminating structure west of Prosser Brook.
- The northwest-trending sidewall structures are coincident with thickness changes in the Horton Group, and overstepping of the Sussex Group onto basement rocks.
- A fundamental change in the end-Tournaisian deformation style occurs across the Sweet Mountain basement block, coincident with a major change in stratigraphy of the Horton Group. West of the basement block, the Albert Formation is underlain by the Memramcook and McQuade Brook formations. East of the block, these formations either are not exhumed or are absent along the southern margin of the Moncton Subbasin, adjacent to the Caledonia basement. West of the Sweet Mountain block, the Albert Formation decreases significantly in thickness from west (Elgin) to east (Parkindale), a reflection of post-Horton erosional events coincident with unconformities at the base of the Sussex, Mabou, and Cumberland groups.
- The fold-thrust belt does not continue west of the Sweet Mountain basement block. No evidence for originally low-angle bedding-parallel slippage can be found in rocks of the Horton or Sussex groups farther west. Specifically, faults parallel to bedding around Elgin and along Pollett River are steep features of the strike-slip duplex and did not originate as low-angle slip surfaces such as those in the fold-thrust belt east of Prosser Brook. These faults pre-date, and are overstepped by, the unconformity at the base of the Hillsborough Formation.
- The Prosser Mountain Fault preserved in the hanging wall of the Sweet Mountain basement block is a post-Windsor, pre-Pennsylvania (Bashkirian) feature unrelated to the Tournaisian fold-thrust belt.
- Data from the area of this report and from farther east (Park and St. Peter 2005) together describe the strike-slip duplex west of Prosser Brook and the fold-thrust belt east of Prosser Brook. The combined data define the structural framework for end-Tournaisian inversion of the Moncton Subbasin after deposition of the Sussex Group. Although deformation styles east and west of the Sweet Mountain basement block are fairly different, both are consistent with the inversion having occurred in response to transpressive, right-lateral movement along fundamental basement faults (Fig. 17).

- The unconformity at the base of the Sussex Group cuts downsection into the underlying Horton Group and locally oversteps directly onto pre-Late Devonian basement, reflecting a post-Horton (pre-Sussex) inversion. The present investigation thus can identify this pre-Sussex event, but can not elucidate its structural framework beyond noting that the northwest-trending structures were reactivated, as post-Sussex sidewalls seem to be involved.

ACKNOWLEDGEMENTS

This work was funded by the New Brunswick Department of Natural Resources (NBDNR) and by a PRAC–NSERC grant to David Keighley. Corridor Resources Inc. also provided support. Palynological analysis by Graham Dolby has been instrumental in elucidating stratigraphy throughout the Moncton Subbasin. Field assistance from Shaun Robertson (to AFP) is also acknowledged. We thank Les Fyffe at the NBDNR and Joseph C. White and Bruce E. Broster at the University of New Brunswick for continued support of our work on the Lower Carboniferous. Adrian Park also thanks Sandra Barr and Chris White for discussions about the nature and affinities of basement rocks associated with the Sweet Mountain block and along northern margins of the Caledonia Uplift.

REFERENCES

Barr, S.M., and White, C.E. 1996. Contrasts in Late Precambrian–Early Paleozoic tectonothermal history between Avalon composite terrane *sensu stricto* and other peri-Gondwanan terranes in southern New Brunswick and Cape Breton Island. *In* Avalonian and Related Peri-Gondwanan Terranes of the North Atlantic. *Edited by* R.D. Nance and M.D. Thompson. Geological Society of America, Special Paper 304, p. 95–108.

Brown, D.F., and Whaley, K.D.A. 1986. Oil shale assessment of the Albert Formation in the Rosevale area of Albert County, New Brunswick. New Brunswick Department of Forests, Mines, and Energy; Mineral Resources Division, Open File Report 86-7, 125 p.

Carr, P.A. 1968. Stratigraphy and spore assemblages, Moncton map-area, New Brunswick. Geological Survey of Canada, Paper 67-29, 47 p.

Chowdhury, A.H., 1995. Sedimentology, diagenesis and organic geochemistry of the Albert Formation, Moncton Subbasin, New Brunswick, Canada. Unpublished Ph.D. thesis, University of New Brunswick, Fredericton, New Brunswick, Canada, 249 p.

Chowdhury, A.H., and Noble, J.P.A. 1992. Porosity evolution in the Albert Formation of the Stoney Creek oil and gas field, Moncton Subbasin, New Brunswick, Canada. American Association of Petroleum Geologists Bulletin, **76** (9), p. 1325–1343.

Chowdhury, A.H., Fowler, M.G., and Noble, J.P.A. 1991. Petroleum geochemistry and geology of the Albert Formation, Moncton Subbasin, New Brunswick, Canada. Bulletin of Canadian Petroleum Geology, **39** (4), p. 315–331.

Dolby, G. 1991. Palynology of samples from the Albert Formation, New Brunswick. Unpublished report (Project 90.11) prepared for the New Brunswick Department of Natural Resources and Energy; Energy Branch, 29 p.

Dolby, G. 1993. Palynology analysis of outcrop samples from New Brunswick. Unpublished report (Project 92.12) prepared for the New Brunswick Department of Natural Resources and Energy; Energy Branch, 30 p.

Dolby, G. 1994. Palynological analysis of Carboniferous outcrop and corehole samples from the NATMAP program, 1993 field season (Sections 5, 6, 7, 8. and 9). Unpublished report (93.05) prepared for the Geological Survey of Canada, p. 26–38.

Dolby, G. 1995a. Palynological analysis of outcrop samples from New Brunswick. Unpublished report (Project 95.04) prepared for the New Brunswick Department of Natural Resources and Energy, 26 p.

Dolby, G. 1995b. Palynological analysis of Carboniferous outcrop and corehole samples from the NATMAP Program, 1994 field season (Sections 8A, 8B, and 8C). Unpublished report (Project 94.07) prepared for the Geological Survey of Canada, Atlantic Geoscience Centre, Bedford Institute of Oceanography, p. 90–103.

Dolby, G. 2000a. Palynological analysis of samples from 14 wells in New Brunswick. Unpublished report (Project 2016) prepared for Columbia Natural Resources Canada Limited, Fredericton, New Brunswick, 19 p.

Dolby, G. 2000b. Palynological analysis of corehole and outcrop samples from New Brunswick. Unpublished report (Project 2015) prepared for the New Brunswick Department of Natural Resources and Energy; Energy Branch, 14 p.

Dolby, G. 2001a. Palynological analysis of cuttings from the McCully #1 and McCully #2 and outcrop samples from New Brunswick. Unpublished report (Projects 2022, 2001/19) prepared for Corridor Resources Inc., Halifax, Nova Scotia, 7 p.

Dolby, G. 2001b. Palynological analysis of core samples from the Columbia Monteagle L-18 well, New Brunswick. Unpublished report (Project 2001/35) prepared for Three-D GeoConsultants Ltd., Fredericton, New Brunswick, 4 p.

Dolby, G. 2001c. Palynological analysis of well and outcrop samples from New Brunswick. Unpublished report (Projects 2001/26, 28) prepared for Corridor Resources Inc., Halifax, Nova Scotia, 13 p.

Dolby, G. 2002a. Palynological analysis of 23 outcrop samples from New Brunswick. Unpublished report (Project 2001/30) prepared for the New Brunswick Department of Natural Resources and Energy; Energy Branch, 10 p.

Dolby, G. 2002b. Palynological analysis of cuttings samples from the McCully P-56 and Urney No. 1 wells, New Brunswick. Unpublished report (Project 2002/1) prepared for Corridor Resources Inc., Halifax, Nova Scotia, 6 p.

Dolby, G. 2003. Palynofacies analysis of 51 outcrop, corehole and well cuttings samples from New Brunswick. Unpublished report (Project 2002/25) prepared for the New Brunswick Department of Natural Resources and Energy; Minerals, Policy and Planning Branch, 18 p.

Dolby, G. 2004. Palynological analysis of corehole and outcrop samples from New Brunswick. Unpublished report (Project 2003.28) prepared for the New Brunswick Department of Natural Resources and Energy; Minerals, Policy and Planning Division, 18 p.

Dolby, G. 2005. Palynological analysis of corehole and outcrop samples from New Brunswick. Unpublished report (Project 2004.16) prepared for the New Brunswick Department of

Natural Resources and Energy; Minerals, Policy, and Planning Division, 18 p.

Dolby, G. 2006a. Palynological analysis of outcrop and corehole samples from New Brunswick. Unpublished report (Project 2005.19a) prepared for the New Brunswick Department of Natural Resources; Minerals, Policy and Planning Division, 6 p.

Dolby, G. 2006b. Palynological analysis of corehole and outcrop samples from New Brunswick. Unpublished report (Project 2005.19b) prepared for the Department of Geology, University of New Brunswick, 5 p.

Dolby, G. 2006c. Palynological analysis of outcrop samples from the Indian Mountain Area, New Brunswick. Unpublished report (Project 2005.19c) prepared for the Department of Geology, University of New Brunswick, 7 p.

Dolby, G. 2006d. Palynological analysis of outcrop samples from New Brunswick. Unpublished report (Project 2005.19d) prepared for the New Brunswick Department of Natural Resources; Minerals, Policy and Planning Division, 7 p.

Foley, S.L. 1989. Geology of the Stoney Creek oil and gas field, and its implications regarding the tectonic evolution of the eastern Moncton Subbasin, New Brunswick. New Brunswick Department of Natural Resources and Energy; Minerals and Energy Division, Geoscience Report 89-1, 77 p.

Greiner, H.R. 1962. Facies and sedimentary environments of Albert shale, New Brunswick. American Association of Petroleum Geologists, Bulletin 46, No. 2, p. 219–234.

Greiner, H.R. 1974. The Albert Formation of New Brunswick: a Paleozoic lacustrine model. Geologische Rundschau Band, **63**, p. 1102–1113.

Gussow, W.C. 1953. Carboniferous stratigraphy and structural geology of New Brunswick, Canada. American Association of Petroleum Geologists, Bulletin, **37** (7), p. 1713–1816.

Hayward, A.B., and Graham, R.H. 1989. Some geometric characteristics of inversion. *In* Inversion Tectonics, *Edited by* M.A. Cooper and G.D. Williams. Geological Society of London, Special Publication 44, p. 17–39.

Hamilton, J.B. 1965. Limestone in New Brunswick. New Brunswick Department of Lands and Mines; Mines Branch, Mineral Resource Report 2, 147 p.

Hinds, S.J., and St. Peter, C. J. 2006. Stratigraphy and structure of the Moncton Subbasin in the Urney-Waterford area, Maritimes Basin, New Brunswick: implications for the McCully natural gas field. *In* Geological Investigations in New Brunswick for 2005. *Edited by* G.L. Martin, New Brunswick Department of Natural Resources; Minerals, Policy and Planning Division, Mineral Resource Report 2006-3, p. 73–102.

McClay, K.R. 1998. Analogue models of inversion tectonics. *In* Inversion Tectonics. *Edited by* M.A. Cooper and G.D. Williams, Geological Society of London, Special Publication 44, p. 41–59.

McCutcheon, S.R. 1981. Stratigraphy and paleogeography of the Windsor Group in southern New Brunswick. Unpublished M.Sc. thesis, Acadia University, Wolfville, Nova Scotia, 206 p. *and* New Brunswick Department of Natural Resources; Mineral Resources Division, Geological Surveys Branch, Open File Report 81-31, 210 p.

McGregor, D.C. 1983a. Palynology of samples of rock from southern New Brunswick (NTS 21H and 21 I), collected by C. St. Peter of the New Brunswick Department of Natural Resources. Geological Survey of Canada, Ottawa Paleontology Section, Report F1-10-

1983-DCM, 4 p.

McGregor, D.C. 1983b. Report to C. St. Peter (New Brunswick Department of Natural Resources) on palynology of samples of rock collected by M.S. Barss in 1969 from near Memramcook, N.B. (NTS 21 I/02E). Geological Survey of Canada, Ottawa Paleontology Section, Report F1-7-1983, 2 p.

McLeod, M.J. 1980. Geology and mineral deposits of the Hillsborough area, map area V-22 and V-23 (Parts of 21 H/15E and 21 H/15W). New Brunswick Department of Natural resources; Mineral Resources Branch, Map Report 79-6, 35 p.

Norman, G.W.H. 1941. Hillsborough map sheet, Albert and Westmorland counties, New Brunswick. Geological Survey of Canada, Map 647A (with marginal notes).

Park, A.F., and St. Peter, C.J. 2005. Deformation of Lower Carboniferous rocks in the Rosevale to Saint-Joseph area (NTS 21 H/15), Albert and Westmorland counties, southeastern New Brunswick. *In* Geological Investigations in New Brunswick for 2004. *Edited by* G.L. Martin. New Brunswick Department of Natural Resources; Minerals, Policy and Planning Division, Mineral Resource Report 2005-1, p. 45–98.

St. Peter, C.J. 1989. Geology of the Albert Formation, Moncton Subbasin. New Brunswick Department of Natural Resources and Energy; Geological Surveys Division, Plates 89-104c, d, and e.

St. Peter, C.J. 1992. Lithologic facies, seismic facies, and strike-slip setting of the Lower Carboniferous alluvial/fluvial/lacustrine Albert Formation of New Brunswick. New Brunswick Department of Natural Resources and Energy; Mineral Resources Division, Geoscience Report 92-2, 145 p.

St. Peter, C.J. 1993. Maritimes Basin evolution: key geologic and seismic evidence from the Moncton Subbasin of New Brunswick. Atlantic Geology, **29**, p. 233–270.

St. Peter, C.J. 2001. Petroleum geology in the Carboniferous of southeastern New Brunswick. *In* Guidebook to Field Trips in New Brunswick and Western Maine. *Edited by* R.K. Pickerill and D.R. Lentz. New England Intercollegiate Geological Conference, 93rd Annual Meeting, September 2001, Fredericton, New Brunswick, p. A4-1 to A4-30.

St. Peter, C.J. 2002. Bedrock geology of the McCully Natural Gas Field area, Moncton Subbasin (parts of 21 H/11, 12, 13, and 14), New Brunswick. New Brunswick Department of Natural Resources and Energy; Minerals and Energy Division, Plate 2002-33 (revised 2004).

St. Peter, C.J. 2006. Geological relationship between the Cocagne Subbasin and Indian Mountain Deformed Zone, Maritimes Basin, New Brunswick. *In* Geological Investigations in New Brunswick for 2005. *Edited by* G.L. Martin. New Brunswick Department of Natural Resources; Minerals, Policy and Planning Division, Mineral Resource Report 2006-3, p. 103–183.

St. Peter, C.J., and Johnson, S.C. 1997. Carboniferous geology of the Hillsborough map area, (NTS 21 H/15). Westmorland and Albert counties, New Brunswick. New Brunswick Department of Natural Resources and Energy; Minerals and Energy Division, Plate 97-8 (revised 2005).

St. Peter, C.J. and Park, A.F. 2006. Bedrock geology of Peck Creek/Weldon Creek area (part of 21 H/15g), Albert County, New Brunswick. New Brunswick Department of Natural

Resources; Minerals, Policy and Planning Division, Plate 2006-44.

Utting, J. 1987. Palynology of the Lower Carboniferous Windsor Group and Windsor–Canso boundary beds of Nova Scotia, and their equivalents in Quebec, New Brunswick and Newfoundland. Geological Survey of Canada, Bulletin, No. 374, 93 p.

Utting, J., Keppie, J.D., and Giles, P.S. 1989. Palynology and stratigraphy of the Lower Carboniferous Horton Group, Nova Scotia. *In* Contributions to Canadian Paleontology, Geological Survey of Canada, Bulletin 396, p. 117–143.

Webb, T.C. 1997. Carboniferous limestones of New Brunswick: geology and development potential. New Brunswick Department of Natural Resources and Energy; Minerals and Energy Division, Open File 97-6, 259 p.

Williams, E.P. 1974. Geology and petroleum possibilities in and around the Gulf of St. Lawrence. American Association of Petroleum Geologists Bulletin, **58**, p. 1137–1155.

Wilson, P. 2004. Syn-sedimentary high-strain zones versus post-lithification shear zones in the Albert Formation of southeastern New Brunswick. Field trip guide, Canadian Tectonics Group, 24th Annual Meeting, October 22–24, 2004, Saint John, New Brunswick. 30 p.

Wilson, P. 2005. Stratigraphy, structural geology, and tectonic history of the McCully area, Moncton Subbasin, southeastern New Brunswick. New Brunswick Department of Natural Resources; Minerals, Policy and Planning Division, Mineral Resource Report 2005-5, 104 p.

Wilson, P., and White, J.C. 2006. Tectonic evolution of the Moncton Basin, New Brunswick, eastern Canada: new evidence from field and sub-surface data. Bulletin of Canadian Petroleum Geology, **54** (4), p. 319-336.

Wright, W.J. 1922. Geology of the Moncton map-area. Geological Survey of Canada, Memoir 129, 69 p.

Mineral Resource Report 2007-1

ISBN 978-1-55396-401-8
ISSN 0548-4014

Price $20.00